A functional analysis of the non-coding RNAs of murine gammaherpesvirus 68

Nila Roy Choudhury

Submitted for the degree of Doctor of Philosophy
The University of Edinburgh
2010

Declaration

I declare that this thesis has been composed by me and that all work included in this thesis is my own except where otherwise stated. No part of this work has been submitted, or will be submitted for any other degree of professional qualification.

Nila Roy Choudhury 2010

Centre for Infectious Diseases
The Roslin Institute and Royal (Dick) School of Veterinary Studies
University of Edinburgh
Summerhall
Edinburgh EH9 1QH

Acknowledgments

I would like to thank my supervisors Dr Bernadette Dutia, Dr Simon Talbot and Professor Alastair Aitken for their help and advice during my PhD. As my main advisor Dr Bernadette Dutia provided guidance and advice at every stage of my work and I am very grateful to have been given the opportunity to do my PhD in her research group.

A big thank you also to Dr Andrew Cronshaw for all his help with the cICAT technique and Amy Buck for her help with the qRT-PCR for miRNAs and general advice. I would also like to thank the rest of the people in the group and all the people in the tower block for creating a fantastic working environment.

Thank you to my family, especially my parents who always encouraged me to work for what I wanted and not give up. Finally, Ewan, thank you for being there supporting me throughout my PhD, encouraging me and believing in me.

Abstract

Murine gammaherpesvirus 68 (MHV-68) is used as a model for the study of gammaherpesvirus infection and pathogenesis. In the left region of the genome MHV-68 encodes four unique genes, eight viral tRNA-like molecules (vtRNAs) and nine miRNAs. The vtRNAs have a predicted cloverleaf-like secondary structure like cellular tRNAs and are processed into mature tRNAs with the addition of 3' CCA termini, but are not aminoacylated. Their function is unknown; however they have been found to be expressed at high levels during both lytic and latent infection and are packaged in the virion. The miRNAs are expressed from the vtRNA primary transcripts during latent infection. All herpesviruses examined to date have been found to express miRNAs. These are thought to aid the viruses in avoiding the host immune response and to establish and maintain latency.

The aim of this project was to investigate the functions of the vtRNAs and miRNAs of MHV-68. MHV-76 is a natural deletant mutant lacking the unique genes, vtRNAs and miRNAs. This virus was previously used in our lab to construct two insertion viruses encoding vtRNAs1-5 and miRNAs1-6. The only difference between MHV-76 and the insertion viruses is therefore the vtRNAs and miRNAs. The B-cell line NS0 was latently infected with the various viruses and the infected cells characterised. *In situ* hybridisation and antibody staining showed that all viruses infect the same proportion of cells. The insertion viruses were confirmed to express the vtRNAs during latency by RT-PCR. In addition, using Northern blot analysis the insertion viruses were shown to express miRNA1 during lytic infection of fibroblast cells; however, not during latent infection of NS0 cells. The lack of miRNA1 expression during latency was confirmed using qRT-PCR and miRNAs3-6 were found to be expressed at a lower level than in MHV-68 infected cells.

Replication and reactivation kinetics of latently infected NS0 cells showed that introduction of vtRNAs and miRNAs into MHV-76 causes a reduction in reactivation and production of lytic virus. To determine if the reduction in reactivation was caused by the miRNAs, they were introduced into infected cells by transfection. Transfection of miRNAs1-6 into MHV-76 infected cells or miRNA1 into insertion virus infected cells did not lead to an increase or decrease in

reactivation. It was confirmed by qRT-PCR that the transfection did result in miRNA levels higher than in insertion virus infected cells. Further, down-regulation of miRNAs using a siRNA against DICER did not lead to a reduction in reactivation. This supports the hypothesis that the vtRNAs rather than the miRNAs are responsible for the reduction of reactivation seen in insertion virus latently infected cells.

To determine the effect of the non-coding RNAs on protein expression, NS0 cells latently infected with MHV-76 and insertion virus were analysed using cleavable ICAT and 1-D PAGE cleavable ICAT. In an ICAT analysis the proteins are labelled and the levels of individual proteins in two samples can be compared using mass spectrometry. These techniques were optimised and several proteins with differences in expression between the viruses were identified. It was, however, difficult to determine any specific functions of the non-coding RNAs from the data.

Contents

Title i

Declaration ii

Acknowledgments iii

Abstract iv

Contents vi

List of Figures xi

List of Tables xiv

Abbreviations xv

1. Chapter One: Introduction 1

1.1. Herpesviruses 2
1.1.1. Classification 2
1.1.1.1. Alphaherpesvirinae 4
1.1.1.2. Betaherpesvirinae 4
1.1.1.3. Gammaherpesvirinae 4
1.1.2. Herpesvirus structure 5
1.1.3. Herpesvirus genome 7
1.1.4. Herpesvirus life cycle 9
1.1.4.1. Entry 9
1.1.4.2. Gene expression 12
1.1.4.3. Replication 12
1.1.4.4. Assembly and egress 13
1.1.4.5. Latency 13
1.2. Gammaherpesviruses 14
1.2.1. Epstein-Barr virus 14
1.2.1.1. EBV latency 15
1.2.1.1.1. Latency transcripts 17
1.2.1.2. EBV infection and associated diseases 19
1.2.2. Kaposi's sarcoma-associated herpesvirus 22
1.2.2.1. KSHV genome 23
1.2.2.2. KSHV epidemiology 23
1.2.2.3. KSHV latency 24
1.2.2.3.1. Latency transcripts 25
1.2.2.4. KSHV infection and associated diseases 27
1.2.2.4.1. Kaposi's sarcoma 27
1.2.2.4.2. Primary effusion lymphoma 28
1.2.2.4.3. Multicentric Castleman's disease 28
1.3. Murine gammaherpesvirus-68 29
1.3.1. Discovery and classification 29
1.3.2. MHV-68 virion 30

1.3.3. MHV-68 genome 30
1.3.4. MHV-68 life cycle 31
1.3.4.1. Entry 31
1.3.4.2. Gene expression 31
1.3.4.3. Viral DNA replication 33
1.3.4.4. Assembly and egress 34
1.3.5. MHV-68 primary infection 34
1.3.6. MHV-68 latency 35
1.3.6.1. Latency *in vitro* 36
1.3.6.2. Latency transcripts 37
1.3.7. MHV-68 evasion of the host's immune system 38
1.3.8. MHV-68 pathogenesis 38
1.3.9. MHV-76 and other related viruses 39
1.3.10. Left-hand end of MHV-68 40
1.3.10.1. M1 40
1.3.10.2. M2 42
1.3.10.3. M3 43
1.3.10.4. M4 43
1.3.10.5. vtRNAs and miRNAs 44
1.4. Non-coding RNAs 45
1.4.1. Viral non-coding RNA molecules 45
1.4.1.1. Alphaherpesvirus non-coding RNA molecules 45
1.4.1.1.1. HSV LATs 45
1.4.1.2. Gammaherpesvirus non-coding RNA molecules 47
1.4.1.2.1. EBV EBERs 47
1.4.1.2.2. HVS U RNAs 50
1.4.1.2.3. KSHV PAN RNAs 51
1.4.1.3. Adenovirus non-coding RNAs 52
1.4.1.3.1. VAI and VAII 52
1.4.2. tRNAs 53
1.4.2.1. tRNA structure 53
1.4.2.2. tRNA expression 55
1.4.2.3. tRNA functions 56
1.4.2.3.1. Translation 56
1.4.2.3.2. Amino acid starvation 56
1.4.2.4. tRNA genes and chromatin 57
1.4.2.5. tRNA functions during viral infections 58
1.4.2.6. tRNA-like molecules 58
1.4.2.6.1. Plant virus tRNA-like molecules 59
1.4.2.6.2. Transfer messenger RNA 59
1.4.2.6.3. The threonyl-tRNA synthetase gene of E.coli 60
1.4.3. miRNAs 60
1.4.3.1. miRNA biogenesis 60
1.4.3.2. miRNA functions 63
1.4.3.3. Viruses and miRNAs 64
1.5. Project outline 69

2. Chapter Two: Materials and methods 70

2.1. Cell Culture techniques 71
2.1.1. Maintenance of cell lines 71
2.1.2. Harvesting and counting cells 71
2.1.3. Cytospins 71
2.1.4. Transfection 72
2.2. Virological methods 72
2.2.1. Preparation of virus stocks 72
2.2.2. Virus titration 73
2.2.3. Infection of NS0 cells for virus characterisation studies 73
2.2.4. Infective centre assay 74
2.2.5. GFP labelled viruses 74
2.2.6. Cloning of infected cells 74
2.2.7. Staining for lytic proteins 75
2.3. In situ hybridisation 75
2.3.1. Generation of labelled RNA probe 75
2.3.2. *In situ* hybridisation of cytospins 77
2.4. DNA isolation and manipulation 78
2.4.1. Plasmid preps 78
2.5. RNA isolation and manipulation 79
2.5.1. microRNA isolation 79
2.5.2. DNase treatment of RNA 79
2.5.3. Reverse transcription of RNA 79
2.5.4. *In vitro* transcription of vtRNAs 80
2.6. Polymerase chain reaction (PCR) 80
2.6.1. Standard PCR 80
2.6.2. Whole cells and virus stock PCR 80
2.6.3. qRT-PCR for miRNAs 81
2.7. Agarose gel electrophoreses 82
2.8. Northern analysis 82
2.8.1. Electrophoresis and blotting 82
2.8.2. Prehybridisation and hybridisation 83
2.8.3. Generation of radiolabelled probe 83
2.8.4. Stripping of membranes for re-probing 84
2.9. Protein techniques 84
2.9.1. Protein extraction 84
2.9.2. Protein fractionation 84
2.9.3. Protein concentrations 84
2.9.4. Acetone precipitation 85
2.9.5. SDS-PAGE gel 85
2.9.6. Digestion of proteins in solution 86
2.9.7. ICAT 86
2.9.7.1. Cleavable ICAT ® 86
2.9.7.2. 1-D PAGE cleavable ICAT 87
2.9.8. Mass spectrometry 88
2.9.8.1. Matrix-assisted laser desorption/ionization (MALDI) 88
2.9.8.2. LC-MS/MS analysis 89

2.10. Stock solutions **90**
2.11. Synthetic oligonucleotides used for in vitro transcription **91**
2.12. Primers **92**

3. Chapter Three: Characterisation of viruses 93

3.1. Aims **94**
3.2. Determining the percentage of infected NS0 cells **96**
3.2.1. GFP labelled viruses 96
3.2.2. *In situ* hybridisation 97
3.2.3. Cloning of infected cells 100
3.2.4. Staining for lytic proteins 100
3.3. miRNA expression **103**
3.3.1. Northern blot analysis 103
3.3.2. qRT-PCR 105
3.4. vtRNA expression **109**
3.5. Discussion **109**

4. Chapter Four: Investigating the functions of the non-coding RNAs 116

4.1. Aims **117**
4.2. Replication and reactivation kinetics **118**
4.2.1. Preliminary experiment 118
4.2.2. Experiment with Int2 virus 123
4.2.3. Experiment with revertant virus 123
4.2.4. *In vivo* reactivation kinetics 129
4.3. Transfection of non-coding RNAs and plasmids **132**
4.3.1. miRNA transfections 132
4.3.2. Dicer 135
4.3.3. ORF50 139
4.3.4. vtRNAs 139
4.3.5. pL2a5 142
4.4. Discussion **142**

5. Chapter Five: Investigating the effects of the non-coding RNAs on protein synthesis in latently infected cells 148

5.1. Aims **149**
5.2. cICAT **153**
5.2.1. BSA 153
5.2.2. MHV-76 vs. Int9 latently infected NS0 cells 157
5.2.3. Troubleshooting protein extraction techniques 161
5.2.4. MHV-76 vs. Int9 latently infected NS0 cells- Vivaspin 165

5.2.5. MHV-76 vs. Int9 latently infected NS0 cells- freeze-dryer 171
5.3. 1-D PAGE cICAT **176**
5.3.1. Assay setup 176
5.3.2. BSA 180
5.3.3. MHV-76 vs. Int9 latently infected NS0 cells 182
5.4. Discussion **192**

6. Chapter Six: Conclusions **197**

7. References **205**

8. Appendix **254**

List of figures

1.1 Herpesvirus virion 6

1.2 Herpesvirus genome organisations 8

1.3 The arrangement of core gene blocks of the three herpesvirus subfamilies 10

1.4 Comparing the genome of MHV-68 with that of KSHV and HVS 32

1.5 The unique genes in the left side of the genome, vtRNA/miRNA transcript and predicted cloverleaf structure of vtRNA5 41

1.6 Viral non-coding RNA molecules 48

1.7 Secondary and tertiary structure of a typical tRNA molecule 54

1.8 An overview of miRNA processing 62

3.1 Showing the differences between MHV-68, MHV-76 and insertion viruses 95

3.2 Percentage of NS0 cells expressing GFP 98

3.3 *In situ* hybridisation for vtRNAs1-4 on NS0 cells 99

3.4 *In situ* hybridisation for vtRNAs1-4 on S11 cells 101

3.5 Identifying MHV-76 and Int9 infected clones by PCR analysis 102

3.6 Staining of virus infected cells using a polyclonal serum raised against lytically infected rabbit kidney cells 104

3.7 Northern blot analysis of miRNA1 expression- BHK and NS0 106

3.8 Northern blot analysis of miRNA1 expression- NS0 with Int2 107

3.9 qRT-PCR amplification plots- uninfected/infected 108

3.10 qRT-PCR for miRNAs- Int9 and Int2 110

3.11 RT-PCR analysis of vtRNAs1, 2, 4 and 5 111

4.1 Supernatant and cell associated virus titres- preliminary experiment 119

4.2 Cell numbers- preliminary experiment 120

4.3 Supernatant virus titres- preliminary experiment 121

4.4 Cell associated virus titres- preliminary experiment 121

4.5 Percentage of NS0 cells reactivating virus- preliminary experiment 122

4.6 Percentage of infective centres- with Int2 124

4.7 Comparing the percentage of infective centres between the two experiments 124

4.8 Supernatant and cell associated virus titres- with Rev 125

4.9 Cell numbers –with Rev 126

4.10 Supernatant virus titres- with Rev 127

4.11 Cell associated virus titres- with Rev 127

4.12 Percentage of NS0 cells reactivating virus- with Rev 128
4.13 Possible miRNA1 target sequence in the ORF50 3' UTR 130
4.14 Infective centres- MLN 131
4.15 Infective centres averages- MLN 131
4.16 Percentage of infective centres- miRNA transfection 24 and 72hours 133
4.17 Percentage of infective centres- miRNA transfection 24 and 48 hours 134
4.18 Supernatant virus titres- miRNA transfection 24 hours and 48 hours 134
4.19 Percentage of infective centres- miRNA transfection 24 hours 136
4.20 Relative quantity of miRNA3 as determined by qRT-PCR 136
4.21 Percentage of infective centres following transfection with DICER siRNA 137
4.22 qRT-PCR amplification plots for miRNA4 138
4.23 Relative quantity of miRNA3 and 4 as determined by qRT-PCR 138
4.24 Percentage of infective centres- ORF50 plasmid transfection Int9 140
4.25 Percentage of infective centres- ORF50 plasmid transfection MHV-68 and Int9 140
4.26 Percentage of infective centres- vtRNA1 transfection 141
4.27 Percentage of infective centres- vtRNA1, 4 and 5 transfection 141
4.28 Percentage of infective centres- pL2a5 transfection 24 hours 143
4.29 Percentage of infective centres- pL2a5transfection 48 hours 143
5.1 Step-by-step schematic description of the cICAT labelling 150
5.2 Demonstrating the fragmentation of a peptide 152
5.3 MALDI analysis of BSA peptides generated by trypsin treatment of unlabelled control BSA or BSA labelled with light cICAT reagent 154
5.4 MALDI analysis of BSA derived peptides labelled with light cICAT following cation-exchange column and after the avidin column 156
5.5 MALDI analysis of the final BSA samples 158
5.6 MALDI results of the BSA sample labelled with light cICAT 159
5.7 LC-MS/MS results of BSA labelled with light cICAT 160
5.8 MALDI analysis of peptides- MHV-76 vs. Int9 162
5.9 MALDI analysis of the final sample- MHV-76 vs. Int9 163
5.10 SDS-PAGE showing the protein bands present in samples 164
5.11 MALDI analysis of tryptic digestions of 10μg BSA 166
5.12 SDS-PAGE of cytoplasmic proteins- MHV-76 and Int9 168
5.13 LC-MS/MS results of labelled peptides- MHV-76 and Int9, Vivaspin 169
5.14 MALDI analysis of labelled peptides- MHV-76 and Int9, Vivaspin 170

5.15 SDS-PAGE of cytoplasmic proteins- MHV-76 and Int9 172
5.16 MALDI analysis of labelled peptides- MHV-76 and Int9, freeze-dryer 173
5.17 MALDI analysis of labelled peptides- MHV-76 and Int9, freeze-dryer 174
5.18 LC-MS/MS results of labelled peptides- MHV-76 and Int9, freeze-dryer 175
5.19 Step-by-step schematic description of the 1-D PAGE cICAT protocol 177
5.20 MALDI analysis of 100ng BSA in the vacuum drying test 178
5.21 MALDI analysis of peptides from 200ng and 300ng BSA 179
5.22 MALDI analysis of peptides from BSA labelled with light cICAT 181
5.23 MALDI analysis of band 3 peptides in the 1-D PAGE cICAT assay 183
5.24 LC-MS/MS results of labelled peptides from band 3 184
8.1 qRT-PCR dissociation curves- uninfected/infected 255
8.2 qRT-PCR dissociation curves for miRNA expression 256

List of tables

1.1 Classification of herpesviruses in the order of *Herpesvirales* 3
1.2 EBV gene expression pattern during latent infection 16
1.3 List of identified viral miRNAs 65
1.4 Viral and cellular mRNA targets of viral miRNAs 67
5.1 Listing the predicted BSA derived peptides 155
5.2 Peptide pairs (light/heavy) identified from band 3 186
5.3 Peptide pairs (light/heavy) identified from band 3, protein score 0 187
5.4 Ratios of proteins from band 3 188
5.5 Rations of individual peptide pairs of heat shock protein 90-beta 189
5.6 Ratios of proteins from bands 1, 2, 4, 5, 7, 9, and 11 191

Abbreviations

ABC	Ammonium bicarbonate
ACN	Acetonitrile
AIDS	Acquired immune deficiency syndrome
ALH	Atypical lymphoid hyperplasia
AREs	AU-rich elements
ATF	Activating transcription factor
BAC	Bacterial artificial chromosome
BARTs	BamA rightward transcripts
BCA	Bicinchoninic acid
BHK	Baby Hamster Kidney fibroblast
BL	Burkitt's lymphoma
BMV	Brome mosaic virus
bp	Base pair
BSA	Bovine serum albumin
cdk	Cyclin-dependent kinase
cICAT	Cleavable Isotope-coded affinity tags
CMV	Cytomegalovirus
dig	Digoxigenin
DNA	Deoxyribonucleic acid
ds	Double stranded
E.coli	*Escherichia coli*
EBERs	EBV encoded small RNAs
EBNA	EBV nuclear antigen
EBV	Epstein-Barr virus
EMSA	Electric mobility shift assay
ESI	Electrospray ionisation
FLIP	FLICE inhibitory protein
GAGs	Glycosaminoglycans
gC	Glycoprotein C
GFP	Green Fluorescent Protein
gp	Glycoprotein
HAART	Highly active anti-retroviral therapy

HCMV	Human cytomegalovirus
HCV	Hepatitis C virus
HHV	Human herpesvirus
HIV	Human immunodeficiency virus
HL	Hodgkin's lymphoma
HSUR	Herpesvirus saimiri unique RNA
HSV	Herpes simplex virus
HVS	Herpesvirus saimiri
IFN	Interferon
Ig	Immunoglobulin
IL	Interleukin
IM	Infectious mononucleosis
IRF	Interferon regulatory factor
Kbp	Kilo base pairs
KSHV	Kaposi's sarcoma-associated herpesvirus
La	Lupus erythematosis-associated antigen
LANA	Latency-associated nuclear antigen
LAT	Latency- associated transcript
LC	Liquid chromatograph
LMP	Latent membrane protein
m/z	Mass-to-charge
MALDI	Matrix-assisted laser desorption/ionization
MAP	Mitogen-activated protein
MCD	Multicentric Castleman's disease
MCMV	Mouse cytomegalovirus
MDV	Marek's disease virus
MHC	Major histocompatibility complex
MHV	Murine herpesvirus
miRNA	MicroRNA
MLN	Mediastinal lymph node
MOI	Multiplicity of infection
mRNA	Messenger RNA
MS	Mass spectrometry
MS/MS	Tandem mass spectrometry

ND-10	Nuclear domain 10
NFκB	Nuclear factor κB
NK cells	Natural killer cells
NPC	Nasopharyngeal carcinoma
nt	Nucleotide
ORF	Open reading frame
*ori*Lyt	Origin of lytic replication
PAGE	Polyacrylamide gel electrophoresis
PAN RNA	Polyadenylated nuclear RNA
PBS	Phosphate buffered saline
PCR	Polymerase chain reaction
PEL	Primary effusion lymphoma
pfu	Plaque forming units
PKR	Protein kinase R
PTLD	Posttransplantation lymphoproliferative disease
RBC	Reed-Sternberg cells
RISC	RNA-induced silencing complex
rLCV	Rhesus lymphocryptovirus
RNA	Ribonucleic acid
RPMI	Rosewell Park Memorial Institute
RT	Reverse transcriptase
rta	Replication and transcription activator
SDS	Sodium dodecyl sulphate
SINES	Short interspersed elements
siRNA	Small interfering RNA
SMN	Survival of motor neurons
snRNPs	Small nuclear ribonucleoproteins
ssDNA	Single stranded DNA
Taq	*Thermus aquaticus*
TBS	Tris-buffered saline
TLS	tRNA-like structures
tmRNA	Transfer messenger RNA
TMV	Tobacco mosaic virus
TOF	Time of flight

TYMV	Turnip yellow mosaic virus
UTR	Untranslated region
v	Viral prefix
v/v	Volume per volume
vtRNAs	Viral transfer RNAs
VZV	Varicella-zoster virus
w/v	Weight per volume
WMHV	Wood mouse herpesvirus

1. Chapter One: Introduction

1.1. Herpesviruses **2**
1.1.1. Classification 2
1.1.2. Herpesvirus structure 5
1.1.3. Herpesvirus genome 7
1.1.4. Herpesvirus life cycle 9
1.2. Gammaherpesviruses **14**
1.2.1. Epstein-Barr virus 14
1.2.2. Kaposi's sarcoma-associated herpesvirus 22
1.3. Murine gammaherpesvirus-68 **29**
1.3.1. Discovery and classification 29
1.3.2. MHV-68 virion 30
1.3.3. MHV-68 genome 30
1.3.4. MHV-68 life cycle 31
1.3.5. MHV-68 primary infection 34
1.3.6. MHV-68 latency 35
1.3.7. MHV-68 evasion of the host's immune system 38
1.3.8. MHV-68 pathogenesis 38
1.3.9. MHV-76 and other related viruses 39
1.3.10. Left-hand end of MHV-68 40
1.4. Non-coding RNAs **45**
1.4.1. Viral non-coding RNA molecules 45
1.4.2. tRNAs 53
1.4.3. miRNAs 60
1.5. Project outline **69**

1.1. Herpesviruses

Herpes can be traced back to the ancient Greeks describing the lesions appearing to "creep or crawl" along the skin (Roizman and Whitley 2001). The order of *Herpesvirales* is a very large order of viruses containing approximately 135 members found to infect most animal species ranging from humans to frogs and oysters (Davison *et al.* 2009). The different members are diverse in terms of genomic sequence; however, they are all similar in terms of structure and genome organisation. There is large variation in the diseases caused by the viruses, e.g. encephalitis, chickenpox and cancer; however, they share several significant biological properties. They all encode a variety of enzymes involved in nucleic acid metabolism, DNA synthesis and protein processing. The genome replication and capsid assembly takes place in the nucleus, while the final processing of the virion takes place in the cytoplasm. Upon release of new virus particles the cell is destroyed. Another common feature among the members is the ability to remain latent in the host with the possibility of reactivation to a lytic infection at a later stage. During latency the viral genome is maintained as circularised DNA in an episome with very limited gene expression (Pellet and Roizman 2007).

There are also differences in the biological properties of the viruses: some have very narrow host cell ranges and some wider, while replication cycles can be long or very short. The cell choice for latency also differs between viruses. Most animal species can be infected by at least one herpesvirus; however, few viruses infect more than one species (Pellet and Roizman 2007). There are eight herpesviruses associated with human disease (Table 1.1).

1.1.1. Classification

The herpesviruses were initially ordered under the *Herpesviridae* family into three subfamilies based on biological properties: the *Alphaherpesvirinae*, the *Betaherpesvirinae*, and the *Gammaherpesvirinae*. The viruses have further been classified using DNA sequence homology, similarities in genome sequence

Herpesvirales	Genus	Virus	Disease in humans
Family *Herpesviridae* **Subfamily** *Alphaherpesvirinae*	*Simplexvirus*	Herpes simplex virus 1 and 2	Encephalitis, Genital herpes
	Varicellovirus	Varicella-zoster virus	Chickenpox, Herpes zoster
	Mardivirus	Marek's disease virus	
	Iltovirus	Pacheco's disease virus	
Subfamily *Betaherpesvirinae*	*Cytomegalovirus*	Human cytomegalovirus	Mononucleosis
	Muromegalovirus	Mouse cytomegalovirus	
	Roseolovirus	Human herpesvirus 6 and 7	Roseola infantum, Encephalitis
	Proboscivirus	Elephant endotheliotropic herpesvirus	
Subfamily *Gammaherpesvirinae*	*Lymphocryptovirus*	Epstein-Barr virus	Infectious mononucleosis, Burkitt's lymphoma
	Rhadinovirus	Kaposi's sarcoma-associated herpesvirus	Kaposi's sarcoma, Castleman's disease
		Murine herpesvirus 68	
		Herpesvirus saimiri	
	Macavirus	Malignant catarrhal fever virus	
	Percavirus	Equine herpesvirus 2 and 5	
Family *Alloherpesviridae*	*Ictalurivirus*	Channel catfish virus	
Family *Malacoherpesviridae*	*Ostreavirus*	Oyster herpesvirus	

Table 1.1 Classification of herpesviruses in the order of *Herpesvirales*, with examples of viruses for each genus. The eight human herpesviruses are in red. Adapted from Davison *et al.* 2009.

arrangement, and relatedness of important viral proteins (Pellet and Roizman 2007). Recently this led to a revision of the herpesvirus classification by the Herpesvirus Study Group of the International Committee on Taxonomy of Viruses (ICTV). A new order, the *Herpesvirales*, was established which includes three virus families (Table 1.1): the *Herpesviridae* (the herpesviruses of mammals, birds and reptiles, still under three subfamilies), the *Alloherpesviridae* (fish and frog viruses), and the *Malacoherpesviridae* (bivalve viruses) (Davison *et al.* 2009). Subsequent chapters will focus on the family *Herpesviridae.*

1.1.1.1. Alphaherpesvirinae

The alphaherpesvirus subfamily includes the genera *Simplexvirus* (e.g. Herpes simplex virus 1 and 2 (HSV-1 and HSV-2)), *Varicellovirus* (e.g. Varicella-zoster virus (VZV)), *Mardivirus* (e.g. Marek's disease virus (MDV)) and *Iltovirus* (e.g. Pacheco's disease virus (PDV)). The alphaherpesviruses have a variable host range and relatively short replication cycle with rapid spread in culture, leading to efficient destruction of the host cell. These viruses establish latency primarily but not exclusively in sensory ganglia (Pellet and Roizman 2007). MDV is different from the other alphaherpesviruses in that it establishes latency in T-cells and causes T-cell lymphoma (Osterrieder *et al.* 2006).

1.1.1.2. Betaherpesvirinae

The betaherpesvirus subfamily consists of genetically diverse viruses in the genera *Cytomegalovirus* (e.g. Human cytomegalovirus (HCMV)), *Muromegalovirus* (e.g. Mouse cytomegalovirus (MCMV)), *Roseolovirus* (Human herpesvirus 6 and 7 (HHV-6 and HHV-7)), and *Proboscivirus* (Elephant endotheliotropic herpesvirus). These viruses exhibit restricted host range and have a long replication cycle and slow replication in cell culture. Infection of cells often leads to the characteristic cytomegalia, enlargement of the cell. The betaherpesviruses can persist in mononuclear cells, salivary glands, kidneys and other tissues (Mocarski *et al.* 2007).

1.1.1.3. Gammaherpesvirinae

The members of the gammaherpesvirus subfamily are characterised by having a narrow host range both in terms of the cell type and the host species they infect.

In vitro work is limited as the viruses have varied ability to replicate in cultured cells, with only some of the viruses being able to undergo lytic replication in epithelial and fibroblast cell lines. The gammaherpesviruses have slow replication cycles and establish latency in lymphocytes. These viruses are often associated with lymphoproliferative disease. This subfamily includes the genera *Lymphocryptovirus* (e.g. Epstein-Barr virus (EBV)), *Rhadinovirus* (e.g. Kaposi's sarcoma-associated herpesvirus (KSHV), Murine gammaherpesvirus 68 (MHV-68) and Herpesvirus saimiri (HVS)), *Macavirus* (e.g. Malignant catarrhal fever virus) and *Percavirus* (e.g. Equine herpesvirus 2 and 5).

1.1.2. Herpesvirus structure

The herpesvirus virions consist of four distinct structures: the core, capsid, tegument and envelope (Figure 1.1). The core containing the linear double stranded (ds) DNA genome is found within an icosahedral (triangulation number T=16) capsid, 100nm in diameter, composed of 162 capsomeres (150 hexons and 12 pentons) (Pellet and Roizman 2007). The capsid consists of five conserved proteins: the major capsid protein, the triplex monomer and dimer proteins, the small capsomer-interacting protein and the portal protein (Mettenleiter *et al.* 2006). The capsid is surrounded by the tegument, an amorphous layer consisting of several proteins both viral and cellular, that links the capsid and the envelope, the outer layer of the virion made up of host-cell derived lipid membranes containing viral proteins and glycoproteins of varying numbers. Herpesvirus virions vary in size from 120 to 260nm; partly because of the variability of the thickness of the tegument (Pellet and Roizman 2007).

The virions contain a varying number of viral and host proteins with between 14 and 71 viral proteins and up to 71 host proteins identified. Several herpesvirus virions have also been reported to include viral and cellular messenger RNAs (mRNAs), both through apparent selective (Bechtel *et al.* 2005; Bresnahan and Shenk 2000; Cliffe *et al.* 2009b; Sciortino *et al.* 2001) and non-selective uptake (Greijer *et al.* 2000; Terhune *et al.* 2004). In addition to mRNAs, non-coding RNAs have been found to be present in herpesvirus virions; the non-coding the polyadenylated nuclear (PAN) RNA in KSHV virions (Bechtel *et al.* 2005) and viral tRNAs (vtRNAs) in

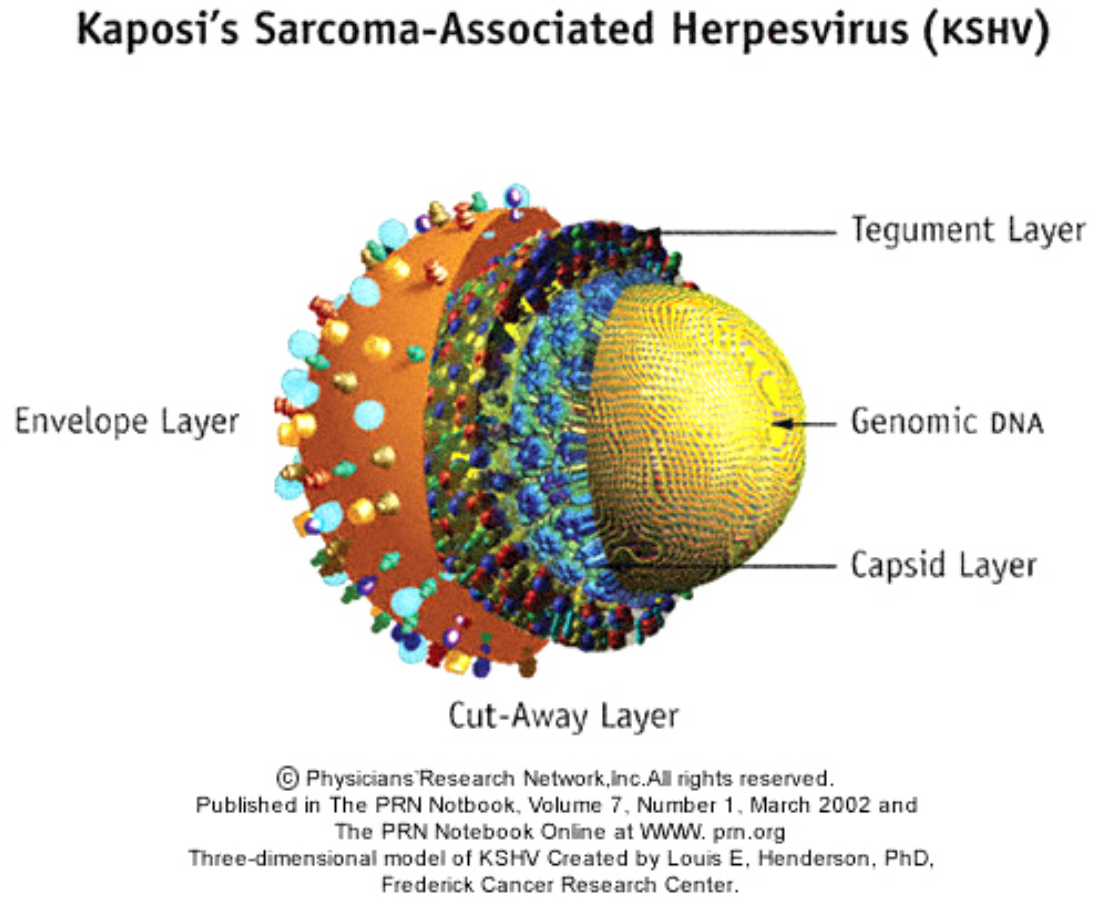

Figure 1.1 The structure of the KSHV virion, used as a representation of a typical herpesvirus virion. Showing the four distinct structures: the core, capsid, tegument and envelope. Taken from PRN Notebook; www.prn.org

MHV-68 virions (Cliffe *et al.* 2009b). The reason for the presence of viral and host proteins and RNAs in the virion is not clear. Packaging them in the virion would mean that they are available for the virus immediately following infection of the cell, facilitating the takeover of the cell. Alternatively, they may have a structural role in the virion, perhaps by forming the tegument.

1.1.3. Herpesvirus genome

Genomes of the *Herpesviridae* consist of large, linear, dsDNA ranging from 124 kbp (Simian VZV) to 241 kbp (Chimpanzee CMV); however, upon entry into the cell the DNA circularises forming an episome. The genomes also have great variation in nucleotide composition with the G+C content varying from 31% to 77%. The herpesvirus genomes can be divided into six groups based on the presence and localisation of internal and terminal repeat regions (A-F, Figure 1.2) (Pellet and Roizman 2007). The variation in genome lengths of the viruses is the result of varying copy numbers of the terminal and internal repeats.

The majority of herpesvirus genomes encode between 70 and 200 open reading frames (ORFs). A typical ORF is flanked by 5' and 3' non-translated sequences of 30 to 300 bp and 10 to 30 bp respectively, with a polyadenylation signal at the 3' end. The transcription initiation site is 20 to 25 bp downstream of a TATA box, which is 50 to 200 bp downstream of the promoter and regulatory sequences (Pellet and Roizman 2007). The majority of genes are transcribed by RNA polymerase II; however, a few genes such as the EBV encoded small RNAs (EBERs) of EBV are transcribed by RNA polymerase III. Most genes are not spliced and beta- and gammaherpesviruses have more intron-containing genes than alphaherpesviruses (McGeoch *et al.* 2006).

The number of predicted ORFs is most likely an underestimation since the herpesvirus genomes are complex with alternative splicing, translational frame shifting, and antisense and overlapping ORFs. It is common for herpesvirus genomes to have clusters of genes overlapping at the 3' end and sharing a polyadenylation site, leading to 3' co-terminal transcripts. The coding regions of these genes usually do not overlap by more than a few codons (Pellet and Roizman 2007). The herpesvirus genomes also encode a great variety of non-coding RNAs, for example the

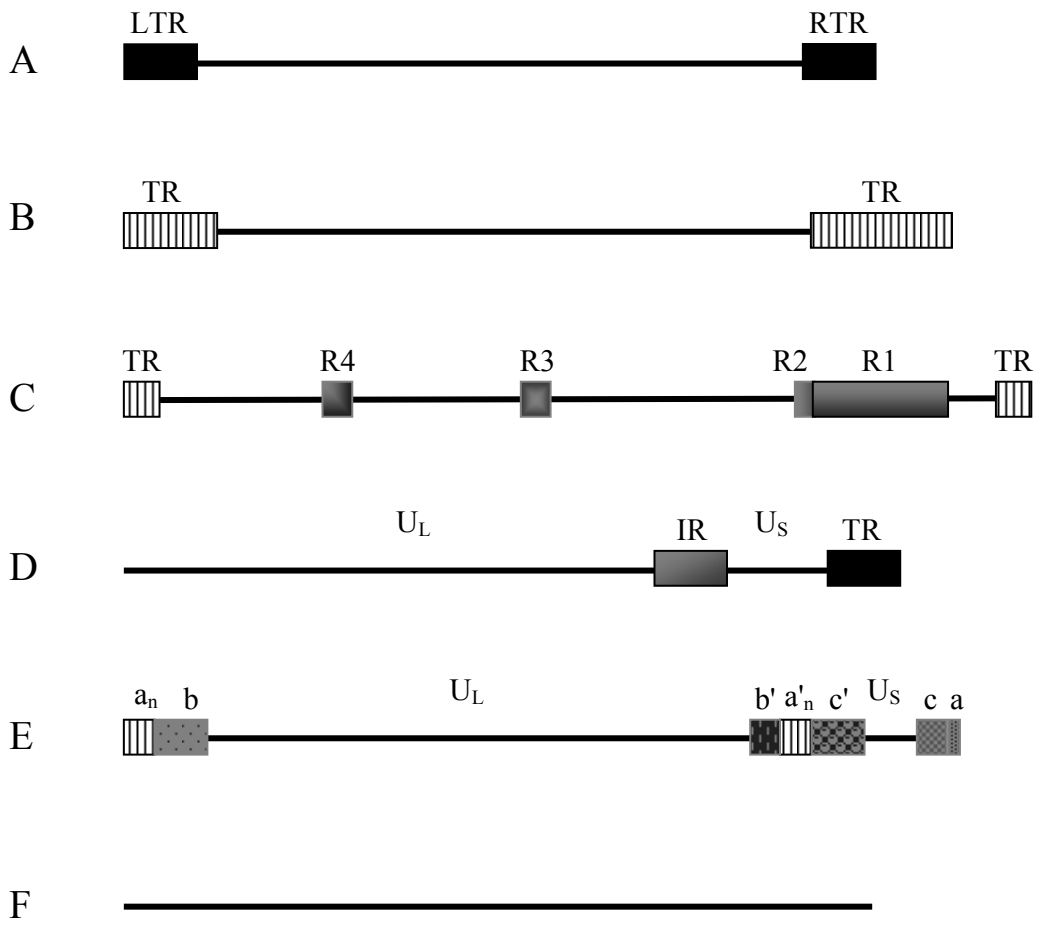

Figure 1.2 The genome organisations for the different classes of herpesviruses (A-F). Group A viruses (e.g. HHV-6) have large sequences of terminal repeats at each end (LTR and RTR). Members of group B (e.g. HVS) also have two terminal repeats (TR); however, these have a varying copy number of repeats at each end. Group C viruses (e.g. EBV) have shorter terminal repeats, but also have internal repeats (IR1-IR4) in the unique region of the genome. In group D viruses (e.g. VZV) the terminal repeat is repeated in the reverse orientation within the unique region of the genome, dividing the genome into the unique long (U_L) and unique short (U_S) region. The short region can invert relative to the large sequence, allowing for two different isomers. The terminuses of group E viruses (e.g. HSV and HCMV) consist of two parts. On one end there is a repeat sequence (a) of varying copy number next to a larger sequence (b). The other end has one copy of the a sequence next to a repeat sequence (c). These terminal ab and ca sequences are found inverted in the unique region (b'a'_nc'), separating the genome into the unique long (U_L) and unique short (U_S) regions. In group E viruses both the U_L and U_S can be inverted, creating the possibility of four isomers of the virus. Group F viruses (e.g. tupaia herpesvirus) do not have any terminal or internal repeats. Adapted from Pellet and Roizman 2007.

latency-associated transcript (LAT) of HSV, EBERs of EBV, PAN RNA of KSHV and vtRNAs of MHV-68. In addition, all herpesviruses examined to date encode microRNAs (miRNAs).

Most herpesvirus proteins have several different functions. They can be divided into structural proteins that make up the virion particle and non-structural proteins that are necessary for viral replication. There are 43 core genes that are conserved between the alpha-, beta- and gammaherpesviruses that make up seven core gene blocks containing two to 12 genes (Figure 1.3). Within each gene block the gene order and orientation is conserved (Pellet and Roizman 2007). Between the family members the order and orientations of the gene blocks vary; however, between members of the same subfamily it is usually conserved. Most of the core genes are involved in the lytic replication of the virus (McGeoch *et al.* 2006). Gene conservation also exists at the subfamily level; betaherpesviruses encode a block of 14 genes that are unique to that subfamily. Herpesvirus genomes also contain cellular homologues captured from host DNA relatively recently; KSHV expresses at least 12 cellular homologues (Choi *et al.* 2001). These proteins have either kept their cellular function, allowing the virus to produce it when needed, or have been modified to alter their function. Many of the captured genes are involved in regulation of host cell defences (McGeoch *et al.* 2006).

1.1.4. Herpesvirus life cycle

The viral life cycle involves two different stages: the lytic stage with viral replication and production of virions, and the latent stage where the viral DNA persists in the cell as an episome with no production of virions and expression of only a few genes. The lytic life cycle can be divided into four different stages: entry of the virus into the cell, viral gene expression, replication of viral DNA and assembly and egress of virus particles. The viral life cycle of HSV-1 is extensively studied and as such the herpesvirus life cycle is described below as it is known for HSV-1.

1.1.4.1. Entry

The first step of virus entry into the host cell, the attachment, involves a reversible binding of virion glycoproteins to a receptor, in most cases to cell surface

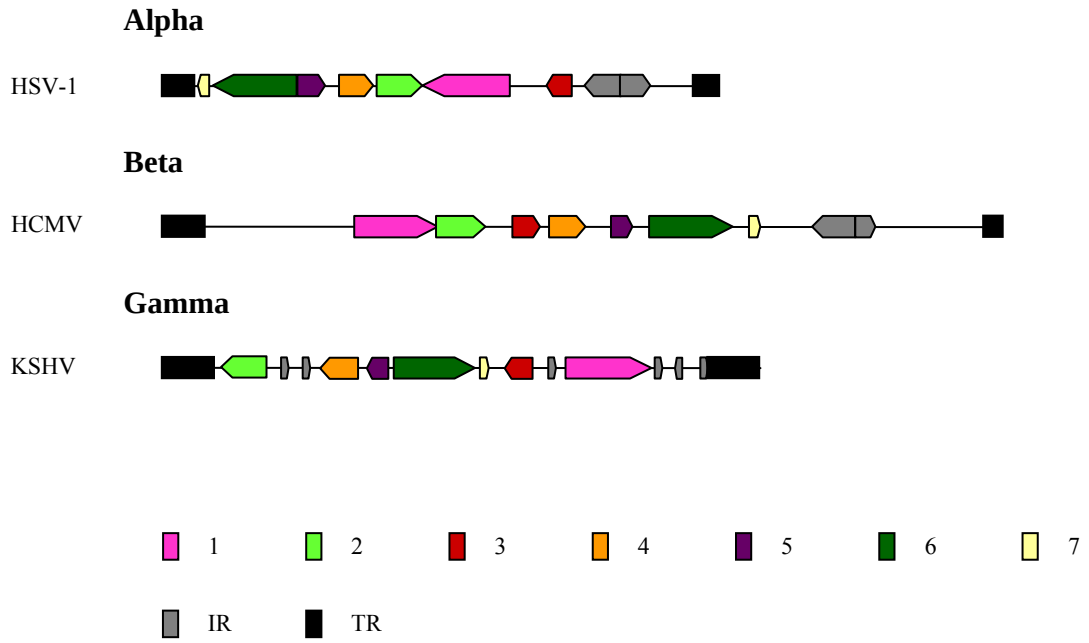

Figure 1.3 The arrangement of core gene blocks of the three herpesvirus subfamilies. There are 43 core genes in seven gene blocks. The gene order and orientation within the gene blocks is conserved; however, between the different subfamilies the orientation and order of gene blocks vary. Within the same subfamily the order and orientation of gene blocks is usually conserved. Abbreviations; Terminal repeats, TR; internal repeats, IR. Adapted from Pellet and Roizman 2007.

glycosaminoglycans (GAGs). In the case of HSV-1 the virion glycoprotein C (gC) and/or gB bind to the heparin sulphate of the cell surface proteoglycans (HSPGs) (Herold *et al.* 1991; Herold *et al.* 1994; Shieh *et al.* 1992). This first attachment step does not seem to be necessary for infection; however, it leads to an increased efficiency (reviewed in Spear and Longnecker 2003).

Following attachment the virions enter the cell by fusion of the virion envelope with a cell membrane, promoting uptake of the virion by fusion or endocytosis. Three glycoproteins seem to be essential for herpesvirus entry: gB, gH and gL; although additional virus specific receptor-binding glycoproteins may be necessary. HSV-1 entry initiates with the irreversible binding of gD to one of three classes of receptors: nectins-1 or -2, herpesvirus entry mediator (HVEM) or heparin sulphate specifically modified by 3-0-sulfotransferases (3-OS-HS) (Geraghty *et al.* 1998; Montgomery *et al.* 1996; Shukla *et al.* 1999; Warner *et al.* 1998). The binding of gD to its receptor promotes a conformation change that allows gD binding to gB and gH/gL which is sufficient to enable fusion of the membranes (Pertel *et al.* 2001; Turner *et al.* 1998).

Binding to different co-receptors enables the viruses to infect a variety of cell types and also allows the viruses to exhibit different cellular tropism during different stages of infection. A good example is EBV which only needs gB and gH/gL to infect epithelial cells, but requires glycoprotein 42 (gp42) binding to major histocompatibility complex (MHC) class II to allow entry into B-cells. Virions released by B-cells have very little gp42 which lead them to infect epithelial cells, while virions released by epithelial cells have more gp42 and infect B-cells (Heldwein and Krummenacher 2008).

Following fusion with the plasma membrane and de-envelopment of the virion the HSV capsid and tegument are released into the cytoplasm. Some of the tegument proteins remain in the cytoplasm, such as virion host shut off protein which causes degradation of host mRNA. Other proteins, like VP1-2, follow the capsid to the nuclear pore; whereas VP16, which is involved in viral gene expression, localises to the nucleus on its own. The capsid is transported to the nucleus along microtubules where the viral DNA enters via nuclear pores, circularises, and localises to nuclear domain 10 (ND-10) sites (Roizman *et al.* 2007).

1.1.4.2. Gene expression

The host RNA polymerase II transcribes the viral DNA in the nucleus with protein synthesis taking place in the cytoplasm. The expression of lytic viral genes takes place in a highly regulated cascade fashion, with the genes being classed as α/immediately-early, β/early or γ/late genes (Honess and Roizman 1974). The α genes are expressed very soon following infection in the absence of *de novo* viral protein synthesis. During HSV-1 infection the tegument protein VP16 acts as a transactivator of α genes and promotes active chromatin on the α gene promoters, enabling transcription of six α genes (ICP0, 4, 22, 27, 47 and $U_S1.5$) (Roizman *et al.* 2007). Five of these proteins can promote β gene expression, which requires α gene expression but not viral DNA replication (Honess and Roizman 1974). The β proteins are involved in replication of viral DNA (e.g. DNA polymerase) and nucleotide metabolism (e.g. thymidine kinase), and can be further subgrouped into β_1 and β_2 proteins depending on the time of their expression (Roizman *et al.* 2007). The γ proteins are dependent on viral protein expression and are either stimulated by (γ_1 genes) or dependent on (γ_2 genes) DNA replication (Roizman *et al.* 2007). These proteins are mainly structural proteins that make up the virion.

1.1.4.3. Replication

Several of the β proteins, the DNA replication proteins, localise with viral DNA near ND-10 sites and assemble DNA replication complexes in prereplicative sites (Roizman *et al.* 2007). DNA synthesis initiates on the circular molecule with the binding of the origin binding protein and the single stranded DNA (ssDNA) binding protein to the origin sequence, followed by the recruitment of the helicase-primase proteins and viral polymerase complex. Seven viral proteins are necessary for viral DNA synthesis. Even though the replication starts in the theta replicative form it soon switches to a rolling circle replication producing long continuous DNA, concatemeric molecules (reviewed in Boehmer and Lehman 1997). As replication progresses the prereplicative sites become replication compartments that enlarge and eventually fill the nucleus (Quinlan *et al.* 1984). The concatemeric DNA is cleaved

in genome length molecules and packaged into empty capsids (Boehmer and Lehman 1997).

1.1.4.4. Assembly and egress

Following their synthesis in the cytoplasm the γ structural proteins localise to the nucleus where the capsid assembly takes place. The five conserved capsid proteins (section 1.1.2) are assembled around a scaffold which is cleaved and removed as the viral DNA is packaged through the portal complex. Proteins required for cleavage and encapsidation are also conserved among the herpesviruses (Mettenleiter *et al.* 2009).

There are three models of how virion envelopment and egress takes place, as reviewed in Roizman *et al.* 2007. In the first model the capsids are enveloped at the inner nuclear membrane and transported to the plasma membrane in perinuclear vesicles which fuse with the membrane releasing the virions. The second model proposes that the capsid envelopes at the inner nuclear membrane, deenvelops through fusion with the outer nuclear membrane and reenvelopes at cytoplasmic membranes, possibly of the trans-Golgi network or endosomal, by budding into vesicles. The third model suggests that the majority of virions exit the nucleus through the nuclear pores and are enveloped at cytoplasmic membranes, while a minority of virus follow the route of the first model.

The tegument is obtained through a complex network of protein-protein interactions forming an inner capsid-associated and an outer envelope-associated tegument. The enveloped virions exit the cell by transportation of the vesicle to the cell surface and fusion of the vesicle with the cell membranes, releasing the virions into the extracellular space (Mettenleiter *et al.* 2009).

1.1.4.5. Latency

Herpesviruses are able to remain latent in the host with the possibility of reactivation at a later stage. During latency the virus genome circularises and associates with nucleosomes; hence chromosome organisation is important for the establishment and maintenance of latency by determining which genes are active (Knipe and Cliffe 2008; Tempera and Lieberman 2009). The different herpesviruses differ in their

preferred cell type for latency and the mechanisms for latency do not seem to be conserved, with no common pattern of gene expression. Some viruses have a very limited gene expression during latency; LAT is the only abundant transcript during HSV-1 latent infection (Stevens *et al.* 1987). In contrast EBV encodes several proteins during latency with various patterns of gene expression observed.

1.2. Gammaherpesviruses

Gammaherpesviruses undergo productive replication in epithelial cells and usually establish latency in lymphocytes. The latently infected lymphocytes have the ability to reactivate and infect nearby epithelial cells, allowing spread of the viruses to non-infected individuals (Pellet and Roizman 2007). The gammaherpesvirus subfamily includes the genera *Lymphocryptovirus*, *Rhadinovirus, Macavirus* and *Percavirus* (Table 1.1). The two human gammaherpesviruses, EBV and KSHV, belong to the *Lymphocryptovirus* and *Rhadinovirus* genera respectively. The Rhadinoviruses also include the well studied HVS, which causes T-cell lymphomas in new world primates, and MHV-68. The genus *Macavirus* includes the veterinary important Ovine herpesvirus 2 and Alcelaphine herpesvirus 1, which are non-pathogenic in their hosts, sheep and wildebeest respectively, but cause malignant catarrhal fever in other species (Davison *et al.* 2009).

1.2.1. Epstein-Barr virus

EBV was discovered in 1964 by Epstein, Achong and Barr, through electron microscopy of cultures from Burkitt's lymphoma (BL) tissue (Epstein *et al.* 1964). Four years later EBV was identified as the causative agent of infectious mononucleosis (IM), a self-limiting lymphoproliferative disease (Henle *et al.* 1968). As the first candidate human tumour virus EBV has since been associated with several cancers, such as nasopharyngeal carcinoma (NPC), non-Hodgkin's lymphoma, oral hairy leukoplakia, T-cell lymphomas and Hodgkin's lymphoma (HL) (Cohen 2000; Weiss *et al.* 1987; Ziegler *et al.* 1982; zur Hausen *et al.* 1970). EBV is an ubiquitous virus infecting over 90% of the human adult population persisting for life, in most cases causing no disease (Rickinson and Kieff 2007). In the developing world the majority of infections occur within the first three years of

life. In the developed world 50% of children have not been infected by the age of 10, delaying the primary infection to adolescence (Rickinson and Kieff 2007), which leads to a 25% risk of developing IM (Crawford *et al.* 2006).

The EBV genome is a 184 kbp long group C genome (Figure 1.2) with four internal repeats within the unique part of the genome, and encodes nearly 100 proteins. There are two subtypes of EBV, EBV-1 and EBV-2, which share extensive homology but differ in the regions encoding the EBV nuclear antigens (EBNAs) (Kieff and Rickinson 2007).

EBV has a very restricted host range and efficient infection *in vitro* is restricted to primary human B lymphocytes. Infection of these cells leads to transformation of the cells resulting in lymphoblastoid cell lines. Lytic infection *in vitro* is usually studied by inducing latently infected B-cells to reactivate and allow lytic replication (Kieff and Rickinson 2007).

1.2.1.1. EBV latency

EBV expresses a restricted subset of genes during latent infection, with different patterns for gene expression observed (Table 1.2) (Kerr *et al.* 1992). These viral genes are six viral nuclear antigens (EBNA-1, -2, -3A, -3B, -3C, and –LP), three membrane proteins (LMP-1, -2A, -2B), the viral bcl-2 homologue (BHRF1), EBERs, several spliced transcripts from the BamA rightward transcripts (BARTs) and miRNAs (Kelly *et al.* 2009; Kieff and Rickinson 2007). These gene products work to maintain the latent infection and to immortalise the B-lymphocytes (Kieff and Rickinson 2007).

The virus establishes latency in resting memory B-cells (Babcock *et al.* 1998; Miyashita *et al.* 1997). How it enters these cells is debated. In the main model EBV infects naïve tonsillar B-cells and drive the cells into memory cells by changing the gene expression pattern (program) to mimic physiologic antigen driven differentiation of the B-cell (Babcock *et al.* 2000). Thus, the infected naïve tonsillar B-cells express the growth program driving the cells to undergo proliferation, while a switch to the default program causes the cells to pass through germinal centres and mature into memory B-cells, at which point the cells shut down the protein expression and enter the latency program (Thorley-Lawson and Gross 2004). This is

Latency program	Genes expressed	Disease examples
Growth	EBNA-1, 2, 3A-C, LP; LMP1-, 2A, 2B; BHRF1; EBERs; BARTs	Posttransplantation lymphoproliferative disease
Default	EBNA-1; LMP-1, LMP-2A; EBERs; BARTs	Hodgkin's lymphoma, Nasopharyngeal carcinoma
Latency	EBNA-1; LMP-2 (in dividing cells); EBERs; BARTs	Burkitt's lymphoma

Table 1.2 EBV gene expression pattern during latent infection and associated diseases. Abbreviations: EBNA, EBV-encoded nuclear antigen; LMP, Latent membrane protein; EBERs, EBV-encoded RNAs; BARTs, *Bam A* rightward transcripts. BHRF1 encodes the vbcl-2.

supported by the findings that the only type of B-cell expressing the growth program in the tonsil is the naïve B-cell, while germinal-centre and tonsillar memory B-cells express the default program and peripheral memory cells the latency program (Babcock *et al.* 2000; Joseph *et al.* 2000). The memory B-cells circulate between the peripheral blood and the tonsils in the latency program, expressing EBNA-1 and possibly LMP2 during cells division (Young and Rickinson 2004). Since memory B-cells rarely die and viral protein production is at a minimal, avoiding detection by the immune response, the virus can persist for a long time. Occasionally the memory B-cell may receive plasma cell signals activating lytic virus production, allowing spread of virus to nearby epithelial cells in mucosal sites and cause shedding of virus (Rickinson and Kieff 2007). Other programmes of latency have also been described; around 15% of BLs express the Wp-restricted latency program, characterised by EBNA-1, -3A, -3B, -3C, -LP, and BHRF1 expression, with the genome lacking EBNA2 (Kelly *et al.* 2009).

1.2.1.1.1. Latency transcripts

The EBV-encoded nuclear antigens

EBNA-1: EBNA-1 is essential for the maintenance and replication of the EBV episome in dividing cells, binding to the plasmid origin of replication, *ori*P (Rawlins *et al.* 1985; Yates *et al.* 1984). During cell division it tethers the episome to the chromosome ensuring even distribution of viral genomes (Kanda *et al.* 2001). EBNA-1 can also act as a transcriptional activator of the EBNAs and LMP-1 (Young and Rickinson 2004). It avoids $CD8^+$ T-cell recognition by inhibiting its own translation, through a glycine-alanine repeat sequence that is thought to delay translation initiation, but since it simultaneously blocks degradation the levels of EBNA-1 remain stable (Apcher *et al.* 2009; Yin *et al.* 2003).

EBNA-2: EBNA-2 is essential for transformation of B-lymphocytes (Cohen *et al.* 1989). It up-regulates the viral latency genes, as well as several cellular proteins, through interactions with the DNA binding protein RBP-Jκ (Kieff and Rickinson 2007).

EBNA-3: The EBNA-3 family of proteins also regulate protein expression. They modulate the EBNA-2-mediated up-regulation of viral and cellular genes by competing with EBNA-2 for RBP-Jκ binding (Kieff and Rickinson 2007).

EBNA-LP: EBNA-LP is transcribed with EBNA-2 at the start of infection and interacts with EBNA-2 to up-regulate viral and cellular genes (Harada and Kieff 1997).

The EBV-encoded latent membrane proteins

LMP-1: LMP-1 is the main EBV transforming protein, functioning as a constitutively activated member of the TNF receptor family (Mosialos *et al.* 1995). It activates several signalling pathways, including nuclear factor κB (NFκB), by mimicking the functions of the B-cell receptor CD40; thereby driving cell growth and differentiation (Uchida *et al.* 1999), and up-regulating cell-surface adhesion molecules, anti-apoptotic proteins and cytokines (Young and Rickinson 2004).

LMP-2: LMP-2A inhibits EBV reactivation from latency in B-lymphocytes by blocking B-cell receptor signal transduction by interacting with the tyrosine kinases (Miller *et al.* 1994). It also provides survival signals by providing surrogate B-cell receptor signalling (Caldwell *et al.* 1998). LMP-2B is reported to negatively regulate the function of LMP-2A (Rechsteiner *et al.* 2008).

BHRF1

vbcl-2: The viral bcl-2 homologue was recently shown to be expressed during the growth programme of latency and the Wp-restricted latency found in around 15% of BLs (Kelly *et al.* 2009). This protein has anti-apoptotic properties and protects the BL cells from cell death (Watanabe *et al.* 2009).

EBV-encoded RNAs

EBERs: These non-polyadenylated small non-coding RNAs are the most abundant EBV RNAs in latently infected cells and have been found to interact with several proteins. These will be discussed further in section 1.4.1.2.1.

Bam A rightward transcripts

BARTs: The BARTs is a set of alternatively spliced transcripts expressed during both lytic and latent infection containing several possible ORFs; however, the protein

products have not been detected. The introns of BART encode miRNAs, which will be discussed in chapter 1.4.3.

1.2.1.2. EBV infection and associated diseases

EBV is spread by oral secretions and infects cells of the oropharynx of naïve individuals. Whether these cells are B-lymphocytes or epithelial cells is still debated; perhaps it is a co-operation where binding of EBV to the B-cell aids entry into epithelial cells (Rickinson and Kieff 2007). The virus enters the memory B-cell pool as previously described and the EBV infection is brought under control by humoral and cell mediated responses, with natural killer (NK) cells and $CD4^+$ and $CD8^+$ cytotoxic T-cells playing an important part (Cohen 2000).

Whereas most EBV infections are asymptomatic some do cause diseases such as IM. IM is usually cleared by immunocompetent individuals after a few weeks; however, can cause severe problems in immunosuppressed individuals. In addition, EBV is associated with three lymphoid tumours of B-cell origin: B-lymphoproliferative disease in the immunocompromised hosts, Burkitt's lymphoma and Hodgkin's lymphoma; as well as other tumours such as nasopharyngeal carcinoma.

Infectious mononucleosis

IM usually occurs during primary EBV infection of young adults with 25% developing IM (Crawford *et al.* 2006). The reason for this age difference is not known; however, it may be related to the viral dose and the host immune response (Rickinson and Kieff 2007). The symptoms include fever, sore throat, swollen and enlarged lymph glands, and fatigue. IM is thought to be an immunopathological disease where the symptoms arise from an exaggerated $CD8^+$ cytotoxic T-cell response that results in an increased cytokine release (Williams and Crawford 2006).

Posttransplantation lymphoproliferative disease

EBV can also cause disease in people with acquired T-cell deficiencies, for example people on immunosuppressant therapy following transplantations. Between 0.5% and 30% of transplant recipients develop Posttransplantation lymphoproliferative disease (PTLD) as a result of immunosuppressive therapy (Thompson and Kurzrock 2004). This is a heterogeneous collection of disorders which results from an uncontrolled expansion of B-lymphocytes. The risk factors include the degree of

immunosuppressive therapy and primary EBV infection; those that undergo primary infection during the immunosuppression have a higher risk of PTLD (Crawford 2001). Around 90% of tumours are EBV infected and most cells express the growth program. The reason for development of PTLD is not clear; however, it is possible that the impaired T-cell response fails to eliminate EBV infected proliferating abnormal cells or directly infected memory cells (Thorley-Lawson and Gross 2004).

Burkitt's lymphoma

BL first described by Burkitt in 1958 as a tumour in the jaw of children in equatorial Africa (Burkitt 1958) is the most common childhood cancer in this area. These endemic cases of BL are prevalent in areas of holoendemic malaria in Africa and New Guinea, and 96% are associated with EBV. The association of EBV with BL in other parts of the world (sporadic BL) is however lower, ranging from 50-70% in some parts of the world and around 20% in North America and Europe (Crawford 2001). BL is also common in human immunodeficiency virus (HIV) infected individuals where EBV is found in 30-40% of BL tumours (Rickinson and Kieff 2007).

All BL tumours carry one of three chromosomal translocations that brings the c-*myc* oncogene under the influence of the immunoglobulin (Ig) heavy- or light-chain genes, leading to its dysregulation (Klein 1983). This over-expression of c-*myc* drives the cell to proliferate and inhibits its differentiation, and even though this over-expression is not sufficient for BL development it seems to be necessary (Bornkamm 2009). The majority of EBV-positive tumours are germinal centre cells that contain EBV clonal genomes expressing the latency program, indicating that EBV infection occurs prior to translocation (Bornkamm 2009; Thorley-Lawson and Gross 2004).

In endemic BL at least three factors co-operate to cause BL, these include malaria, EBV and c-*myc* translocation (reviewed in Crawford 2001; Thompson and Kurzrock 2004). EBV is thought to promote survival of the B-cell, perhaps by inhibiting apoptosis, and avoids detection by the immune system by only expressing EBNA-1 (Bornkamm 2009).

Hodgkin's lymphoma

HL accounts for around 20% of all lymphomas in the western world. In these tumours the malignant cells, large mono- or multinuclear Reed-Sternberg cells (RBC) and Hodgkin's cells, make up a minority of cells (1-2%) with a heavy inflammatory infiltrate of reactive mononuclear cells making up the rest of the tumour (Crawford 2001). Activation of the NFκB-signalling pathway has been suggested as a possible cause of HL (Staudt 2000).

The association of EBV with HL was confirmed when clonal EBV DNA was detected in tumour cells (Weiss *et al.* 1987) and later also in RSCs (Wu *et al.* 1990). These EBV positive cells express the default program of latent gene expression (Table 1.2). The EBV association varies depending on the type of tumour, geographical location, and age; ranging from 40-50% in developed countries up to almost 100% in cases in South America (Crawford 2001).

RSCs contain hypermutated Ig genes and are believed to be B-cells that have arrested at the centrocyte stage during B-cell differentiation in the germinal centre and do not express IgG molecules. These abnormal B-cells would normally be prone to apoptosis; however, it is possible that EBV provides survival signals keeping the cells alive and proliferating (Andersson 2006; Crawford 2001). LMP-1 mimics CD40 replacing the T-cell signal needed during memory cell selection (Uchida *et al.* 1999), while LMP-2A mimics B-cell receptor signalling from surface Ig, replacing antigen binding (Caldwell *et al.* 1998). LMP-1 also activates NFκB (Hammarskjold and Simurda 1992), indicating that both EBV- positive and negative tumours may use the same pathway to induce HL. One hypothesis is that EBV associated HL occurs when a mutation in a germinal centre B-cell prevents its differentiation. If this cell is infected with EBV it will express LMP-1 and LMP-2, promoting survival and proliferation; thus enhancing tumour growth.

Nasopharyngeal carcinoma

NPC is a tumour of squamous epithelium of the post-nasal space common in southern China, south-east Asia, north Africa and among Inuits in Alaska and Greenland, but rare in the rest of the world. The tumour is more common in men than in women and in southern China it is the most common malignancy in men and second commonest in women (Crawford 2001). NPC can be divided into different

types depending on the level of differentiation of the tumour cells; 70% are classed as undifferentiated and 100% of these tumours are associated with EBV. These tumours are made up of undifferentiated carcinoma cells and a lymphocyte infiltrate, with clonal EBV genomes present only in the epithelial cells expressing the default latency program (Table 1.2) (Brooks *et al.* 1992; Young and Rickinson 2004). Nasopharyngeal epithelial cells do not usually contain EBV, which has led to a model where the genetic events of NCP occur early in the pathogenesis and makes the epithelial cells either more susceptible to EBV infection or more able to maintain the viral genome (Rickinson and Kieff 2007). EBV latent gene expression may then provide survival signals and promote tumour growth. The EBERs confer resistance to Fas-mediated apoptosis by blocking the double-stranded RNA-regulated protein kinase R (PKR) pathway in an human epithelial intestine cell line (Nanbo *et al.* 2005) and may enhance growth of NPC cells by inducing expression of insulinlike growth factor 1 (IGF-1) (Iwakiri *et al.* 2005). LMP-2 promotes the growth of epithelial cells and enhance epithelial cell migration (Rickinson and Kieff 2007). In addition, NPC cells express high levels of BARTs which encode several miRNAs that could be involved in the pathogenesis of NPC (Cai *et al.* 2006).

1.2.2. Kaposi's sarcoma-associated herpesvirus

KS was first described in 1872 by the Hungarian dermatologist Moritz Kaposi when he published the case histories of five patients with a rare idiopathic pigmentation of the skin (Kaposi 1872). Initially considered a non-aggressive disease of elderly men in the Mediterranean, it was given further attention during the emergence of the HIV pandemic in the 1980s, when KS became the most common neoplasm in patients with acquired immune deficiency syndrome (AIDS) (Beral *et al.* 1990). The finding that KS was more prevalent among patients that had acquired HIV by sexual contact than parentally suggested that KS was spread by a sexually transmitted infectious agent (Beral *et al.* 1990). In 1994 Chang *et al.* identified two short fragments from a new herpesvirus (KSHV) in AIDS associated KS tissues using representational difference analysis. These sequences were homologous to capsid and tegument genes of the gammaherpesviruses EBV and HVS (Chang *et al.* 1994).

1.2.2.1. KSHV genome

Sequencing of the viral genome further revealed that KSHV was a *Rhadinovirus* with linear dsDNA of 165 to 170 kbp made up of a central unique region of 140.5 kbp flanked by a variable number of 801 bp terminal repeat sequences (Renne *et al.* 1996; Russo *et al.* 1996). The unique region encodes at least 86 ORFs, with 66 conserved herpesvirus genes involved in virus replication and structure grouped together in gene blocks interspersed with non-conserved genes (Russo *et al.* 1996). KSHV also encodes several homologues of cellular proteins involved in DNA synthesis, cell cycle regulation, and signalling; at least 12 of these were captured from the host. These include cell-cycle regulators (e.g. vcyclin), inhibitors of apoptosis (e.g. vbcl-2 and vFLIP) and immunomodulatory proteins (e.g. vIRF-1 and vIL-6) (Moore and Chang 2001; Russo *et al.* 1996). Most of the captured genes are functionally similar to cellular genes induced by EBV infection, indicating that the two viruses use different ways of achieving the same thing. The KSHV genome also encodes miRNAs and a lytic polyadenylated non-coding RNA, PAN, that localises to the nucleus.

1.2.2.2. KSHV epidemiology

Although KSHV is found all over the world the prevalence varies significantly by geographical region. In Europe, North America, and Asia the prevalence in the general population is low, ranging from 0%-15%, and the virus is mainly spread by sexual transmission, particularly among homosexual men. In Mediterranean and Eastern European countries, where KS is more common, there is a higher prevalence ranging from 4% to 24%, while there is a very high prevalence in African regions with rates over 50%. In the latter two cases the virus is thought to spread by both sexual contact and parentally thorough saliva with infection often starting in childhood (Ganem 2007; Jenson 2003). KSHV has been divided into subtypes based on the sequence of the ORF K1. These subtypes A-H show distinct geographical distributions suggesting that KSHV is an ancient human infection with the subtypes reflecting the migration of human populations out of Africa (Boshoff and Weiss 2001; Hayward 1999).

1.2.2.3. KSHV latency

KSHV infection *in vivo* is restricted to humans making it difficult to study viral infection in the host. Most of the knowledge of KSHV latent infection comes from cultivation of primary effusion lymphoma (PEL) cell lines derived from patients with advanced AIDS. These cells are latently infected with the KSHV genome maintained as a circular episome, but following cultivation 1% to 5% of cells produce virus. This can be enhanced by treatment with chemicals or viral replication and transcription activator (rta), and thus allows for production of viral stocks and study of gene expression. However, this will not entirely represent gene expression *in vivo*. KSHV can latently infect several cell lines such as human fibroblasts, endothelial, and epithelial cells. Fibroblasts and epithelial cells have not been found to be infected *in vivo*, while B-cells, which are the site of latency *in vivo*, have been very difficult to infect *in vitro* (Ganem 2007).

During latent infection only a few of the viral genes are expressed. In PEL cells most latently expressed transcripts are expressed from a region at the far right end of the genome. Latency-associated nuclear antigen-1 (LANA-1), vcyclin and vFLIP are transcribed through a program of alternative splicing and internal translational initiation. The kaposin locus gives rise to a family of proteins; kaposin A, B, and C, as well as miRNAs (Ganem 2007). LANA-2 lies outside of this region and is a B-cell specific latency gene not expressed in KS tumours (Rivas *et al.* 2001).

It is possible that the latency expression in PEL cells gives a restricted view of KSHV latency. EBV has a complex program of latency expression and the B-cell limited expression of LANA-2 may be an indication that KSHV latency expression is more complex than thought. In addition, a large number of infected B-cells in Castleman's disease express a variety of proteins including proteins that are not classed as latent (Katano *et al.* 2000; Parravicini *et al.* 2000). It is not clear if this represents an expanded pattern of latent gene expression, or if these are cells undergoing lytic virus replication (Chang and Moore 2001).

1.2.2.3.1. Latency transcripts

Latency-associated nuclear antigen-1

LANA-1 is a large, highly immunogenic, protein expressed in all latently infected cells where it localises to the nucleus. It is a multifunctional protein with DNA replication, anti-apoptotic, cell cycle regulatory and gene regulatory functions, most of which are exerted by interactions with other proteins (Kaul *et al.* 2007). LANA-1 is essential for the establishment and maintenance of the latent viral episome in the nucleus. It activates the semiconservative replication of the episome by binding to DNA sequences within the terminal repeats; thus showing functional resemblance to EBV EBNA-1 binding to the *ori*P sequence (Grundhoff and Ganem 2003; Hu *et al.* 2002). Further, LANA-1 tethers the viral episome to host chromosomes during cell division to allow efficient segregation of the viral DNA to both daughter cells (Ballestas *et al.* 1999; Cotter and Robertson 1999). It is also involved in the regulation of several pathways affecting cell growth and survival; however, LANA-1 itself does not seem to be sufficient for transformation (Watanabe *et al.* 2003). LANA-1 up- and down-regulates a range of host and viral genes, including the latency genes, through binding to the DNA in the terminal repeats and interacting with components of the transcriptional machinery (Garber *et al.* 2001; Renne *et al.* 2001). It also inhibits lytic replication by decreasing the expression of the lytic transactivator rta and antagonising its function (Lan *et al.* 2004).

Viral cyclin

vcyclin is a homologue of the cellular protein cyclin D and acts in a similar fashion in regulating the cell cycle. It forms functional complexes with cellular cyclin-dependent kinase 6 (cdk6) which leads to phosphorylation of pRB; thus stimulating cell cycle progression (Chang *et al.* 1996). However, the viral cyclin has several differences from the cellular cyclin D. It has a wider range of substrates, such as histone H1 (Godden-Kent *et al.* 1997) and origin recognition complex 1 (Laman *et al.* 2001), suggesting that vcyclin may regulate several cell-cycle phases as well as stimulate the replication of both host and viral genome. In addition, vcyclin is able to evade the inhibitors that regulate the activity of cellular cyclin-cdk complexes (Swanton *et al.* 1997).

Viral FLIP

vFLIP is a homologue of the FLICE inhibitory protein (FLIP) and like its homologue has antiapoptotic activities; it up-regulates the antiapoptotic transcription factor NFκB by interacting with the inhibitory κB kinase complex (Liu *et al.* 2002). Since vFLIP also is a homologue of caspase 8 it may act as a functional homologue in activating the NFκB signalling pathway; thus enhancing cellular proliferation (Chugh *et al.* 2005). Activation of the NFκB signalling pathway has several effects, including inhibition of apoptosis by up-regulation of several antiapoptotic molecules (Guasparri *et al.* 2004). It also promotes latency by inhibiting the expression of rta and lytic replication (Ye *et al.* 2008; Zhao *et al.* 2007), is responsible for the spindle cell phenotype seen in KSHV infected endothelial cells (Matta *et al.* 2007) and up-regulates cytokines (Sun *et al.* 2006). vFLIP has also been shown to directly inhibit KSHV lytic gene expression by binding to lytic promoters (Matta *et al.* 2008).

Kaposins

The kaposin locus gives rise to at least three proteins by differential initiation of translation, as well as several miRNAs. Kaposin A is a transmembrane protein found to transform cultured cells and drives tumorigenesis in nude mice (Muralidhar *et al.* 1998). Kaposin A-transformed cells show enhanced activation of several serine/threonine kinase pathways, some of which are known to regulate cell proliferation (Muralidhar *et al.* 2000). It also binds cytohesin-1 activating the ERK1/2 pathway, which is thought to be important for transformation (Kliche *et al.* 2001). Kaposin B binds and activates mitogen-activated protein (MAP) kinase-associated protein kinase 2 (MK2), a target of the p38 MAP kinase signalling pathway and known inhibitor of decay of mRNAs with AU-rich elements (AREs). Kaposin B thereby increases the expression of cytokines by blocking the degradation of their mRNAs, which are usually unstable because they contain AREs (McCormick and Ganem 2005).

Latency-associated nuclear antigen-2

LANA-2, also called viral interferon regulatory factor 3 (vIRF-3), is a B-cell specific protein (Rivas *et al.* 2001) required for proliferation and survival of PEL cells (Wies *et al.* 2008). It has several functions including inhibition of apoptosis induced by p53 (Rivas *et al.* 2001) and PKR, an interferon (IFN)-regulated anti-viral product

(Esteban *et al.* 2003). It also inhibits NFκB activation (Seo *et al.* 2004), IRF-7 activity (which leads to suppression of alpha interferon (IFN-α) production and IFN-mediated immunity) (Joo *et al.* 2007), as well as virus-mediated transcriptional activation of the IFN-A promoter (Lubyova and Pitha 2000). In contrast, LANA-2 has also been shown to enhance the binding of IRF-3 and IRF-7 to IFN promoters; thus upregulating virus-mediated induction of IFN responses (Lubyova *et al.* 2004). LANA-2 has recently been found to disrupt the ND-10 sites in the nucleus and interfere with the tumour suppressor PML (Marcos-Villar *et al.* 2009).

1.2.2.4. KSHV infection and associated diseases

Primary KSHV infection is thought to be asymptomatic in most cases; however, fever and rash has been described in immunocompetent children (Andreoni *et al.* 2002). In a study of HIV-negative men mild symptoms such as fever, diarrhoea, fatigue, rash and enlarged lymph nodes was associated with primary KSHV infection; unlike primary EBV infection there were was no increase in T-lymphocyte numbers (Wang *et al.* 2001). Primary KSHV infection is brought under control by MHC class I-restricted cytotoxic T-lymphocyte responses (Osman *et al.* 1999; Wang *et al.* 2001). KSHV encodes two proteins (MIR-1 and MIR-2) that have been found to reduce cell surface MHC class I expression by increasing its endocytosis; thus enabling the virus to evade the immune response (Coscoy and Ganem 2000; Coscoy *et al.* 2001). Asymptomatic carriers harbour the virus mainly in $CD19^+$ B-cells (Ambroziak *et al.* 1995). Most people remain asymptomatic unless they acquire an immunodeficiency and severe KSHV associated disease is a rare occurrence.

1.2.2.4.1. Kaposi's sarcoma

KS lesions can occur in several tissues, but is most commonly located in the skin where it forms brownish-purple raised nodules. The disease can be divided into four epidemiological forms: classic, endemic, post-transplant or iatrogenic, and HIV- associated KS. HIV- associated KS is the most common neoplasm in patients with AIDS and in the early days KS in AIDS patients was at least 20 000 times more common than in the general population (Beral *et al.* 1990). However, the introduction of HAART (highly active anti-retroviral therapy) has resulted in a

reduction of KS in AIDS patients in the developed world (Schwartz *et al.* 2008). HIV-associated KS is extremely aggressive.

KS is not a classical tumour, but is a complex lesion made up of spindle cells, infiltrating monocytes, T-lymphocytes, plasma cells and neovascular channels. The spindle cells are the main proliferating cells of the lesion and they are thought to be endothelial cells, possibly of lymphatic origin (Ganem 2007). KSHV is necessary for the development of KS, but is not sufficient for it. Various findings support this; including the correlation of seroprevalence and KS risk and that KSHV DNA is present in all KS tumours where nearly all spindle cells are latently infected (Boshoff and Weiss 2001; Ganem 2007). Lytic replication may have an important role in KS development since ganciclovir, a drug that blocks lytic replication, reduces the occurrence of new KS tumours in patients with advanced AIDS (Martin *et al.* 1999).

1.2.2.4.2. Primary effusion lymphoma

PEL is a rare disease that occurs mainly in HIV-infected individuals with advanced AIDS and presents as a proliferation of B-cells in the body cavities lacking detectable tumour mass. PEL is a classic malignancy with clonal expansion of B-cells and every tumours cell harbours KSHV genomes as circular episomes at very high copy numbers (Boshoff and Weiss 2001). The tumour cells are often co-infected with EBV; however, PEL is not seen without KSHV infection (Ganem 2007). PEL cells express the latent proteins and viral interleukin 6 (vIL-6) (Parravicini *et al.* 2000) which might drive tumorigenesis. Both vFLIP and LANA-2 have been found to be essential for PEL cell survival *in vitro* (Guasparri *et al.* 2004; Wies *et al.* 2008).

1.2.2.4.3. Multicentric Castleman's disease

Multicentric Castleman's disease (MCD) is an aggressive, lymphoproliferative, systemic illness, resulting in sustained fever, weakness, enlarged lymph nodes and spleen (Ganem 2007). MCD occurs more frequently in AIDS patients and in these cases are always associated with KSHV, while in HIV-negative cases only 40-50% are associated with KSHV (Boshoff and Weiss 2001). MCD is a polyclonal lesion with KSHV present in plasmablasts that localise mainly to the mantle zones surrounding the germinal centres (Du *et al.* 2001; Dupin *et al.* 2000). These

plasmablasts are not present in KSHV-negative MCD. It is thought that KSHV infects naïve B-cells and drives their differentiation into plasmablasts, bypassing the germinal centre reaction (Du *et al.* 2001). The IL-6 receptor is expressed in the majority of KHSV-infected cells and vIL-6 is highly expressed in a proportion of cells, indicating that the IL-6 pathway may drive both the differentiation of KSHV infected cells and the development of lymphoproliferative lesions. The vIL-6 may also induce expression of human IL-6, and in line with this increased levels of human IL-6 have been described in patients with MCD and this is thought to be responsible for the systemic manifestation of the disease (Du *et al.* 2001). In contrast to HIV-associated KS, HIV-associated MCD does not usually resolve following HAART (Boshoff and Weiss 2001).

1.3. Murine gammaherpesvirus-68

1.3.1. Discovery and classification

MHV-68 (also known as murid herpesvirus 4; MuHV-4) was originally isolated in 1976 from bank voles together with two other viruses, MHV-60 and MHV-72, and two viruses isolated from wood mice, MHV-76 and MHV-78 (Blaskovic *et al.* 1980) These viruses are considered strains of MHV-68. The growth characteristics of the viruses in cell lines and virion structures as observed by electron microscopy led to their classification as herpesviruses (Blaskovic *et al.* 1980; Ciampor *et al.* 1981). They were further classified as part of the *Alphaherpesvirinae* based on their cytopatic effects, growth characteristics, and wide host range in different cell cultures (Svobodova *et al.* 1982a), as well as structural polypeptide similarities to HSV-1 (Stancekova *et al.* 1987). However, *in vivo* studies with MHV-68 showed a pathogenesis inconsistent with alphaherpesviruses; the mice showed no neurological disease, but severe pneumonia with widespread haematogenous viral spread with the virus replicating predominantly in lung alveolar cells (Blaskovic *et al.* 1984; Rajcani *et al.* 1985). Short nucleotide sequence analysis of the MHV-68 genome revealed that it was actually closely related to the gammaherpesviruses EBV and HVS in terms of genome organisation, content, and structure (Efstathiou *et al.* 1990a; Efstathiou *et al.* 1990b), and that the genome organisation was more similar to that of

Rhadinoviruses, e.g. HVS and KSHV. Partial and full sequencing of the MHV-68 genome further corroborated this (Mackett *et al.* 1997; Virgin *et al.* 1997).

Although MHV-68 was initially isolated from bank voles subsequent epidemiological surveys of MHV-68 infection in free-living rodents found that the virus is endemic in wood mice, striped field mouse and yellow-necked mouse, and not bank voles, suggesting that the wood mouse and related mouse species are likely to be the natural hosts (Blasdell *et al.* 2003; Ehlers *et al.* 2007). At least three other mouse herpesviruses have been reported; MHV-Brest and wood mouse herpesvirus (WMHV) are thought to be strains of the same virus species (Chastel *et al.* 1994; Hughes *et al.* 2009).

Since MHV-68 can infect mice it provides a small animal model for the study of virus-host interactions, virus pathogenesis and latency. MHV-68 can also be studied *in vitro* as it establishes productive and latent infections in several cell lines. In addition, the MHV-68 genome has been cloned into a bacterial artificial chromosome (BAC) which makes it relatively easy to generate virus mutants (Adler *et al.* 2000).

1.3.2. MHV-68 virion

The virion structure of MHV-68 as determined by electron microscopy and antigen analysis was early on found to be similar to other herpesviruses (Ciampor *et al.* 1981; Svobodova *et al.* 1982b). The sequencing of the genome revealed that MHV-68 does indeed encode homologues for several herpesvirus structural proteins (Virgin *et al.* 1997). Analysis of proteins associated with the MHV-68 virion identified a number of homologues of capsid, tegument, and envelope proteins, along with proteins not previously associated with virions, as well as cellular proteins such as annexin I, annexin II and a cytoplasmic β-actin homologue (Bortz *et al.* 2003). As described for other viruses (section 1.1.2) MHV-68 packages mRNAs, in addition to the vtRNAs (Cliffe *et al.* 2009b). The reason for the packaging of the non-coding RNAs is not known.

1.3.3. MHV-68 genome

The MHV-68 genome comprises a unique region of 118 kbp DNA with two internal repeats of 40 respectively 100 bp, flanked by terminal repeat regions made up of

variable numbers of 1.213 kbp repeat units (Efstathiou *et al.* 1990a; Virgin *et al.* 1997). The genome encodes 73 protein-coding ORFs, most of which are homologues of HVS and KSHV genes and many also of EBV genes. The genome consists of conserved herpesvirus gene blocks separated by virus specific genes and can be aligned with other Rhadinoviruses such as KSHV and HVS (Figure 1.4) (Virgin *et al.* 1997). MHV-68, like the other gammaherpesviruses, encodes a number of cellular homologues, such as vcyclin, vGPCR, and vbcl-2 (Nash *et al.* 2001; Virgin *et al.* 1997). At the left end of the genome MHV-68 encodes four genes unique to the virus, eight vtRNAs and nine miRNAs (Bowden *et al.* 1997; Pfeffer *et al.* 2005; Virgin *et al.* 1997).

1.3.4. MHV-68 life cycle

1.3.4.1. Entry

The mechanism by which MHV-68 enters the cells appears to be a complex process involving several molecules. Like other herpesviruses (1.1.4.1) the virion binds heparin sulphates via gH/gL or gp70 (Gillet *et al.* 2007a; Gillet *et al.* 2008) and entry also involves gB (Gillet and Stevenson 2007) and gp150 (Gillet *et al.* 2007a). While gH is essential for infectivity, gL is not (Gill *et al.* 2006; Gillet *et al.* 2007b). gp150 appears to have an inhibitory role, blocking heparin sulphate-independent cell binding until the virion is already bound by gH/gL or gp70 (Gillet *et al.* 2009). The MHV-68 ORF75c tegument protein is involved in moving incoming capsids to the nucleus (Gaspar *et al.* 2008). It also disrupts the ND-10 sites, like LANA-2 of KSHV (Gaspar *et al.* 2008; Ling *et al.* 2008).

1.3.4.2. Gene expression

Following entry and DNA translocation to the nucleus the expression of viral genes, like that of all herpesviruses (section 1.1.4.2), takes place in a highly regulated cascade fashion (Ebrahimi *et al.* 2003; Martinez-Guzman *et al.* 2003). Viral gene expression starts as early as three hours post infection *in vitro* (Ahn *et al.* 2002) with lytic infection in cultured fibroblasts having a similar transcription program to infected lungs of mice (Martinez-Guzman *et al.* 2003). One of the immediate early genes, ORF 50, encodes the rta which is a well conserved viral replication and

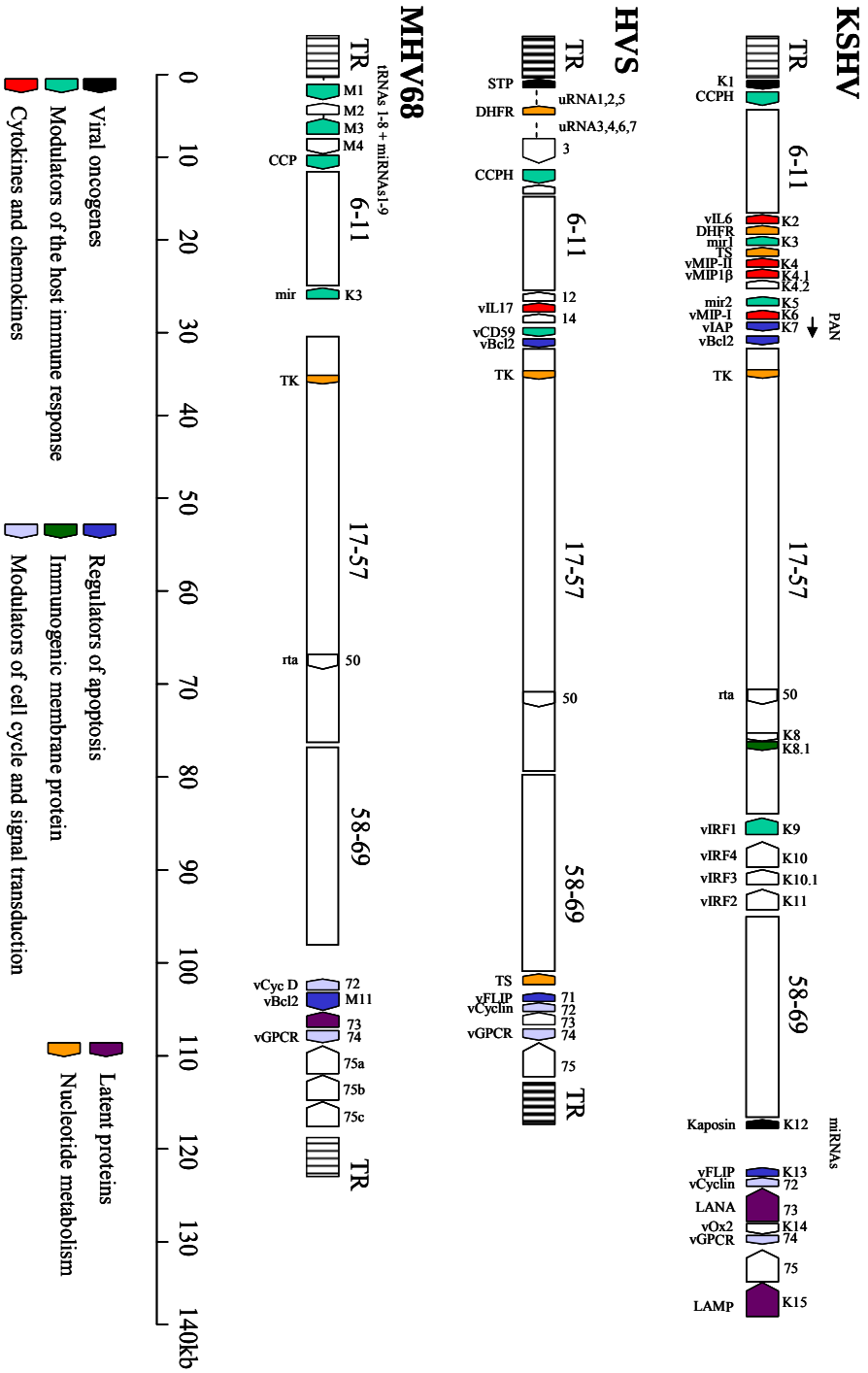

Figure 1.4 Comparing the genome of MHV-68 with that of KSHV and HVS. Open boxes represent conserved gene blocks. The orientations of additional ORFs are shown as pointed boxes. Abbreviations: CCP, Complement control protein; TK, Thymidine kinase; rta, Replication and transcription activator; vGPCR, Viral G-protein coupled receptor; STP, Simian transformation-associated protein; DHFR, Dihydrofolate reductase; TS, Thymidylate synthase; vFLIP, Viral FLICE-like inhibitory protein; LANA, Latency associated nuclear antigen; LAMP2, Latent membrane protein 2. Adapted from Nash *et al.* 2001.

transcription activator of gammaherpesviruses. The rta is essential for lytic replication, activating not only early genes but affecting all genes during both reactivation and de novo infection (Martinez-Guzman *et al.* 2003; Wu *et al.* 2001). Over-expression of rta was found to induce expression of specific lytic cycle genes, but repress the transcription of ORF 73 which is essential for establishment of latency (Hair *et al.* 2007). The mechanisms for MHV-68 rta transcription induction and repression are not known; however, the rta of KSHV has been found to activate a number of genes either through direct binding to promoter sequences or through other proteins. In addition, KSHV rta targets transcriptional suppressors for proteasomal degradation via an E3 ubiquitin ligase activity (Gould *et al.* 2009).

1.3.4.3. Viral DNA replication

MHV-68 has homologues of six of the seven herpes proteins required for viral DNA synthesis (see section 1.1.4.3)(Virgin *et al.* 1997). The seventh protein, a protein with origin binding function which differs between herpesviruses (U_L9 of HSV, Zta of EBV and K8 of KSHV), has not been found for MHV-68 (Gong *et al.* 2009). MHV-68, like KSHV, has two origins of lytic replication (*ori*Lyt) located at either end of the genome and a packaging signal in the terminal repeats (Adler *et al.* 2007; Deng *et al.* 2004). The cellular transcription factor NF-Y has recently been found to bind to the *ori*Lyt sequences and is important for MHV-68 lytic replication (Gong *et al.* 2009)

The generation of a MHV-68 BAC plasmid has simplified the construction of mutant viruses. This enabled two studies using signature-tagged mutagenesis to identify candidate viral genes involved in virus replication. In these studies 16 and 41 essential genes were identified, respectively; many of which are conserved between herpesviruses, including gB, gH, gM and rta (Moorman *et al.* 2004; Song *et al.* 2005). Further studies on individual genes, using the BAC system, have found that some of the genes (ORF 18, 24, 30 and 34) required for infectious virus production are essential for late gene expression, but dispensable for viral DNA replication (Arumugaswami *et al.* 2006; Wong *et al.* 2007; Wu *et al.* 2009). While some, like rta, are essential for both gene expression and DNA replication (Pavlova *et al.* 2003)

1.3.4.4. Assembly and egress

Following capsid assembly the virion is enveloped and released as described in section 1.1.4.4. ORF 52 and ORF33 of MHV-68 encode virion-associated tegument proteins important for envelopment and egress into the cytoplasm (Bortz *et al.* 2007; Guo *et al.* 2009). The glycoprotein gp150 is important for virus release into the extra-cellular space, but not for cell-to-cell spread which is thought to be the major spread of virus during *in vivo* infection, avoiding the host immune response (de Lima *et al.* 2004). ORF58 and gp48 are both important for cell-to-cell spread, with ORF58 transporting gp48 to the cell surface where it induces outgrowths of actin-based membrane projections to create intercellular networks for virion spread (Gill *et al.* 2008; May *et al.* 2005b; May *et al.* 2005a).

1.3.5. MHV-68 primary infection

MHV-68 infection *in vivo* is studied by intranasal or intraperitoneal infection of laboratory mice. Intranasal infection seems most likely to mimic natural infection, since the main site of viral replication in wood mice is the lung and by comparison to other gammaherpesviruses (Blasdell *et al.* 2003). Following intranasal infection of anaesthetised mice primary MHV-68 replication takes place in the respiratory tract, mainly in alveolar epithelial cells but also mononuclear cells and in the nose, with replication spreading to distal epithelial sites such as the adrenal gland (Milho *et al.* 2009; Sunil-Chandra *et al.* 1992b). Primary infection induces an inflammatory infiltrate in the lung, made up mainly of macrophages, monocytes, $CD4^+$ and $CD8^+$ T-cells, leading to bronchiolitis and interstitial pneumonia (Sarawar *et al.* 2002; Sunil-Chandra *et al.* 1992b). The lytic infection is controlled by day 10 post infection and the inflammation is resolved by the second week, with both $CD4^+$ and $CD8^+$ T-cells contributing to the control of virus replication (Christensen *et al.* 1999; Stevenson *et al.* 1999). The $CD4^+$ T-cell antiviral response is dependent on IFN-γ but not $CD8^+$ T-cells or B-cells (Christensen *et al.* 1999; Sparks-Thissen *et al.* 2004; Sparks-Thissen *et al.* 2005).

1.3.6. MHV-68 latency

Following clearance of lytic virus from the lung low levels of persistent virus can still be detected in epithelial cells and during long-term latency virus persists in B-cells (Flano *et al.* 2003; Stewart *et al.* 1998). The lung has been found to be a major site of persistence both in laboratory mice and wood mice (Blasdell *et al.* 2003; Stewart *et al.* 1998). From the lung the virus spreads to the mediastinal lymph node (MLN) where dendritic cells, macrophages and B-cells are infected (Nash *et al.* 2001). The B-cells undergo a $CD4^+$ T-cell dependent proliferation leading to lymphadenopathy and an increase in the number of infected B-cells which spread to the spleen and other lymphoid organs where the virus establishes latency (Stewart *et al.* 1998; Usherwood *et al.* 1996b). During latency in the spleen MHV-68 can be detected within germinal centre B-cells, macrophages and dendritic cells (Flano *et al.* 2000; Sunil-Chandra *et al.* 1992a; Weck *et al.* 1999). Like EBV MHV-68 utilises the B-cell differentiation pathway to gain entry into the B-cell memory pool, ensuring life-long persistence (Kim *et al.* 2003). Splenomegaly occurs by day 10 with an increase in both size and numbers of germinal centres and a 2-3 fold increase in spleen cells, such as B-cells, $CD4^+$ and $CD8^+$ T-cells (Sunil-Chandra *et al.* 1992b; Usherwood *et al.* 1996a). Infected B-cells and $CD4^+$ T-cells are necessary for the development of splenomegaly (Ehtisham *et al.* 1993; Usherwood *et al.* 1996c; Usherwood *et al.* 1996b). Splenomegaly is however not a requirement for establishment of latency in the spleen (Usherwood *et al.* 1996b). The number of latently infected cells peak at around day 10-14 and decline to a low level with long-term latency maintained in germinal centre and memory B-cells, as well as macrophages and dendritic cells (Flano *et al.* 2003; Sunil-Chandra *et al.* 1992b; Usherwood *et al.* 1996c; Willer and Speck 2003).

Following splenomegaly there is a massive expansion of $CD8^+$ T-cells in the peripheral blood, dominated by $V\beta4^+$ $CD8^+$ T-cells, causing an IM-like syndrome (Tripp *et al.* 1997). This selective expansion seems to be MHC-independent, but like splenomegaly dependent on $CD4^+$ T-cells and B-cells (Brooks *et al.* 1999; Coppola *et al.* 1999; Flano *et al.* 1999). The oligoclonal expansion of $V\beta4^+$ $CD8^+$ T-cells is driven by a ligand encoded by the M1 gene that is expressed by latently infected

germinal centre B-cells (Coppola *et al.* 1999; Evans *et al.* 2008; Hardy *et al.* 2000). Even though these T-cells have the ability to exert effector functions they are not essential for the control of latent infection; however, they may function as a back-up defence (Braaten *et al.* 2006; Flano *et al.* 2004).

$CD4^+$ T-cells are important for the control of latent infection. Despite a functional $CD8^+$ T-cell response, long term MHV-68 infection of mice lacking $CD4^+$ T-cells leads to reactivation of virus in the respiratory tract and a chronic wasting disease (Belz *et al.* 2003; Cardin *et al.* 1996; Stevenson *et al.* 1998). The $CD4^+$ T-cell control of latent infection is not only mediated by IFN-γ but also by direct cytotoxicity (Sparks-Thissen *et al.* 2005; Stuller and Flano 2009). The IFN-γ control however seems to be cell type specific, suppressing reactivation in macrophages but not B-cells (Steed *et al.* 2007). $CD4^+$ T-cells are also needed to drive B-cell proliferation and maturation leading to a polyclonal non-specific antibody response. This is followed by a slow-developing virus-specific antibody response which plays a role in the control of latent infection (Kim *et al.* 2002; Sangster *et al.* 2000; Stevenson and Doherty 1998). The $CD4^+$ T-cells remain activated during the latent infection (Christensen and Doherty 1999) with cells specific for viral gp150 and ORF11 peptides making up 10-20% of the virus specific population (Flano *et al.* 2001).

Despite being insufficient in controlling latency, $CD8^+$ T-cells regulate the latent load by a single epitope within the M2 protein (Husain *et al.* 1999; Marques *et al.* 2008).

1.3.6.1. Latency *in vitro*

In vitro MHV-68 establishes latency in mouse myeloma B-cell lines, such as NS0 (Sunil-Chandra *et al.* 1993). During latent infection of NS0 cells approximately 5% undergo reactivation to lytic infection (Nash *et al.* 2001). Several B-cell lines derived from mice with MHV-68 associated lymphomas e.g. S11 have been established (Usherwood *et al.* 1996a). Infection of primary B-cells leads to phenotypic changes such as increased proliferation, however the cells are not transformed and the genome does not circularise (Dutia *et al.* 1999).

1.3.6.2. Latency transcripts

In common with other herpesviruses the switch from lytic to latent MHV-68 infection is accompanied by a shutdown of gene expression, with only a subset of genes expressed. Genes expressed during the establishment of latency include M1-M4, K3, ORF 72 (vcyclin), ORF 73, ORF 74 (vGPCR), M11 (vbcl-2), ORF 65, and the vtRNAs and miRNAs (Bowden *et al.* 1997; Diebel *et al.* 2010; Marques *et al.* 2003). The gene expression is cell type dependent, with B-cells of different differentiation stages, macrophages and dendritic cells expressing different genes, indicating the existence of latency programs (Marques *et al.* 2003). The gene expression during long-term latency has not been well defined.

The latency associated genes of MHV-68, like that of other gammaherpesviruses, play a role in establishment of latency, maintenance of the episome and promoting reactivation from latency. ORF 73, a positional homologue of KSHV LANA-1 with 24.2% sequence homology, is important for the establishment of latency (Fowler *et al.* 2003; Moorman *et al.* 2003b; Virgin *et al.* 1997). It is thought to have functions similar to the LANA-1 (see section 1.2.2.3.1) in tethering the viral episome to the host chromosome during cell division and inhibiting the activity of rta. ORF73 and rta thereby regulate each others expression, with the balance between ORF73 and rta determining between latency and reactivation. Other latency associated proteins also play a part in the establishment of latency in the spleen. These include M11 (vbcl-2) (de Lima *et al.* 2005), M2 (Jacoby *et al.* 2002; Macrae *et al.* 2003; Simas *et al.* 2004), M3 (Bridgeman *et al.* 2001), M4 (Evans *et al.* 2006; Geere *et al.* 2006) and K3 (Stevenson *et al.* 2002). M2, ORF 72 (vcyclin) and ORF 74 (vGPCR) (Moorman *et al.* 2003a) promote reactivation from latency (Herskowitz *et al.* 2005; Jacoby *et al.* 2002; van Dyk *et al.* 2000).

Cellular proteins are also involved in the establishment and maintenance of latency: NFκB inhibits viral replication and IFN-α/β regulates the viral gene expression, thereby directing the switch between lytic and latent infection and inhibiting reactivation from latency (Barton *et al.* 2005; Brown *et al.* 2003; Krug *et al.* 2009).

1.3.7. MHV-68 evasion of the host's immune system

MHV-68, like other herpesviruses, has evolved strategies to avoid the host immune response, especially during latency amplification. The K3 protein (a homologue of KSHV MIR-1) down-regulates MHC class I expression by degrading the MHC class I heavy chains and TAP, thereby avoiding $CD8^+$ T-cell recognition during latency amplification (Boname and Stevenson 2001; Boname *et al.* 2004; Lybarger *et al.* 2003; Stevenson *et al.* 2002). M3 is a chemokine binding protein that blocks chemokine signalling and thus leukocyte recruitment, including $CD8^+$ T-cells, enabling the amplification of latent virus in lymphoid tissue (Bridgeman *et al.* 2001; Martin *et al.* 2006; Parry *et al.* 2000; van Berkel *et al.* 2000). ORF36 encodes a multifunctional kinase that is conserved among herpesviruses. This protein binds to the activated form of IRF-3 and thereby inhibits the virus-induced type-I IFN response, promoting persistent infection (Hwang *et al.* 2009). The episome maintenance protein encoded by ORF73 has a *cis*-acting $CD8^+$ T-cell evasion mechanism, like EBNA-1, so that it can avoid recognition by the immune system (see section 1.2.1.1.1) (Yin *et al.* 2003). Disruption of this evasion mechanisms leads to a reduction in latency (Bennett *et al.* 2005).

1.3.8. MHV-68 pathogenesis

MHV-68 associated diseases vary in severity from splenomegaly to lymphoproliferative disorders. The outcome of infection depends on the type and immunological status of the infected mouse; with severe disease usually not occurring in immunocompetent mice. Infection of inbred BALB/c mice leads to both lymphoid and non-lymphoid lymphomas in 10% of infected mice, with the number of virus DNA positive lymphocytes varying from low to very high numbers. The incidence of lymphoma was increased following treatment with the immunosuppressant drug cyclosporine A (Sunil-Chandra *et al.* 1994). Infection of BALB/c mice with MHV-72 leads to a similar incidence of lymphomas (Mistrikova *et al.* 1996). MHV-68 infection of BALB β_2-microglobulin deficient mice is associated with a higher occurrence of lymphoproliferative disease than BALB/c mice, with two types of lesions observed: B-cell lymphoma and atypical lymphoid hyperplasia (ALH). The AHL lesions, resembling EBV-associated PTLD, commonly

contained MHV-68 infected cells, while lymphomas contained few infected cells (Tarakanova *et al.* 2005). The MHV-68 positive B-cell line S11 induces tumours when introduced into nude mice, with $CD4^+$ T-lymphocytes found to be important for tumour regression (Robertson *et al.* 2001; Usherwood *et al.* 1996a).

There are several candidate viral genes for transformation of cells, including ORF72 (vcyclin), ORF-74 (vGPCR) and M11 (vbcl-2). vcyclin is an oncogene that binds and activates cellular cdks, promoting cell cycle progression and inhibiting T-lymphocyte differentiation (Upton *et al.* 2005; van Dyk *et al.* 1999). vcyclin is important for *in vivo* replication and reactivation from latency; with its role in reactivation at least in part cdk-independent (Upton and Speck 2006; van Dyk *et al.* 2000). The vGPCR is expressed during both lytic infection and latency and has the ability to transform cells *in vitro* (Wakeling *et al.* 2001). The viral bcl-2 homologue is expressed during lytic and latent infection and inhibits apoptosis and autophagy; thus promoting cell survival and tumour formation (Ku *et al.* 2008; Roy *et al.* 2000; Wang *et al.* 1999). vbcl-2 and vcyclin have been shown to be involved in the development of ALH in MHV-68 infected BALB β_2-microglobulin deficient mice, while vGPCR is not (Tarakanova *et al.* 2008).

MHV-68 is also involved in other disorders in immunocompromised mice. Infection of young or immunocompromised mice lacking IFN-γ response or B-cells is associated with arthritis of large elastic arteries, eventually leading to death (Weck *et al.* 1997). Infection of IFN-γ receptor deficient mice is also associated with fibrosis and atrophy of lymphoid tissue, liver, and lungs, with at least splenic fibrosis being dependent on a Th2 response (Dutia *et al.* 1997; Ebrahimi *et al.* 2001; Gangadharan *et al.* 2008; Mora *et al.* 2005). Pulmonary inflammation was found to lead to more severe disease over time, with 80% developing lymphoid hyperplasia or pulmonary lymphoma after 12 months (Lee *et al.* 2009b).

1.3.9. MHV-76 and other related viruses

MHV-76 and MHV-72 were discovered at the same time as MHV-68 and are considered strains of MHV-68. MHV-76 is identical to MHV-68 except for a 9538 bp deletion in the left end of the genome, encompassing M1-M4, the eight vtRNAs, and nine miRNAs (Macrae *et al.* 2001). MHV-76 thereby appears to be a deletant

virus occurring during either *in vivo* or *in vitro* passaging. This was further supported by the generation of a spontaneous deletion mutant with a nearly identical deletion affecting the same genes through *in vitro* passaging (Clambey *et al.* 2002). MHV-76 replicates with similar kinetics to MHV-68 *in vitro*. However, following intranasal infection of mice MHV-76 shows an attenuated phenotype (Macrae *et al.* 2001). During acute infection in the lungs, MHV-76 induces a greater inflammatory response and is cleared more rapidly. In addition, the virus does not induce splenomegaly to the same degree and establishes latency in the spleen at a much lower level. Following establishment of latency MHV-76 is able to persist in the spleen, but not in the lungs. MHV-72 lacks the first 7 kbp of the genome, encompassing M1-M3, vtRNAs and miRNAs (Oda *et al.* 2005).

MHV-Brest and WMHV are closely related viruses with 99.2% sequence identity considered strains of viruses related to MHV-68 (Chastel *et al.* 1994; Hughes *et al.* 2009). WMHV has 85% sequence identity with MHV-68, with the left end region highly conserved, particularly M1 and M4 and the vtRNAs, while five of the miRNAs are less conserved (Hughes *et al.* 2009). The left end of MHV-Brest is also highly conserved, with least sequence similarities in the M2 gene (Chastel *et al.* 1994).

1.3.10. Left-hand end of MHV-68

The left end of the genome contains the genes that are unique to MHV-68; M1-M4, the vtRNAs and miRNAs (Figure 1.5A). The functions of these genes are not fully understood, but what is known will be discussed below.

1.3.10.1. M1

The M1 ORF has 25% sequence homology with M3 (van Berkel *et al.* 1999) and is expressed during lytic infection both *in vitro* and *in vivo* and during latent infection in the spleen (Ebrahimi *et al.* 2003; Marques *et al.* 2003; Martinez-Guzman *et al.* 2003; Simas *et al.* 1999). M1 is a secreted protein responsible for the expansion of $V\beta4^+$ $CD8^+$ T-cells during MHV-68 infection (Evans *et al.* 2008). It suppresses viral reactivation through the action of $V\beta4^+$ $CD8^+$ T-cells, apparently by IFN-γ

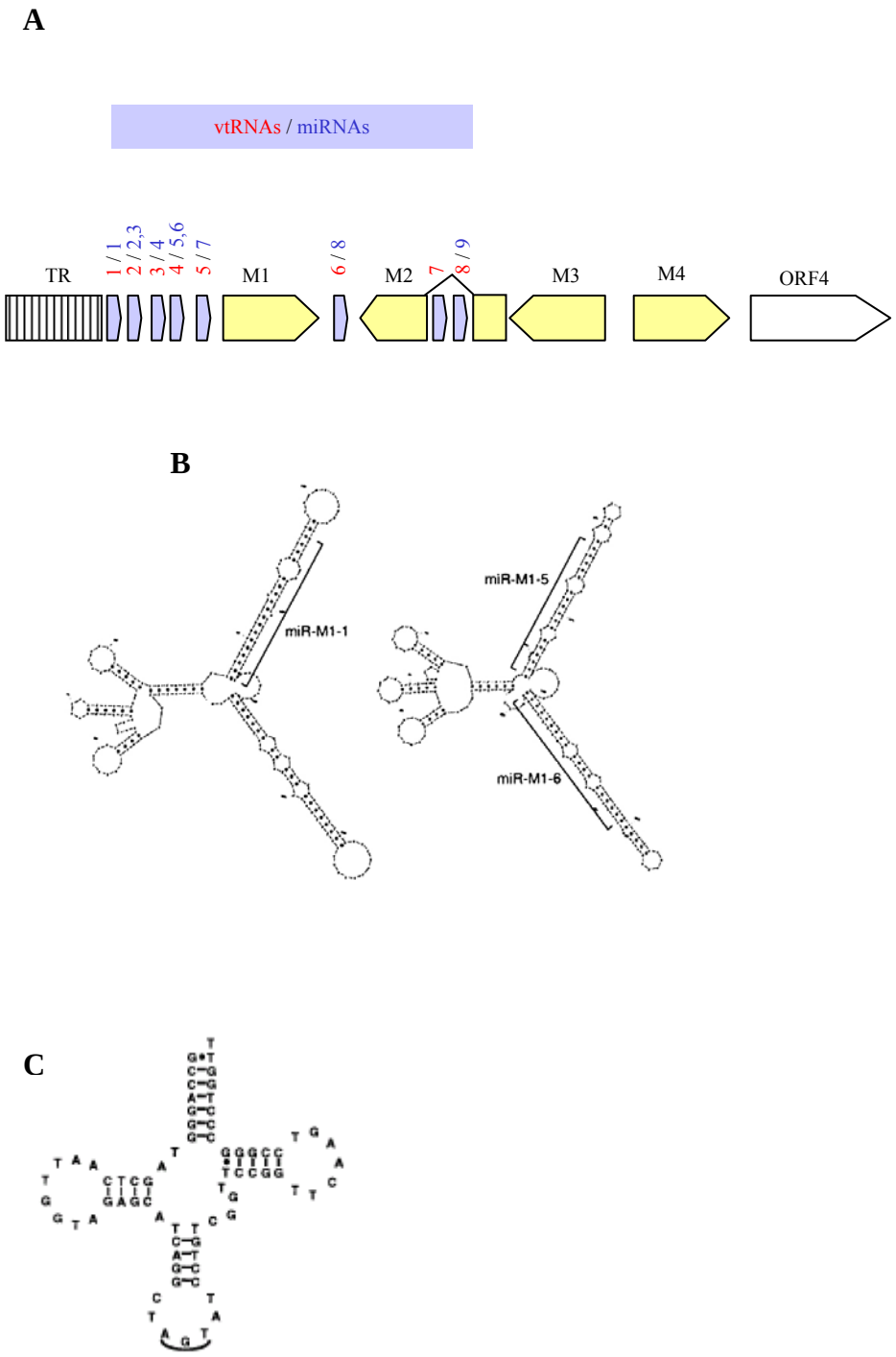

Figure 1.5 (A) The unique genes in the left side of the genome, showing the four unique protein coding genes M1-M4 and the vtRNA and miRNA genes. (B) The miRNAs are transcribed as part of the vtRNA transcripts (taken from Pfeffer *et al.* 2005). (C) Predicted cloverleaf structure of vtRNA5 (taken from Bowden *et al.* 1997).

production (Clambey *et al.* 2000; Evans *et al.* 2008). M1 driven expansion of $V\beta4^+$ $CD8^+$ T-cells causes inflammation and multi-organ fibrosis in IFN-γ receptor deficient mice (Clambey *et al.* 2000; Evans *et al.* 2008). In contrast, M1 was found to repress the severity of the lymphoproliferative disease seen in MHV-68 infected BALB β_2-microglobulin deficient mice (Tarakanova *et al.* 2008). The M1 driven expansion of $V\beta4^+$ $CD8^+$ T-cells also mediates resistance to transplantation tolerance during latent infection (Stapler *et al.* 2008).

1.3.10.2. M2

M2 is a membrane-associated protein expressed during lytic infection in the lungs and transiently during latent infection in the spleen (Macrae *et al.* 2003; Marques *et al.* 2003; Usherwood *et al.* 2000). This protein has been found to be critical for the efficient establishment of latency in the spleen and reactivation from latency (Herskowitz *et al.* 2005; Jacoby *et al.* 2002; Macrae *et al.* 2003; Simas *et al.* 2004). M2 is not involved in the splenomegaly or expansion of $V\beta4^+$ $CD8^+$ T-cells seen during the establishment of latency (Macrae *et al.* 2003), but is required for colonisation of splenic follicles and the differentiation of these cells into memory B-cells and plasma cells (Herskowitz *et al.* 2005; Liang *et al.* 2009; Simas *et al.* 2004). Lack of M2 has been associated with an increase of latently infected germinal centre B-cells during long-term latency indicating an inability of these cells to differentiate into memory B-cells (Herskowitz *et al.* 2005; Simas *et al.* 2004). M2 promotes B-cell differentiation, proliferation and survival through interactions with the guanine nucleotide exchange factor vav, affecting its activity and thereby lymphocyte signalling (Madureira *et al.* 2005; Rodrigues *et al.* 2006). In primary B-cells M2 was found to increase B-cell production of and sensitivity to IL-10 by modulating B-cell signalling, thereby driving B-cell proliferation and differentiation (Siegel *et al.* 2008). M2 driven proliferation of B-cells into plasma cells is associated with an increase in reactivation (Liang *et al.* 2009). M2 also protects latently infected cells by inhibiting IFN- and apoptosis-mediated innate immunity (Liang *et al.* 2004; Liang *et al.* 2006). In addition, M2 has a $CD8^+$ T-cell epitope that affects the viral latent load during long-term latency (Husain *et al.* 1999; Marques *et al.* 2008).

1.3.10.3. M3

M3 encodes a secreted high-affinity broad spectrum chemokine binding protein with no sequence similarity to known chemokine receptors (Parry *et al.* 2000; van Berkel *et al.* 1999). It is expressed abundantly during lytic infection and the establishment of latency, but does not seem to be expressed during long-term latency in the spleen (Marques *et al.* 2003; Martinez-Guzman *et al.* 2003; Simas *et al.* 1999). M3 is able to bind chemokines from all four subfamilies and by blocking their interaction with both GPCRs and GAGs inhibits chemokine signalling (Alexander *et al.* 2002; Parry *et al.* 2000; van Berkel *et al.* 2000; Webb *et al.* 2004). In mice M3 was found to be critical for the establishment of latency by inhibiting $CD8^+$ T-cell recruitment (Bridgeman *et al.* 2001). This effect on latency was however not seen in a different study, instead M3 was found to be involved in the induction of the lethal meningitis caused by MHV-68 by regulating the inflammatory responses (van Berkel *et al.* 2002). The ability of M3 to block leukocyte recruitment, including $CD8^+$ T-cells, through cytokine binding *in vivo* has been verified in two separate studies using transgenic mice (Jensen *et al.* 2003; Martin *et al.* 2006).

1.3.10.4. M4

M4 encodes a secreted glycoprotein expressed during lytic infection in the lung and establishment of latency in the spleen, but not during long-term latency (Evans *et al.* 2006; Marques *et al.* 2003; Townsley *et al.* 2004). Studies using recombinant viruses either by inserting M4 into MHV-76 or disruption of the M4 gene in MHV-68 have found that M4 is important for the establishment of latency; however, not for the maintenance of long-term latency (Evans *et al.* 2006; Geere *et al.* 2006; Townsley *et al.* 2004). Lack of M4 leads to an increased clearance of virus, suggesting that M4 modulates the immune response (Geere *et al.* 2006); consistent with this M4 has been shown to bind the chemokine CXCL4 and reduce its levels (pers commun Y. Ligertwood and B.M. Dutia). M4 did not have an effect on splenomegaly, again showing that the increase in latent load is not dependent on lymphocytosis (Geere *et al.* 2006; Townsley *et al.* 2004).

1.3.10.5. vtRNAs and miRNAs

MHV-68 encodes eight vtRNAs and nine miRNAs which are transcribed by RNA polymerase III as dicistronic transcripts, with one or two 20-25 bp pre-miRNA hairpins following the tRNA (Figure 1.5B) (Bowden *et al.* 1997; Pfeffer *et al.* 2005). The vtRNA sequences contain internal RNA polymerase III type-2 promoter elements with three overlapping A-box promoter elements and one B-box promoter element (Diebel *et al.* 2010).

The vtRNAs contain up to 75% sequence homology with some cellular tRNAs and are predicted to form cloverleaf-like secondary structures in which the majority of invariant and semi-invariant bases typical of tRNAs are conserved (Figure 1.5C; see section 1.4.2.1) (Bowden *et al.* 1997). However, the prediction of amino acid specificity is difficult because the vtRNAs have atypical anti-codon arms, differing in size and sequence from known cellular tRNAs. In addition, the vtRNAs do not have more similarity to tRNAs sharing the same anticodon than other tRNAs. vtRNA7 contains an intron, but lacks the purine residue needed for splicing, indicating that at least this vtRNA is unlikely to function in translation. The determinant bases (nt73), which are known to be important for recognition by cellular aminoacyl-tRNA synthases, are not conserved; consistent with this at least four of the vtRNAs are not aminoacylated (Bowden *et al.* 1997). At least two of the vtRNAs are however recognised as tRNAs by the cellular machinery and processed into mature tRNAs with the post-transcriptional addition of the 3' CCA sequence. The vtRNAs are expressed at high levels during both lytic infection in the lung and latent infection in the spleen. They can be detected by *in situ* hybridisation in spleens in the absence of viral DNA, which has lead to the vtRNAs being used to detect latently infected cells (Bowden *et al.* 1997). During lytic infection *in vitro* the vtRNAs are located in both the nucleus and cytoplasm of the cell, at later times predominantly in the cytoplasm (Cliffe *et al.* 2009b). The functions of these vtRNAs are not known; however, they are not thought to act as part of the normal translation machinery. They are selectively packaged in the virion, indicating their need either as structural components of the virion or immediately upon entry into the cell (Cliffe *et al.* 2009b).

MHV-68 has been predicted to encode at least 14 miRNAs, with nine identified through cloning (Pfeffer *et al.* 2005). These miRNAs can be detected in both lytically and latently infected tissues *ex vivo* with varying levels of expression (Diebel *et al.* 2010). The miRNAs are able to down-regulate expression of genes containing their target sequence *in vitro*, with three miRNAs able to reduce luciferase expression by at least 50% (Diebel *et al.* 2010). miRNA 8 appears to be post-transcriptionally modified with the addition of uracils (Diebel *et al.* 2010). How the miRNAs are processed from the vtRNA-pre-miRNA transcript into mature miRNAs and what targets and thereby functions they might have is currently not known.

1.4. Non-coding RNAs

1.4.1. Viral non-coding RNA molecules

Several viruses express diverse non-coding RNAs that differ in structure, expression and function. Some of these are reviewed below.

1.4.1.1. Alphaherpesvirus non-coding RNA molecules

1.4.1.1.1. HSV LATs

The only abundant viral transcripts detected during latent infection with HSV-1 are the LATs that were initially detected in latently infected murine (Spivack and Fraser 1987; Stevens *et al.* 1987) and then also rabbit (Rock *et al.* 1987) and human (Krause *et al.* 1988) trigeminal ganglia. The primary LAT transcript is a 8.3-8.5kb capped, polyadenylated, non-coding RNA that is spliced into a stable, non-polyadenylated 2.0 kb intron, which can be further spliced into a 1.5 kb intron in some neurons (Farrell *et al.* 1991; Spivack *et al.* 1991; Wagner *et al.* 1988a; Wagner *et al.* 1988b). The 2.0 kb intron is the most abundant LAT species and is located mainly in the nucleus during latent infection (Stevens *et al.* 1987; Wagner *et al.* 1988b). The introns are unusually stable because of a lariat structure, while the predicted 6.3 kb exon is highly unstable (Kang *et al.* 2006; Thomas *et al.* 2002). The primary LAT transcript is expressed from a neuron-specific promoter or enhancer (Berthomme *et al.* 2000; Zwaagstra *et al.* 1990). The region encoding the LATs, located in the inverted repeats, is complex with several ORFs and transcripts thought

to be encoded. The last 750 bp of the 2.0 kb LAT intron lies anti-sense to the lytic transactivator ICP0. Further, the primary LAT transcript lies anti-sense to ICP4 and $\gamma_1$34.5 and is co-linear with ORF P, L/STs, αX and βX (reviewed in Roizman *et al.* 2007). Several other transcripts have been described that lie within the promoter regulatory region or first 1.5 kb of the LAT coding sequence; some reported to express proteins (UOL, AL and AL3) and some RNAs (AL2, sRNA1 and sRNA2) (Jaber *et al.* 2009; Naito *et al.* 2005; Perng *et al.* 2002; Shen *et al.* 2009). The LAT region has also been shown to encode several miRNAs, six in the unstable large exon and two upstream of LAT (Cui *et al.* 2006; Umbach *et al.* 2008; Umbach *et al.* 2009).

Because of the complexity of the LAT region determining the functions of the LATs has been difficult, with contradictory results obtained with different parts of the LAT region deleted or in different animal models. Even though the LATs do not seem to be critical for latency several studies have implicated LATs in facilitating efficient reactivation, both in mouse and rabbit animal models (Garber *et al.* 1997; Hill *et al.* 1990; Kang *et al.* 2003; Leib *et al.* 1989; Perng *et al.* 1994; Steiner *et al.* 1989). Several of these studies did not find a role for the LATs in establishing latency; however, more sensitive PCR techniques have found a defect in the establishment of latency during infection with deletion mutants, with the decrease in the number of latently infected neurons causing the lack of reactivation (Sawtell and Thompson 1992; Thompson and Sawtell 1997, 2001). The deficiency in establishing latency was caused by an increase in neuronal cell death (Thompson and Sawtell 2001). The region implicated in reactivation, and thus possibly establishment of latency, has been mapped to a 348 bp region of the 5'of LAT (Bloom *et al.* 1996).

The mechanism by which the LATs facilitate the establishment of latency and reactivation is not clear. The LATs have been shown to reduce the production of lytic gene transcripts during both lytic infection and latent infection of mice (Chen *et al.* 1997; Garber *et al.* 1997) and in cultured murine neuronal cells (Mador *et al.* 1998); however, they seem to have the opposite effect during infection of rabbits (Giordani *et al.* 2008). One of the mechanisms by which the LATs inhibit lytic gene expression is by inducing epigenetic changes, with LAT transcription promoting heterochromatin on lytic promoters (Cliffe *et al.* 2009a; Wang *et al.* 2005b). Mutants

lacking LATs have been found to cause more neuronal death, higher mortality in mice and increased apoptosis (Ahmed *et al.* 2002; Branco and Fraser 2005; Perng *et al.* 2000; Thompson and Sawtell 2001; Wang *et al.* 2005b). It is therefore speculated that the LATs protect infected neurons from cell death by inhibiting lytic gene transcription and protecting against apoptosis; thus increasing the number of latently infected cells and preventing their death prior to reactivation.

The 2 kb LAT intron may also have a role in translation. During lytic infection the 2 kb LAT intron locates to the cytoplasm as well as the nucleus, apparently transported there as part of the 60S ribosomal subunit. Its interaction with ribosomal proteins associated with the 60S ribosomal subunit suggests that it may have a structural role of the ribosomal complex and thereby affect the translation machinery (Ahmed and Fraser 2001; Atanasiu and Fraser 2007).

Recently two small RNAs identified within the 5' end of the 2.0 kb LAT intron were found to inhibit apoptosis, reduce infectious virus production, and inhibit expression of the transcription factor ICP4 in *in vitro* studies (Shen *et al.* 2009).

Of the eight miRNAs expressed from the LAT region, two have been found to down-regulate ICP0 and ICP4 (Umbach *et al.* 2008).

1.4.1.2. Gammaherpesvirus non-coding RNA molecules

1.4.1.2.1. EBV EBERs

The two EBERs, EBER-1 and EBER-2, are the most abundant transcripts expressed during latent EBV infection (Lerner *et al.* 1981). Like the vtRNAs expressed by MHV-68, the EBERs are small, non-polyadenylated, uncapped, non-coding RNAs transcribed by RNA polymerase III into RNAs of 167 and 172nt, respectively (Arrand and Rymo 1982; Lerner *et al.* 1981; Rosa *et al.* 1981). However, the presence of RNA polymerase II promoter elements makes it possible that they are also transcribed by RNA polymerase II (Howe and Shu 1989). The EBERs have highly conserved sequences, but only have 54% sequence homology between each other (Arrand *et al.* 1989). They both form very similar stable secondary structures due to extensive base-pairing, forming a number of short stem-loops (Figure 1.6A) (Glickman *et al.* 1988). These predicted secondary structures show similarity to both

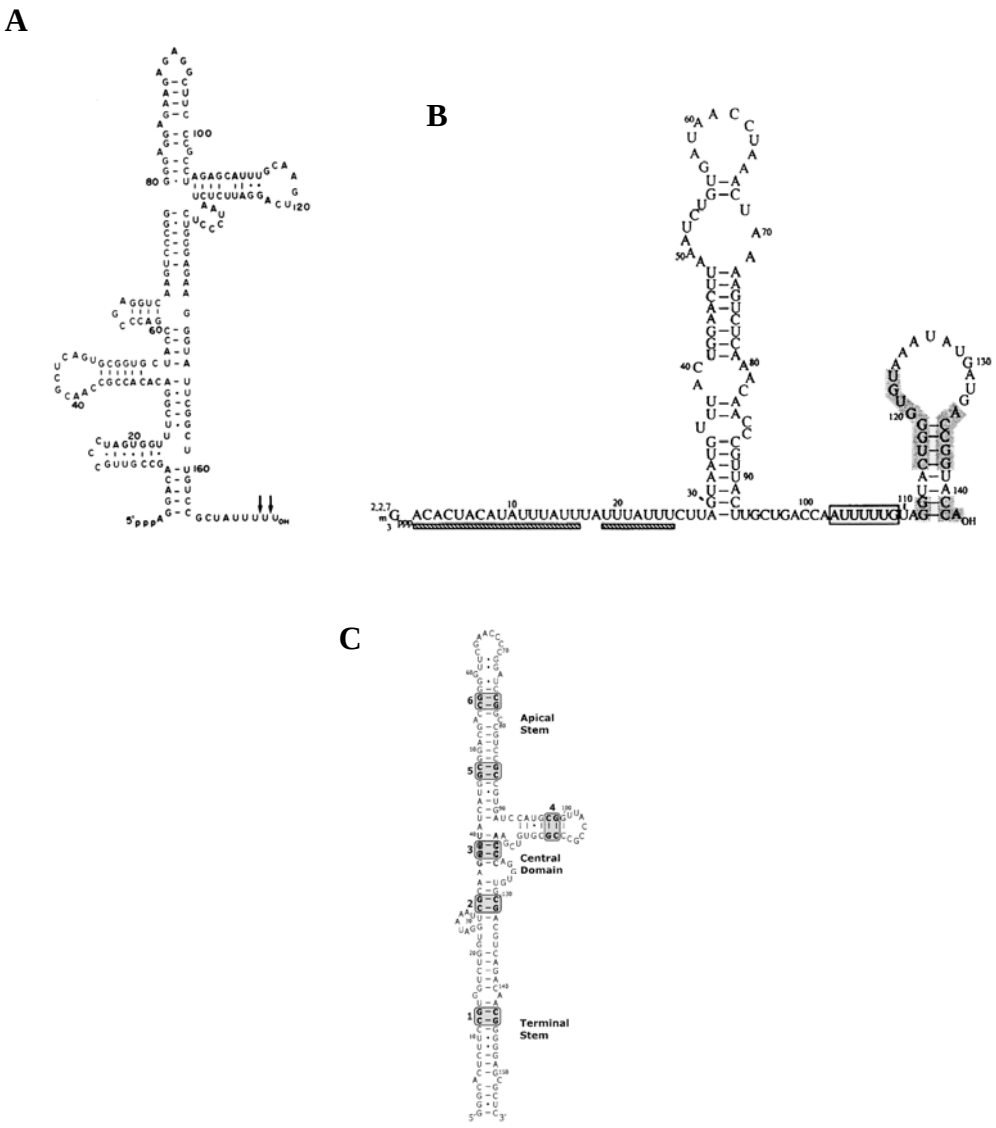

Figure 1.6 Predicted secondary structures of viral non-coding RNA molecules. (A) EBER-2 of EBV (taken from Rosa *et al.* 1981). (B) HSUR-1 of HVS (taken from Lee and Steitz 1990). (C) VAI of adenovirus type 2 (taken from Coventry and Conn 2008).

herpesvirus papio small RNAs and adenovirus VAI and VAII molecules (Howe and Shu 1988; Rosa *et al.* 1981). The biological functions of the EBERs seem to depend on their secondary structures since disruption of the secondary structure by replacing GTP with ITP reduces EBER-1 binding to PKR (Clarke *et al.* 1991). Both EBERs can be detected during all forms of latency, with EBER-1 10 times more abundant than EBER-2 due to differences in half-life (Clarke *et al.* 1992). The EBERs are expressed during many EBV-associated diseases; however, are absent in disorders such as oral hairy leukoplakia that consists of replicating cells (Gilligan *et al.* 1990).

The EBERs seem to localise to both the nucleus and the cytoplasm as they have been found to interact with cellular proteins in both locations. They form complexes with lupus erythematosis-associated antigen (La) (Lerner *et al.* 1981), ribosomal protein L22, RIG-I and PKR. La is a highly abundant nuclear phosphoprotein that binds the 3' end of newly synthesised RNA polymerase III transcripts, protecting them from exonuclease digestion (Wolin and Cedervall 2002). The EBERs also bind to the latent form of PKR and inhibit its phosphorylation by preventing its dimerisation. This inhibits the virus induced phosphorylation and inactivation of the protein synthesis factor eIF-2α and interferes with the inhibition of translation (Clarke *et al.* 1991; McKenna *et al.* 2007; Sharp *et al.* 1993). The EBERs have also been found to prevent the inhibition of protein synthesis in an PKR-independent manner (Laing *et al.* 2002). They are also associated with polyribosomes in the cytoplasm, binding to L22, an abundant ribosomal protein (Toczyski and Steitz 1991). The function of L22 is not clear; however, it has been implicated in the chromosomal 3;21 translocation seen in some cases of acute and chronic myeloid leukaemias (Nucifora *et al.* 1993). The EBERs have multiple binding sites for L22 and it is possible that the EBERs may have an affect on translation by interacting with the ribosome (Fok *et al.* 2006). However, binding of L22 to the EBERs out-competes other proteins, e.g. PKR, and thus interferes with the EBERs' PKR-dependent and -independent regulation of protein synthesis (Elia *et al.* 2004). EBER binding to RIG-I leads to its activation and induction of IL-10, as well as type-I IFNs and thereby apoptosis, through phosphorylation of NFκB and IRF-3 (Samanta *et al.* 2006; Samanta *et al.* 2008). To avoid apoptosis the EBERs inhibit IFN-α-mediated

as well as Fas-mediated apoptosis by interaction with PKR (Nanbo *et al.* 2002; Nanbo *et al.* 2005).

Several studies have shown that the EBERs have growth-promoting properties. The EBERs are responsible for the malignant phenotype seen in BL cells and contribute to tumorigenicity in SCID mice (Komano *et al.* 1999) (Ruf *et al.* 2000). EBER-2 is also important for efficient EBV-induced B-lymphocyte growth transformation, promoting growth by inducing IL-6 production (Wu *et al.* 2007). The EBERs also induce other cytokines in different cell types, e.g. IL-10, IGF-I, IL-9, which all act as autocrine growth factors (Iwakiri *et al.* 2005; Samanta *et al.* 2008; Yang *et al.* 2004). A recent study showed that the EBERs released from EBV-infected cells activate toll-like receptor 3 (TLR3) signalling, thereby inducing type-I IFNs and proinflammatory cytokines which contribute to the immunopathological diseases caused by EBV-infection (Iwakiri *et al.* 2009).

1.4.1.2.2. HVS U RNAs

HVS causes T-cell lymphomas in new world primates. The most abundant viral gene products in latently infected transformed T-cells are seven small nuclear U RNAs, HSURs (Figure 1.6B) (Albrecht and Fleckenstein 1992; Lee *et al.* 1988; Murthy *et al.* 1986; Wassarman *et al.* 1989). These HSURs are 75 to 143nt long and are encoded by a cluster of genes at the left end of the genome, which is essential for oncogenicity and immortalisation, but is not required for replication (Desrosiers *et al.* 1986). The HSURs are not required for viral transformation *in vitro* (Ensser *et al.* 1999; Murthy *et al.* 1989). The HSURs have no sequence similarity to cellular U RNAs, but share several other features: they are transcribed by RNA polymerase II and have the same typical promoters, enhancers and 3'-end signals, acquire 5' trimethylguanosine caps and have the Sm protein binding site sequences (Lee *et al.* 1988). Like cellular U RNAs that form small nuclear ribonucleoproteins (snRNPs) involved in RNA maturation such as splicing and polyadenylation, HSURs associate with snRNPs, of the class Sm, using the cellular protein survival of motor neurons (SMN) (Golembe *et al.* 2005). The HSURs have a high affinity for SMN and can out-compete host U RNAs for snRNP assembly; the significance of this is not clear.

The 5'-ends of HSURs 1, 2 and 5 have conserved AUUUA sequences of different copy numbers. Similar AUUUA motifs, known as AREs, are present in the 3' untranslated region (UTR) of short-lived mRNAs such as protooncogenes, cytokines, and lymphokines and target these mRNAs for degradation. Given that the HSURs bind proteins known to bind AREs and regulate mRNA stability, such as HuR which protects ARE-containing mRNAs, they are thought to compete with these cellular proteins and alter the expression of cytokines and protooncogenes (Fan and Steitz 1998; Myer *et al.* 1992; Myer *et al.* 1997). However, HSUR1 and HSUR2 were not found to affect the levels of ARE-containing mRNAs *in vitro*, but they were found to up-regulate a small number of genes associated with T-cell activation in transformed cells (Cook *et al.* 2004; Cook *et al.* 2005). The HSUR1 ARE was also found to induce degradation of small nuclear RNAs, including itself, HSUR2 and cellular U1 (Fan *et al.* 1997).

1.4.1.2.3. KSHV PAN RNAs

The PAN RNA is an early lytic 1.2 kb polyadenylated non-coding RNA of unknown function that accumulates to high levels in the nucleus (Sun *et al.* 1996; Zhong *et al.* 1996; Zhong and Ganem 1997). It has features of both U RNAs and mRNAs in that it is transcribed by RNA polymerase II, lacks a 5' trimethylguanosine cap, is not associated with polyribosomes and has several parts with sequence homology to U1 RNA, 5' sequence elements typical of regulatory regions of U RNAs and 33% uracils content typical of U RNAs (Sun *et al.* 1996). In addition, it associates with Sm forming ribonucleoprotein complexes in the nucleus (Sun *et al.* 1996; Zhong and Ganem 1997). The high level of PAN expression is attributed to two factors. First, PAN expression is up-regulated by the transactivators rta and Mta, with rta binding to a very strong rta-response element (RRE) located in the promoter (Chang *et al.* 2002; Kirshner *et al.* 2000; Palmeri *et al.* 2007; Song *et al.* 2001; Song *et al.* 2002). In addition, PAN contains a cis-acting element PAN-ENE (PAN RNA expression and nuclear retention element) that protects polyadenylated intronless transcripts from rapid decay by interactions with the poly-A tail and retains these transcripts in the nucleus (Conrad and Steitz 2005; Conrad *et al.* 2006; Conrad *et al.* 2007).

1.4.1.3. Adenovirus non-coding RNAs

1.4.1.3.1. VAI and VAII

All adenoviruses examined encode one or two non-coding RNAs known as VAI and VAII that vary in sequence and length, 149-174nt, between different viruses (Ma and Mathews 1996; Ohe and Weissman 1971; Reich *et al.* 1966; Soderlund *et al.* 1976). The VA RNAs are transcribed by RNA polymerase III early during the infection. VAI is synthesised in increasing amounts during the later stages to become the most abundant RNA in the cytoplasm, while VAII is slightly less abundant (Soderlund *et al.* 1976). The VAs form highly structured and stable secondary structures consisting of three major domains: terminal stem, central domain and apical stem; with specific functions attributed to each domain (Figure 1.6C) (Coventry and Conn 2008; Ma and Mathews 1993).

VAI was found to be critical for efficient translation when a deletion mutant lacking VAI showed impaired growth (Thimmappaya *et al.* 1982). It was further found that VAI blocks the antiviral activation of PKR (Kitajewski *et al.* 1986; O'Malley *et al.* 1986) using the same mechanism as the EBERs (see section 1.4.1.2.1) (McKenna *et al.* 2007). In fact it was the similarities of gene organisation, size and predicted secondary structure between the VAs and EBERs that lead to the idea that the EBERs, like the VAs, may influence translation. The EBERs were subsequently shown to substitute for the VAs and rescue translation during infection with deletion mutants lacking the VAs (Bhat and Thimmappaya 1983, 1985). The apical stem of VAI is important for binding to PKR, while the central domain is critical for inhibition of PKR (Clarke *et al.* 1994; Coventry and Conn 2008; Ghadge *et al.* 1991; Ghadge *et al.* 1994). The terminal stem is however dispensable for PKR inhibition (Wahid *et al.* 2008). In addition to regulating translation VAI may also regulate RNA editing since it binds the RNA-specific adenosine deaminase, ADAR, and inhibits its interferon-inducible RNA-editing activity (Lei *et al.* 1998). VAII has limited ability to block PKR but is able to bind other proteins with double stranded-binding motifs, such as RNA helicase A and nuclear factor 90 (NF90), both involved in transcriptional regulation (Liao *et al.* 1998; Ma and Mathews 1993; Reichman *et al.*

2002). Like the EBERs both VAI and VAII form ribonucleoprotein complexes with La (Rosa *et al.* 1981). The significance of these interactions is not known.

The VAs also inhibit RNA interference (RNAi). As discussed in section 1.4.2, RNAi is a posttranscriptional gene silencing mechanism where 21-23nt RNAs generated from cytoplasmic processing of endogenous distinct hairpin structures (miRNAs), either degrade or inhibit translation of mRNA targets. The VAs out-compete binding to the Exportin-5 nuclear export factor and Dicer, preventing the export of pre-miRNAs from the nucleus and their processing into functional miRNAs that can be incorporated into the RNA-induced silencing (RISC) complex (Andersson *et al.* 2005; Lu and Cullen 2004). In addition, the terminal stem is cleaved by Dicer generating miRNAs named svaRNAs or mivaRNAs (Andersson *et al.* 2005; Aparicio *et al.* 2006; Sano *et al.* 2006). 80% of RISC complexes are associated with mivaRNAs and VAII mivaRNAs account for 60% of small RNAs in RISC complexes, indicating that cellular miRNAs are out-competed (Xu *et al.* 2007). The mivaRNAs are thought to be functional because: they are able to inhibit the expression of genes with complementary sequences, were detected on polyribosomes, and inhibition of VAI mivaRNAs affects virus production (Aparicio *et al.* 2006; Sano *et al.* 2006; Xu *et al.* 2007). Recently 30 cellular genes involved in cell growth, transcription, RNA metabolism and DNA repair were found to be down-regulated in adenovirus infected or transfected cells expressing mivaRNAs. Of these TIA-1, a splicing and translational regulator, is a direct target of mivaRNAI-138 and is down-regulated both at mRNA and protein level (Aparicio *et al.* 2009).

1.4.2. tRNAs

1.4.2.1. tRNA structure

The tRNAs are small RNA molecules, usually 74 to 95nt, that play a central role in translation by providing the link between mRNA and protein. As one of the first nucleic acids to be sequenced the tRNAs were found to form a predicted canonical cloverleaf secondary structure (Figure 1.7A) with three arms and loop regions, a variable loop and acceptor arm (Holley *et al.* 1965). The acceptor arm made up of

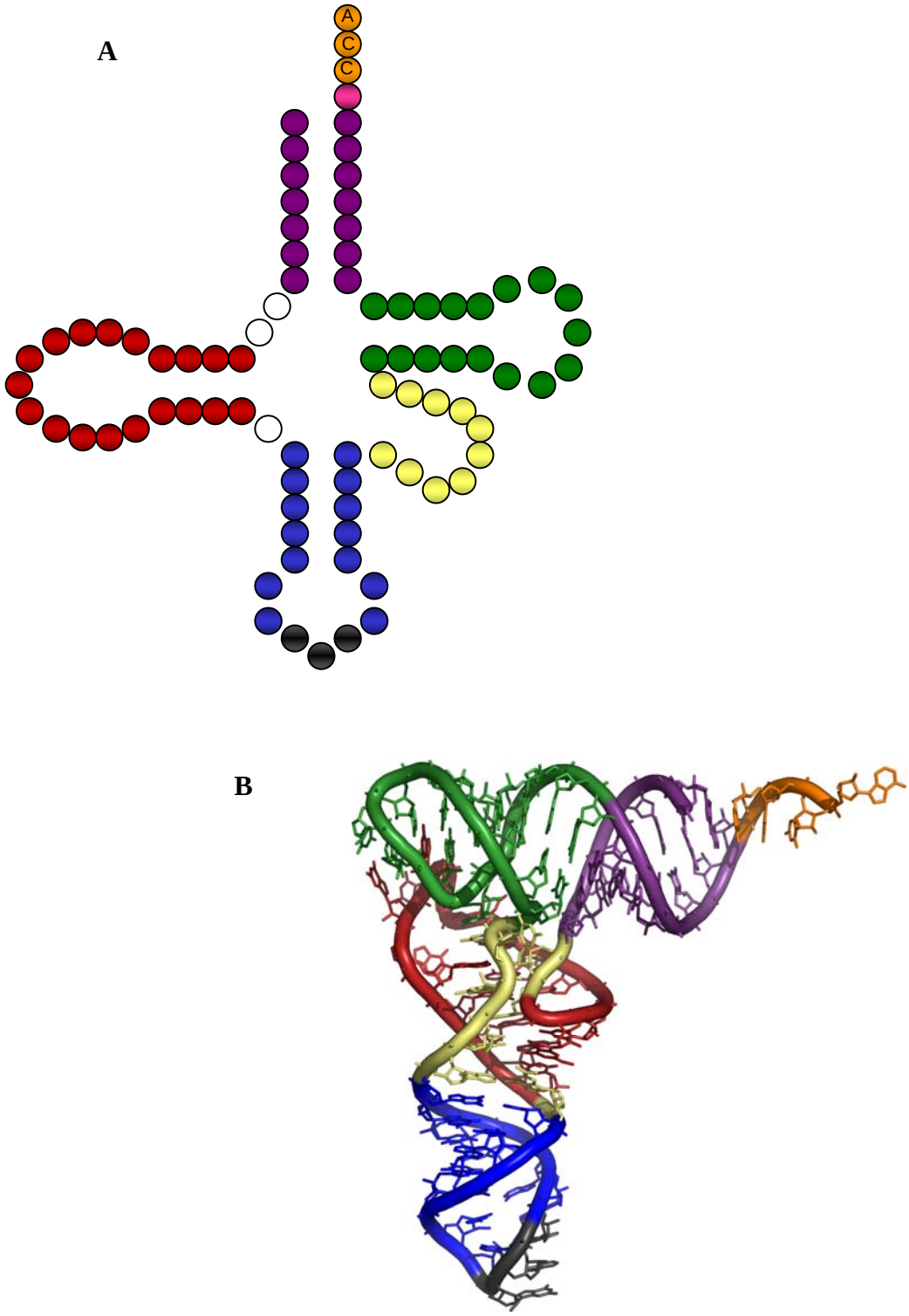

Figure 1.7 Secondary (A) and tertiary (B) structure of a typical tRNA molecule, showing the acceptor stem (purple) with the CCA tail (orange) and discriminator nucleotide (pink), D arm and loop (red), T arm and loop (green), variable loop (yellow) and anticodon arm and loop (blue) with the anticodon (black). Tertiary structure (B) reproduced with the kind permission of N.R. Voss.

seven base pairs has a 3' CCA invariant sequence added transcriptionally to which the amino acid is attached. The D arm has three or four base pairs, while the T and anticodon arms have five base pairs (Dirheimer *et al.* 1995). The loops vary more in length with the anti-codon and T loops comprising seven nucleotides, while the D and V loops vary in length. The tRNAs have several invariant (the same nucleotide) and semi-invariant (always purine or always pyrimidine) nucleotides, that often are important for the tertiary structure of the tRNA (Dirheimer *et al.* 1995). Using X-ray crystallography the tRNAs were found to form a stable L-shaped tertiary structure through base pairing of nucleotides in the D and T loops (Figure 1.7B) (Robertus *et al.* 1974; Suddath *et al.* 1974). The acceptor arm thereby folds onto the T arm creating the acceptor stem and the D arm onto the anticodon arm creating the anticodon stem (Dirheimer *et al.* 1995).

1.4.2.2. tRNA expression

Unlike mRNAs, tRNAs are transcribed by RNA polymerase III. The eukaryotic tRNA genes have internal promoters made up of highly conserved box-A and box-B promoter elements which form the binding site for the multisubunit transcription factor TFIIIC (Sprauge 1995). TFIIIC recruits TFIIIB to a ~50bp conserved sequence pattern upstream of the transcription start site (Giuliodori *et al.* 2003). TFIIIB forms a stable complex with the DNA and recruit RNA polymerase III promoting multiple rounds of transcription initiation. Transcription is terminated at a short run of T residues and is dependent on upstream promoter elements in the TFIIIB binding site (Sprauge 1995). The TATA-box binding protein (TPB) is a component of TFIIIB that binds to a TATA-like sequence and is necessary for transcription (Dieci *et al.* 2007). This region has also been implicated in regulation of transcription and tissue specific expression of tRNAs (Sprauge 1995). A number of viruses up-regulate RNA polymerase III transcription. The adenovirus E1a protein increases the amount of TFIIIC; thus increasing the transcription of RNA polymerase III genes such as tRNAs and VAs (Berger and Folk 1985; Yoshinaga *et al.* 1986). EBV induces TFIIIC and BDP1, one of the subunits of TFIIIB, stimulating transcription of the EBERs as well as other RNA polymerase III transcripts such as tRNAs (Felton-Edkins *et al.* 2006). In addition, transcription of tRNAs is

up-regulated in cancers by oncoproteins such as c-Myc, while controlled by tumour suppressors (White 2008). Up-regulated tRNA expression, in particular the initiation tRNA ($tRNA_i^{Met}$) has been implicated in cellular transformation (Marshall *et al.* 2008)

Following transcription the tRNAs go through further processing, e.g. removal of extra 3'and 5' sequences, modification of residues, excision of any introns, and the addition the CCA sequence, which requires several enzymes.

1.4.2.3. tRNA functions

1.4.2.3.1. Translation

The tRNAs function during translation is well known and will not be described in detail here. During translation the tRNAs interact with several proteins and RNAs, some are specific for that type of RNA and some interact with all tRNAs; thus requiring highly conserved regions. The attachment of the correct amino acid to the tRNA requires interaction between the correct aminoacyl-tRNA synthetase and the anticodon loop (which specifies the amino acid), acceptor arm with the discriminator nucleotide at position 73, as well as individual nucleotides in the D and T arms (Meinnel 1995). Through associations with the ribosome and different factors the tRNAs recognise the codon sequence in the mRNA through complementary base-pairing with the anticodon and line up the amino acids, forming the polypeptide.

1.4.2.3.2. Amino acid starvation

It is important for the survival of the cell to have sufficient amounts of aminoacylated tRNAs available. Uncharged tRNAs as a result of amino acid starvation have been found to play important roles in the regulation of protein synthesis in both eukaryotic and prokaryotic cells. In bacteria the binding of an uncharged tRNA to the ribosome stalls translation and triggers a stringent response with production of specific signalling nucleotides, (p)ppGpp, which act as global transcription regulators lowering the cell's metabolism, while over-expressing genes involved in amino acid synthesis (Jain *et al.* 2006). In gram-positive bacteria aminoacyl-tRNA synthetase genes and genes involved in amino acid synthesis have

riboswitch leader elements (T boxes) to which specific tRNAs bind that allow for monitoring of amino acid conditions. Binding of an aminoacylated tRNA to the T box leads to the formation of a terminator helix and termination of transcription. However, the binding of an uncharged tRNA leads to the stabilisation of an anti-terminator and transcription can proceed (Green *et al.* 2010). Uncharged tRNAs have also been implicated in regulation of replication of ColE1-like replicons in *E.coli*, by binding to or mediating tRNA-dependent cleaving of RNA I, a negative regulator of replication (Wang *et al.* 2006; Wegrzyn and Wegrzyn 2008).

In eukaryotic cells the response to amino acid starvation is different. The build up of uncharged tRNAs activates the protein kinase GCN2 which phosphorylates and inactivates eIF-2, leading to a reduction in global protein synthesis (Wek *et al.* 1995). In yeast phosphorylation of eIF-2 also induces translation of GCN4 mRNA, a transcriptional activator of a large number of amino acid biosynthesis genes and genes encoding aminoacyl-tRNA synthetases (Hinnebusch 2005). In mammalians the translation of the activating transcription factor 4 (ATF4) is induced, leading to activation of several genes and pathways, as well as ATF3 and ATF5, ultimately leading to regulation of gene expression at different levels, such as chromatin structure, mRNA splicing, export and translation (Harding *et al.* 2000; Jiang *et al.* 2004; Kilberg *et al.* 2005; Zhou *et al.* 2008).

1.4.2.4. tRNA genes and chromatin

tRNA genes have been shown to regulate gene expression by affecting the chromatin organisation (McFarlane and Whitehall 2009). tRNA genes can act as chromatin barriers that limit the spread of heterochromatin (silencing) into a euchromatin (transcriptional active) region in budding and fission yeast (Biswas *et al.* 2009; Donze *et al.* 1999; Donze and Kamakaka 2001; Scott *et al.* 2006; Scott *et al.* 2007; Simms *et al.* 2004). The functions of these tRNAs are dependent on the ability of the gene to be transcribed. However, in both fission and budding yeast ectopic B-box elements not linked to functional polymerase III genes have been found to act as chromatin barriers (reviewed in McFarlane and Whitehall 2009). In mammals short interspersed elements (SINES), believed to derive from tRNAs and containing B-box

elements, are thought to protect promoters from spread of heterochromatin; this was found for an Alu SINE element in transgenic mice (Willoughby *et al.* 2000).

tRNA genes have also been shown to block enhancers or silencers from affecting promoters of nearby genes in yeast (Bolton and Boeke 2003; Hull *et al.* 1994). In one study this was found to be dependent on the localisation of tRNA genes in or near the nucleolus (Wang *et al.* 2005a). Some of the ectopic B-box elements have also been found to have repressive effects on nearby genes (McFarlane and Whitehall 2009).

1.4.2.5. tRNA functions during viral infections

In retroviruses the ssRNA genome is converted into dsDNA by the reverse transcriptase (RT) for integration into the host genome. This DNA synthesis, as well as that of retrotransposons and plant pararetroviruses, is primed by specific tRNAs. In retroviruses and plant pararetroviruses the primer binding site is complementary to 18 respective 8-12 nucleotides in the 3' end of the primer tRNA, while retrotransposons can bind both the 3' end and internal regions (Marquet *et al.* 1995). However, there are also other interactions between the primer and RNA molecule which are not understood. The tRNA used for priming differs, e.g. Rous sarcoma virus (RSV) uses $tRNA^{Trp}$, and HIV-1 $tRNA^{Lys3}$ (Harada *et al.* 1975; Wakefield *et al.* 1995). The primer tRNA is selectively packaged in the virion (Jiang *et al.* 1993; Sawyer and Dahlberg 1973), and in the case of HIV-1 the cognate aminoacyl-tRNA synthetase is as well (Cen *et al.* 2001).

Bacteriophages carry tRNA genes that are thought to compensate for the codon differences in the phage and host genomes (Bailly-Bechet *et al.* 2007; Desai *et al.* 1986; Weiss *et al.* 1968).

1.4.2.6. tRNA-like molecules

Many tRNA-like molecules with structural or functional resemblance to tRNA molecules have been identified that have various functions, such as initiation and regulation of replication, intron splicing, regulation of gene expression, and tagging of abnormal proteins for proteolysis (Giege *et al.* 1998). Some of these will be discussed here.

1.4.2.6.1. Plant virus tRNA-like molecules

Plant viruses of a number of virus genera have tRNA-like structures (TLSs) at their 3' termini. Three aminoacyl identities have been identified: valine, histidine and tyrosine; however, not all of the TLSs are dependent on aminoacylation for function and the ability of aminoacylation varies between TLSs (reviewed in Dreher 2009; Florentz and Giege 1995). The TLS-containing viruses are exemplified by: Turnip yellow mosaic virus (TYMV; valin), Tobacco mosaic virus (TMV; histidine) and Brome mosaic virus (BMV; tyrosine). The TLS of TYMV is the one that most closely resembles cellular tRNAs: it has an anticodon-D stem and a pseudoknot structured acceptor-T stem that allows for the typical L-shape (Rietveld *et al.* 1983). In addition to being recognised by cellular aminoacyl-tRNA synthetases, the TLSs are adenylated by CCA nucleotidyltransferases and form ternary complexes with eEF1A elongation factor. TYMV is also cleaved by Ribonuclease P (RNase P) and is further processed by tRNA modifying enzymes (Dreher 2009; Guerrier-Takada *et al.* 1988).

Various functions have been attributed to the TLSs. The promoters for minus strand replication by the replicase are located within the TLSs opposite the 3' C of TYMV, BMV, and TMV. However, initiation of replication is not dependent on the TLS structure, though it might help to present the promoter elements in the correct conformation (Dreher 2009). The TLS of TYMV has high affinity for eEF1A and through this interaction it acts as a translational enhancer, a function that is dependent on aminoacylation (Dreher *et al.* 1999; Matsuda and Dreher 2004). However, binding of eEF1A to the TLS represses minus strand synthesis, and it is therefore speculated that the TLS down-regulates minus-strand synthesis and enhance translation until replicase levels increase and can out-compete eEF1A for binding to the TLS (Matsuda *et al.* 2004). The TLS of BMV, like that of TYMV, is also a regulator of translation. In addition it functions as a telomere with the host CCA nucleotidyltransferase maintaining intact termini and is also required for virion assembly (Barends *et al.* 2004; Choi *et al.* 2002; Rao *et al.* 1989).

1.4.2.6.2. Transfer messenger RNA

The transfer messenger RNA (tmRNA) is a bacterial molecule with features of both tRNAs and mRNAs. Aminoacylated tmRNAs recognise stalled ribosomes, move the

started polypeptide to its amino acid and replace the faulty mRNA with an ORF within the tmRNA to tag the protein for proteolysis (reviewed in Dulebohn *et al.* 2007).

1.4.2.6.3. The threonyl-tRNA synthetase gene of E.coli

The threonyl-tRNA synthetase (ThrRs) gene of *E.coli* regulates its own translation. When there is a high level of ThrRs it binds to tRNA-like structures in the operator that mimic the anticodon arm of *E.coli* $tRNA^{Thr}$, thereby blocking translation (Romby *et al.* 1996).

1.4.3. miRNAs

The first small RNA was discovered in 1993 during studies of genes controlling the timing of developmental stages of *Caenorhabditis elegans* (*C. elegans*) larva. The lin-4 gene, known to control timing, was found to not encode a protein but two small RNAs of 22 and 61nt (Lee *et al.* 1993). It was further found that the small lin-4 RNAs had sequences complementary to 3' sequences of lin-14 and that this interaction reduced the amount of lin-14 protein without affecting the mRNA levels (Wightman *et al.* 1993). Since then these small RNAs, now called miRNAs, have been found in worms, flies, and mammals, and affect many cellular pathways including control of development, cellular differentiation, proliferation and apoptosis. Dysregulation of miRNAs have been found in human disorders, including cancers (Iorio and Croce 2009). More than 700 miRNAs have been identified in human cells to date (MiRBase) and since one miRNA might have hundreds of targets, thousands of genes may be regulated by miRNAs (Selbach *et al.* 2008). Many miRNAs are conserved between species; around 50% of *C. elegans* miRNAs have homologues in humans, indicating the importance of these miRNAs (Ibanez-Ventoso *et al.* 2008).

1.4.3.1. miRNA biogenesis

miRNAs are transcribed by RNA polymerase II or III in the form of long primary miRNAs (pri-miRNAs) that can form stable hairpin structures (Borchert *et al.* 2006; Cai *et al.* 2004; Lee *et al.* 2004). It was originally thought that miRNAs were transcribed only by RNA polymerase II, and the MHV-68 miRNAs were the first

found to be transcribed by RNA polymerase III. Recent research show that tRNA or tRNA-like coding units such as Alu elements can drive expression of miRNAs in mammalian genomes and it is estimated that more than 20% of human miRNAs could be transcribed by polymerase III (Borchert *et al.* 2006). The pri-miRNA transcripts often contain several miRNA sequences clustered together, can be capped and adenylated, and encoded from non-coding sequences or from introns, exons or UTRs of protein-coding sequences (Cai *et al.* 2004; Lee *et al.* 2002; Lee *et al.* 2004; Saini *et al.* 2007). miRNA expression is under the control of transcription factors and depends on the methylation status of the gene (Weber *et al.* 2007). Mammalian miRNAs often have multiple isoforms that may have some overlapping functions, but may also have distinct functions depending on target binding and different expression patterns (Tanzer and Stadler 2004; Ventura *et al.* 2008).

Following transcription the hairpin structure with unpaired flanking regions is recognised and cleaved by the microprocessor complex, made up of at least two subunits (Figure 1.8) (Gregory *et al.* 2004). DGCR8 binds to the pri-miRNA and determines the cleavage site for Drosha, a RNase III enzyme, that makes a double stranded cleavage near the base of the hairpin generating a pre-miRNA hairpin with a 3' 2nt overhang and a 5' terminal phosphate (Han *et al.* 2004; Han *et al.* 2006; Landthaler *et al.* 2004; Lee *et al.* 2003; Zeng and Cullen 2005; Zeng *et al.* 2005). Drosha cleavage occurs co-transcriptionally and, in the case of miRNAs present within introns, prior to splicing (Morlando *et al.* 2008). Following processing by the microprocessor the pre-miRNA is exported out of the nucleus through the nuclear pore complex by a protein complex containing the nucleoplasmic transport factor Exportin-5 and RanGTP (Lund *et al.* 2004; Yi *et al.* 2003). Exportin-5 binding is not dependent on sequence, but the length of the stem and 3' overhang (Lund and Dahlberg 2006; Zeng and Cullen 2004). This interaction also protects the nuclear pre-miRNA from degradation (Zeng and Cullen 2004).

In the cytoplasm the pre-miRNA is processed by the RISC loading complex (RLC), a multi-protein complex made up of Dicer, TRBP, PACT and Argonaute-2 (Ago2) (Chendrimada *et al.* 2005; Gregory *et al.* 2005; Lee *et al.* 2006; Maniataki and Mourelatos 2005). Dicer, a RNase III enzyme, cleaves the pre-miRNA into small RNA duplexes of ~22bp, removing the hairpin loop and generating 3' 2nt overhangs

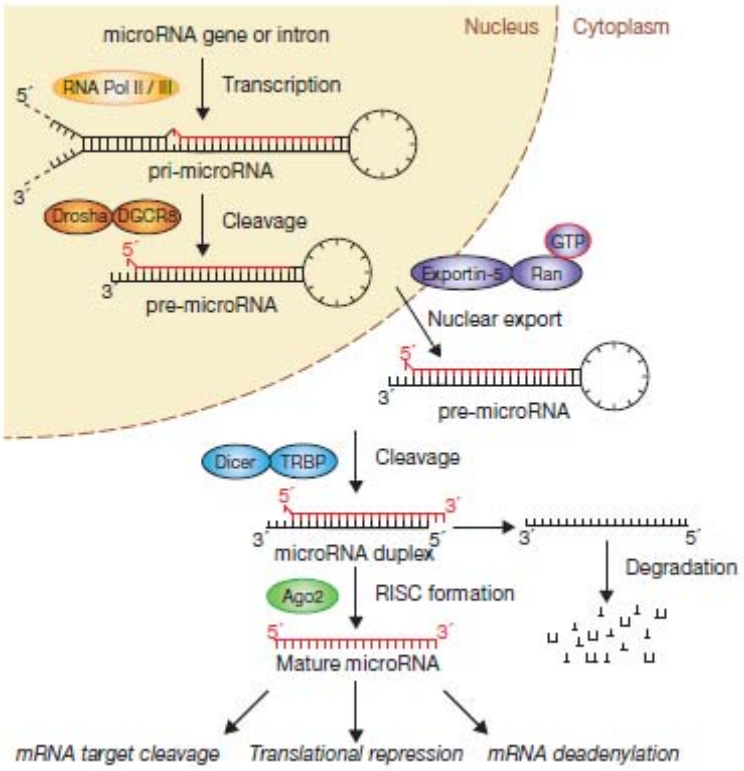

Figure 1.8 An overview of miRNA processing, showing the different processing steps. For more information see the text. Taken from Winter *et al.* 2009.

and 5' terminal phosphates (Bernstein *et al.* 2001; Elbashir *et al.* 2001; Hutvagner *et al.* 2001). Following cleavage one arm of the miRNA duplex, usually the one with less stable base pairs at its 5' end, is loaded onto Ago2, making up the core subunit of the RISC complex which is made up of over 50 proteins (Gregory *et al.* 2005; Hock *et al.* 2007; Khvorova *et al.* 2003; Liu *et al.* 2004; Maniataki and Mourelatos 2005). The RISC complex then uses the mature miRNA bound to Ago to silence fully or partially complementary target genes.

The above description of miRNA biogenesis is the general one; specific steps for individual miRNAs have been reported. In addition, each of the steps of the miRNA processing is under regulatory influence. Lin-28 has been found to inhibit both Drosha and Dicer cleavage of let-7, while let-7 targets Dicer mRNA creating a feedback loop (reviewed in Winter *et al.* 2009). Subunits of the microprocessor have been found to act as specificity factors and to regulate each others expression. In addition, factors binding individual pri-miRNAs enhance their cleavage by Drosha (Winter *et al.* 2009). By blocking or enhancing Drosha or Dicer cleavage tissue and cell type specific expression of miRNAs can be achieved (Obernosterer *et al.* 2006). The miRNAs are also subject to editing with ADAR changing adenines to inosines, which may affect processing or target specificity of the miRNA (Kim *et al.* 2009; Winter *et al.* 2009). The ends of the miRNA can also be subject to 1-2nt deletions or additions, most often uracil and adenine (Kim *et al.* 2009).

1.4.3.2. miRNA functions

In mammals the RISC complexes usually bind to partially complementary binding sites leading to translational arrest or RNA destabilisation; although Ago2 catalysed cleavage of fully complementary targets have been reported (Davis *et al.* 2005; Yekta *et al.* 2004). In addition, other types of regulation including heterochromatin formation have been reported (Bao *et al.* 2004; Kim *et al.* 2008).

Binding of the miRNA to the target usually involves the 5' seed region (nucleotides 2-8) of the miRNA, with partial pairing of the 3'end supplementing or sometimes compensating for a single nucleotide mismatch in the seed region (Bartel 2009). The binding site is most often in the 3' UTR of the mRNA, although binding to ORFs and 5' UTRs have also been reported, including miRNAs that bind

with their 3' end to the 5' UTR and 5' end to the 3'UTR of a mRNA (Bartel 2009; Lee *et al.* 2009a). Some mRNAs have multiple binding sites for the same or different miRNAs that work independently or cooperate to control protein synthesis (Bartel 2009).

The mechanism of translation repression is debated; however, inhibition of translation initiation and post-initiation steps as well as co-translational protein degradation have been reported (reviewed in Chekulaeva and Filipowicz 2009; Eulalio *et al.* 2008; Filipowicz *et al.* 2008). In addition, protein translation is inhibited by deadenylation of mRNAs leading to destabilisation and sometimes degradation or sequestering of mRNAs within P bodies (reviewed in Eulalio *et al.* 2008; Filipowicz *et al.* 2008; Nilsen 2007). During certain circumstances miRNAs are able to up-regulate the expression of genes (reviewed in Chekulaeva and Filipowicz 2009). In one example the liver specific mir-122 up-regulates Hepatitis C virus (HCV) replication when binding to the 5'UTR of the HCV RNA; however, insertion of the binding site into the 3'UTR leads to repression of replication (Henke *et al.* 2008; Jopling *et al.* 2005; Jopling *et al.* 2008).

miRNAs can act to switch off protein synthesis, but most often they fine-tune the protein expression to keep proteins at optimal levels; this means that although some proteins can be down-regulated by 50-80%, individual miRNAs often only reduce protein expression by less than 50% and often not by more than a third (Bartel 2009).

1.4.3.3. Viruses and miRNAs

The first virally encoded miRNAs were identified in 2004 in EBV (Pfeffer *et al.* 2004). Since then every herpesvirus examined have been found to express several miRNAs, with several other DNA viruses found to encode one miRNA (Table 1.3) The most likely reason that all of these viruses are nuclear DNA viruses is that Drosha cleavage takes place in the nucleus and would destroy a RNA genome encoding RNAs. A miRNA that avoids the Drosha cleavage step has been proposed for HIV-1 (Ouellet *et al.* 2008); however, this miRNA has not been found in other studies (Pfeffer *et al.* 2005). For viruses with short life cycles the use of miRNAs would be limited as the miRNAs may not have time to affect the protein pool; consistent with this DNA viruses that are capable of establishing latency or persistent

Virus family	Subfamily	Name	Number of pre-miRNAs	References
Herpesvirus	alpha	HSV-1	8	Cui *et al.* 2006; Umbach *et al.* 2008; Umbach *et al.* 2009
		HSV-2	6	Tang *et al.* 2008; Tang *et al.* 2009; Umbach *et al.* 2010
		MDV 1	14	Burnside *et al.* 2006; Yao *et al.* 2008
		MDV 2	17	Waidner *et al.* 2009; Yao *et al.* 2007
		HVT	17	Waidner *et al.* 2009; Yao *et al.* 2009
		BV	3	Besecker *et al.* 2009
		BoHV-1	10	Glazov *et al.* 2010
		ILTV	7	Rachamadugu *et al.* 2009; Waidner *et al.* 2009
	beta	HCMV	11	Grey *et al.* 2005; Pfeffer *et al.* 2005
		MCMV	18	Buck *et al.* 2007; Dolken *et al.* 2007
	gamma	EBV	25	Cai *et al.* 2006; Grundhoff *et al.* 2006; Pfeffer *et al.* 2004; Zhu *et al.* 2009
		rLCV	16	Cai *et al.* 2006
		KSHV	12	Cai *et al.* 2005; Grundhoff *et al.* 2006; Pfeffer *et al.* 2005; Samols *et al.* 2005
		RRV	7	Schafer *et al.* 2007
		MHV-68	9	Pfeffer *et al.* 2005
Polyomavirus		SV40	1	Sullivan *et al.* 2005
		SA12	1	Cantalupo *et al.* 2005
		MCV	1	Seo *et al.* 2009
		BKV	1	Seo *et al.* 2008
		JCV	1	Seo *et al.* 2008
		mPy	1	Sullivan *et al.* 2009
Adenovirus		hAV	1	Aparicio *et al.* 2006; Sano *et al.* 2006
Ascovirus		HvAV	1	Hussain *et al.* 2008

Table 1.3 List of identified viral miRNAs. Abbreviations: HSV, Herpes simplex; MDV, Marek's disease virus; HVT, Herpesvirus of Turkeys; BV, Herpes B virus; BoHV-1, Bovine herpesvirus-1; ILTV, Infectious laryngotracheitis virus; HCMV, Human cytomegalovirus; MCMV, Mouse cytomegalovirus; EBV, Epstein-Barr virus; rLCV, Rhesus Lymphocryptovirus; KSHV, Kaposi's sarcoma-associated herpesvirus; RRV, Rhesus monkey Rhadinovirus; MHV-68, Murine gammaherpesvirus 68; SV40, Simian virus 40; SA12, Simian agent 12; MCV, Merkel cell polyomavirus; BKV, BK polyomavirus; JCV, JC polyomavirus; mPy, Murine polyomavirus; hAV, Human adenovirus; HvAV, *Heliothis virescens* ascovirus.

infection have been found to encode most of the miRNAs. The viral miRNAs are expressed during lytic, latent or both stages of infection, in clusters that can be expressed differently, or scattered. The miRNAs are advantageous to the viruses as they allow regulation of specific genes, one miRNA is capable of regulating several genes, they do not take up much space in the genome, and they are non-immunogenic.

Viral miRNAs can target viral or cellular mRNAs or both (Table 1.4). Most viral mRNA targets identified encode proteins that would be targets of the host immune response (e.g. SV40 miR-S1 that cleaves the T antigen mRNAs), or viral gene regulators (e.g. HSV-1 miR-H2-3p targeting ICP0 and miR-H6 ICP4, both important for initiating productive infection) (Sullivan *et al.* 2005; Umbach *et al.* 2008). Most cellular mRNA targets are either regulators of apoptosis (e.g. EBV miR-BART5 targeting PUMA) or immunomodulators (e.g. HCMV miR-UL112-1 targeting MICB) (Choy *et al.* 2008; Stern-Ginossar *et al.* 2007). However, the effect of these viral miRNAs *in vivo* still needs to be investigated. Viral targets can lie antisense to the miRNA leading to cleavage of the mRNA (e.g. EBV miR-BART2 and the viral DNA polymerase), or just down-regulation of the protein (HSV-1 miR-H2-3p and ICP0) or show partial complementary to an mRNA in other parts of the genome (Barth *et al.* 2008; Umbach *et al.* 2008). Fully complementary cellular targets have not been found. Some viral miRNAs mimic cellular miRNAs. KSHV miR-K12-11 and MDV-1 miR-M4 have identical seed regions to the oncogenic cellular miR-155, while EBV instead induces miR-155 expression (Gottwein *et al.* 2007; Lu *et al.* 2008; Skalsky *et al.* 2007; Yin *et al.* 2008; Zhao *et al.* 2009). MHV-68 miR-M1-4 shares a seed region with murine miR-151 of unknown function, and EBV miR-BART5, rhesus lymphocryptovirus (rLCV) miR-rL1-8 and MHV-68 miR-M1-7-5p with cellular miR-18 and miR18b, which are encoded within the oncogenic miR-17-92 cluster (Gottwein and Cullen 2008).

In addition, virus infection has been shown to induce or inhibit cellular miRNAs in general or specific miRNAs, presumably to create a more optimal environment. It has been suggested that cellular miRNAs directly target viral transcripts. This seems unlikely since many cellular miRNAs are conserved between species, while viruses are not, and viruses that were not targeted by miRNAs would have been selected;

Viral targets

Virus	miRNA	mRNA target	Function of protein	Reference
EBV	miR-BART2	BALF5	DNA polymerase	Barth *et al.* 2008
	miR-BART1-5p /16/17-5p	LMP1	Signalling molecule	Lo *et al.* 2007
	MiR-BART22	LMP2A	Immunogenic antigen	Lung *et al.* 2009
HvAV	miR-1	ORF1	DNA polymerase	Hussain *et al.* 2008
SV40	miR-S1	T antigens	Transcription factors, recognised by T-cells	Sullivan *et al.* 2005
HSV-1	miR-H2-3p	ICP0	Initiate productive infection	Umbach *et al.* 2008
	miR-H6	ICP4	Initiate productive infection	Umbach *et al.* 2008
HSV-2	miR-H2-3p	ICP0	Initiate productive infection	Tang *et al.* 2009
	miR-H3/H4	ICP34.5	Neurovirulence factor	Tang *et al.* 2008; Tang *et al.* 2009
HCMV	miR-UL112	IE1	Transcription activator	Grey *et al.* 2007; Murphy *et al.* 2008
	miR-UL112	UL114	Uracil DNA glycosylase	Stern-Ginossar *et al.* 2009
KSHV	miR-K12-9*	rta	Replication and transcription activator	Bellare and Ganem 2009

Cellular targets

Virus	miRNA	mRNA target	Function of protein	Reference
KSHV	miR-K12-11 (seed miR-155)	BACH1 and others	Transcriptional suppressor	Gottwein *et al.* 2007; Skalsky *et al.* 2007
	miR-K12-6-3p + others	THBS1	Anti-angiogenic, chemoattractant etc.	Samols *et al.* 2007
	miR-K5/9/10	BCLAF1	apoptotic factor	Ziegelbauer *et al.* 2009
	miR-K1	IκBα	Inhibitor of NFκB complexes	Lei *et al.* 2010
	miR-K12-7	MICB	NK cell-surface receptor ligand	Nachmani *et al.* 2009
HCMV	miR-UL112	MICB	NK cell-surface receptor ligand	Stern-Ginossar *et al.* 2007
EBV	miR-BART5	PUMA	Proapoptotic factor	Choy *et al.* 2008
	miR-BHRF1-3	CXCL11	Chemokine, T-cell chemoattractant	Xia *et al.* 2008
	miR-BART2-5p	MICB	NK cell-surface receptor ligand	Nachmani *et al.* 2009
MDV-1	miR-M4 (seed miR-155)	BACH1 and others	Transcriptional suppressor	Zhao *et al.* 2009

Table 1.4 Viral and cellular mRNA targets of viral miRNAs. KSHV miR-K12-11 and MDV-1 miR-M4 both have seeds identical to the cellular miR-155 and target at least some of the same mRNAs.

unless the virus could take advantage of the cellular miRNAs (Mahajan *et al.* 2009). This is the case for HCV whose replication is induced by 5'UTR binding of the liver specific miR-122 (Henke *et al.* 2008; Jopling *et al.* 2005). It is also possible that viruses could use cellular miRNAs to limit viral replication and facilitate the establishment of latency. Viruses can up-regulate cellular miRNAs that are beneficial to the virus or down-regulate anti-viral miRNAs. EBV infection leads to a reduction in cellular miRNAs and following initiation of the lytic cycle the immunomodulator miR-146a is induced by LMP1 (Godshalk *et al.* 2008; Motsch *et al.* 2007). MDV-1 induces the expression of miR-221 and miR-222, which are involved in tumorigenesis (Lambeth *et al.* 2009). MCMV on the other hand down-regulates the anti-viral miR-27a and miR-27b (Buck *et al.* 2010). It is possible that the cellular miRNAs can be used as a part of the immune response against viruses by acting on cellular targets affecting the virus, without targeting the virus it self.

The herpesvirus miRNAs are generally not well conserved; the exception being EBV and rLCV which have eight miRNAs that are highly similar and encoded at a similar location in the genomes (Cai *et al.* 2006). Even though there is poor sequence conservation the miRNA locations in the genomes are conserved in closely related viruses such as HSV-1 and HSV-2, MDV-1 and MDV-2, KSHV and RRV, and HCMV and MCMV. The lack of sequence similarity does not mean that the miRNAs do not have similar effects; they could have evolved to target different regions of the same mRNA or different mRNAs in the same cellular pathway. An example is the NK cell-surface receptor ligand MICB which is a target for HCMV miR-UL122-1, EBV miR-BART2-5p and KSHV miR-K12-7 as well as cellular miRNAs, leading to reduced NK cell killing of infected cells (Nachmani *et al.* 2009; Stern-Ginossar *et al.* 2007; Stern-Ginossar *et al.* 2008). These viral miRNAs do not have any sequence homology and all target the 3'UTR at sites that do not overlap.

1.5. Project outline

The role of the vtRNAs and miRNAs of MHV-68 during infection has not been extensively characterised and their biological functions are unknown. The functions of these non-coding RNAs were examined in a previous experiment using two viruses made through insertion of five of the vtRNAs and six of the miRNAs into MHV-76, which lacks the non-coding RNAs. These viruses behaved like MHV-76 during lytic infection *in vitro* and during *in vivo* infection; like MHV-76 they were cleared more rapidly and established low levels of latency in the spleen compared to MHV-68 (Cliffe 2005).

The aim of this study was to investigate the role of the non-coding RNAs during latent infection *in vitro*, utilising the insertion viruses. The initial objective was to determine if the mouse B-cell line NS0 was appropriate as an *in vitro* model to study the non-coding RNAs during latency and to study the expression of the vtRNAs and miRNAs. A second objective was to study the effects of the non-coding RNAs on the replication and reactivation kinetics *in vitro*. The final objective was to investigate differences in protein expression between cells latently infected with MHV-76 and insertion virus by analysing the global protein expression profiles of the cells.

It was hypothesised that by characterising the effects of the non-coding RNAs during latent infection *in vitro*, possible functions of these, as well as other non-coding RNAs would be elucidated.

2. Chapter Two: Materials and methods

2.1. Cell Culture techniques **71**
2.2. Virological methods **72**
2.3. In situ hybridisation **75**
2.4. DNA isolation and manipulation **78**
2.5. RNA isolation and manipulation **79**
2.6. Polymerase chain reaction (PCR) **80**
2.7. Agarose gel electrophoreses **82**
2.8. Northern analysis **82**
2.9. Protein techniques **84**
2.10. Stock solutions **90**
2.11. Synthetic oligonucleotides used for in vitro transcription **91**
2.12. Primers **92**

2.1. Cell Culture techniques

2.1.1. Maintenance of cell lines

All cell lines were cultured in tissue flasks (Nunc, UK) at 37°C + 5% CO_2. Baby Hamster Kidney fibroblast 21 (BHK-21) cells were maintained in Glasgow's Modified Eagle's Medium (Invitrogen, UK), containing 10% (v/v) newborn calf serum (Invitrogen, UK), 10% (v/v) tryptose phosphate broth (Invitrogen, UK), 2mM L-glutamine (Invitrogen, UK), and 100U/ml penicillin and streptomycin. NS0 and S11 cells were cultured in Rosewell Park Memorial Institute 1640 (RPMI-1640) medium (Invitrogen, UK), supplemented with 10% (v/v) fetal calf serum (Sera laboratories international), 2mM L-glutamine (Invitrogen, UK), and 100U/ml penicillin and streptomycin.

2.1.2. Harvesting and counting cells

BHK-21 cells were detached by trypsin treatment. Growth medium was decanted and cells washed with 0.02% (w/v) versene, prior to adding 0.05% (w/v) trypsin-EDTA (Invitrogen, UK). The trypsin was inactivated by addition of an equal volume of medium and the cells pelleted by centrifugation at 470 x g for 5 min at room temperature. NS0 and S11 cells were scraped down from the flask and pelleted by centrifugation at 470 x g for 5 min at room temperature. The pellet was re-suspended in medium and an aliquot diluted 1:1 with 0.4% (w/v) trypan blue (Sigma, UK). The unstained, viable cells, were counted in a haemocytometer.

2.1.3. Cytospins

The cells were counted, fixed in 4% (w/v) paraformaldehyde for 10 min, washed and re-suspended in phosphate buffered saline (PBS) to $1x10^5$ cells/ml. Subsequently, 200µl of cells were pelleted onto polylysine slides (VWR international) at 1000 rpm for 5 min using a cytospin (Shandon cytospin 2). The slides were fixed in 4% (w/v) paraformaldehyde for 15 min, washed in PBS and left to dry.

2.1.4. Transfection

Transfection of NS0 cells was preformed using a nucleofector (Lonza, UK) with a pre-optimised protocol (Amaxa, Lonza, UK). NS0 cells, cultivated in RPMI-1640 medium (Invitrogen, UK) supplemented with 10% (v/v) fetal calf serum (Sera laboratories international), 2mM L-glutamine (Invitrogen, UK), and 100µg/ml Normocin (Amaxa, Lonza, UK), were infected with viruses at a multiplicity of infection (MOI) of 5 plaque forming units (pfu)/cell, 4 days or 2 hours prior to transfection or 48 hours post transfection. For each transfection reaction $2x10^6$ cells were pelleted at 90 x g at room temperature for 10 min and the medium removed. The cell pellet was resuspended in 100µl Nucleofector solution C (Amaxa, Lonza, UK) prior to the addition of 0.5µg miRNA (miScript miRNA mimics, Qiagen), negative small interfering RNA (siRNA) (Qiagen), or 2µg plasmid DNA and 66.5pmol siGLO red (Thermo Scientific Dharmacon, UK). The cells were moved to a cuvette and transfected using programme T-005. Following transfection 500µl pre-warmed RPMI-1640 (supplemented as above) was added to the cuvette and the cells transferred to a 6-well plate with 1.4ml pre-warmed medium per well, using a plastic pipette. The plate was incubated at 37°C with 5% CO_2. The transfection efficiency was determined 24 hours post transfection by counting the number of red fluorescing cells using a fluorescent microscope.

2.2. Virological methods

2.2.1. Preparation of virus stocks

BHK-21 cells were harvested as described previously, counted, and infected at a MOI of 0.001 pfu/cell. The virus was left to infect the cells for 1 hour at 37°C while shaking. The cells were subsequently incubated in T175 flasks at $3x10^6$ cells per flask for around six days, until there was complete cytopatic effect (CPE). The cells were removed by scraping and pelleted by centrifugation at 1900 x g for 20 min at 4°C and the pellet re-suspended in PBS, in a volume of about 1/3 of the number of flasks used (e.g. 10 ml for 30 flasks). The cells were homogenised in a glass dounce 20-30 times and subsequently sonicated in an ice bath for 15 min before being pelleted by centrifugation at 1900 x g for 20 min at 4°C and the supernatant

collected. The pellet was re-suspended in 1ml of PBS and homogenised again, pelleted by centrifugation at 1900 x g for 20 min at 4°C and the supernatant pooled with the previous. The virus suspension was aliquoted and stored at -80°C.

2.2.2. Virus titration

BHK-21 cells were harvested as described previously and counted. The virus, at an unknown concentration, was ten-fold serial diluted 10^{-2} to 10^{-9} in medium, following which $2x10^6$ BHK-21 cells were added to each dilution and the tube incubated for 1 hour at 37°C while shaking. Each dilution was plated onto two 60mm Petri dishes, resulting in $1x10^6$ cells per dish. Uninfected cells were plated as negative controls for each experiment. The plates were incubated for 4 days at 37°C + 5% CO_2, following which the medium was decanted and the cells fixed with 10% (v/v) neutral buffered formaldehyde (Surgipath Europe Ltd) for 1 hour, prior to staining with 0.1% (w/v) toluidine blue (BDH Laboratory supplies). The plaques formed by the virus particles were counted by light microscope. The titre was calculated as: (no. of plaques x dilution)/ final dilution volume added to plate.

For titrations of cell associated virus, $1x10^5$ virus infected cells in 1ml medium were lysed by freeze thawing three times. The cells were centrifuged at 850 x g for 10 min at room temperature to remove cell debris, prior to serial dilution.

2.2.3. Infection of NS0 cells for virus characterisation studies

NS0 cells were harvested and $5x10^6$ cells were infected with each virus at a MOI of 5 pfu/cell, followed by incubation at 37°C for 1 hour while shaking. The cells were subsequently counted and $2x10^6$ cells incubated in two T25 flasks for each virus, in 9ml of medium. Alternatively, $3x10^6$ cells were infected with each virus in duplicate and $2x10^6$ cells incubated in T25 flasks, in 9ml of medium. A sample of the supernatant was frozen for titration of infectious virus and $1x10^5$ cells in 1ml medium frozen for titration of cell associated virus. The cells were split as appropriate and the cells harvested 5 and 9 days post infection, with some or all of the cells taken and pelleted by centrifugation at 470 x g for 5 min at room temperature. A sample of the supernatant was frozen for titration of the infectious virus produced by the viruses. The pellet was resuspended in 3ml medium and the

cells counted prior to washing the cells 3 times in medium. The cells were subsequently counted again and $1x10^5$ cells in 1ml medium frozen for titration of cell associated virus, $1x10^5$ cells taken for infective centres, and on occasions some cells taken for cytospins.

2.2.4. Infective centre assay

50, 100, and 1000 NS0 cells were co-cultivated with 10^6 BHK-21 cells in 60mm Petri dishes in 5ml complete RPMI medium for 5 days at 37°C + 5% CO_2. Following incubation the medium was decanted and the cells fixed with 10% (v/v) neutral buffered formaldehyde (Surgipath Europe Ltd) for 1 hour, before staining with 0.1% (w/v) toluidine blue (BDH Laboratory supplies). The infective centres formed by reactivating virus particles were counted by light microscope. Uninfected controls were included for each experiment.

2.2.5. GFP labelled viruses

To determine the percentage of NS0 cells infected at different MOIs, two Green Fluorescent Protein (GFP) labelled viruses were utilised, LHΔgfp and MHV-76GFP. LHΔgfp was previously constructed by co-transfection of BHK-21 cells with MHV-68 DNA and DNA containing a HCMV GFP cassette (Dutia *et al.* 2004). MHV-76GFP has a GFP cassette downstream of a murine PGK promoter in the left end of the MHV-76 genome (personal communication with Simon Talbot).

NS0 cells were infected at a MOI of 1, 5 and 10 pfu/cell with either LHΔgfp or MHV-76GFP, followed by incubation at 37°C for 1 hour while shaking. The cells were seeded out in a 24 well plate at $1x10^5$ cells/ well. At days 2 and 6 cells were harvested and cytospins made. The slides were mounted in Vectashield (Vector laboratories).

2.2.6. Cloning of infected cells

NS0 cells were infected with MHV-76 or Int9 at a MOI of 5 pfu/cell, followed by incubation at 37°C for 1 hour while shaking. The infected cells were subsequently incubated at 37°C + 5% CO_2 for 5 days, when they were cloned at 0.5 cells/well in a 96-well plate in 1ml of medium (50:50, pre-conditioned: new media). The cells were

given fresh medium and split appropriately. When the clones had grown to larger numbers, they were moved to larger plates and then flasks.

2.2.7. Staining for lytic proteins

Cytospins were washed in PBS and blocked with Cas block (Invitrogen, UK) for 30 min at room temperature. The slides were incubated with primary antibody, Rabbit A (a polyclonal sera raised against MHV-68 lytically infected rabbit cells (Sunil-Chandra *et al.* 1992b)) diluted 1/1000 in Cas block, for 2 hours at room temperature. After washing the slides 2x10 min in PBS they were incubated with the secondary antibody, biotinylated goat anti-rabbit (Sigma, UK) diluted 1/750 in Cas block, for 1 hour at room temperature. The slides were washed as previously and incubated with streptavidin/alexa fluor 488 (Invitrogen, UK) and Topro 3 (Invitrogen, UK) both diluted 1/1000 in PBS, for 45 min. Following another wash the slides were mounted in Mowiol mounting media (25% (v/v) glycerol; 10% (w/v) Mowiol 4-88 (Calbiochem); 50% (v/v) 200mM Tris-HCl (pH 8.5)).

2.3. In situ hybridisation

2.3.1. Generation of labelled RNA probe

A digoxigenin (dig) antisense probe was constructed from a plasmid (pEH1.4) consisting of nucleotides 106 to 1517, covering vtRNA1-4 (Bowden *et al.* 1997). This plasmid has both T7 and SP6 promoters.

E.coli containing the plasmid were cultured and the DNA prepared as in section 2.4.1. The plasmid DNA was digested with *Hind*III and purified with a Qiaquick® PCR Purification kit (Qiagen), according to the manufacturer's instructions. In brief, the DNA was bound to the silica-gel membrane of the column and any contaminants washed away. Five volumes of Buffer PBI was added to the sample, the solution applied to the column and the DNA bound to the membrane by centrifugation at 10 000 x g for 60 seconds, prior to washing with Buffer PE. The DNA was eluted with 50µl Buffer EB and run on a 0.8% (w/v) agarose gel, to check that complete cleavage of the plasmid had occurred.

The riboprobe was in vitro transcribed by T7 RNA polymerase using the DIG RNA labelling kit (Roche). 1µg DNA template was mixed with 1mM each of ATP, CTP and GTP, 0.65mM UTP, 0.35 DIG-11-UTP, 1x Transcription buffer and 36 units T7 polymerase, to a final volume of 20µl, and the solution incubated for 2 hours at 37°C. The reaction was stopped by addition of 2µl 0.2M EDTA (pH 8.0). The labelled RNA was precipitated by addition of 1µl yeast tRNA (1mg/ml), 2.5 volumes of cold 100% ethanol and 0.1 volumes of 3M sodium acetate (pH 5.5), followed by incubation on dry ice for at least 1 hour. The RNA was subsequently pelleted by centrifugation at 10 000 x g for 30 min at 4°C and the supernatant removed. The RNA pellet was washed in cold 70% (v/v) ethanol and air dried before being resuspended in 45µl RNase free water.

Alkaline hydrolysis was performed to digest the labelled probe to approximately 170 nucleotides. The probe was incubated with 5µl 0.4M $NaHCO_3$, 0.6M Na_2CO_3 (pH 9.8) for 47 min at 60°C. The optimum time was calculated as: $t = L_0\text{-}L_f / (K \times L_0 \times L_f)$, where t=time, L_0= initial fragment length, L_f= final fragment length and K=0.11. The digested probe was precipitated by addition of 2.5 volumes of cold 100% ethanol and 0.1 volumes of 3M sodium acetate (pH 5.5), followed by incubation at -70°C over night. Subsequently, the RNA was pelleted by centrifugation at 10 000 x g for 30 min at 4°C, the pellet washed in cold 70% ethanol and air dried prior to being resuspended in 45µl RNase free water.

The probe was quantified by visual comparison between serial dilutions of the probe to a known control. Serial dilutions of the probe at 1/10 to 1/100000 were made in RNase free water and the control dig-labelled neo antisense RNA was 10-fold serial diluted from 10µg/ml to 0.1 ng/ml. 5µl RNA was dotted onto a nylon membrane and left to air dry, prior to crosslinking with the auto-crosslink function on a Stratalinker 2400 (Stratagen, UK). The membrane was washed in buffer I (0.1M maleic acid, 0.15M NaCl, pH 7.5, 3 x 5 min), prior to blocking with buffer II (buffer I containing 0.1% (v/v) normal sheep serum), for 30 min with constant agitation. The membrane was subsequently incubated with anti-dig/alkaline phosphatase (AP) conjugated antibody (Roche, Germany) diluted 1/5000 in buffer II, for 1 hour. The membrane was washed with buffer I containing 0.3% (v/v) tween-20 (3 x 5 min), followed by

buffer III (0.1M Tris-HCl, 0.1M NaCl, 50mM $MgCl_2$, pH 9.5, 1 x 5 min). AP was detected by incubation with 5-bromo-4-chloro-3-indolyl phosphate/nitroblue tetrazolium (BCIP/NBT, Sigma UK). The approximate concentration of the probe was determined by comparison of the colour intensity of the probe to that of the control.

2.3.2. *In situ* hybridisation of cytospins

NS0 cells were infected with MHV-68 at a MOI of 5 pfu/cell, followed by incubation at 37°C for 1 hour while shaking. The infected cells were incubated at 37°C + 5% CO_2 for 5 days, when cytospins were made. Cytospins were washed in PBS three times for 10 min, prior to permeabilisation in 0.5% (v/v) Triton X-100 in PBS for 10 min at 4°C, and rinsing in PBS three times for 10 min. The slides were subsequently washed in 2 x SSC for 5 min, prior to pre-hybridisation with prehybridisation buffer (50 % (v/v) formamide; 5 x salts (0.05M EDTA; 0.05M PIPES; 0.6M NaCl, pH 6.8), 5 x Denhardt's, 0.25mg/ml salmon sperm DNA (Sigma UK, boiled for 2 min at 95°C), 0.25mg/ml yeast tRNA (Sigma, UK), 20U/ml heparin, 0.1% (w/v) sodium dodecyl sulphate (SDS)) for 1 hour at 55°C. The hybridisation buffer was made by adding 50mg/ml dextran sulphate and 200ng/ml of labelled probe to the prehybridisation buffer and the buffer was subsequently boiled for 2 min at 95°C prior to addition of 10mM DTT. The slides were incubated with the hybridisation buffer over night at 55°C, while covered with parafilm. Following hybridisation the slides were rinsed in 4 x SSC and unbound probe removed by washing with 2 x SSC (2 x15 min at 37°C), 1 x SSC (2 x15 min at 37°C) and 0.2 x SSC (2 x15 min at 55°C).

The slides were blocked in Cas block (Invitrogen, UK) for 30 min at room temperature and incubated with primary anti-dig antibody made in sheep (0.4ng/µl in Cas block, Roche) for 1.5 hours. The slides were subsequently rinsed in Tris-buffered saline (TBS; 3 x 15 min) and incubated for 1 hour with secondary biotinylated anti-sheep antibody (10ng/µl in Cas block, Vector laboratories). The slides were rinsed in TBS (3x15 min) and incubated for 45 min with streptavidin/alexa fluor 488 (Invitrogen, UK) diluted 1/1400 in TBS. The slides were again rinsed in TBS (3x15 min) followed by processing in 100% ethanol (2 x 5 min)

and xylene (2 x 3 min), prior to mounting in Vectashield mounting media for fluorescence with propidium iodide (Vector laboratories).

On some occasions Mowiol mounting media (25% (v/v) glycerol; 10% (w/v) Mowiol 4-88 (Calbiochem); 50% (v/v) 200mM Tris-HCl (pH 8.5)) was used. In that case Topro 3 (Invitrogen, UK) was added as a nuclear stain at 1/1000 in TBS, together with the alexa fluor 488.

2.4. DNA isolation and manipulation

2.4.1. Plasmid preps

E. coli containing the plasmid pEH1.4 was cultured in L-Broth and 100µg/ml ampicillin over night at 37°C in an orbital shaker. The culture was pelleted by centrifugation at 3000 x g for 5 min and the DNA extracted by alkaline lysis of the bacteria using a QIAprep Spin Miniprep kit (Qiagen), according to the manufacturer's instructions. The bacterial pellet was resuspended in 250µl Buffer P1 and 250µl Buffer P2 was added prior to mixing by inversion of the tube, lysing the bacteria. 350µl of Buffer P3 was added and the solution mixed immediately by inversions to avoid localised precipitation of DNA. The lysed bacteria were pelleted by centrifugation at 17 900 x g for 10 min and the supernatant applied to a QIAprep spin column. The DNA was bound to the column by centrifugation at 17 900 x g for 60 seconds and washed with Buffer PE, prior to elution with 50µl water.

An EndoFree Plasmid Maxi Kit (Qiagen) was used according to the manufacture's instructions to produce plasmid for transfection. In brief, the DNA was extracted by alkaline lysis and the lysate filtered through a QIA filter Maxi Cartridge. The endotoxins were removed by addition of buffer ER and the lysate loaded onto a anion exchange tip to which the plasmid DNA binds. Contaminants such as RNA and proteins were washed away prior to eluting the DNA. The DNA was further concentrated and salts removed by isopropanol precipitation.

2.5. RNA isolation and manipulation

2.5.1. microRNA isolation

Small RNAs were isolated from infected or uninfected cells with a mirVana miRNA isolation kit (Ambion, UK). This kit lyses the cells in a denaturing lysis solution, which stabilises RNA and inactivates RNases. Most cellular components are removed by an acid-phenol:chloroform extraction, and the solution is further purified by bringing the solution to 25% (v/v) ethanol and passing it through a glass-fibre filter. Larger RNAs are immobilised and smaller RNAs can be collected in the filtrate. By increasing the ethanol concentration to 55% (v/v) small RNAs become immobilised when passing the solution through a second glass-fibre filter. RNAs of ≤ 200 nucleotides are then eluted with a low ionic strength solution.

2.5.2. DNase treatment of RNA

Contaminating DNA was removed from RNA samples by recombinant turbo DNA-free (Ambion, UK). 1µg of miRNA enriched RNA was treated with 3µL (6U) Turbo DNA free in 0.1 volume 10x Turbo DNase buffer for 1 hour at 37°C. Another 3µL (6U) Turbo DNA free was then added and the reaction incubated at 37°C for 1 hour. Following the DNase treatment the reaction was stopped by the addition of 0.1 volume (at least 2 µl) inactivation reagent and the samples incubated at room temperature for 5 min. The inactivation reagent was pelleted by 5 min centrifugation at 10 000 x g and the supernatant moved to a fresh tube for RT-PCR analysis.

2.5.3. Reverse transcription of RNA

cDNA was generated from RNA using SuperScript™ III Reverse Transcriptase (Invitrogen). 8µL of DNase treated RNA was incubated with 50ng random primers and 1µL 10mM dNTP mix in a total volume of 13µL for 5 min at 65°C. The mixture was immediately chilled on ice and spun down briefly. 4µL 5x First-strand buffer, 1µL 0.1M DTT, 1µL (40 U) RNase OUT and 1µL SuperScript III RT (200U) was added to the RNA/primer mix and the reaction gently mixed by pipetting. The reaction was subsequently incubated at room temperature for 5 min and then 50°C for 1 hour prior to inactivating the reaction at 70°C for 15 min. The cDNA was

cooled on ice before the addition of 1μL (2U) *E. coli* RNase H and the reaction incubated at 37°C for 20 min to remove RNA complementary to the cDNA. 2μL cDNA was used per PCR reaction.

2.5.4. *In vitro* transcription of vtRNAs

vtRNA1, 4 and 5 templates were initially annealed with T7 promoter (vtRNA1 and 5) or forward strand (vtRNA4) by heating to 75°C for 2 min and cooling to 50°C, prior to addition of 1 μl 0.1M $MgCl_2$. The vtRNAs were subsequently transcribed using a MEGAshortscript™ kit (Ambion), which utilises T7 polymerase to *in vitro* transcribe short transcripts. Unincorporated nucleotides were removed by Micro Bio-spin® 30 columns (BioRad, UK), which purifies nucleic acids larger than 20 bases or base pairs. The vtRNAs were subsequently folded by heating to 80°C for 90 seconds, prior to cooling to room temperature and adding $MgCl_2$ to a final concentration of 20mM and placing the tubes on ice.

2.6. Polymerase chain reaction (PCR)

2.6.1. Standard PCR

60-100ng template DNA was mixed with 1x PCR buffer (20mM Tris-HCl, pH8.4; 50mM KCl, Invitrogen), 3mM $MgCl_2$, 200μM each of dNTPs and 1μM of each primer, in a final volume of 50μl. The reactions were overlaid with mineral oil (Sigma, UK) and incubated at 94°C for 3 min. The program was paused at 80°C for the addition of 1 unit of *Taq* DNA polymerase (Invitrogen). The program continued with 35-40 cycles of denaturing at 94°C for 45 seconds, annealing at 51-56°C for 45 seconds, followed by elongation for 1 min at 72°C. When all the cycles were finished the reactions were incubated at 72°C for 5 min and then allowed to cool down to room temperature.

2.6.2. Whole cells and virus stock PCR

20μl of cells or 1μl of virus stock was mixed with master mix containing 0.4μg/μl proteinase K, 1x PCR buffer (20mM Tris-HCl, pH8.4; 50mM KCl, Invitrogen), 3mM $MgCl_2$, 200μM each of dNTPs and 1μM of each primer, in a final volume of

50µl. The reactions were overlaid with mineral oil (Sigma, UK) and incubated at 65°C for 15 min to allow the proteinase K to act, followed by 95°C for 5 min to inactivate the proteinase K. The program was paused at 80°C for the addition of 1 unit of *Taq* DNA polymerase (Invitrogen). The program continued with 35-40 cycles of denaturing at 94°C for 45 seconds, annealing at 51-56°C for 45 seconds, followed by elongation for 1 min at 72°C. When all the cycles were finished the reactions were incubated at 72°C for 5 min and then allowed to cool down to room temperature. The reactions were run on a 1% agarose gel.

2.6.3. qRT-PCR for miRNAs

The levels of miRNAs in infected cells were compared using qRT-PCR, with an Invitrogen NCode miRNA First-Strand cDNA Synthesis Kit and Platinum SYBR Green qPCR SuperMix-UDG, according to a protocol optimised by Amy H Buck to use less of the reagents. A poly(A) tail was added to the 3' end to increase the size of the miRNA, prior to reverse transcribing the miRNA using a universal RT primer. dsDNA was produced using a forward primer specific to the miRNA and a universal qPCR primer, in a PCR reaction. The levels of dsDNA produced were then determined using the intercalating dye SYBR green.

Forward primers corresponding to the whole mature miRNA sequences were purchased from Invitrogen and resuspended to 100µM and aliquots of 1 µM made in PCR strips. Poly(A) tails were added to the miRNAs by incubating 4µl miRNA enriched RNA (section 2.5.1) with 1.25µl 5x miRNA Reaction Buffer, 0.625µl 25mM $MgCl_2$, 0.25µl ATP (10mM diluted 1:(1250/ng RNA used)), and 0.125µl Poly A Polymerase for 15 min at 37°C in a PCR machine. The universal primer was annealed to the polyadenylated RNA by incubating 2µl polyadenylated RNA with 0.5µl 2x Annealing Buffer and 1.5µl 25µM Universal RT primer for 5 min at 65°C and chilling the reaction on ice for 1 min. The reverse transcription reaction was set up by adding 5µl 2x First-Strand Reaction mix and 1µl Superscript III/RNase OUT enzyme mix to the RNA and the tube was incubated at 50°C for 50 min before stopping the reaction at 85°C for 5 min. The cDNA was subsequently chilled on ice. 5µl of the diluted forward primers for the Real Time PCR were added to wells of a

96-well plate (giving a final concentration of 200nM). A Real Time mastermix was set up consisting of 12.5µl 2x SYBR Green qPCR Supermix UDG, 0.5µl 10µM Universal qPCR primer and 7µl DEPC water, for each well used. 3-5µl cDNA was added to the mastermix, and 20µl of the mix added to each well. The plate was spun down and run on a MxPro3000 Real Time PCR machine (Stratagene). The reaction was started by a 50°C step for 2 min and an initial denaturing step of 95°C for 2 min, activating the Taq polymerase. 45 cycles of amplification was performed, consisting of denaturing at 95°C for 15 seconds, annealing at 60°C for 15 seconds and extension at 72°C for 20 seconds. The reaction was finished with a 1 min 95°C step and a melting curve was created by measuring the fluorescence from 55°C to 95°C.

The levels of 5S ribosomal RNA and mouse miR-16 were used to normalise the levels of amplified PCR product.

2.7. Agarose gel electrophoreses

Agarose (SeaKem®, Flowgen, UK) gels were prepared in TAE or TBE buffer at varying concentrations depending of the size of DNA examined. Ethidium bromide was added to the gel to a concentration of 0.75µg/ml. The samples were mixed with appropriate volume of 10 x loading buffer (0.25% (w/v) orange G; 0.15% (w/v) Ficoll), loaded onto the gel, and electrophoresed at 60-90V in TAE or TBE buffer, prior to visualisation of bands by UV transilluminator.

2.8. Northern analysis

2.8.1. Electrophoresis and blotting

1µg miRNA enriched RNA was mixed with an equal volume gel loading buffer II, boiled for 2-5 min at 95-100°C and loaded on 15% Polyacrylamide TBE-Urea Gels (8M Urea). The gels were electrophoresed at 180V in TBE and the RNA transferred to a nylon membrane (GE healthcare) by electroblotting. A stack of 3 blotting papers soaked in 0.5 x TBE was placed above and below the gel/membrane (soaked in 0.5 x TBE) and the RNA transferred at 200mA for 30 min. Following blotting, the RNA

was UV crosslinked to the membrane with the auto-crosslink function on a Stratalinker 2400 (Stratagen UK).

A Decade^{TM} marker (Ambion, UK) was used to determine the sizes of bands. A 150nt transcript was 5' end-labelled by T4 polynucleotide kinase and ^{32}P-ATP, and cleaved to generate a set of radiolabelled markers of 100, 90, 80, 70, 60, 50, 40, 30, 20 and 10nt. These were run alongside the samples on the gel.

2.8.2. Prehybridisation and hybridisation

The membrane was prehybridised with ULTRAhyb®-Oligo Hybridization Buffer (Ambion, UK) for 30 min at 42°C. Hybridisation was then performed by incubating the membrane with ULTRAhyb®-Oligo Hybridization Buffer and 10µl ^{32}P-UTP-labelled probe for miRNA1 over night at 42°C. Following hybridisation the membrane was washed three times at 42°C for 30 min with washing solution (2x SSC and 0.5% (w/v) SDS). The blot was wrapped in plastic film and exposed to x-ray film.

2.8.3. Generation of radiolabelled probe

The probe was generated with a *mir*Vana^{TM} miRNA probe construction kit (Ambion). Initially, a target-specific DNA oligonucleotide template was converted to dsDNA with a T7 promoter. This was done by hybridising a DNA oligonucleotide template (corresponding to the target RNA and with a 8nt sequence complementary to the T7 Promoter primer) with the T7 Promoter Primer, by incubating them at 70°C for 5 min in hybridisation buffer and then leaving them at room temperature for 5 min to allow for hybridisation to occur. Exo-Klenow, dNTPs and Klenow reaction buffer was then added and the solution incubated at 37°C for 30 min, in order to produce the dsDNA template. Next, a ^{32}P-labelled antisense RNA probe was transcribed in vitro by incubating the dsDNA template with T7 RNA polymerase, ATP, CTP, GTP, ^{32}P-UTP and transcription buffer, for 10-30 min at 37°C. The DNA template was then removed by DNase I treatment for 10 min at 37°C. Unincorporated nucleotides were removed by Micro Bio-spin® 30 columns (BioRad, UK), which purifies nucleic acids larger than 20 bases or base pairs.

2.8.4. Stripping of membranes for re-probing

The blot was rinsed in distilled water, prior to washing twice with boiling 0.1% (w/v) SDS in distilled water. The blot was then washed in 6 x SCC before pre-hybridisation.

2.9. Protein techniques

2.9.1. Protein extraction

Around $4x10^7$ cells were washed with PBS and pelleted by centrifugation at 212 x g. The pellet was resuspended in 5 pellet volumes of CE buffer (10mM HEPES, 60mM KCl, 1mM EDTA, 0.075% (v/v) NP40, 1mM DTT, 1mM Pefa block) and incubated on ice for 3 min prior to centrifuging at 100-150 x g for 4 min. The cytoplasmic extract was removed from the pellet to a clean tube and spun at max speed for 10 min to pellet any nuclei. The supernatant was transferred to a clean tube and stored at -70°C.

2.9.2. Protein fractionation

A ProteoExtract® Subcellular Proteome Extraction Kit (Calbiochem, Merck UK) was used to extract and fractionate cellular proteins, according to the manufacturer's protocol. The kit utilises the different solubilities of the cellular compartments to produce four different fractions of proteins (cytosolic, membrane/organelle, nuclear and cytoskeletal), through the addition of different extraction buffers and centrifugation.

2.9.3. Protein concentrations

The total protein concentration of protein extracts from NS0 cells was determined by bicinchoninic acid (BCA) Protein Assay (Pierce). In brief, this assay utilises the reduction of Cu^{2+} to Cu^{1+} by the peptide bonds of proteins in an alkaline solution, followed by the chelation of BCA with Cu^{1+} forming a purple-coloured product of which an absorbance can be measured. The amount of Cu^{1+} formed, and thereby the intensity of the colour, is directly proportional to the amount of protein in the sample.

0.1ml of bovine serum albumin (BSA) or sample (diluted in water, to an appropriate concentration range) was mixed with 2ml working reagent (50:1, reagent A:B) and the tubes incubated at 60°C for 30 min. After cooling to room temperature the absorbance of the samples was measured at 562nm. A standard curve was prepared by diluting BSA with the diluted sample buffer to a working range of 5-250µg/ml and plotting the absorbance against the concentration. The protein concentrations of the samples were determined by the equation produced by the Polynomial trendline of the standard curve.

2.9.4. Acetone precipitation

2-3 times sample volumes of acetone containing 60mM DTT was added to the sample. The sample was incubated at -20°C for 2 hours prior to centrifuging at 12500 x g for 15 min. The pellet was washed with cold acetone containing 20mM DTT and spun at 12500 x g for 5 min prior to air-drying the pellet.

2.9.5. SDS-PAGE gel

Proteins were separated by 12% SDS- Polyacrylamide gel electrophoresis (PAGE) to demonstrate that the protein extracts contained numerous different proteins, prior to ICAT analysis. The resolving gel (12% (w/v) acrylamide (30% acrylamide/0.8% bisacrylamide, Severn Biotech ltd.); 375mM Tris-HCl pH 8.7; 0.1% (w/v) SDS; 0.1% (w/v) ammonium persulphate; 0.1% (v/v) TEMED) was poured, layered with isobutanol and left to polymerise. The isobutanol was subsequently poured off and the gel rinsed with a small amount of stacking gel, prior to pouring the stacking gel (3.5% (w/v) acrylamide (30% acrylamide/0.8% bisacrylamide, Severn Biotech ltd.); 144mM Tris-HCl pH 6.8; 0.1% (w/v) SDS; 0.06% (w/v) ammonium persulphate; 0.1% (v/v) TEMED).

Samples and 10µl prestained protein marker (broad range 6-175 kDa, Biolabs, UK) were mixed with 5µl sample buffer (2% (w/v) SDS; 20% (v/v) glycerol; 0.125M Tris-HCl pH 6.8; 0.004% (w/v) bromophenol blue; 5% (v/v) 2-mercaptoethanol) and boiled for 5 min before loading. Gels were run in 1x Tris-Glycine SDS (Severn Biotech) at 200V until the dye front had reached the bottom of the gel.

The gels were stained in Coomassie blue for 1 hour (0.25% (w/v) Coomassie blue R250 (Sigma), 5% (v/v) acetic acid, 50% (v/v) methanol) prior to destaining (10% (v/v) acetic acid, 20% (v/v) methanol) over night.

2.9.6. Digestion of proteins in solution

10µl of protein solution was mixed with 40µl 50mM ammonium bicarbonate (ABC) and DTT added to a final concentration of 5mM. The sample was subsequently heated at 60°C for 30 min, prior to cooling to room temperature. Iodoacetamide was added to a final concentration of 15mM and the sample placed in the dark for 30 min, prior to the addition of 0.8µg trypsin and the sample incubated at 37°C for 2 hours for digestion.

2.9.7. ICAT

2.9.7.1. Cleavable ICAT ®

To investigate differences in protein expressions between cells infected with different viruses, cleavable isotope-coded affinity tag labelling (cICAT) was performed using a cICAT Reagent Kit from Applied Biosystems. This method tags the cysteines with heavy or light biotin labelled isotope-coded tags ($C_{10}H_{17}N_3O_3$), with the heavy tag containing 9x ^{13}C and the light 9x ^{12}C, thus allowing the identification and quantification of individual proteins in two samples following mass spectrometry. The kit protocol was followed with some adjustments.

The two protein samples were concentrated and cleaned separately by acetone precipitation or by using Vivaspin 500 (Sartorius group) with a molecular weight cut off of 3000, according to the manufacturer's instructions. The samples were denatured and reduced by the addition of Denaturing buffer and Reducing reagent and 10 min boiling on a heat block. The proteins were labelled by either light or heavy ICAT reagent resuspended in acetonitrile, during a 2 hour incubation at 37°C. The protein samples were subsequently combined and the proteins trypsin-digested over night at 37°C. The resulting peptides were run through a cation-exchange column to wash away TCEP (reducing agent that breaks disulfide bonds), SDS and unused ICAT reagents. The labelled peptides were selected by utilising an avidin

column to bind the biotin molecule on the isotope tag. The biotin molecule was subsequently cleaved off the tag by drying down the sample by vacuum or freeze dryer and incubation for 2 hours with cleavage reagents A and B at 37°C. The peptides were again dried down by vacuum dryer and resuspended in 0.5% (v/v) acetic acid, prior to running the sample on a LC-MS/MS system (LCQDeca or LTQ, ThermoScientific).

2.9.7.2. 1-D PAGE cleavable ICAT

The 1-D PAGE cICAT is a variation of the cICAT. The protocol for 1-D PAGE cleavable ICAT reagent applications development kit for targeted protein ID and quantification (Applied Biosystems) was followed with some adjustments. Reagents from the cICAT kit were used.

The two protein samples were concentrated and cleaned separately by using Vivaspin 500 (Sartorius group) with a molecular weight cut off of 3000 MW, according to the manufacturer's instructions. The samples were denatured and reduced by the addition of Denaturing buffer and Reducing reagent and 10 min boiling on a heat block. The proteins were labelled by either light or heavy ICAT reagent resuspended in acetonitrile, during a 2-hour incubation at 37°C. The protein samples were subsequently combined and the sample vacuum dried to reduce the volume prior to mixing with 3x loading buffer and boiling for 10 min. The sample was run on a 1.5mm 12% SDS- Polyacrylamide gel with a 5% stacking gel at 180-200V. The gel was subsequently washed in distilled water and stained with Coomassie blue (Sigma) for about 10 min before being destained. The gel was washed in distilled water for 1 hour prior to excising the bands and cutting them into small pieces (1x1mm), and storing them at -20°C. The gel pieces were subsequently washed three times in 500µl gel washing buffer (50% (v/v) Acetonitrile (ACN) in 100mM ABC) at room temperature for 20 min and dehydrated with 100µl 100% ACN for 5 min at room temperature, the solution removed and the gel pieces left to air-dry. The proteins were in-gel trypsin digested by the addition of 60µl trypsin solution (0.8µg trypsin in 60µl 50mM ABC). The gel pieces were left to rehydrate with the trypsin solution for 10 min and more 50mM ABC added if needed to cover the gel pieces. The gel pieces were left to digest over night at 32°C. The peptides were extracted by sonicating the

gel pieces for 20 min in a sonic ice water bath and the supernatant transferred to a fresh tube. A 10µl ZipTip® (Millipore, UK), that has a bed of chromatography media in the tip, was used to concentrate the sample using a table top centrifuge at 144 x g. The ZipTip® was washed with 5µl 100% methanol, followed by 10µl 0.1% (v/v) TFA, and the sample loaded onto the ZipTip®. The bound peptides were washed with 2 x 10µl 0.1% (v/v) TFA and eluted with 2 x 10µl 80% (v/v) ACN in 0.1% (v/v) TFA. The labelled peptides were purified using an avidin column according to the protocol, and the solution concentrated using a ZipTip® as above and the concentrated peptide solution dried using a vacuum dryer for 10 min. The biotin tag was subsequently cleaved off by the addition of cleavage reagents A and B and incubation for 2 hours at 37°C, and the sample vacuum dried before re-suspension in 60µl 0.5% acetic acid. The peptides were loaded onto a ZipTip®, as above, eluted and dried down in a vacuum dryer prior to loading onto the LC-MS/MS (LCQdeca or LTQ, ThermoScientific).

On some occasions the peptide extraction involved addition steps. Following the initial sonication, extraction solvent was added (50% (v/v) ACN, 0.1% (v/v) TFA) and the gel pieces sonicated for 20 min in a sonic ice water bath. This was repeated three times. In addition, on some occasions vacuum drying and freeze drying was used instead of the ZipTip® prior to loading the sample onto the avidin column, and freeze drying prior to cleaving.

2.9.8. Mass spectrometry

2.9.8.1. Matrix-assisted laser desorption/ionization (MALDI)

A Voyager DE STR MALDI–TOF MS (Applied Biosystems) was used for analysis of some protein and peptide samples. 0.5µl of sample was spotted on to a MALDI plate with 0.5µl CHCA matrix (10mg/ml CHCA (Sigma), 0.3% (v/v) TFA, 50% (v/v) ACN) for peptides and sinapinic acid matrix (10mg/ml (Sigma), 0.3% (v/v) TFA, 50% (v/v) ACN) for proteins. The spots were left to air dry prior to MALDI analysis.

2.9.8.2. LC-MS/MS analysis

A LCQdeca or LTQ (Thermo Scientific) nanoLC-MS system was used to analyse peptide samples.

The LCQdeca system consisted of a Famos autosampler, Switchos column switching unit, Ultimate nanoLC (Dionex) and LCQdeca mass spectrometer (ThermoScientific) fitted with a nanoLC ESI source interfaced to the MS with a PicoTip (New Objective). Separation of peptides was performed at 200µl/min on a PepMap C18 column (3µm particle size, 75µm x 15cm), monitored at 214nm and the hplc method controlled by Chromeleon software (Dionex). The column was equilibrated with solvent A (0.1% (v/v) formic acid) and eluted with a linear gradient from 0 to 70% solvent B (0.1 % (v/v) formic acid in 100% acetonitrile) over 45 min.

The LTQ system consisted of an Agilent 1200 Series hplc (Agilent technologies) with a Kasil sealed fused silica pre-column (Next Advance) packaged to a length of approximately 3cm with Pursuit C18 5µm particle size (Varian), and a PicoTip Emitter analytical column (New Objective) packaged to a length of approximately 20cm with Pursuit C18 5µm particle size (Varian). The column was equilibrated with solvent A (0.1% (v/v) formic acid in 2.5% (v/v) acetonitrile) and eluted with a linear gradient from 0 to 8% over 6 to 8 min; from 8 to 60% over 8 to 35 min; from 60 to 100% over 35 to 40 min; solvent B (0.1% (v/v) formic acid, 0.025% (v/v) TFA in 90% (v/v) acetonitrile) over 45 min at a flow rate of 5µl/min. The LTQ mass spectrometer (ThermoScientific) was fitted with a nanoLC-ESI source.

For both systems data dependent acquisition was controlled by Xcalibur software and database searching achieved using MASCOT software (Matrix Science).

2.10. Stock solutions

10x TBS buffer	100mM Tris-base 1500mM NaCl pH 7.5 with HCl
TBE buffer	0.44M Tris-base 0.44M Boric acid 12mM EDTA
PBS (pH 7.4)	150mM NaCl 2.5mM KCl 10mM Na_2HPO_4 1mM KH_2PO_4
20 x SSC	3M NaCl 300mM sodium citrate (pH 7.0)
50 x Denhardt's buffer	1% (w/v) Ficoll 400 1% (w/v) Polyvinylpyrrolidone 1% (w/v) Bovine serum albumin fraction V
Paraformaldehyde	4% (w/v) paraformaldehyde 10mM NaOH 1 x PBS pH 7.4 with 1M HCl filtered through a 0.45 μm membrane filter
L-broth (pH 7.5)	1% (w/v) tryptone 0.5% (w/v) yeast extract 1% (w/v) NaCl

2.11. Synthetic oligonucleotides used for in vitro transcription

miRNA Northern probe

template

TAGAAATGGCCGTACTTCCTTTCCTGTCTC

Sequence of the DNA oligonucleotide template used for making the miRNA1 probe. The template corresponds to the target RNA and also has a 8nt sequence complementary to the T7 Promoter primer, shown in red.

vtRNA transcription

T7 promoter

5'- AATTTAATACGACTCACTATA -3'

vtRNA1 reverse

5'-TGGGACCAGAGCTCGGACTTGAACCGAGAACCAGGATCGGTGACCTG
TTGCTCTACCAATTGAGCTACTCTGGCCCTATATAGTGAGTCGTATTAAAT
T-3'

vtRNA4 forward

5'-GATCCTAATACGACTCACTATAGGGTCGGGGTAGCTCAATTGGTAGAG
CGGCAGGCTCATCCCCTGCAGGTTCTCGGTTCAATCCCGGGTCCCGACGC
CA-3'

vtRNA4 reverse

5'-TGGCGTCGGGACCCGGGATTGAACCGAGAACCTGCAGGGGATGAGCC
TGCCGCTCTACCAATTGAGCTACCCCGACCCTATAGTGAGTCGTATTAG-
3'

vtRNA5 reverse

5'-TGGAACCAGGGCCCGGACTTGAACCGGAACCGACAGGATACTAGCC
TGATGCTCTACCAATTGAGCTACCCTGGCCCTATATAGTGAGTCGTATTA
AATT-3'

The T7 promoter is shown in red and the 3' CCA coding sequence in blue.

2.12. Primers

Forward (F) Reverse (R)	Primer pair	Anneal temp	Amplified region
ORF46-F ORF46-R	5'- CAT GCT TAC TGC CAT TGA TCA G -3' 5'- GGT TTG GCC TTT AGT GTT CAT G -3'	55°C	ORF 46
vtRNA1-F vtRNA1-R	5'- TAGAGCAACAGGTCACCGATC -3' 5'- TGGACCCACTTCCTCGACCAG -3'	56°C	vtRNA1 nt 146-215 70bp product
vtRNA2-F vtRNA2-R	5'- GGTAGAGCAGCGGTTCCT -3' 5'- ACTCCCCCTCTCAACCA -3'	56°C	vtRNA2 nt 505-573 69bp product
vtRNA4-F vtRNA4-R	5'- GCGGCAGGCTCATC -3' 5'- ATCTCAACTCTGCGTCGG -3'	56°C	vtRNA4 nt 1205-1266 62bp product
vtRNA5-F vtRNA5-R	5'- TAGAGCATCAGGCTAGTA -3' 5'- CTCCACCTTTAACCAG -3'	51°C	vtRNA5 nt 1607-1669 63bp product
vtRNA8-F vtRNA8-R	5'- CCCATCCTGTTGGTT -3' 5'- CGCGGGTAGCTAGTC -3'	51°C	vtRNA8 nt 5418-5471 54bp product

3. Chapter Three: Characterisation of viruses

3.1. Aims **94**
3.2. Determining the percentage of infected NS0 cells **96**
3.2.1. GFP labelled viruses 96
3.2.2. *In situ* hybridisation 97
3.2.3. Cloning of infected cells 100
3.2.4. Staining for lytic proteins 100
3.3. miRNA expression **103**
3.3.1. Northern blot analysis 103
3.3.2. qRT-PCR 105
3.4. vtRNA expression **109**
3.5. Discussion **109**

3.1. Aims

The aim of this project was to investigate the functions of the viral tRNAs and miRNAs encoded by MHV-68. The natural deletant virus MHV-76 is useful for this purpose as it is missing these genes. By infecting cells with MHV-68 and MHV-76 and comparing the phenotypes (cell numbers, percentage of reactivating virus and amount of infectious virus), as well as gene and protein expression, a possible function for the viral tRNAs and miRNAs might be found. However, MHV-76 is also missing the four unique genes M1-M4, meaning that any phenotype found could be the action of any of these proteins. M2, M3 and M4 are all important for the establishment of latency (Bridgeman *et al.* 2001; Evans *et al.* 2006; Geere *et al.* 2006; Jacoby *et al.* 2002; Macrae *et al.* 2003; Simas *et al.* 2004). M2 also promotes reactivation (Herskowitz *et al.* 2005; Jacoby *et al.* 2002), while M1 suppresses reactivation from latency (Clambey *et al.* 2000; Evans *et al.* 2008). To overcome this MHV-76 can be utilised to construct a recombinant knock-in virus, by re-inserting the genes of interest into the left end of the genome without the risk of disrupting any viral genes. This has previously been done in this laboratory, by inserting the M4 ORF to look at the role of the M4 gene during infection (Townsley *et al.* 2004), as well as inserting vtRNAs1-5 and miRNAs1-6 (pers commun Yvonne Ligertwood; Cliffe 2005). Two independent insertion viruses were made in our laboratory by using the recombinant cassette pL2a5, consisting of vtRNAs1-5 and miRNAs1-6 flanked by partial M4 and ORF4 from MHV-76 and a *Pst*I fragment of the terminal repeats (Figure 3.1). These viruses, named Int2 and Int9, will serve as important tools to investigate the functions of the non-coding RNAs, since the only difference between MHV-76 and the insertion viruses is the vtRNAs and miRNAs. As a control a revertant virus made from Int9 was constructed by recombination using a cosmid (cM1) covering part of the MHV-76 genome from nt115587 to nt26842 (Macrae *et al.* 2001). This virus was plaque purified and analysed by Southern hybridisations and it was determined that the vtRNAs had been removed from the insertion virus and the genome reverted back to that of MHV-76 (Cliffe 2005).

A mouse myeloma B-cell line, NS0, was used to study latent infection. MHV-68 establishes long-term latency in B-cells *in* vivo and NS0 cells have been shown

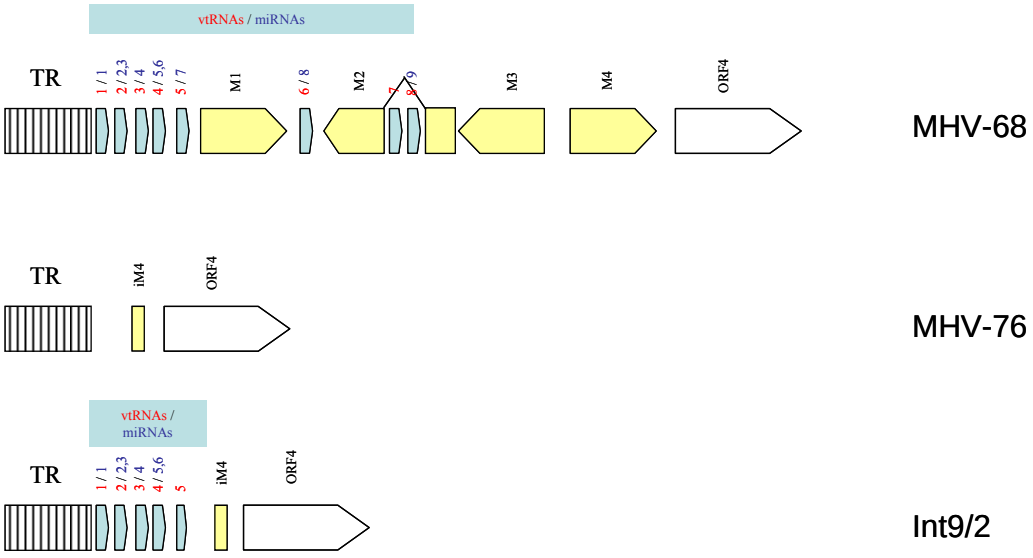

Figure 3.1 Diagram showing the differences between MHV-68, MHV-76 and the insertion viruses (Int9 and Int2) in the left side of the genome.

previously to support latent infection (Sunil-Chandra *et al.* 1993). Prior to any major experiment, infection of NS0 cells was examined to ensure this provided a suitable model to study latent infection.

To be able to use the insertion viruses to compare subtle differences in protein expression and phenotypes of virus infected cells during latent infection, a very high percentage of cells need to be infected. It was not known how the infectivity of BHK cells, on which virus titration was performed, compared to that of NS0 cells. In addition, it was not known if the different viruses infected the same proportion of cells. Therefore, the percentage of infected NS0 cells needed to be determined.

The insertion viruses have previously been shown to express the vtRNAs during lytic infection by RT-PCR and the levels of expression found to be similar to that of MHV-68 by northern blot analysis using a probe specific for vtRNA 1-4 (Cliffe 2005). However, it had not been confirmed that the insertion viruses express the vtRNAs during latent infection of NS0 cells. Further, the insertion viruses had not been shown to express the miRNAs. The miRNAs are known to be expressed in latently infected S11 cells (Pfeffer *et al.* 2005); however, their expression had not been shown in MHV-68 infected NS0 cells or during lytic infection. Hence, the expression of the vtRNAs and miRNAs during lytic and latent infection was investigated.

3.2. Determining the percentage of infected NS0 cells

3.2.1. GFP labelled viruses

The initial experiment to determine the number of infected NS0 cells utilised GFP-labelled viruses, LHΔgfp and MHV-76GFP. LHΔgfp is a recombinant MHV-68 virus which carries a CMV-GFP cassette in the left end of the genome resulting in a deletion of nt 1-3223 (Dutia *et al.* 2004). The MHV-76GFP virus has a GFP cassette downstream of a murine PGK promoter (for the house keeping gene phosphoglycerate kinase) in the left end of the genome (pers commun Simon Talbot).

NS0 cells were infected with the two viruses at a MOI of 1, 5 and 10 pfu/cell and cytospins were made at days 2 and 6 post infection. The GFP expressing cells were

counted using a fluorescent microscope at 40x magnification. MHV-76GFP did not generate any visible fluorescence. The reason for this is unknown, though it has been observed previously with this virus in NS0 cells. This virus has a promoter for a house keeping gene that should not be affected by latency. LHΔgfp did result in fluorescent cells; however, at a much lower level than expected (Figure 3.2). Since the virus has a CMV promoter that might be shut down during latency more cells could be infected but are not expressing the fluorescence. The best approach would be to infect the cells with the wild-type virus to avoid any effects of the inserted cassette and promoters.

A MOI of 10 was found to affect the cell viability and since a MOI of 5 pfu/cell has previously been used in published studies (Simas *et al.* 1999; Sunil-Chandra *et al.* 1993) it was decided that this MOI would be used for future experiments.

3.2.2. *In situ* hybridisation

To detect MHV-68 infected cells within a population of cells, *in situ* hybridisations were carried out with a dig-labelled anti-sense probe consisting of nucleotides 106 to 1517, covering vtRNA1-4. The vtRNAs are commonly used as markers for latent infection as they are expressed at high levels (Bowden *et al.* 1997). In addition, there are currently no antibodies for any of the latent proteins.

NS0 cells were infected with MHV-68 at a MOI of 5 pfu/cell and at day 5 post infection they were harvested and cytospins made. Initially the dig-labelled probe was detected by anti-dig/AP conjugated antibody and BCIP/NBT (results not shown). However, this approach was not sufficiently sensitive and a fluorescent antibody was used instead which allowed the use of confocal microscopy, giving greater resolution. A primary sheep anti-dig antibody was used to detect the dig-labelled probe, followed by a secondary biotinylated anti-sheep antibody and streptavidin/alexa fluor 488. The slides were blocked in Cas block (Invitrogen, UK), as this gave the least background staining. The majority of MHV-68 infected NS0 cells were positive for vtRNAs (Figure 3.3), meaning that they were virus infected. The vtRNAs appeared to localise in the cytoplasm and be peri-nuclear, which is consistent with previous findings in latently infected S11 cells (Cliffe 2005).

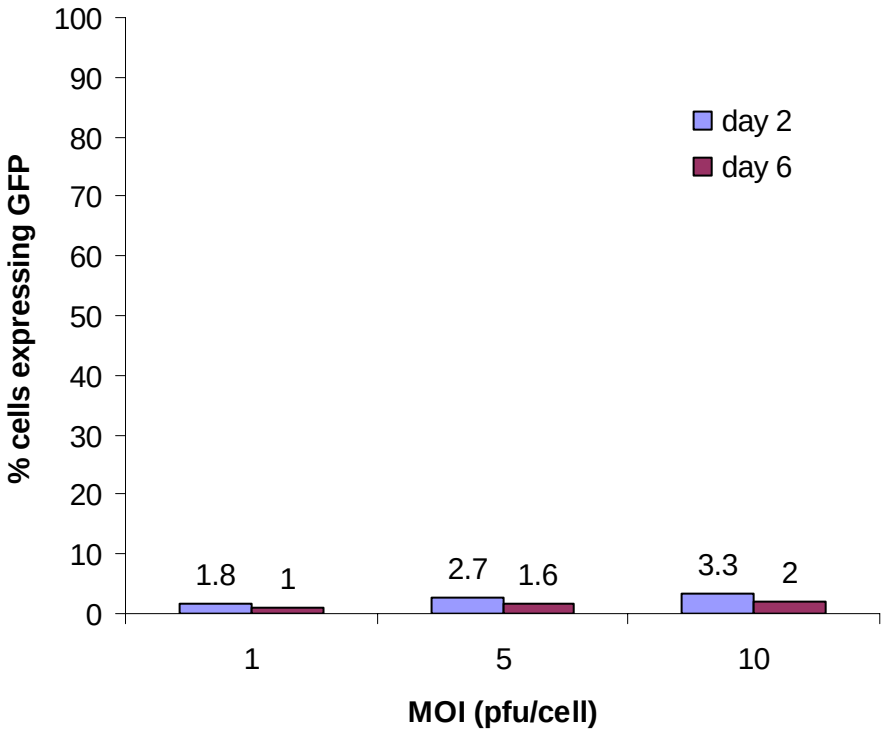

Figure 3.2 Percentage of NS0 cells expressing GFP, 2 and 5 days post infection with LHΔgfp at a MOI of 1, 5 and 10 pfu/cell. The GFP expressing cells were counted using a fluorescent microscope at 40x magnification.

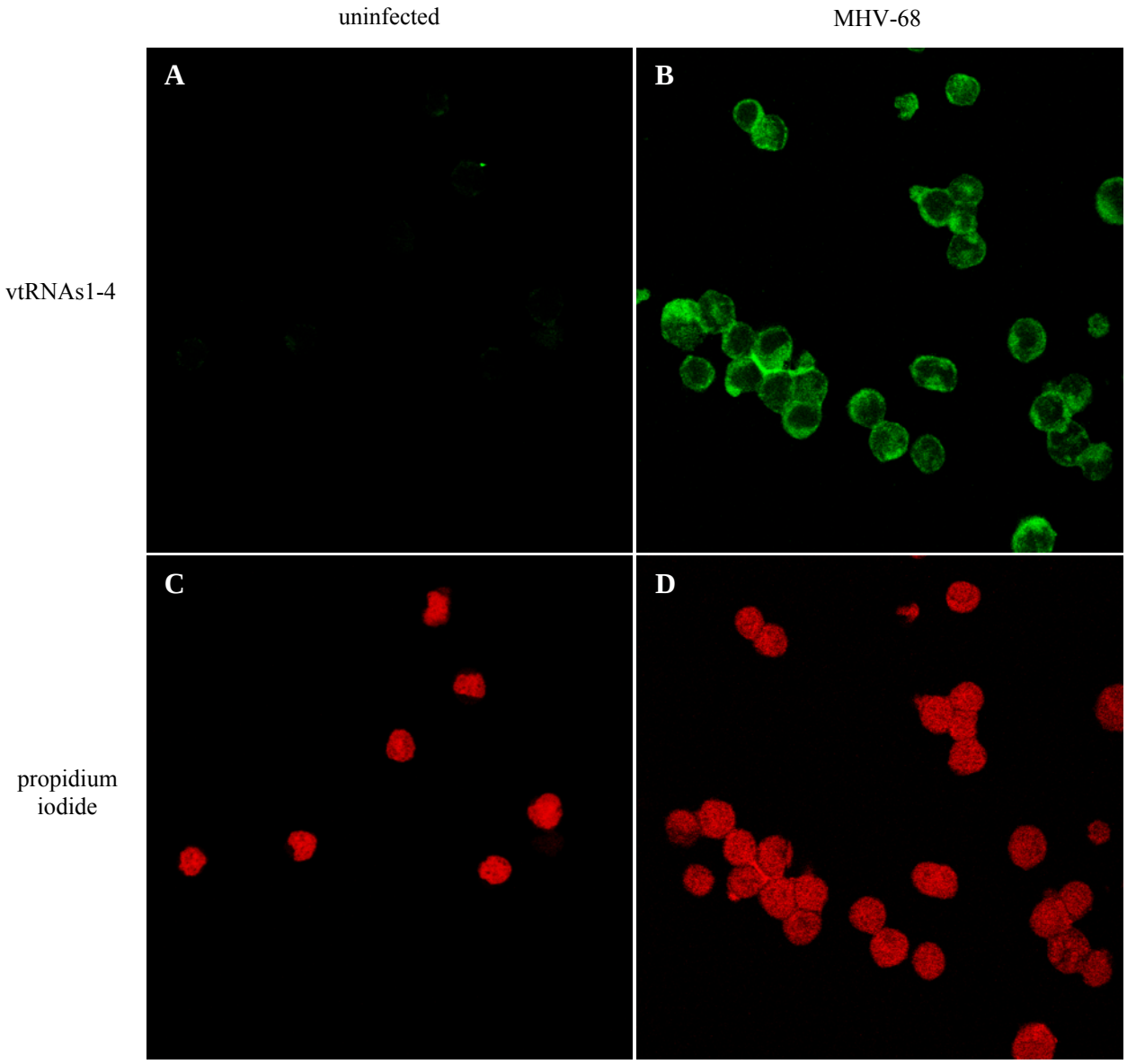

Figure 3.3 *In situ* hybridisation for vtRNAs1-4 on uninfected NS0 cells (A and C) and NS0 cells infected with MHV-68 at a MOI of 5 pfu/cell (B and D). The dig-labelled probe was detected by a primary anti-dig antibody, a secondary biotinylated antibody, and streptavidin/alexa fluor 488 (A and B). The cells were nuclear stained by propidium iodide (C and D). Confocal microscope was used at x63 magnification.

As a positive control *in situ* hybridisation was also carried out on S11 cells with and without the vtRNA probe (Figure 3.4). The S11 cells were positive for vtRNAs after *in situ* hybridisation with the probe and again the vtRNAs seemed to localise in the cytoplasm. There was some non-specific fluorescence around the edges of the S11 cells even when no probe had been used for the *in situ* hybridisation (Figure 3.4). The cause of the slightly high background was found to be the secondary antibody. As no alternative antibody was available the antibody was titred; however, a lower concentration of antibody led to a loss of signal (results not shown).

3.2.3. Cloning of infected cells

Another method of generating a very high percentage of virus infected cells would be to clone infected cells. NS0 cells were infected at a MOI of 5 pfu/cell with MHV-76 or Int9 and incubated for 5 days before being cloned at 0.5 cells/well in a 96-well plate. Wells with only one clone were kept growing and the cells moved to larger plates and eventually flasks as the cells grew in numbers. PCR was carried out to determine if the clones were virus infected using primers for ORF 46, a viral uracil DNA glycosylase (Virgin *et al.* 1997), and the products visualised on a 1% agarose gel. Of the 12 clones tested (six MHV-76 and six Int9) all were positive for viral DNA (Figure 3.5), indicating that a very high percent of cells are infected at a MOI of 5 pfu/cell.

Although the clones would give a high number of infected cells they would not represent a population of cells; any phenotypes found could be a feature of that particular clone. Since a high percentage of infected cells could be achieved in a diverse population of cells, it was decided that the clones would not be used for further analysis.

3.2.4. Staining for lytic proteins

During latent infection a small number of cells will reactivate and cause a lytic infection. Around 3% of S11 cells and 5% of MHV-68 infected NS0 cells undergo spontaneous reactivation (Nash *et al.* 2001; Usherwood *et al.* 1996a). To determine the percentage of lytically infected cells, staining was performed using a polyclonal serum raised against lytically infected rabbit cells. NS0 cells were infected

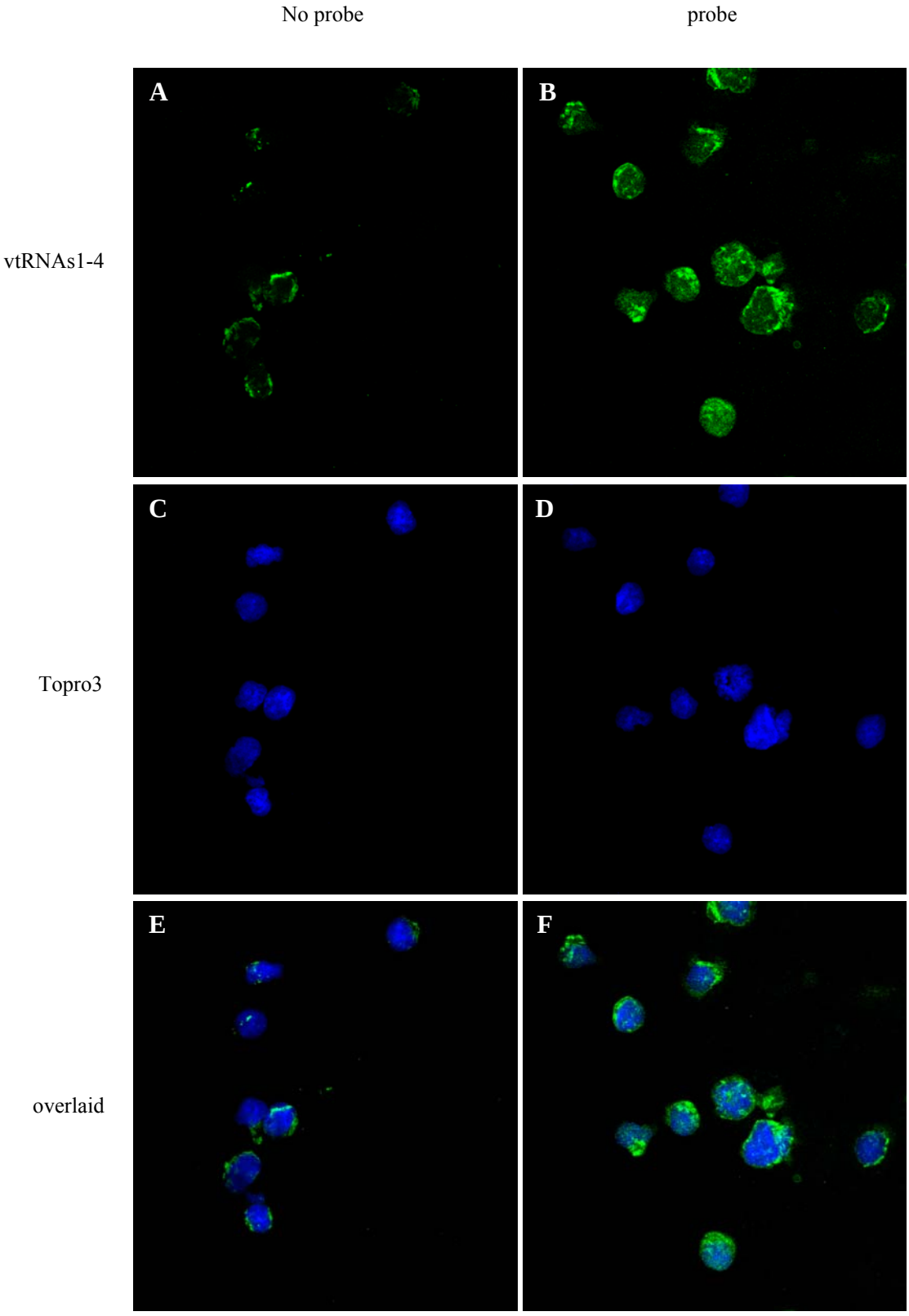

Figure 3.4 *In situ* hybridisation for vtRNAs1-4 on S11 cells without probe (A, C and E) and with probe (B, D and F). The dig-labelled probe was detected by a primary anti-dig antibody, a secondary biotinylated antibody, and streptavidin/alexa fluor 488 (A and B). The cells were nuclear stained by Topro3 (C and D), with E and F showing the alexa fluor and nuclear stain overlaid. Confocal microscope at 63x magnification.

MHV-76 clones

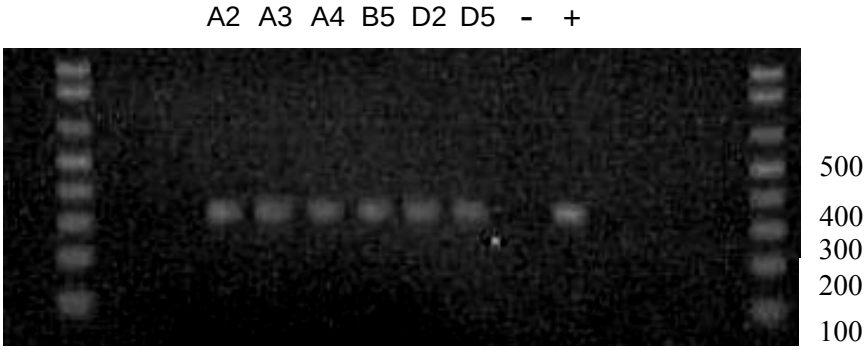

Int9 clones

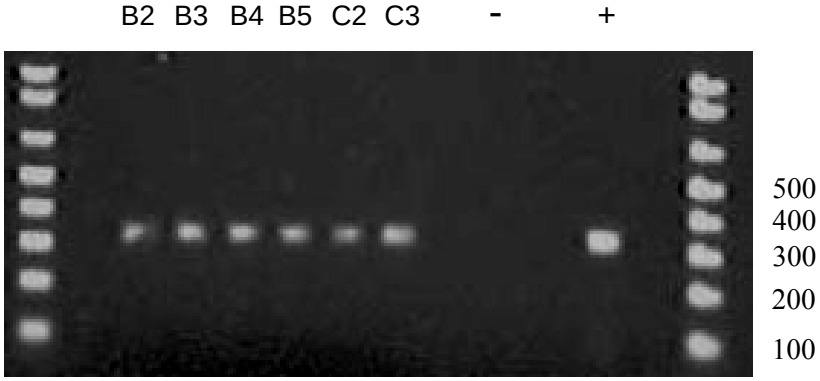

Figure 3.5 Identifying MHV-76 and Int9 infected clones by PCR analysis with primers for ORF46. The PCR products were visualised on a 1% agarose gel. The size of molecular weight markers in bp is shown to the right. Water control (–) and viral DNA as a positive control (+) were included in the PCR reaction.

with MHV-68, MHV-76, Int9, Int2 and revertant virus at a MOI of 5 pfu/cell and at day 5 post infection they were harvested and cytospins made. A secondary biotinylated anti-rabbit antibody and streptavidin/alexa fluor was used to detect the antibodies that had bound to viral antigens. The number of positive cells was counted using a fluorescent microscope at x40 magnification.

The antibodies bound weakly to latently as well as lytically infected cells. However, there were clear differences, with brightly stained cells indicating lytic infection (Figure 3.5). The serum was raised during a lytic infection but may contain antibodies to antigens expressed during latent infection. However, this proved useful as it confirmed that a very high percentage of cells are infected at a MOI of 5 pfu/cell. The percentage of lytically infected cells was estimated as 1% for MHV-68, 8% for MHV-76, and 0.1% for Int9 infected NS0 cells.

3.3. miRNA expression

3.3.1. Northern blot analysis

To ensure that MHV-68 and the insertion viruses express the miRNAs during latent infection of NS0 cells and during lytic infection, northern blot analysis was performed using a probe for miRNA1.

Small RNAs were extracted from lytically infected BHK cells and latently infected NS0 cells that had been mock-infected or infected with MHV-68, MHV-76, Int9 or revertant virus at a MOI of 5 pfu/ml for 24 hours or 5 days respectively, using a mirVana miRNA isolation kit (Ambion, UK), as well as from latently infected S11 cells. The RNA was separated by electrophoresis on a 15% TBE-Urea gel, transferred to a nylon membrane by electroblotting, and hybridisation carried out using ULTRAhyb®-Oligo Hybridization Buffer (Ambion, UK) and a radiolabelled probe specific for miRNA1. The probe was generated using a *mir*Vana™ miRNA probe construction kit to *in vitro* transcribe the probe using T7 RNA polymerase. A Decade™ marker (Ambion, UK) was used to determine the sizes of bands.

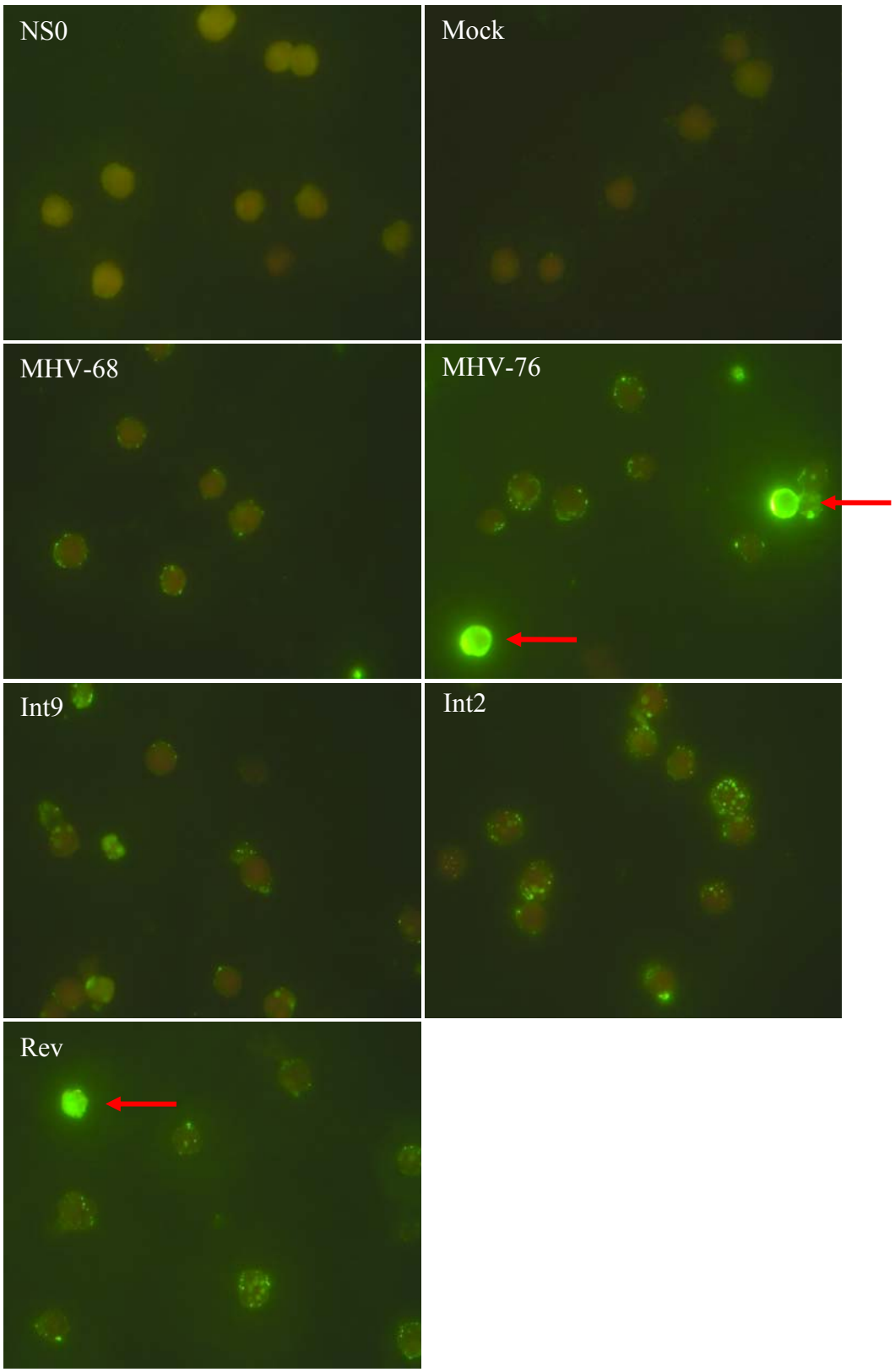

Figure 3.6 Staining of virus infected cells using a polyclonal serum raised against lytically infected rabbit cells. A secondary biotinylated anti-rabbit antibody and streptavidin/alexa fluor was used to detect the antibodies that had bound to viral antigens. The stained cells were visualised using a fluorescent microscope at x100 magnification. The red arrows indicate lytically infected cells.

The northern analysis confirmed that latently infected S11 cells express miRNA1 (Figure 3.7). It also confirmed that MHV-68 and Int9 express miRNA1 during lytic infection of BHK cells, while, as expected, MHV-76 and the revertant do not. In addition it showed that miRNA1 is expressed in NS0 cells latently infected with MHV-68; however, not with Int9. This was surprising as miRNA1 was expressed by Int9 during lytic infection.

To confirm the lack of miRNA1 expression another northern blot analysis was performed on RNA from latently infected NS0 cells. The cells were infected with the viruses, including the second insertion virus Int2, at a MOI of 5 pfu/cell and small RNAs extracted 24 hours and 5 days post infection. In addition, 2μg of RNA from Int9 infected NS0 cells was loaded into one well, instead of the usual 1 μg, to see if the miRNA was expressed at a very low level. The second northern blot confirmed the previous result; while MHV-68 expressed miRNA1 during latent infection of NS0 cells both 24 hours and 5 days post infection, the insertion viruses did not (Figure 3.8). To further confirm this result and to examine the expression of the other miRNAs, a more sensitive qRT-PCR analysis was performed.

3.3.2. qRT-PCR

To confirm that the insertion viruses do not express miRNA1 and to determine if the other miRNAs are expressed, a qRT-PCR analysis for the miRNAs was performed using an Invitrogen NCode miRNA First-Strand cDNA Synthesis Kit and Platinum SYBR Green qPCR SuperMix-UDG. Using this kit a poly(A) tail was added to the 3' end and the miRNA reverse transcribed using a universal RT primer. dsDNA was produced using a forward primer specific to the miRNA and a universal qPCR primer in a PCR reaction. The levels of dsDNA produced were determined using the intercalating dye SYBR green.

In an initial experiment small RNAs extracted from mock and MHV-68 infected NS0 cells using a mirVana miRNA isolation kit (Ambion, UK) were used. All six miRNAs examined were detected in all MHV-68 infected cells and none in mock-infected cells (Figure 3.9); however, the dissociation curve for miRNA2 was not good and no specific product seemed to be detected (see Appendix Figure 8.1). This is possibly because of the high C content of the miRNA and it was decided that this

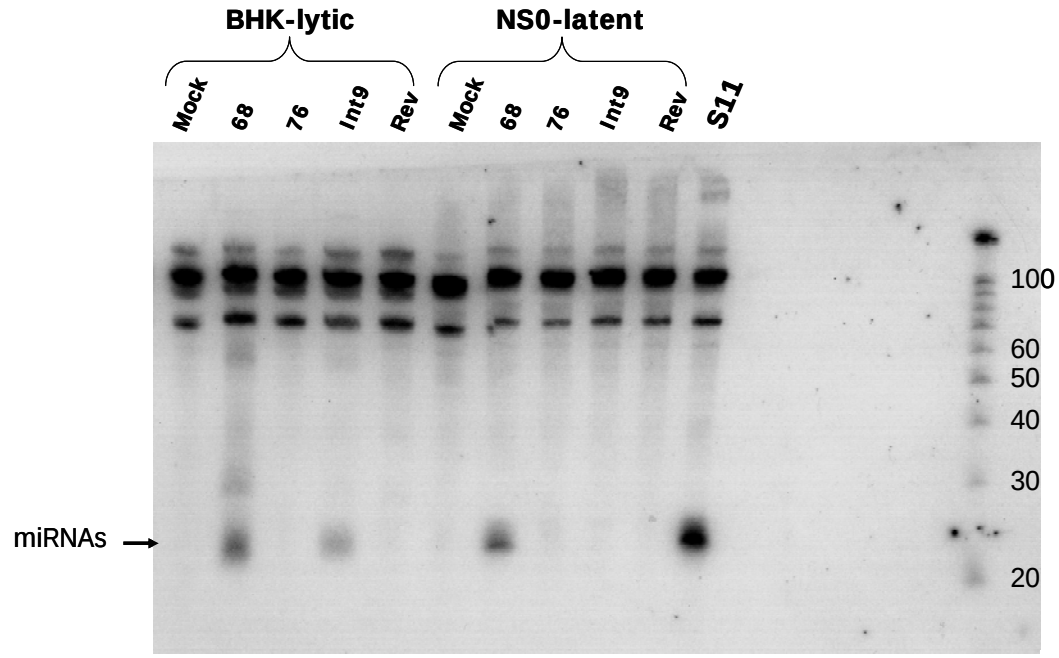

Figure 3.7 Northern blot analysis of miRNA1 expression by MHV-68, MHV-76, Int9 and revertant (Rev) viruses during lytic and latent infection. BHK cells were infected for 24 hours and NS0 cells for 5 days at a MOI of 5 pfu/cell and small RNAs extracted with a mirVana miRNA isolation kit (Ambion, UK). Hybridisation was carried out using ULTRAhyb®-Oligo Hybridization Buffer (Ambion, UK) and a radiolabelled probe specific for miRNA1. A Decade™ marker (Ambion, UK) was used to determine the sizes of bands.

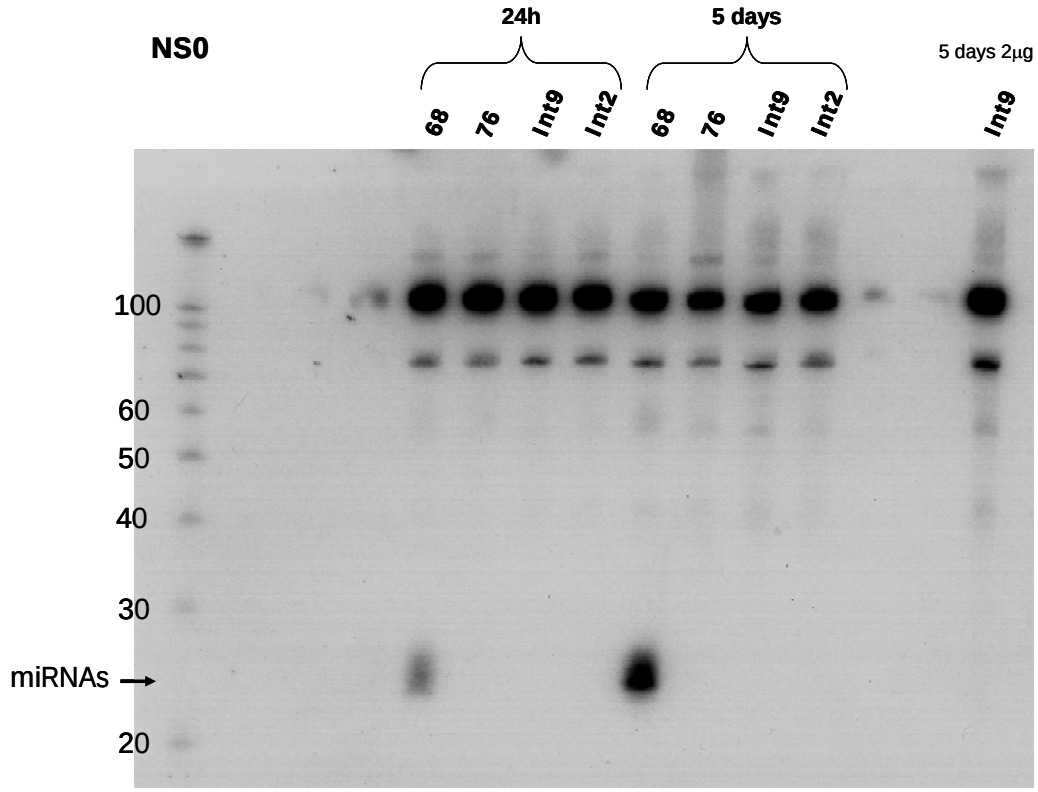

Figure 3.8 Northern blot analysis of miRNA1 expression by MHV-68, MHV-76, Int9 and Int2 during latent infection. NS0 cells were infected for 24 hours or 5 days at a MOI of 5 pfu/cell and small RNAs extracted with a mirVana miRNA isolation kit (Ambion, UK). One well was loaded with twice as much RNA, 2μg, from Int9 infected NS0 cells. Hybridisation was carried out using ULTRAhyb®-Oligo Hybridization Buffer (Ambion, UK) and a radiolabelled probe specific for miRNA1. A Decade™ marker (Ambion, UK) was used to determine the sizes of bands.

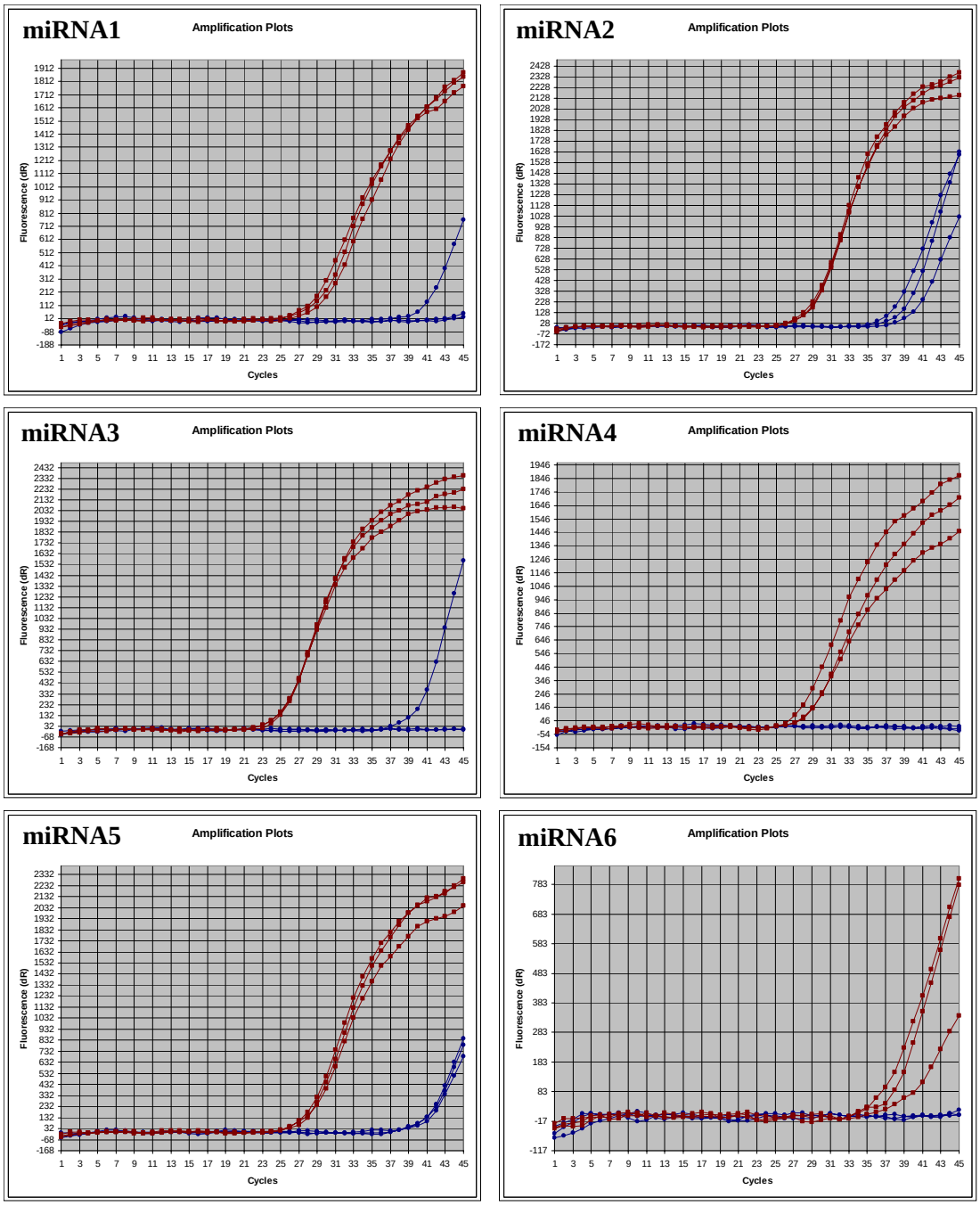

Figure 3.9 qRT-PCR amplification plots for miRNA1-6 on RNA from mock (blue) and MHV-68 (red) infected NS0 cells.

miRNA could not be quantified using this method. The miRNA5 primer seemed to pick up some non-specific products as well (see Appendix Figure 8.1); however this primer was used for further analysis to see if the dissociation curve could be improved.

The miRNA expression by the insertion viruses, Int9 and Int2, during latent infection was subsequently compared to that of MHV-68 by qRT-PCR for miRNA1, 3, 4, 5 and 6. The relative quantity of the miRNAs was normalised against cellular 5S ribosomal RNA, to compensate for differences in the amount of RNA used for the reverse transcription. The qRT-PCR results confirmed the previous northern analyses; the insertion viruses express miRNA1 at very low levels during latent infection (Figure 3.10). In addition, miRNA3, 4, 5 and 6 were all expressed at a lower level than by MHV-68. This time the dissociation curve for miRNA5 was slightly better, but amplification of some non-specific products still occurred (see Appendix Figure 8.2). However, it could still be concluded that NS0 cells latently infected with the insertion viruses contain less of the miRNAs than MHV-68 infected cells.

3.4. vtRNA expression

To ensure that the insertion viruses express the vtRNAs during latent infection, RT-PCR analysis was carried out on miRNA enriched RNA from mock-infected NS0 cells or infected with MHV-68, MHV-76, Int9, or Int2 for five days. The RNA was DNase treated and RT-PCR carried out using primers specific for four of the vtRNAs and the products visualised on a 2% agarose gel. All four vtRNAs examined were expressed during latency (Figure 3.11).

3.5. Discussion

Two insertion viruses had previously been made by inserting five of the vtRNAs and six of the miRNAs into the natural deletant virus MHV-76. This generated two viruses with the only difference from MHV-76 being the vtRNAs and miRNAs. In addition a revertant virus had been made by reverting the insertion virus Int9 back to MHV-76 genome. These were to be used to investigate the functions of the

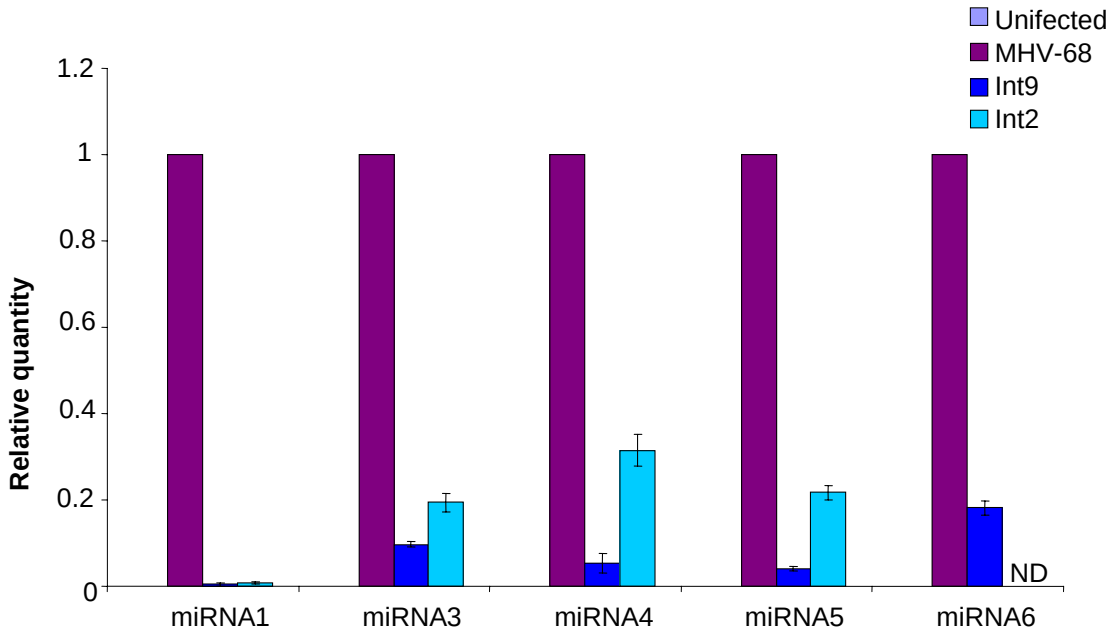

Figure 3.10 qRT-PCR for miRNAs. Showing the levels of miRNAs expressed by the insertion viruses (Int9 and Int2) relative to the expression by MHV-68. Error bars show the standard deviation. Values were normalised against cellular 5S ribosomal RNA levels to adjust for differences in the amount of RNA used. ND, not done.

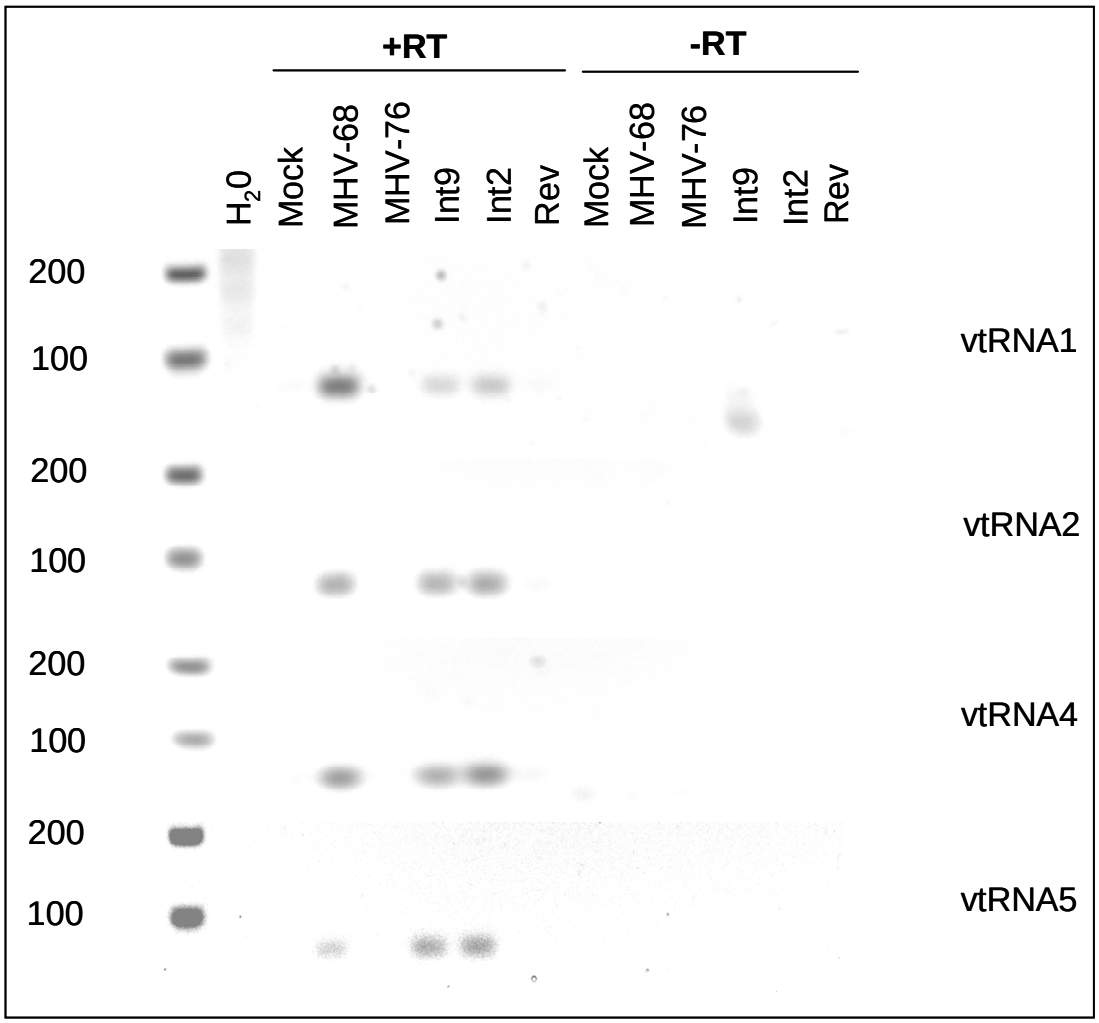

Figure 3.11 RT-PCR analysis showing the expression of vtRNAs1, 2, 4 and 5 from NS0 cells latently infected with MHV-68, MHV-76, Int9, Int2 and revertant (Rev), as well as mock-infected cells. The RNA was DNase treated, RT-PCR carried out for the vtRNAs (+RT) and the products visualised on a 2% agarose gel. Control RT-PCR reactions without reverse transcriptase (-RT) were also carried out, as well as a water control (H_20) for the PCR reaction.

non-coding RNAs. However, prior to any major studies with the viruses they needed to be characterised. The recombinant viruses had already been analysed by Southern blot analysis to confirm correct insertion of the DNA fragments into the viral genome of the insertion viruses and that the revertant was identical to MHV-76. The expression of the vtRNAs by the insertion viruses during lytic infection had also been confirmed (Cliffe 2005).

To compare subtle differences in phenotypes and protein expression a large proportion of cells need to be infected, and the viruses need to infect a similar proportion of cells. The viruses were titred on BHK-21 fibroblast cells, determining the number of pfu per ml in the virus stocks. It was not known if the viruses had similar infectivity on NS0 cells. In this study it was shown that five days post infection at a MOI of 5 pfu/cell the viruses (MHV-68, MHV-76, Int9, Int2 and revertant) have all infected close to 100% of the NS0 cells, and that the cells are healthy and growing well following infection.

The initial experiment using GFP-labelled viruses was unsuccessful, probably due to the promoters driving the GFP expression not being fully active, perhaps being shut-down due to chromatin remodelling during latency. However, the *in situ* hybridisations carried out for vtRNAs in MHV-68 infected NS0 cells were more successful. In addition to showing that close to 100% of cells were infected with MHV-68, the *in situ* hybridisation also showed that the vtRNAs appear to localise in the cytoplasm during latency. The vtRNA1-4 probe has previously been used for *in situ* hybridisations and has been shown to bind specifically to vtRNAs (Bowden *et al.* 1997; Cliffe 2005; Simas *et al.* 1999). However, since MHV-76 and the revertant virus do not express the vtRNAs the *in situ* hybridisation could not be used for all viruses.

There are no antibodies available for any proteins expressed during latency; however, a polyclonal serum raised against lytically infected rabbit cells proved useful as it bound to antigens produced at low levels during latent infection. It could thereby be confirmed that all the viruses infect close to 100% of NS0 cells. It was clear that MHV-76 and the revertant virus had a higher proportion of lytically infected cells, while the insertion viruses had a very low number.

In parallel to the other experiments, virus infected clones were grown up. All the clones tested were virus positive, corroborating that 100% of cells are infected at a MOI of 5 pfu/cell. It is possible that the virus infected cells are more viable; thus making it more likely that the surviving clones are virus infected. However, virus infected cells do not increase in cell numbers compared to uninfected cells (see chapter four), therefore virus infection does not seem to increase cell viability. The clones would have been useful if a high number of infected cells could not be achieved through infection of NS0 cells. However, it was decided that it was better to use a population of infected cells, instead of a clone.

The viruses were further characterised in regards to vtRNA and miRNA expression. The insertion viruses were known to express the vtRNAs during lytic infection (Cliffe 2005) and we confirmed by RT-PCR that the vtRNAs are expressed during latent infection as well. This was expected since MHV-68 expresses the vtRNAs during both lytic and latent infection. We corroborated that MHV-68 expresses the miRNAs during latent infection of S11 cells and confirmed that they are expressed in latently infected NS0 cells. We further showed that MHV-68 expresses the miRNAs during lytic infection, which was expected since the vtRNAs are expressed. This had not been shown at that point, but has since been published (Diebel *et al.* 2010). Since MHV-68 expresses the miRNAs during both lytic and latent infection, it was surprising to find that during latent infection of NS0 cells the insertion viruses do not express miRNA1 at detectable levels and the other miRNAs at lower levels than MHV-68, especially since they express miRNA1 during lytic infection.

The lack of miRNA1 expression by the insertion viruses during latency could be because promoter elements needed during latent infection are missing. Eukaryotic tRNA genes have upstream promoter elements around -30 relative to the transcription initiation site that can regulate tRNA transcription (reviewed in Dieci *et al.* 2007). The insert used for making the insertion viruses consists of nt 112-1694, covering vtRNA1-5 and miRNA1-6. vtRNA1 starts at nt 127 and since the promoter regions of the vtRNA/miRNA transcripts are not fully mapped and there may be unknown promoter/enhancer regions, it is possible that more of the sequence should have been included in the insert. If this is the case the vtRNA1 expression by the insertion viruses would be expected to be very low as well; however, since only a

non-quantitative RT-PCR was performed for the expression of the vtRNAs it is not known if this is the case.

The lower expression of the miRNAs by the insertion viruses during latency is interesting. It is possible that the presence of the non-coding RNAs affect the copy number of the viruses. If there are fewer copies of the viral genome, lower amounts of miRNAs would be expressed. Preliminary qPCR data (not shown) indicates that this might be the case; however, this would need to be examined further. It would be interesting to see if the insertion viruses also express the vtRNAs at a lower level, which would be expected if the deficiency is at the level of transcription, since the vtRNAs and miRNAs are expressed on the same transcript. In addition, it is not known if there is a difference in expression levels of the non-coding RNAs between MHV-68 and the insertion viruses during lytic infection. Perhaps the unique genes are needed for efficient expression of the non-coding RNAs.

Several methods to detect and/or quantify miRNAs have been made available during the last few years. Initially northern blot analysis was used; however, the development of qRT-PCR for miRNAs has made detection more sensitive, less time consuming and enables large scale analysis. The initial difficulty with qRT-PCRs was the short miRNAs sequence, making primer design difficult. This has been overcome by making the miRNA larger by using stem-loop primers (Ambion), adding a poly(A) tail (Invitrogen), or by using LNA nucleotides that allows for shorter primers (Exiqon). In this study we used the Invitrogen NCode miRNA First-Strand cDNA Synthesis Kit and Platinum SYBR Green qPCR SuperMix-UDG. This kit allows for designing of a miRNA primer specific for the miRNA, while other kits use pre-designed primers that do not include viral miRNAs. Because the primer used corresponds to the whole miRNA it is difficult in some cases to obtain specific products and good dissociation curves as there is little sequence variation allowed, as seen with miRNA2 and 5. In addition, if all miRNAs are to be analysed in one qRT-PCR experiment it is difficult to chose an annealing temperature suitable for all miRNA primers. For future experiments a possible alternative would be the TaqMan microRNAs assay (Applied Biosystems) to which specific stem loop primers for MHV-68 miRNAs can be ordered.

The aim of this study was to characterise the vtRNA and miRNA expression profiles of the viruses and determine whether infection of NS0 cells provided a suitable model to study differences in phenotypes and protein expression during latent infection. In conclusion, although some differences are observed, the NS0 cells provide a suitable model; a very high percentage of infected cells can be achieved and the non-coding RNAs are expressed.

4. Chapter Four: Investigating the functions of the non-coding RNAs

4.1. Aims **117**
4.2. Replication and reactivation kinetics **118**
4.2.1. Preliminary experiment 118
4.2.2. Experiment with Int2 virus 123
4.2.3. Experiment with revertant virus 123
4.2.4. *In vivo* reactivation kinetics 129
4.3. Transfection of non-coding RNAs and plasmids **132**
4.3.1. miRNA transfections 132
4.3.2. Dicer 135
4.3.3. ORF50 139
4.3.4. vtRNAs 139
4.3.5. pL2a5 142
4.4. Discussion **142**

4.1. Aims

The roles of the non-coding RNAs of MHV-68 during infection have not been extensively characterised and it is not know what their biological functions are. The lack of the vtRNAs, miRNAs and M1-4 seen in MHV-76 leads to an attenuated phenotype, with the virus being cleared more rapidly and showing a deficiency in establishing latency (Macrae *et al.* 2001). However, the unique proteins are known to be important during infection (see section 1.3.10). In contrast, deletion of vtRNA1-4, miRNAs1-7 and M1 from MHV-68 did not result in a difference in either replication during *in vitro* infection or the ability of the virus to reactivate from latency *in vivo* compared to wild type virus (Simas *et al.* 1998). However, this was a limited study investigating infection in only four mice for each virus at one time point, with varying results obtained between mice. In addition, the non-coding RNAs may have similar functions so deleting just some of them might not abolish their effect. M1 is a multifunctional protein and deletion of M1 has since been shown to result in an increase in reactivation, which is inconsistent with the above study (Clambey *et al.* 2000; Evans *et al.* 2008).

The insertion viruses, Int9 and Int2, provide useful tools to study the non-coding RNAs, since the only difference between the two insertion viruses and MHV-76 are the five vtRNAs and six miRNAs, and any phenotype found will be caused by these. However, the insertion viruses will not tell us if the phenotype is caused by the vtRNAs or miRNAs. A previous *in vivo* study showed that, like MHV-76, the insertion viruses are cleared more rapidly and establish latency at a lower level in the spleen than MHV-68 (Cliffe 2005). Since a phenotype for the insertion viruses could not be found *in vivo,* we decided to investigate the functions of the non-coding RNAs during latent infection *in vitro*.

NS0 cells were latently infected with the different viruses at a MOI of 5 pfu/cell and the replication and reactivation kinetics analysed by plaque assay and infective centre assay.

4.2. Replication and reactivation kinetics

4.2.1. Preliminary experiment

$5x10^6$ NS0 cells were mock-infected or infected with MHV-68, MHV-76, or Int9 at a MOI of 5 pfu/cell for one hour and $2x10^6$ of the infected cells incubated in T25 flasks in duplicate for each virus, for five days. These viruses had been titrated at the same time on the same BHK cells. Mock lysate was used to bring the virus solutions to the same volume, to minimise differences in the amount of cell debris present in the samples. On the day of infection and five and nine days post infection, cell numbers and titres of cell associated virus and virus in the supernatant were determined. In addition, infective centre assays were performed five and nine days post infection, by co-cultivating latently infected NS0 cells with BHK cells, to determine the percentage of NS0 cells reactivating virus.

The titres of supernatant virus and cell associated virus following adsorption for one hour was determined to ensure that the same pfu of each virus had been used to infect the cells (Figure 4.1). The cell numbers showed that the virus infection did not give the cells a survival advantage (as discussed for the clones in the previous chapter), but infection with MHV-68 and MHV-76 seemed to lead to slightly reduced cell numbers (Figure 4.2); however this was not observed in subsequent experiments (Figure 4.9). There was a significantly larger amount of virus produced by MHV-68 and MHV-76 compared to Int9 (Figure 4.3). This difference was also seen in the amount of virus present in the cells; with Int9 infected NS0 cells having significantly lower levels of cell associated virus (Figure 4.4). The difference became more apparent when looking at the percentage of cells reactivating virus; Int9 reactivated at a significantly lower level than MHV-68 and MHV-76 (Figure 4.5). At five days post infection MHV-76 also reactivated at a significantly higher level than MHV-68 and produced significantly more virus than MHV-68 both five and nine days post infection.

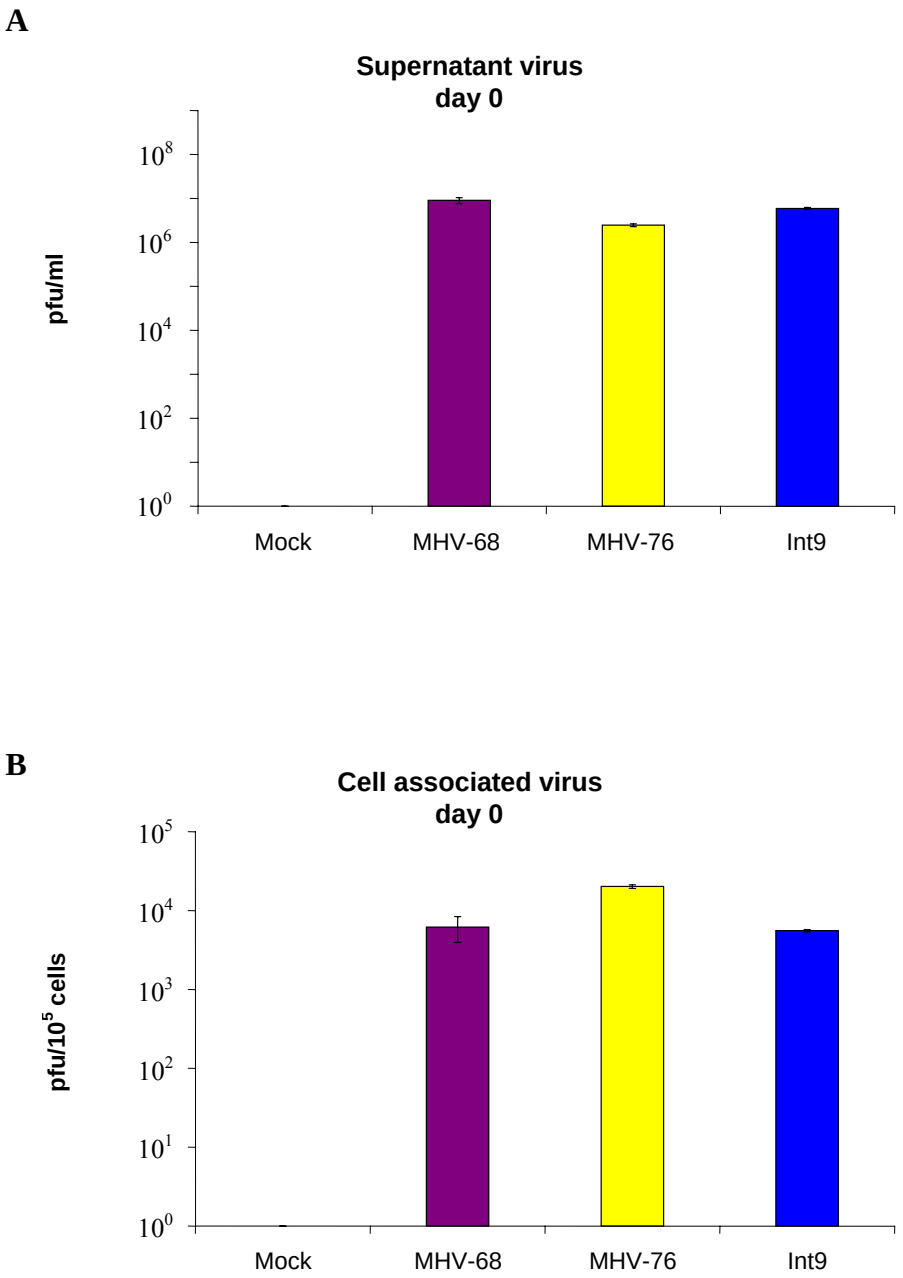

Figure 4.1 Supernatant (A) and cell associated (B) virus titres (pfu/ml and pfu/10^5 cells) from NS0 cells mock-infected or infected with MHV-68, MHV-76 or Int9 at a MOI of 5 pfu/cell, following one hour of adsorption. Each bar shows the mean of two biological replicates, each with two technical replicates. Error bars represent the standard deviation.

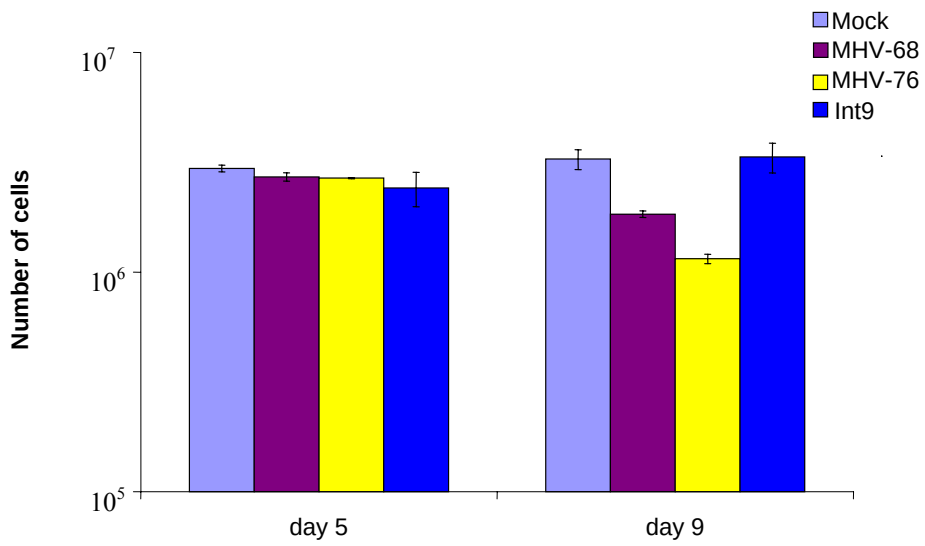

Figure 4.2 Cell numbers from NS0 cells mock-infected or infected with MHV-68, MHV-76 or Int9 at a MOI 5 pfu/cell, five and nine days post infection. Each bar shows the mean of two biological replicates. Error bars represent the standard deviation.

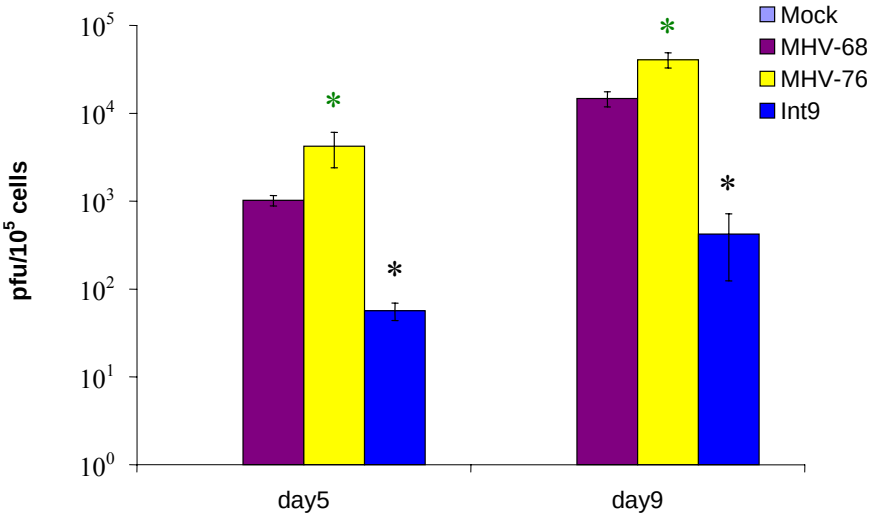

Figure 4.3 Supernatant virus titres (pfu/10^5 cells) from NS0 cells mock-infected or infected with MHV-68, MHV-76 or Int9 at a MOI 5 pfu/cell, five and nine days post infection. Each bar shows the mean of two biological replicates, each with two technical replicates. Error bars represent the standard deviation. * Int9 produced significantly less virus than MHV-68 and MHV-76 five days ($p<0.025$) and nine days ($p<0.0025$) post infection. * MHV-76 produced significantly more virus than MHV-68 both five ($p<0.05$) and nine ($p<0.005$) days post infection, as determined by Student's t-test.

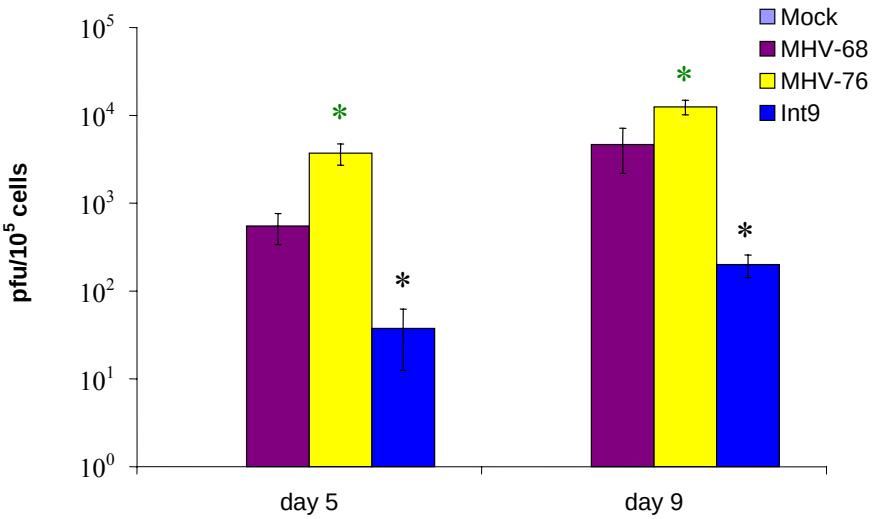

Figure 4.4 Cell associated virus titres (pfu/10^5 cells) from NS0 cells mock-infected or infected with MHV-68, MHV-76 or Int9 at a MOI 5 pfu/cell, five and nine days post infection. Each bar shows the mean of two biological replicates, each with two technical replicates. Error bars represent the standard deviation. * Int9 infected NS0 cells had significantly less cell associated virus than MHV-68 and MHV-76 infected cells five days ($p<0.025$) and nine days post infection ($p<0.05$). * MHV-76 infected NS0 cells had significantly more cell associated virus than MHV-68 both five ($p<0.01$) and nine ($p<0.005$) days post infection, as determined by Student's t-test.

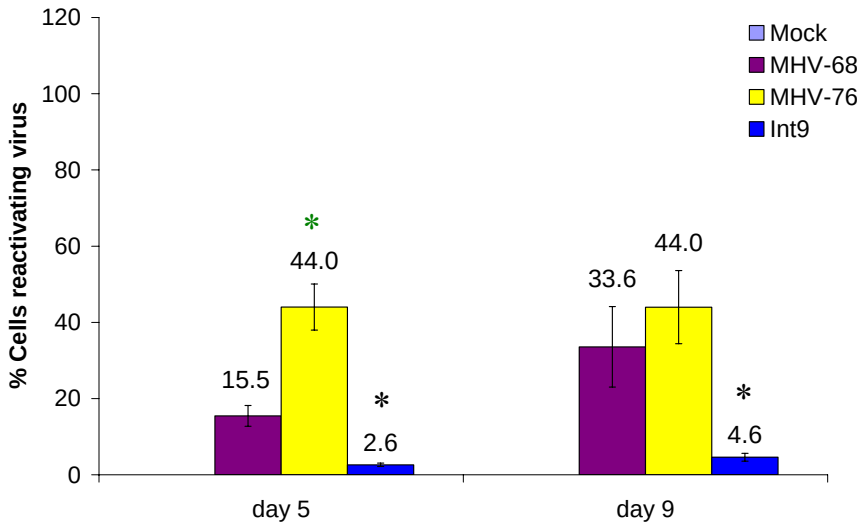

Figure 4.5 Percentage of NS0 cells reactivating virus, mock-infected or infected with MHV-68, MHV-76 or Int9 at a MOI 5 pfu/cell, five and nine days post infection. The percentage of cells reactivating virus was calculated by subtracting the cell associated virus titres from the infective centres. Each bar shows the mean of two biological replicates, each with two technical replicates. Error bars represent the standard deviation. * Int9 reactivated at a significantly lower rate than MHV-68 and MHV-76 both five days ($p<0.0025$) and nine days ($p<0.01$) post infection. * MHV-76 reactivated at a higher frequency than MHV-68 five days ($p<0.001$) but not nine days post infection, as determined by Student's t-test.

4.2.2. Experiment with Int2 virus

To confirm the reduction in reactivation seen with Int9 the experiment was repeated to include the second insertion virus Int2, which had been made independently of Int9. This time only the infective centres assay was performed five days post infection. The percentages of infective centres were analysed without subtracting the cell associated virus titre.

The second insertion virus reactivated at the same level as Int9, strongly suggesting that the lower reactivation rate was due to the insert (Figure 4.6). The infective centres from this experiment replicated the results from the previous experiment (Figure 4.7). The cell associated virus titres did not have a great impact on the percentage of cells reactivating virus, since the same differences in reactivation between the viruses were observed even without subtracting the cell associated virus titres from the infective centres (Figure 4.5, Figure 4.7). This showed that the infective centres alone give a good measurement of reactivation.

4.2.3. Experiment with revertant virus

The replication and reactivation kinetics experiment was repeated with the revertant virus to confirm that the insertion viruses do reactivate at a lower level and produce less infectious virus. This time $3x10^6$ NS0 cells were infected in duplicate for each virus (MHV-68, MHV-76, Int9, Int2 and revertant virus) at a MOI of 5 pfu/cell for one hour and $2x10^6$ of the infected cells subsequently incubated in T25 flasks for five days. As previous, cell numbers and titres of cell associated virus and virus in the supernatant were determined on the day of infection and five and nine days post infection. Also, the percentage of cells reactivating virus was determined five and nine days post infection.

The supernatant and cell associated virus titres following one hour of adsorption were similar for all viruses (Figure 4.8). In this experiment MHV-68 and MHV-76 did not have lower cell numbers nine days post infection (Figure 4.9), as seen in the first assay. Both insertion viruses produced significantly less lytic (Figure 4.10), and cell associated virus (Figure 4.11), and reactivated at a significantly lower level (Figure 4.12) than MHV-68, MHV-76 and the revertant virus. Insertion of the

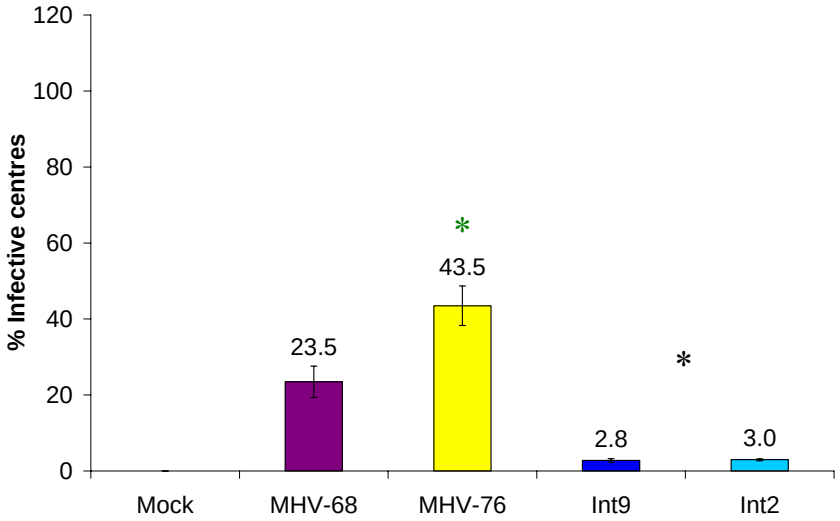

Figure 4.6 Percentage of infective centres from NS0 cells mock-infected or infected with MHV-68, MHV-76, Int9 or Int2 at a MOI 5 pfu/cell, five days post infection. Each bar shows the mean of two biological replicates, each with two technical replicates. Error bars represent the standard deviation. * Int9 and Int2 infected cells reactivated at a significantly lower level than MHV-68 and MHV-76 ($p<0.0025$). * MHV-76 reactivated at a significantly higher frequency than MHV-68 ($p<0.001$), as determined by Student's t-test.

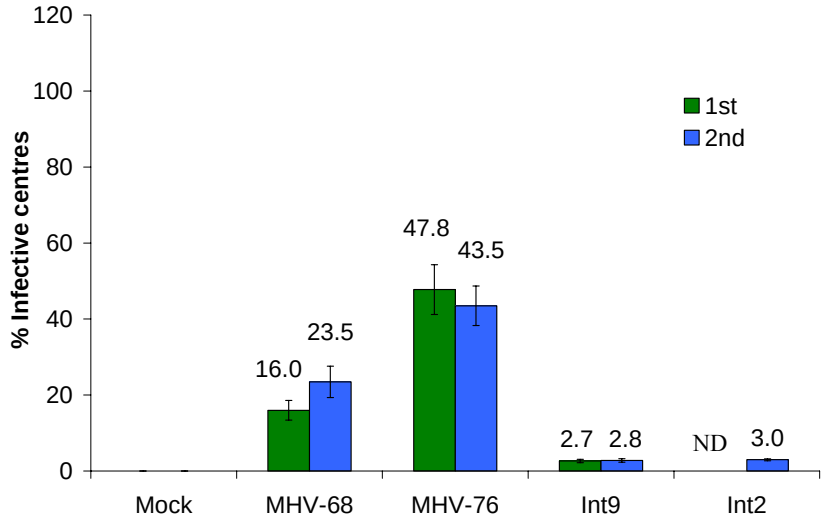

Figure 4.7 Comparing the percentage of infective centres between the two experiments, five days post infection of NS0 cells mock-infected or infected with MHV-68, MHV-76, Int9 or Int2 at a MOI 5 pfu/cell. Each bar shows the mean of two biological replicates, each with two technical replicates. Error bars represent the standard deviation. ND, not done.

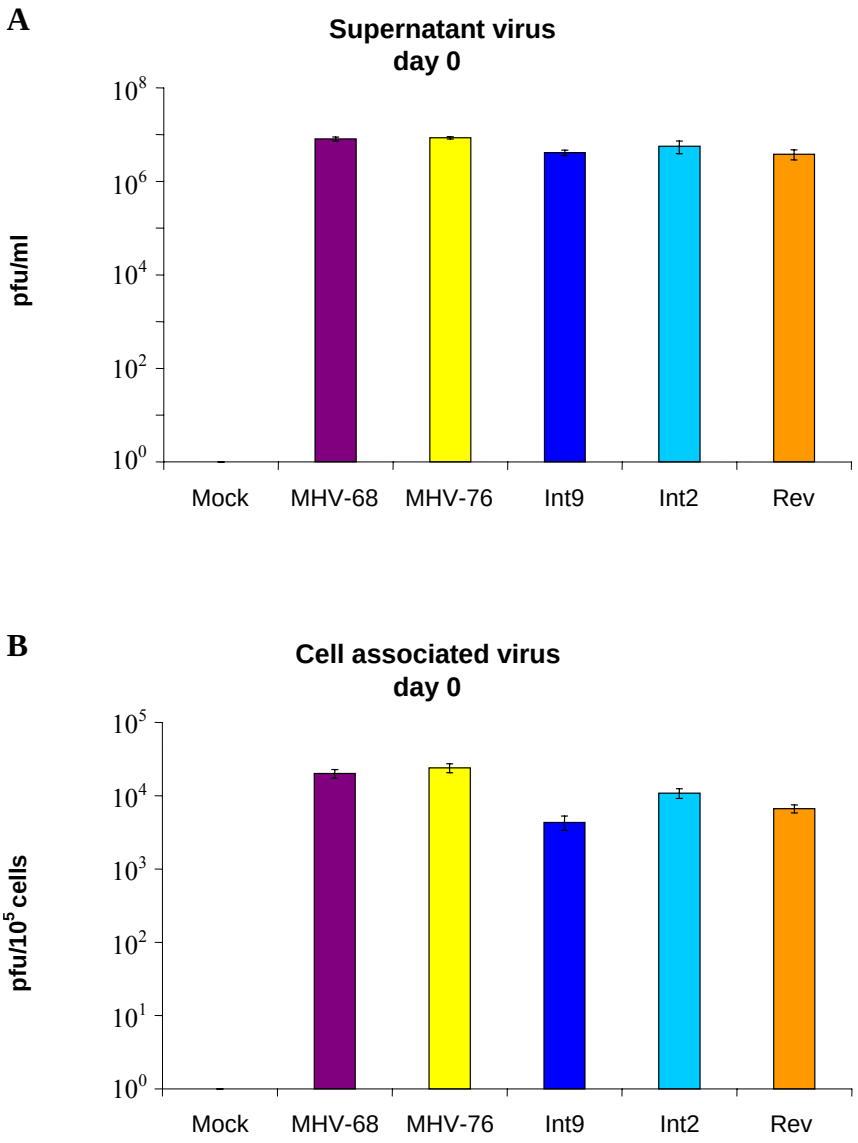

Figure 4.8 Supernatant (A) and cell associated (B) virus titres (pfu/ml and pfu/10^5 cells) from NS0 cells mock-infected or infected with MHV-68, MHV-76, Int9, Int2 or revertant virus (Rev) at a MOI 5 pfu/cell, following one hour of adsorption. Each bar shows the mean of two biological replicates, each with two technical replicates. Error bars represent the standard deviation.

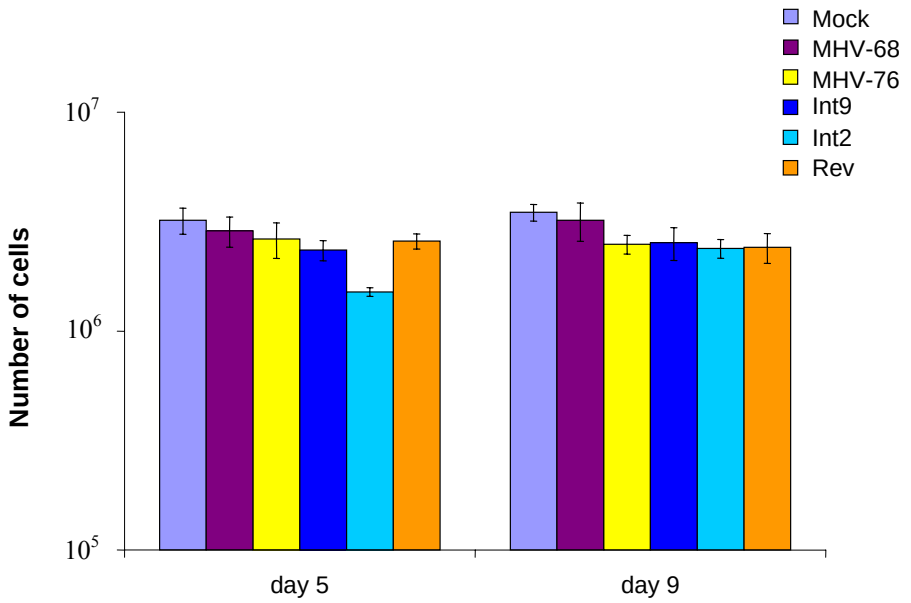

Figure 4.9 Cell numbers from NS0 cells, mock-infected or infected with MHV-68, MHV-76, Int9, Int2 or revertant virus (Rev) at a MOI 5 pfu/cell, five and nine days post infection. Each bar shows the mean of two biological replicates. Error bars represent the standard deviation.

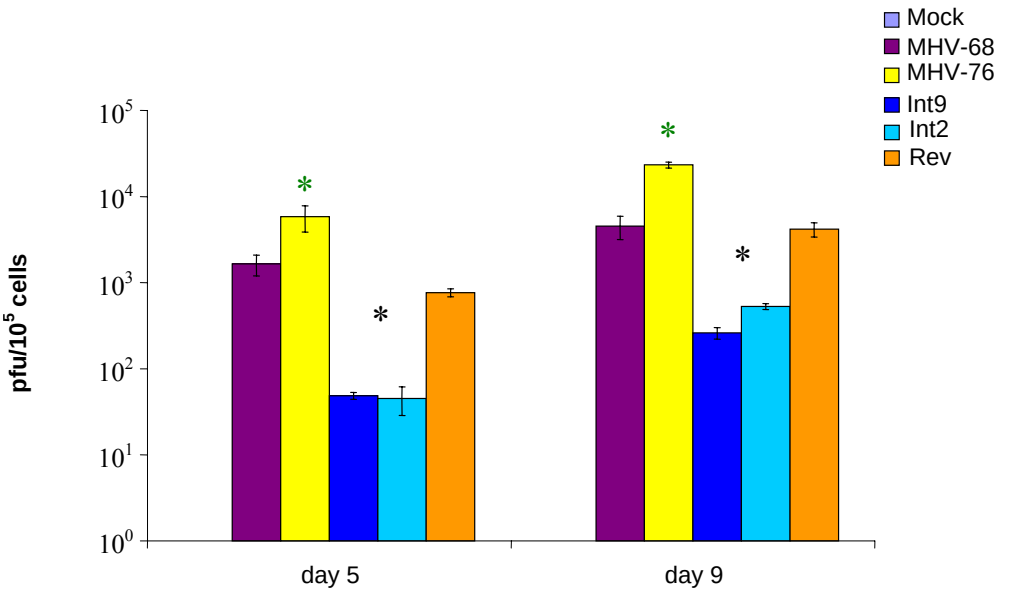

Figure 4.10 Supernatant virus titres (pfu/10^5 cells) from NS0 cells, mock-infected or infected with MHV-68, MHV-76, Int9, Int2 or revertant virus (Rev) at a MOI 5 pfu/cell, five and nine days post infection. Each bar shows the mean of two biological replicates, each with two technical replicates. Error bars represent the standard deviation. * Int9 and Int2 produced significantly less virus than MHV-68, MHV-76 and the revertant virus both five days ($p<0.01$) and nine days ($p<0.01$) post infection. * MHV-76 produced significantly more virus than MHV-68 and the revertant virus five days ($p<0.025$) and nine days ($p<0.00005$) post infection, as determined by Student's t-test.

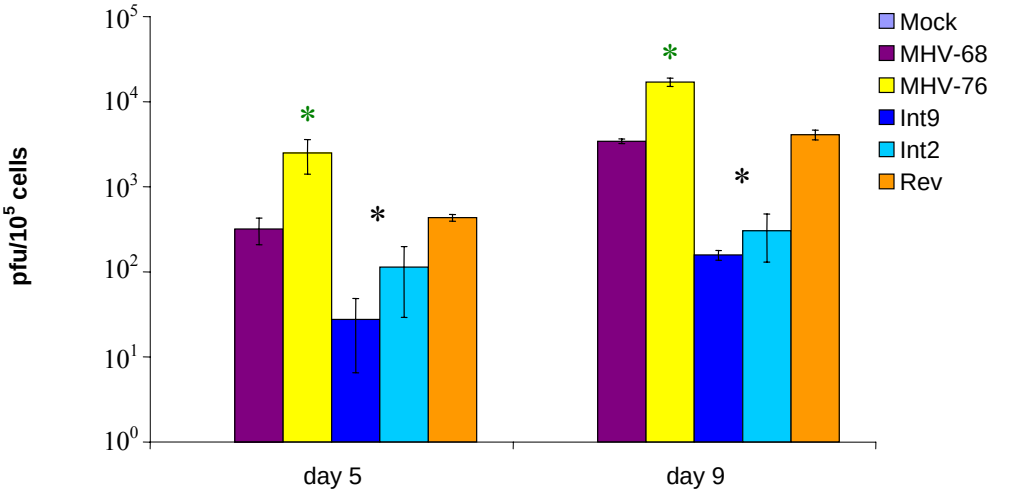

Figure 4.11 Cell associated virus titres (pfu/10^5 cells) from NS0 cells, mock-infected or infected with MHV-68, MHV-76, Int9, Int2 or revertant virus (Rev) at a MOI 5 pfu/cell, five and nine days post infection. Each bar shows the mean of two biological replicates, each with two technical replicates. Error bars represent the standard deviation. * Int9 and Int2 infected NS0 cells had significantly less cell associated virus than MHV-68, MHV-76 and the revertant virus both five days ($p<0.05$) and nine days ($p<0.001$) post infection. * MHV-76 infected cells had significantly more cell associated virus than MHV-68 and the revertant virus five days ($p<0.05$) and nine days ($p<0.001$) post infection, as determined by Student's t-test.

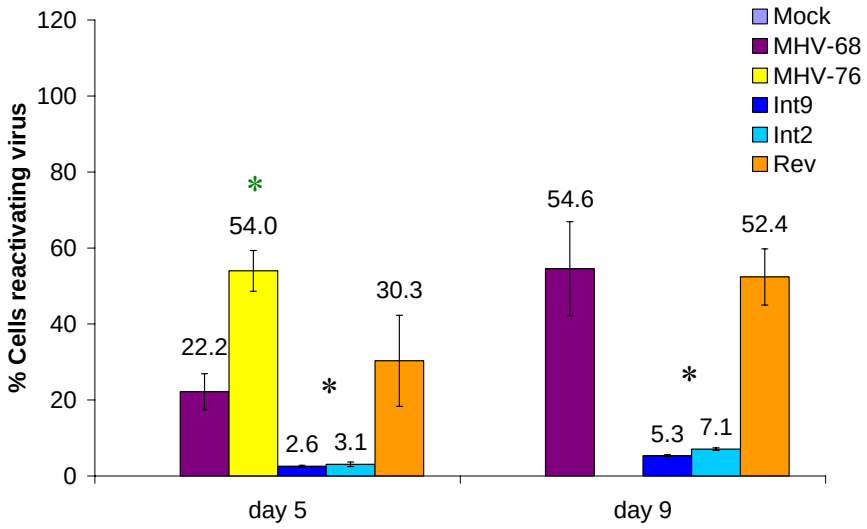

Figure 4.12 Percentage of NS0 cells reactivating virus, mock-infected or infected with MHV-68, MHV-76, Int9, Int2 or revertant virus (Rev) at a MOI 5 pfu/cell, five and nine days post infection. The percentage of cells reactivating virus was calculated by subtracting the cell associated virus titres from the infective centres. Each bar shows the mean of two biological replicates, each with two technical replicates. Error bars represent the standard deviation. Nine days post infection the infective centres from MHV-76 infected cells could not be counted as there were too many on the plates. * Int9 and Int2 reactivated at a significantly lower level than MHV-68, MHV-76 and the revertant virus both five days ($p<0.025$) and nine days ($p<0.005$) post infection. * MHV-76 reactivated at a higher frequency than MHV-68 and the revertant virus five days post infection ($p<0.025$), as determined by Student's t-test.

vtRNAs and the miRNAs into the genome of MHV-76 led to a decrease in reactivation and production of lytic virus 10-fold or greater compared to revertant virus. MHV-76 reactivated at a higher rate and produced more lytic virus than both MHV-68 and the revertant virus (Figure 4.10, Figure 4.12).

miRNA1 has a predicted target site in the 3' UTR of the ORF50 gene that encodes the rta that is important for reactivation (Figure 4.13; pers commun Simon Talbot), which would be expected to lead to a reduction in ORF50 and thus a decrease in reactivation. However, since the insertion viruses express miRNA1 at very low levels during latent infection; this is unlikely to be the reason for the lower reactivation rates seen.

4.2.4. *In vivo* reactivation kinetics

To investigate if the lower reactivation rate seen by the insertion viruses could also be observed *in vivo*, a small study was performed where five BALB/c mice were infected intranasally with $4x10^5$ pfu of MHV-76 and five with Int9. Previous *in vivo* studies had shown that Int9, like MHV-76, is cleared more rapidly than MHV-68 and established latency at a very low level in the spleen (Cliffe 2005); a feature that must therefore be because of the lack of the unique proteins M1-M4, and not the vtRNAs and miRNAs. However, these studies did not examine the MLN and it is possible that the establishment of latency is different in this location. Therefore, we investigated the reactivation kinetics of latently infected MLN cells. The cells were collected by disrupting the MLN with a scalpel, washing the cells by centrifugation and letting the debris settle, prior to removing the supernatant with the cells. The cells were counted and infective centres assays set up with 10^5 or 10^6 MLN cells.

Although there were large variations in infectious centres between different mice, there did not appear to be a difference in reactivation between MHV-76 and Int9 infected MLN cells (Figure 4.14, Figure 4.15). A larger study involving a larger number of mice may be useful.

A

TAGCCACAGGGATACGCCTGTCCAGCATATTGTGCAATCTGGCTCAACGCCCGC
CCCGCCAATTGTTGAGCCTCAGGGACAAGATTTTGTTGGAAAACAGGATGAGAC
ATGTTCCAACGTGTTCCCAGAACAAATTACTCAGGAAGCGTGTCCCGGATCATCT
GAGGACGCGTTCATCGATGATGCTATAAAGGAAATATTTGCATCGCTGGACTCT
ATGGCAAACCAGGACACTGCTGACAGTGACACATGTTCCATACTTGACCCCCAA
TCACCCACTCCCCCACCCTCCGTTCCCCCAATAACTACACTCTCGTTGTATGACA
TTTATGCCAGCATACTTAGTCCACTCGACCCAAACAGCCTGGAGTCATAAACGG
TGCCAAATACAAGACATTTCTAAATCCTTAAGTATAATGTTTATATTTAACTGAA
TAAAAGAAGTGACGCTATAAAACCCTCAACATGTGTGGCGTTAAA-3'

Coding region
Stop codon
miRNA1 binding site
seed region binding site
poly (A) signal

miRNA1

B

```
TAAACGGTGCCAAA TACAAGACATTTCTAAATCCTTAAGTATAATGTTTATATTTAACTGAATAAA
 UUU CC      UUCAUG CCGGUAAAGAU
```

C

```
    C  TGCCA       AA A
TAAA GG      AA TAC  G CATTTCTA
 UUU CC      UU AUG  C GUAAAGAU
               C     C G


    CGGTGCCAAA    AA A
TAAA           TAC  G CATTTCTA
 UUU           AUG  C GUAAAGAU
    CCUUC           C G
```

Figure 4.13 Showing the possible miRNA1 target sequence in the ORF50 3' UTR. (A) The 3' end of ORF50. (B) The possible binding site of miRNA1 to the ORF50 3' UTR. (C) Possible binding conformations. (Pers commun Simon Talbot)

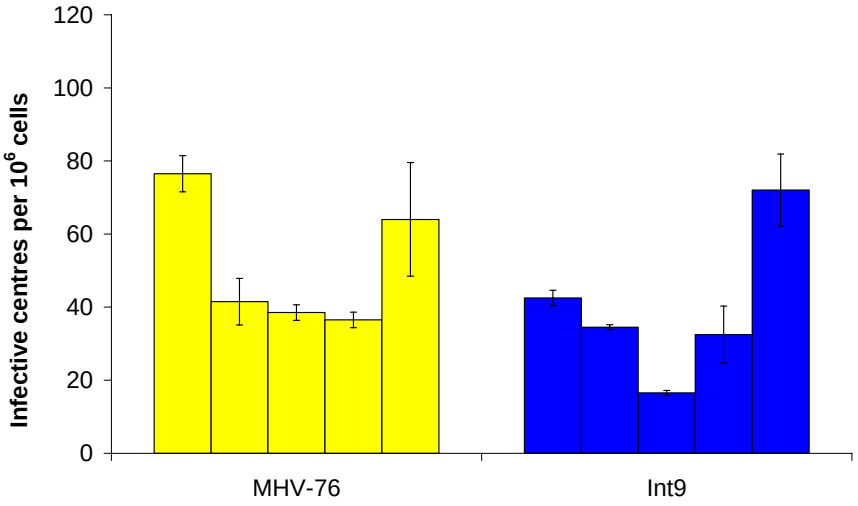

Figure 4.14 Infective centres per 10^6 MLN cells from mice infected intranasally with $4x10^5$ pfu of MHV-76 or Int9, five mice for each virus. Error bars represent the standard deviation.

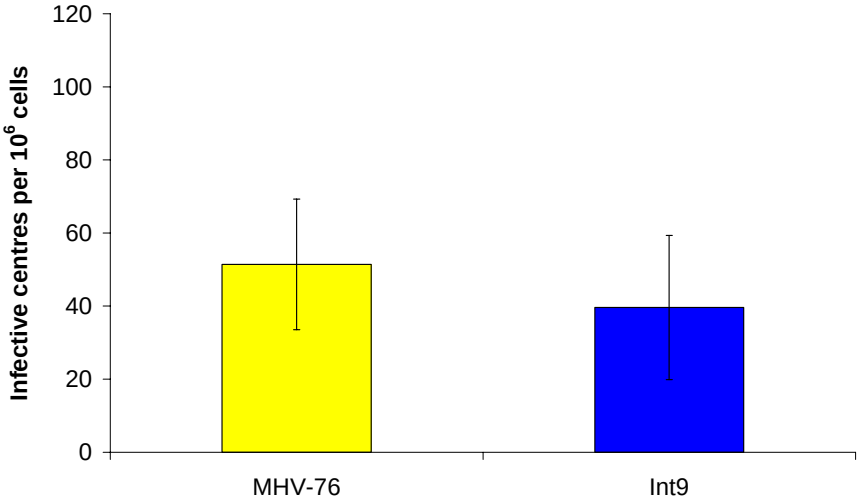

Figure 4.15 Infective centres per 10^6 MLN cells from mice infected intranasally with $4x10^5$ pfu of MHV-76 or Int9, five mice for each virus. Showing the mean number of infective centres for mice infected with each virus. Error bars represent the standard deviation.

4.3. Transfection of non-coding RNAs and plasmids

4.3.1. miRNA transfections

The insertion viruses could not be used to distinguish whether the vtRNAs or miRNAs are responsible for the reduction in reactivation. Therefore, to determine if the miRNAs caused the reduction in reactivation, miRNAs1-6 were transfected into MHV-76 infected NS0 cells.

Initially, the cells were infected with MHV-76 at a MOI of 5 pfu/cell for two hours prior to transfection with 0.5μg miRNA1-6 mimics (miScript miRNA mimics, Qiagen) or a negative siRNA and 66.5pmol siGLO red using a nucleofector. siGLO is a fluorescent RNA duplex that when co-transfected with miRNAs gives an indication of the transfection efficiency. The reactivation kinetics were analysed by infective centres assays 24 and 72 hours post transfection. Transfection of the miRNAs into MHV-76 infected cells did not lead to a change in the percentage of cells reactivating virus compared to the negative control; however, the transfection itself led to an increase in reactivation compared to untransfected cells (Figure 4.16).

The previous reactivation experiments examined the infective centres five days post infection. To replicate these conditions NS0 cells were infected with MHV-76 at a MOI of 5 pfu/cell and the infected cells transfected with miRNAs1-6 or negative siRNA after four days, followed by infective centres assays after 24 hours (five days post infection) and 48 hours. In addition, supernatant virus titres were analysed. At 24 hours post transfection, miRNA transfected cells reactivated virus at a significantly lower level than the negative control (Figure 4.17). However, this was not seen at 48 hours post transfection, or in the amount of infective virus produced (Figure 4.18). Again, at 48 hours post transfection, negative siRNA transfected cells had a higher percentage of cells reactivating virus than the untransfected cells, and also produced a larger amount of infectious virus.

To further investigate the difference in reactivation 24 hours post transfection of miRNAs, the previous experiment was repeated. This time NS0 cells infected for five days with Int9 was included as a control of the reactivation assay. The

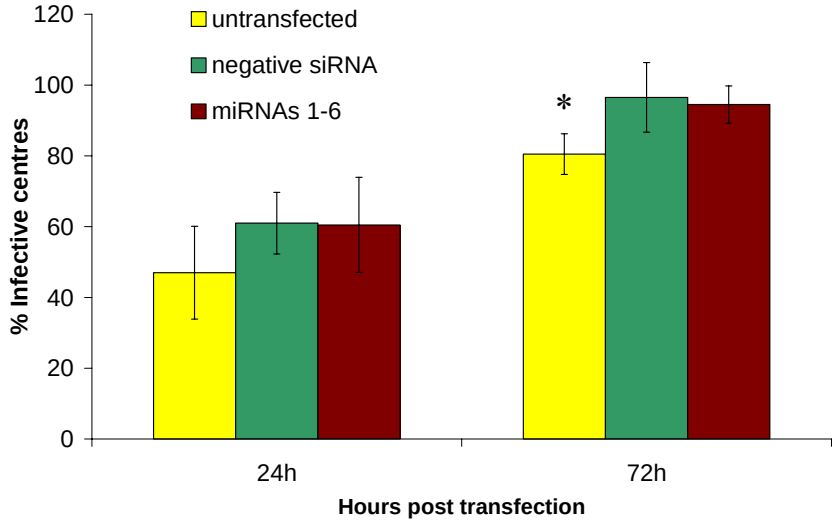

Figure 4.16 Percentage of infective centres from MHV-76 infected NS0 cells, untransfected or 24 and 72 hours post transfection with negative control siRNA or miRNAs1-6. Each bar shows the mean of two biological replicates, each with two technical replicates. The transfection efficiency was around 76%. Error bars represent the standard deviation. * Untransfected cells had significantly ($p<0.05$) lower percentage of infective centres compared to transfected cells 72 hours post transfection, as determined by Student's t-test.

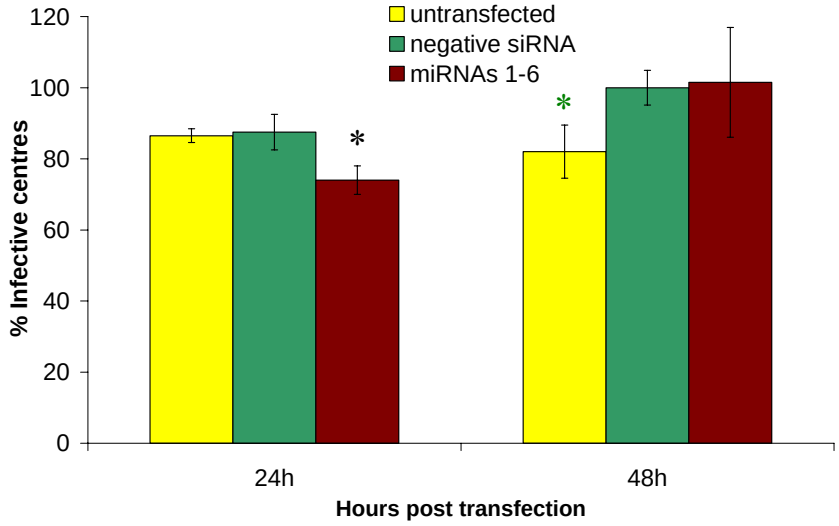

Figure 4.17 Percentage of infective centres from NS0 cells latently infected with MHV-76 for four days, untransfected or 24 and 48 hours post transfection with negative control siRNA or miRNAs1-6. Each bar shows the mean of two biological replicates, each with two technical replicates. The transfection efficiency was around 65%. Error bars represent the standard deviation. * miRNA transfected cells had significantly ($p<0.01$) lower percentage of infective centres compared to negative siRNA transfected cells 24 hours post transfection. * Untransfected cells had significantly lower ($p<0.01$) percentage of infective centres than negative siRNA transfected cells 48 hours post transfection, as determined by Student's t-test.

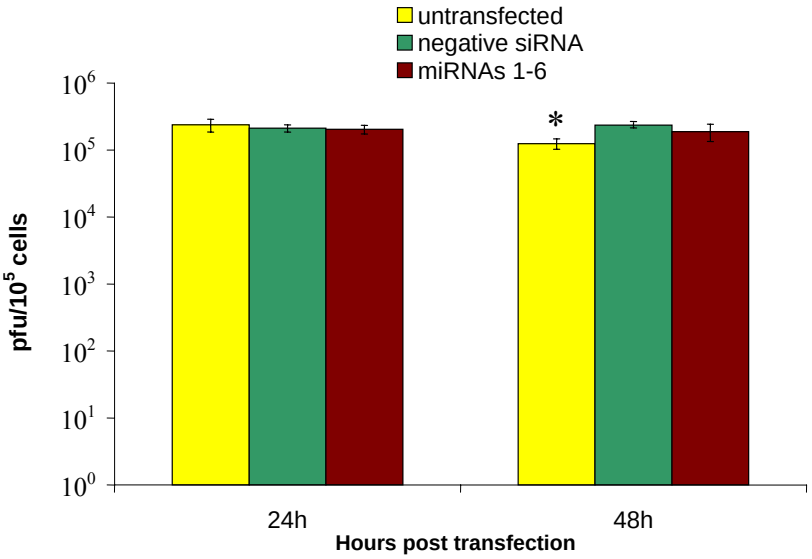

Figure 4.18 Supernatant virus titres (pfu/10^5 cells) from NS0 cells latently infected with MHV-76 for four days, 24 hours and 48 hours post transfection with negative control siRNA or miRNAs 1-6, or untransfected cells. Each bar shows the mean of two biological replicates, each with two technical replicates. The transfection efficiency was around 65%. Error bars represent the standard deviation. * Untransfected cells had significantly ($p<0.05$) lower percentage of infective centres compared to negative siRNA transfected cells 48 hours post transfection, as determined by Student's t-test.

transfection of miRNAs1-6 into MHV-76 infected cells did not lead to a reduction in reactivation at 24 hours post transfection (Figure 4.19), as seen in the previous experiment. Consistent with the previous experiments, the Int9 infected cells reactivated virus at a significantly lower level than MHV-76 infected cells.

To confirm that the transfection led to increased miRNA levels, a qRT-PCR for miRNA3 was performed on small RNAs from the transfected cells. As excepted, untransfected or negative siRNA transfected MHV-76 infected cells did not contain miRNA3. miRNA transfection of MHV-76 infected NS0 cells lead to significantly higher levels of miRNA3 than in Int9 infected NS0 cells (Figure 4.20).

4.3.2. Dicer

To further investigate the role of the miRNAs in virus reactivation, the miRNA processing pathway was disrupted by inhibiting Dicer through transfection of a siRNA targeting the Dicer mRNA. Dicer is a component of the RISC loading complex and cleaves the pre-miRNA into small RNA duplexes approximately 22nt in size. By reducing the production of Dicer, the processing of new miRNAs is inhibited. The siRNA was transfected into NS0 cells and after 48 hours the cells were infected with MHV-68, MHV-76 or Int9, followed by infective centres assays 24 hours post infection. MHV-76 infected cells were included to ensure that cellular miRNAs were not inhibited resulting in a change in reactivation. By waiting 48 hours following transfection the siRNA is allowed to be processed and inhibit Dicer synthesis prior to infection so that viral miRNAs can not be processed. It should not have a major impact on the cellular miRNAs as there should still be a pool of these in complexes with RISC. Transfection with a siRNA against Dicer did not have an effect on the reactivation (Figure 4.21). To ensure that the miRNAs had been knocked down qRT-PCR was performed for miRNAs3 and 4 on small RNAs from the transfected cells. However, because of the low amounts of miRNAs present within Int9 infected cells, an effect of the siRNA against Dicer on viral miRNA levels could not be detected (Figure 4.22, Figure 4.23). Further studies are needed to confirm the results.

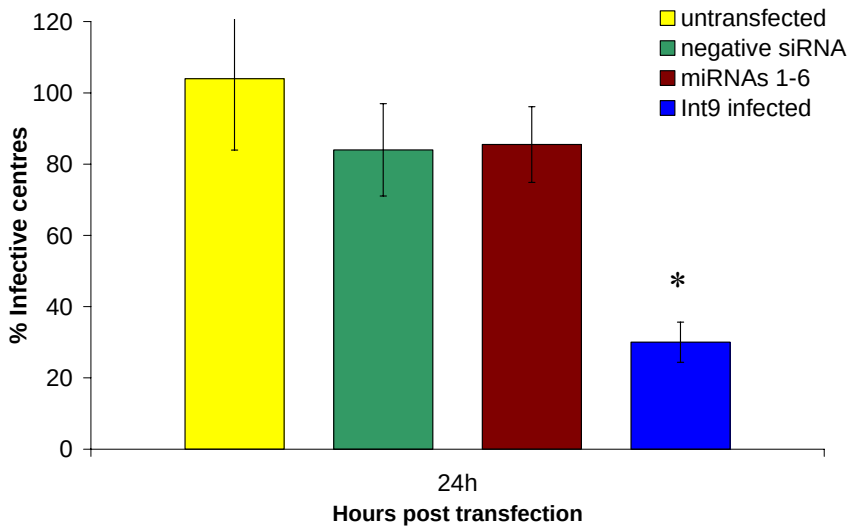

Figure 4.19 Percentage of infective centres from NS0 cells latently infected with MHV-76 for four days, untransfected or 24 hours post transfection with negative control siRNA or miRNAs1-6. Int9 infected NS0 cells were included as a control for reactivation. Each bar shows the mean of two biological replicates, each with two technical replicates. The transfection efficiency was around 36%. Error bars represent the standard deviation. * The Int9 infected NS0 cells reactivated virus at a significantly lower level ($p<0.005$) than MHV-76 infected cells, whether transfected or not, as determined by Student's t-test.

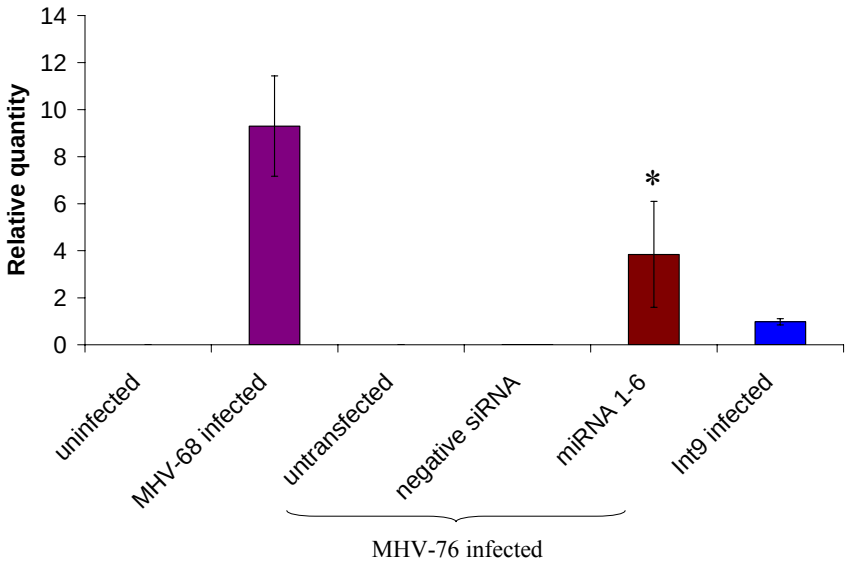

Figure 4.20 Relative quantity of miRNA3 as determined by qRT-PCR, in uninfected, MHV-68 infected, and Int9 infected NS0 cells, and MHV-76 infected NS0 cells: untransfected, negative siRNA transfected or miRNA transfected. Values normalised against cellular mir-16 levels and expressed relative to Int9 expression levels. Error bars represent the standard deviation. * miRNA transfected cells had significantly more ($p<0.05$) miRNA3 than In9 infected NS0 cells, as determined by Student's t-test.

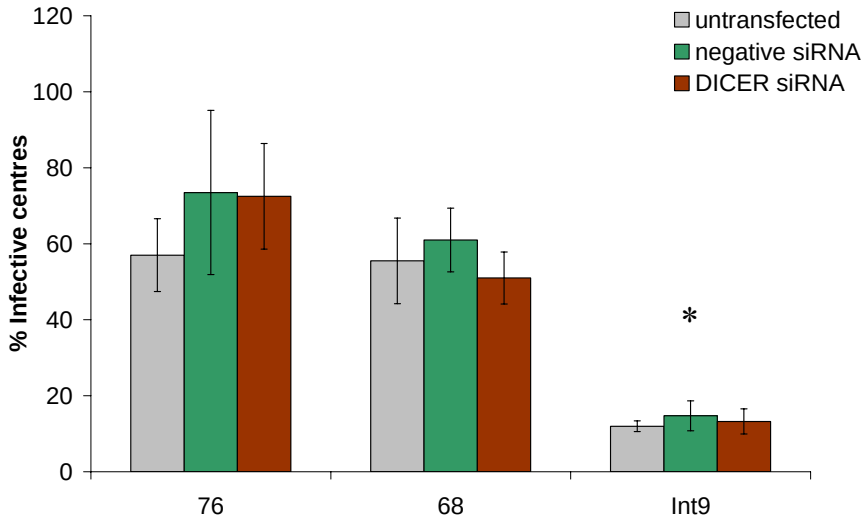

Figure 4.21 Percentage of infective centres following transfection of a siRNA against Dicer. NS0 cells were transfected with siRNA and 48 hours later infected with either MHV-76, MHV-68 or Int9. Each bar shows the mean of two biological replicates, each with two technical replicates. The transfection efficiency was around 37%. Error bars represent the standard deviation. * Int9 infected NS0 cells reactivated virus at a significantly lower ($p<0.005$) percentage than MHV-68 and MHV-76 untransfected NS0 cells, as determined by Student's t-test.

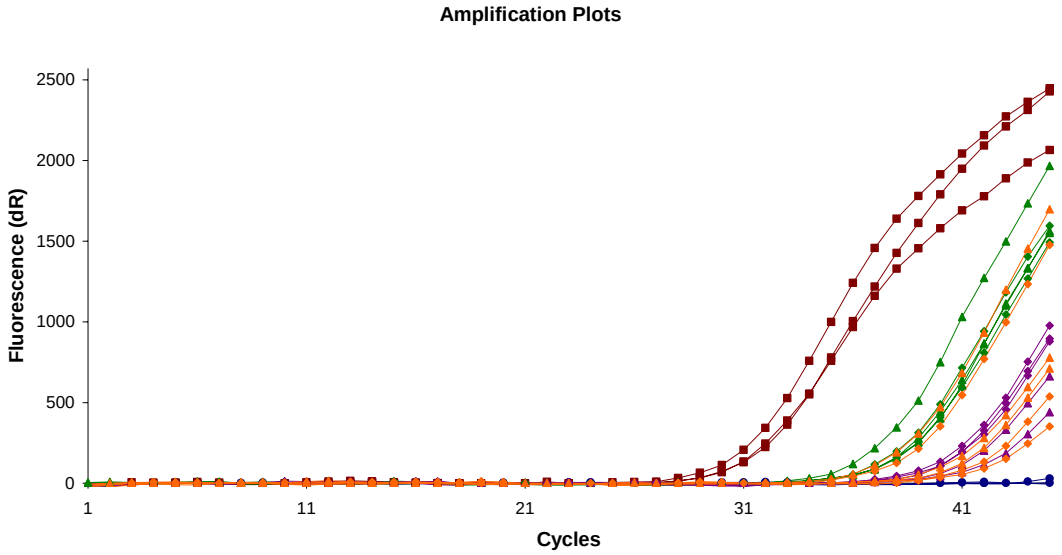

Figure 4.22 qRT-PCR amplification plots for miRNA4. Showing uninfected cells (), MHV-68 infected cells () and Int9 infected cells: untransfected (), negative siRNA () and Dicer siRNA () transfected.

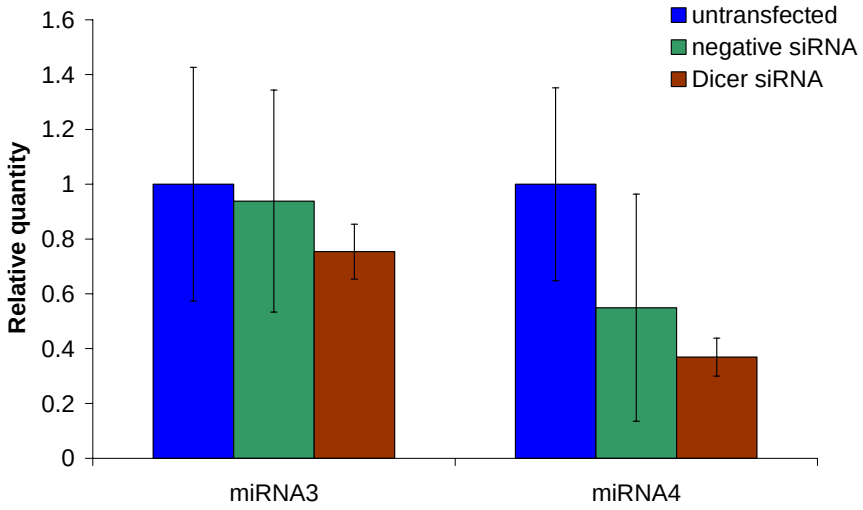

Figure 4.23 Relative quantity of miRNA3 and 4 as determined by qRT-PCR on small RNAs from Int9 infected NS0 cells: untransfected, negative siRNA transfected or miRNA transfected. Values normalised against cellular mir-16 levels and expressed relative to untransfected cell expression levels. Error bars represent the standard deviation.

4.3.3. ORF50

To examine if the Int9 infected NS0 cells were capable of reactivating virus, a plasmid expressing the MHV-68 rta (a gift from Bahram Ebrahimi) was transfected into the cells. This plasmid contains the rta (ORF 50) genomic sequence fused to a flag sequence, under the influence of CMV promoter (Wu *et al.* 2001).

NS0 cells were infected with Int9 at a MOI 5 pfu/cell for four days and the plasmid transfected. After 24 hours infective centres assays were performed. MHV-68 infected NS0 cells were included as a reactivation control. Transfection of rta expressing plasmid did not lead to a significant increase in reactivation ($p=0.06$) compared to negative control plasmid (Figure 4.24). Again, MHV-68 infected cells reactivated virus at a significantly ($p<0.01$) higher frequency than Int9 infected cells.

To further investigate if the lack of induction of reactivation by rta over-expression was due to the inability of Int9 infected cells to reactivate, the experiment was repeated. This time MHV-68 infected cells were transfected as well. Over-expression of rta in MHV-68 infected cells should lead to an increase in reactivation (Wu *et al.* 2000). This time infective centres were performed 48 hours post transfection as well, since over-expression of rta in S11 cells was found to lead to a large increase in the production of lytic virus following reactivation at this time post infection (Wu *et al.* 2000). Over-expression of rta in MHV-68 or Int9 infected cells did not lead to an increase in reactivation (Figure 4.25). However, the transfection itself stressed both MHV-68 and Int9 infected cells to reactivate virus. Due to time constraints this was not followed up.

4.3.4. vtRNAs

Since transfection of miRNAs did not have an effect on the reactivation rates of infected NS0 cells, expression of the vtRNAs might be the cause of the reduction in reactivation seen in Int9 infected NS0 cells. To investigate this further, vtRNA1 was *in vitro* transcribed, folded, and transfected into NS0 cells infected with MHV-76 for four days. Infective centres assays were performed 24 hours post transfection, with Int9 infected cells included as a control. Transfection of vtRNA1 did not lead to a reduction in reactivation of MHV-76 infected NS0 cells (Figure 4.26); however, the

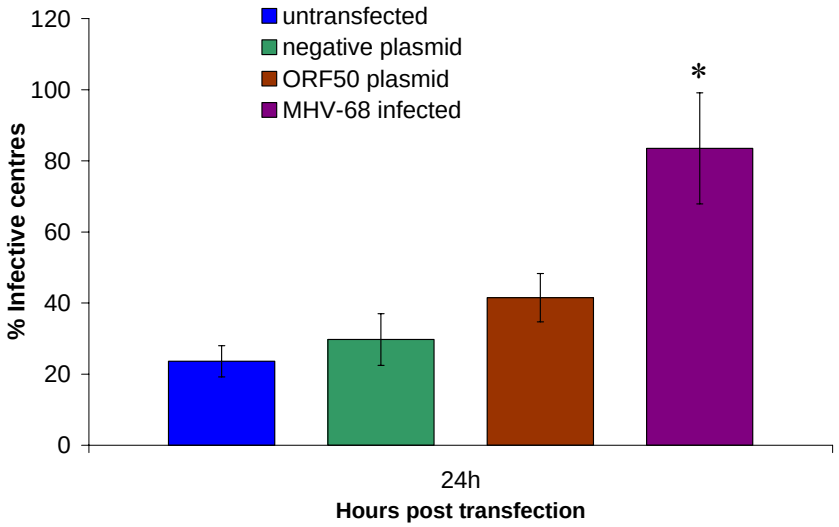

Figure 4.24 Percentage of infective centres 24 hours following transfection of Int9 infected cells with ORF50 plasmid or negative control plasmid. MHV-68 infected cells were included as a control of reactivation. Each bar shows the mean of two biological replicates, each with two technical replicates. The transfection efficiency was around 69%. Error bars represent the standard deviation. * MHV-68 infected cells reactivated virus at a significantly ($p<0.01$) higher frequency than Int9 infected cells, whether transfected or not, as determined by Student's t-test.

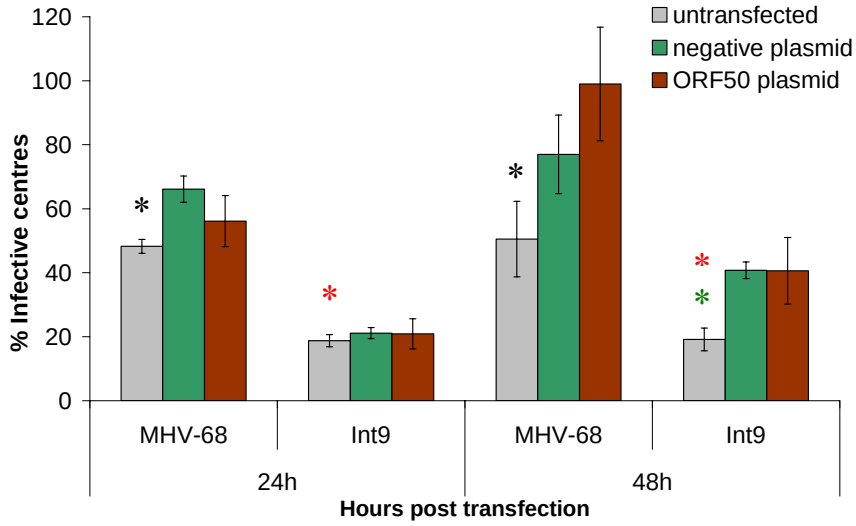

Figure 4.25 Percentage of infective centres 24 and 48 hours following transfection of MHV-68 or Int9 infected cells with ORF50 plasmid or negative control plasmid. Each bar shows the mean of two biological replicates, each with two technical replicates. The transfection efficiency was around 60%. Error bars represent the standard deviation. * MHV-68 infected untransfected cells had significantly lower reactivation rates than negative plasmid transfected cells 24 hours ($p<0.001$) and 48 hours ($p<0.025$). * At 48 hours post transfection Int9 infected untransfected cells had significantly lower reactivation rates ($p<0.0001$) than negative plasmid transfected cells. * Int9 infected untransfected NS0 cells reactivated virus at significantly lower levels than MHV-68 infected untransfected NS0 cells both 24 hours ($p<0.000001$) and 48 hours ($p<0.01$) post transfection, as determined by Student's t-test.

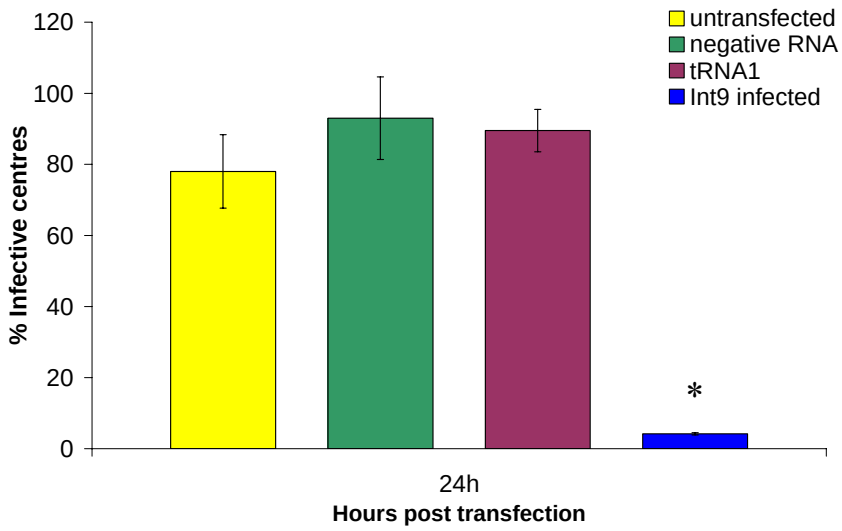

Figure 4.26 Percentage of infective centres from MHV-76 infected NS0 cells, 24 hours post transfection with vtRNA1. Each bar shows the mean of two biological replicates, each with two technical replicates. The transfection efficiency was around 21%. Error bars represent the standard deviation. * Int9 infected cells reactivated virus at a significantly ($p<0.001$) lower level than MHV-76 infected cells, whether transfected or not, as determined by Student's t-test.

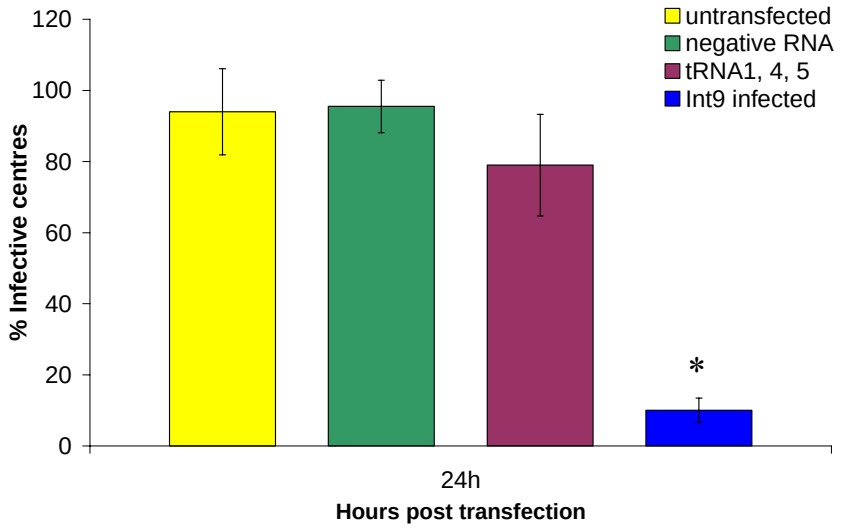

Figure 4.27 Percentage of infective centres from MHV-76 infected NS0 cells, 24 hours post transfection with vtRNA1, 4 and 5. Each bar shows the mean of two biological replicates, each with two technical replicates. The transfection efficiency was around 30%. Error bars represent the standard deviation. * Int9 infected cells reactivated virus at a significantly ($p<0.0025$) lower level than MHV-76 infected cells, whether transfected or not, as determined by Student's t-test.

transfection efficiency was low, 21%. Int9 infected NS0 cells reactivated virus at a significantly lower level than MHV-76 infected NS0 cells.

The vtRNAs may co-operate to reduce reactivation; therefore, the previous experiment was repeated but this time vtRNAs1, 4 and 5 were co-transfected into MHV-76 infected NS0 cells. Transfection of vtRNAs1, 4 and 5 into MHV-76 infected NS0 cells did not lead to a reduction of reactivation (Figure 4.27). This time the transfection efficiency was slightly higher, around 30%. Again, Int9 infected NS0 cells reactivated virus at a significantly lower level than MHV-76 infected NS0 cells.

4.3.5. pL2a5

It is possible that the vtRNAs and miRNAs co-operate and that both are needed to cause a reduction in reactivation. To investigate this further the plasmid used to make the insertion viruses, pL2a5, was transfected into infected cells. NS0 cells were infected with MHV-76 at a MOI of 5 pfu/cell for four days, prior to transfection with pL2a5 or negative control plasmid. Infective centres assays were set up 24 hours post transfection. Transfection of pL2a5 into MHV-76 infected NS0 cells did not led to a reduction in reactivation (Figure 4.28). Int9 infected NS0 cells reactivated virus at a significantly lower level than MHV-76 infected NS0 cells, whether transfected or not.

To give the plasmid longer time to express the non-coding RNAs the previous experiment was repeated and infective centres performed 48 hours post transfection. Transfection of the pL2a5 plasmid into MHV-76 infected NS0 cells did not lead to a reduction in reactivation after 48 hours either (Figure 4.29). Consistent with previous results, Int9 infected NS0 cells reactivated virus at a significantly lower level than MHV-76 infected NS0 cells, whether transfected or not.

4.4. Discussion

In this study we showed that the introduction of vtRNAs and miRNAs into MHV-76 causes a reduction in reactivation and production of lytic virus of latently infected NS0 cells, and provide evidence that this is not caused by the miRNAs.

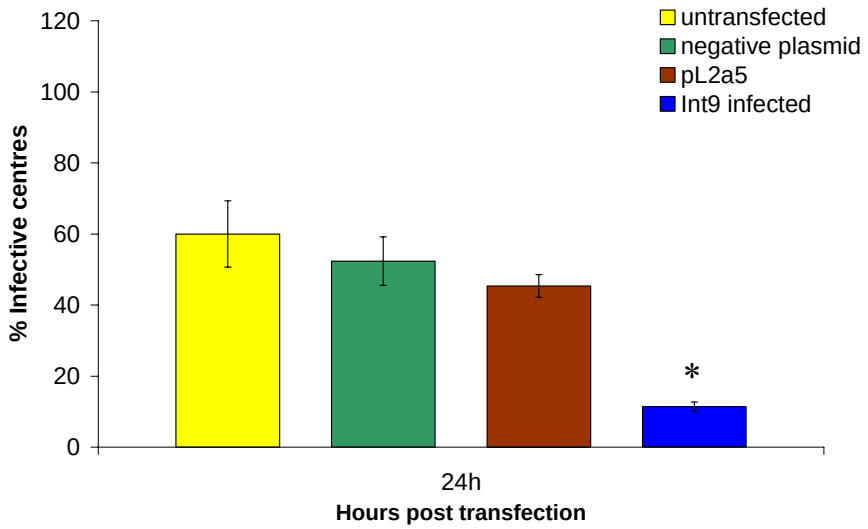

Figure 4.28 Percentage of infective centres from MHV-76 infected NS0 cells, 24 hours post transfection with pL2a5. Each bar shows the mean of two biological replicates, each with two technical replicates. The transfection efficiency was around 66%. Error bars represent the standard deviation. * Int9 infected cells reactivated virus at a significantly ($p<0.0025$) lower level than MHV-76 infected cells, whether transfected or not, as determined by Student's t-test.

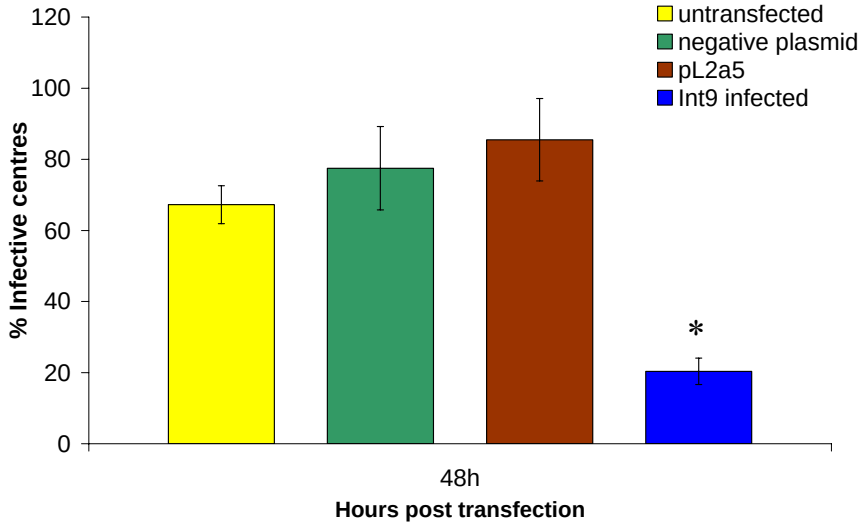

Figure 4.29 Percentage of infective centres from MHV-76 infected NS0 cells, 48 hours post transfection with pL2a5. Each bar shows the mean of two biological replicates, each with two technical replicates. The transfection efficiency was around 78%. Error bars represent the standard deviation. * Int9 infected cells reactivated virus at a significantly ($p<0.001$) lower level than MHV-76 infected cells, whether transfected or not, as determined by Student's t-test.

We utilised insertion viruses, made by homologous recombination to insert the non-coding RNA genes into the left-end of MHV-76, to study the non-coding RNAs. This technique has previously been used to investigate the functions of the unique gene M4 (Townsley *et al.* 2004), and also the KSHV gene K1 (Douglas *et al.* 2004). In addition, MHV-76 was successfully rescued by recombination to generate a virus with growth properties indistinguishable to MHV-68 (Macrae *et al.* 2001). The technique was validated when disruption to M4 confirmed the results from the M4 insertion virus study (Geere *et al.* 2006; Townsley *et al.* 2004). The non-coding RNAs of the insertion viruses are thereby expressed by their natural promoters and they are inserted into their original location in the genome.

The initial replication and reactivation assays showed that the insertion virus Int9 reactivates and replicates at a lower level than MHV-68 and MHV-76. The investigation of the second insertion virus Int2, made independently of Int9, confirmed that this was not a phenotype restricted to Int9. The revertant virus further confirmed the results: the decrease in reactivation and production of lytic virus observed with the insertion viruses was 10-fold or greater compared to revertant virus. Because of the rapid clearance and low levels of latency of MHV-76 and the insertion viruses, as well as large differences between mice, the phenotype could not be confirmed *in vivo*. A larger study involving more mice may be helpful.

Since the only difference between the insertion viruses and MHV-76 and the revertant virus is the five vtRNAs and six miRNAs, these must be the cause of the phenotype. However, miRNA1 which has a predicted target site in the 3' UTR of the viral rta (ORF50) and could be responsible for the reduction in reactivation by targeting the rta is expressed at very low levels by the insertion viruses during latency, so is not likely to affect the reactivation of the insertion viruses. To further investigate if the vtRNAs or miRNAs had a role in virus reactivation, miRNA mimics were transfected into MHV-76 infected cells. miRNA mimics are synthetic RNA oligonucleotides that function like the mature endogenous miRNA following transfection, down-regulating the target protein for up to 72 hours. Even though the levels of miRNA mimics, as assessed by qRT-PCR for miRNA3, were higher than for insertion virus infected cells, they did not cause a reduction in reactivation.

To further confirm that the miRNAs did not cause the reduction in reactivation, a siRNA against Dicer was transfected into virus infected cells. Inhibition of Dicer leads to a decrease in the production of mature miRNAs. However, by limiting the inhibition to 48 hours cellular miRNAs should not be affected. As a control MHV-76 was included in the experiment as it does not encode any viral miRNAs. Transfection of a siRNA against Dicer did not lead to an increase or decrease in reactivation by MHV-68 or Int9 infected NS0 cells. However, the Dicer knock-down could not be confirmed by qRT-PCR of Int9 infected cells, since the miRNA expression is already low in these cells. To further confirm the results, qRT-PCR for miRNA levels in siRNA transfected MHV-68 infected NS0 cells or a western blot analysis looking at changes in the Dicer protein levels would be recommended.

To examine if the Int9 infected NS0 cells were capable of reactivating, the rta was over-expressed in infected cells by transfecting a plasmid containing ORF50 under the influence of a CMV promoter. Over-expression of the rta using this plasmid has previously been found to initiate lytic replication in productively infected cells (Wu *et al.* 2001). In addition, transfection of a similar plasmid construct into S11 cells lead to an increase in reactivation (Wu *et al.* 2000). In the infective centres assay the latently infected NS0 cells are stressed to reactivate the virus and it was thought that over-expression of the rta would lead to higher reactivation levels; however, this was not observed. The transfection itself led to an increase in reactivation that may have masked the effect of the rta. This increase in reactivation caused by the transfection was seen in several of the transfection experiments. This did show that Int9 infected NS0 cells are capable of reactivating. The expression levels of rta by the plasmid were, however, not confirmed due to time constraints.

Since the miRNAs do not appear to be involved in the reduction of reactivation seen in insertion virus infected NS0 cells, it suggested that the vtRNAs are responsible. To further investigate this, vtRNAs were transfected into MHV-76 infected NS0 cells. This did not lead to a decrease in reactivation; however, since it is not known how the vtRNAs are processed and how they function, the transfected vtRNAs may not be functional vtRNAs. In addition, the transfection efficiencies achieved were quite low.

It is possible that expression of both the vtRNAs and miRNAs is needed to decrease the reactivation of infected NS0 cells. To investigate this, the plasmid used to make the insertion viruses was transfected into MHV-76 infected NS0 cells, but it did not result in a reduction in reactivation. This was not an ideal approach since the copy number of the plasmid was not known and the non-coding RNAs would not have been in the viral genome and possibly not expressed appropriately. It should be noted that the expression levels of the vtRNAs and miRNAs following transfection was not examined due to time constraints. Further work would be needed to confirm the results, including transfection of miRNAs and vtRNAs together.

MHV-76 consistently reactivated at a higher level and produced more lytic virus than both MHV-68 and the revertant virus. The reason for this is not known. It is possible that the copy number of MHV-76 in the cell is higher; however, it is not known why the revertant would not have the same copy number since it is identical to MHV-76. A fresh MHV-76 virus stock could be used to see if the same phenotype is achieved. It may also be useful to repeat the transfection experiments using revertant virus infected NS0 cells. Importantly, the insertion viruses consistently reactivated at a much lower rate than the revertant, which is the control virus, as well as MHV-68 and MHV-76.

The experiment described in this chapter point to a role for the non-coding RNAs in virus reactivation. The miRNA transfections show that the reduction in reactivation is not due to the miRNAs alone, even though the miRNAs levels achieved were higher than in Int9 infected cells. The vtRNA transfection experiments did not confirm the role of the vtRNAs in viral reactivation and it is possible that the vtRNAs and miRNAs co-operate, which needs to be further investigated. The expression of the miRNAs by the insertion viruses is lower than that of MHV-68, and it is not known if the vtRNA levels are as well. Due to these problems a better approach would be to make mutations in the MHV-68 genome, which has previously been done to determine the functions of a number of viral genes, such as ORF 73, ORF50, M1 and K3 (Clambey *et al.* 2000; Fowler *et al.* 2003; Pavlova *et al.* 2003; Stevenson *et al.* 2002). To confirm that the vtRNAs are responsible for the reduction in reactivation, it would be useful to create a virus with disruption to the miRNAs which does not affect the processing of the vtRNAs. Since the vtRNAs and miRNAs

are transcribed on the same transcript and the processing of this transcript is not clear, it may not be possible to remove the whole miRNA. An option could be to mutate the seed sequences of the miRNAs. The seed sequence of the miRNA is usually important for target binding; however, this is not always the case and it would be difficult to confirm that the miRNAs actually were not functional since their targets are not known. Another possibility would be to disrupt the stem-loop structure of the vtRNAs; however, it is not know if this would affect the processing of the miRNAs. It may also be useful to insert only one of the vtRNA/miRNA transcripts into MHV-76 to investigate if the same phenotype can be achieved or if more than one vtRNA/miRNA transcript is necessary.

5. Chapter Five: Investigating the effects of the non-coding RNAs on protein synthesis in latently infected cells

5.1. Aims **149**
5.2. cICAT **153**
5.2.1. BSA 153
5.2.2. MHV-76 vs. Int9 latently infected NS0 cells 157
5.2.3. Troubleshooting protein extraction techniques 161
5.2.4. MHV-76 vs. Int9 latently infected NS0 cells- Vivaspin 165
5.2.5. MHV-76 vs. Int9 latently infected NS0 cells- freeze-dryer 171
5.3. 1-D PAGE cICAT **176**
5.3.1. Assay setup 176
5.3.2. BSA 180
5.3.3. MHV-76 vs. Int9 latently infected NS0 cells 182
5.4. Discussion **192**

5.1. Aims

To investigate the functions of the non-coding RNAs, the differences in protein expression during latency between MHV-76 and Int9 infected cells were examined using cICAT. In this method the cysteines of the proteins are labelled with heavy or light isotope-coded tags which allows for identification and quantification of differentially expressed proteins using mass spectrometry. The isotope-coded tags are made up of $C_{10}H_{17}N_3O_3$, with the light tag containing 9 ^{12}C and the heavy 9 ^{13}C resulting in a difference of 9 amu in weight. A biotin affinity tag on the isotope-coded tag enables purification of labelled peptides using an avidin column, decreasing the complexity of the sample. The biotin tag is subsequently cleaved off, reducing the size of the labelled peptide and thus allowing analysis of larger peptides. Samples taken during the labelling to monitor the process are analysed by MALDI (Matrix-assisted laser desorption/ionization) mass spectrometry, while the final labelled sample is separated on a liquid chromatograph (LC) and analysed using on-line tandem mass spectrometry (MS/MS). The cICAT method is described in Figure 5.1.

Mass spectrometry utilises the production of ions that are separated according to their mass-to-charge ratio (m/z). An ionisation source such as electrospray ionisation (ESI) or MALDI is used to charge the peptides, via the addition of one (MALDI) or more (ESI) protons. A singly charged peptide with a molecular mass of 2000 daltons will thus have an m/z of 2001, while a doubly charged ion will have an m/z of 1001. During single mass spectrometry analysis using a MALDI-TOF (Time of flight) the ions enter a flight tube, with the ions travelling faster towards the detector the smaller they are. The ions are accelerated with the same potential at the same point and time, and will therefore be separated by their m/z. The relative abundance of the ions is then plotted for each m/z value in a mass spectrum. The masses of the peaks generated can be matched against databases of theoretical peptides generated from proteins to identify the protein they originated from. A protein score is calculated for each protein match, which indicates the probability that the match is a random event.

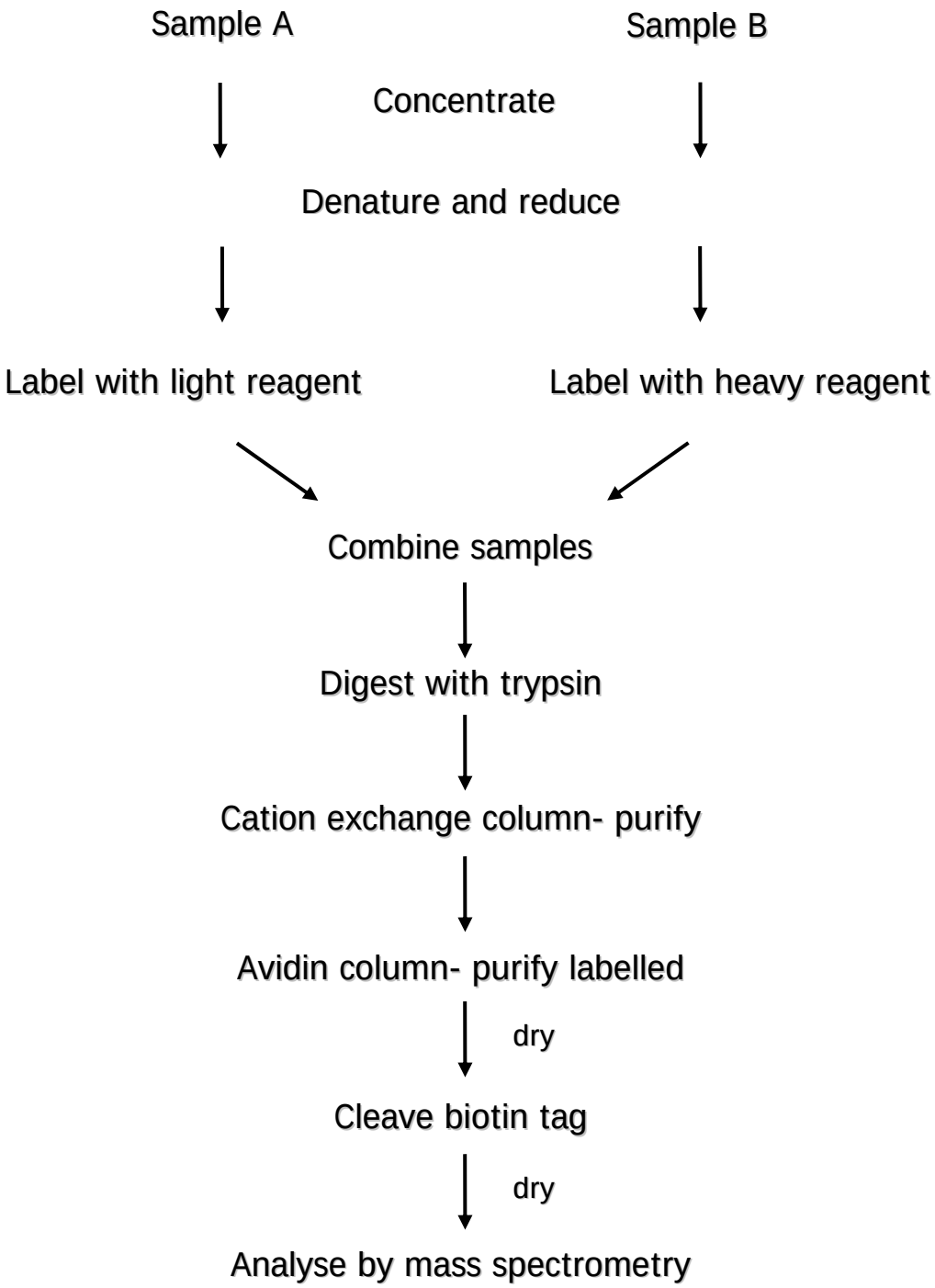

Figure 5.1 Step-by-step schematic description of the cICAT labelling.

During nanoLC-MS/MS, a reverse phase high performance liquid chromatograph (HPLC) separates the peptides according to polarity and they are introduced into the mass spectrometer. Following the single MS, ions are selected on peak intensities to go through a further MS. The selected ion is fragmented into product ions, usually through collision with a neutral gas, with b and y ions being most common (Figure 5.2A). The fragments are separated according to m/z, producing a MS/MS mass spectrum from fragments of that specific peptide (Figure 5.2B). The b and y ions can be identified in the spectra in Figure 5.2B by looking at differences in m/z values of fragment ions between the peptide labelled with light and heavy cICAT reagent. Since the labelled cysteine is in the far left end of this peptide, only b ions will be labelled and have a difference in charge in the two spectra, 9 m/z if the ion is singly charged and 4.5 m/z if doubly charged. The fragment masses generated are matched against a database of theoretical fragment masses of peptide ions of the same mass and an ion score reflecting the absolute probability that the match is a random event is calculated. The peptides identified are matched against proteins in the database and a protein score is derived from the ion scores, with multiple peptide matches for the same protein giving a high protein score and thus indicating a true match.

Since the only difference between MHV-76 and Int9 is the non-coding RNAs, any difference in protein expression found should be caused by the vtRNAs and/or miRNAs. The cICAT would provide a screening method to identify proteins directly and indirectly affected by the non-coding RNAs. This could further be confirmed by western blot analysis to verify changes in protein levels, northern blot analysis to examine if the mRNA levels of the proteins are affected, and electric mobility shift assay (EMSA) to investigate if there is a direct interaction between the protein and the vtRNAs.

A

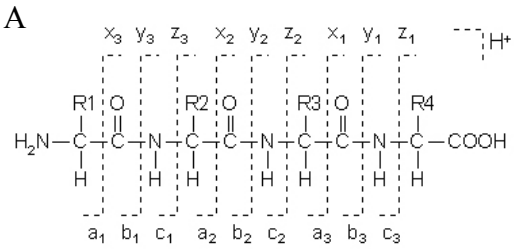

B

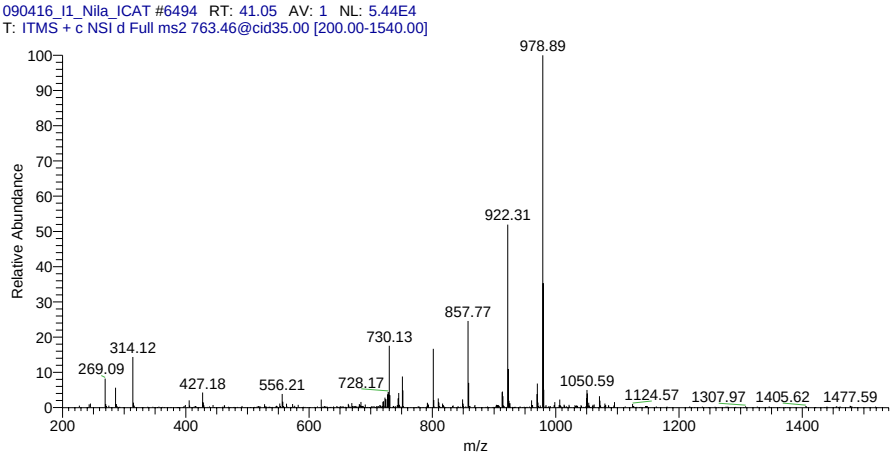

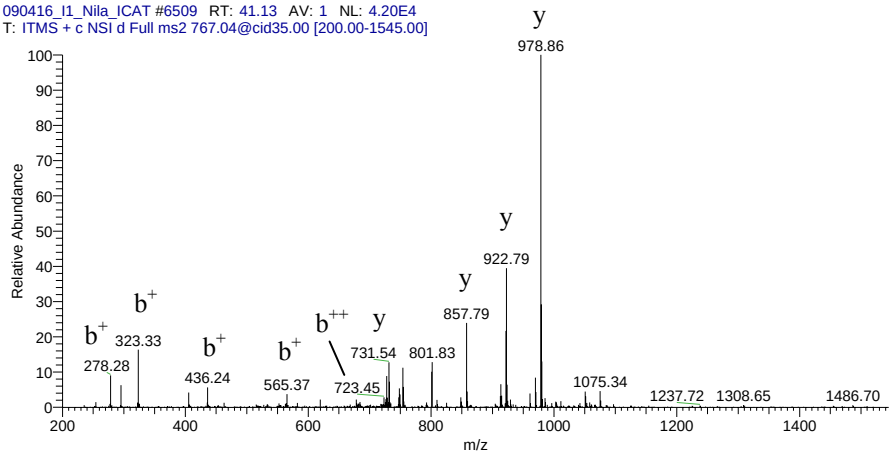

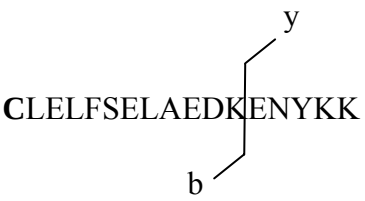

Figure 5.2 Demonstrating the fragmentation of a peptide, showing the different possibilities of fragmentation (A) with b and y ions being most common, and in the MS/MS spectrum (B) of a Hsp90-β peptide, labelled with light (top) and heavy (bottom) cICAT reagent. Since the labelled cysteine is at the far left end of the peptide, only the b ions will be labelled and have different m/z values in the two spectra, 9 m/z if singly charged and 4.5 if doubly charged. y ions will not have a different m/z value.

5.2. cICAT

5.2.1. BSA

Prior to analysing virus infected cells the technique was tested using a known protein, BSA, which was labelled according to the manufacturer's protocol (section 2.9.7.1) with some changes to the volumes used.

Aliquots were collected at each step during the cICAT protocol and analysed by MALDI to monitor the process. 2.5µg BSA was denatured and reduced, and half of the protein solution labelled with light ICAT reagent (36µl protein + 9µl light reagent) and half mixed with acetonitrile as a non-labelled control (36µl protein + 9µl acetonitrile). The proteins were trypsin digested over night at 37°C and the samples analysed by MALDI. The samples yielded mainly the same peptide peaks (Figure 5.3). Labelling of the peptides should yield peaks with m/z ratios that are higher than the unlabelled and not the same m/z, as was observed; however, the majority of the abundant peaks were BSA peptides that do not contain cysteines and would not be labelled (Table 5.1).

The peptides of the cICAT labelled sample were subsequently purified using a cation-exchange column, which removed some of the peaks seen in the previous MALDI analysis (Figure 5.4). Some of these peaks could be from components of the denaturing buffer (SDS), reducing agent (TCEP, breaks disulfide bonds) or unused light cICAT reagent, which will be removed with the cation-exchange column. One of the most abundant peaks, a BSA peptide with an m/z of 1283, was also lost in the cation-exchange column. This indicated that some peptides may be lost, perhaps due to instability or that they do not bind or elute at the pH that was used. Labelled peptides were purified using an avidin column, which changed the MALDI spectrum with previously small peaks becoming more prominent as a results of losing some of the abundant non-labelled peptides and removal of salts that may interfere with the MALDI ionisation (Figure 5.4).

Both the control and labelled peptide solutions were vacuum dried, prior to cleavage of the biotin tag of the labelled peptides, and the peptide samples subsequently dried using a vacuum dryer. The peptides were resuspended in 40µl 0.5% (v/v) acetic acid

Control: post-trypsin

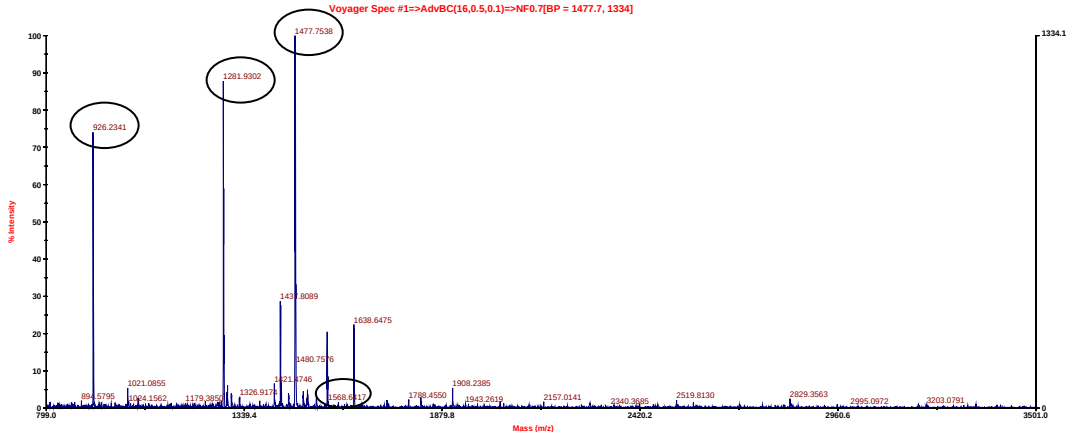

Labelled: post-trypsin

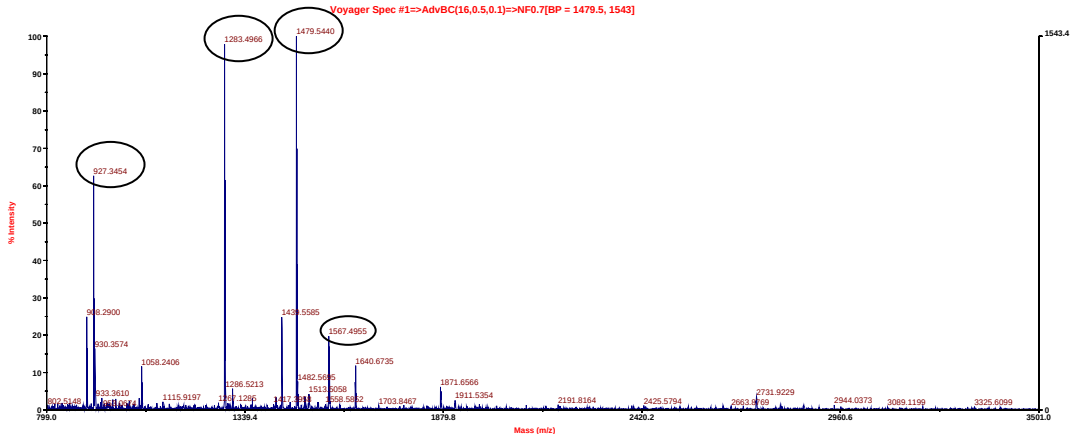

Figure 5.3 MALDI analysis of BSA peptides generated by trypsin treatment of unlabelled control BSA or BSA labelled with light cICAT reagent. Abundant peaks of possible BSA peptides that do not contain cysteines and would not be labelled are circled.

Sequence	No. of cysteines	Unlabelled	Light
GLVLIAFSQYLQQCPFDEHVK	1	2435.24	2662.37
DAIPENLPPLTADFAEDK	0	1955.96	1955.96
HPYFYAPELLYYANK	0	1888.93	1888.93
LFTFHADICTLPDTEK	1	1850.90	2078.03
RPCFSALTPDETYVPK	1	1823.90	2051.03
MPCTEDYLSLILNR	1	1667.81	1894.94
YNGVFQECCQAEDK	2	1633.66	2087.92
ECCHGDLLECADDR	3	1578.60	2259.99
DAFLGSFLYEYSR	0	1567.74	1567.74
LKPDPNTLCDEFK	1	1519.75	1746.88
VPQVSTPTLVEVSR	0	1511.84	1511.84
DDPHACYSTVFDK	1	1497.63	1724.76
LGEYGFQNALIVR	0	1479.80	1479.80
TVMENFVAFVDK	0	1399.69	1399.69
EYEATLEECCAK	2	1388.57	1842.83
YICDNQDTISSK	1	1386.62	1613.75
ETYGDMADCCEK	2	1364.48	1818.74
SLHTLFGDELCK	1	1362.67	1589.80
TCVADESHAGCEK	2	1349.55	1803.81
HLVDEPQNLIK	0	1305.72	1305.72
HPEYAVSVLLR	0	1283.71	1283.71
ECCDKPLLEK	2	1177.56	1631.82
LVNELTEFAK	0	1163.63	1163.63
CCTKPESER	2	1052.45	1506.71
EACFAVEGPK	1	1050.49	1277.62
CCTESLVNR	2	1024.46	1478.72
SHCIAEVEK	1	1015.49	1242.62
QTALVELLK	0	1014.62	1014.62
QNCDQFEK	1	1011.42	1238.55
LVVSTQTALA	0	1002.58	1002.58
NECFLSHK	1	977.45	1204.58
DLGEEHFK	0	974.46	974.46
YLYEIAR	0	927.49	927.49
AEFVEVTK	0	922.49	922.49
DDSPDLPK	0	886.42	886.42
LCVLHEK	1	841.46	1068.59
ATEEQLK	0	818.43	818.43
LVTDLTK	0	789.47	789.47
NYQEAK	0	752.36	752.36
CCAADDK	2	725.26	1179.52
SEIAHR	0	712.37	712.37
VLASSAR	0	703.41	703.41
GACLLPK	1	701.40	928.53
AWSVAR	0	689.37	689.37
TPVSEK	0	660.36	660.36
QEPER	0	658.32	658.32
IETMR	0	649.33	649.33
CASIQK	1	649.33	876.46
AFDEK	0	609.29	609.29
VASLR	0	545.34	545.34
FWGK	0	537.28	537.28
ADLAK	0	517.30	517.30
HKPK	0	509.32	509.32
FGER	0	508.25	508.25
DTHK	0	500.25	500.25
DVCK	1	464.22	691.35

Table 5.1 Listing the predicted BSA derived peptides, with m/z values as expected in the unlabelled control and labelled with light cICAT reagent.

Labelled: pre-avidin

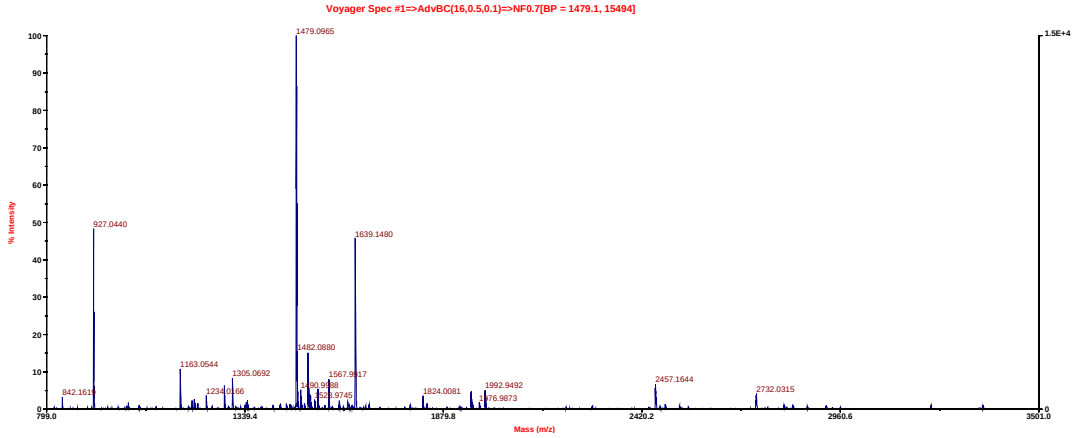

Labelled: post-avidin

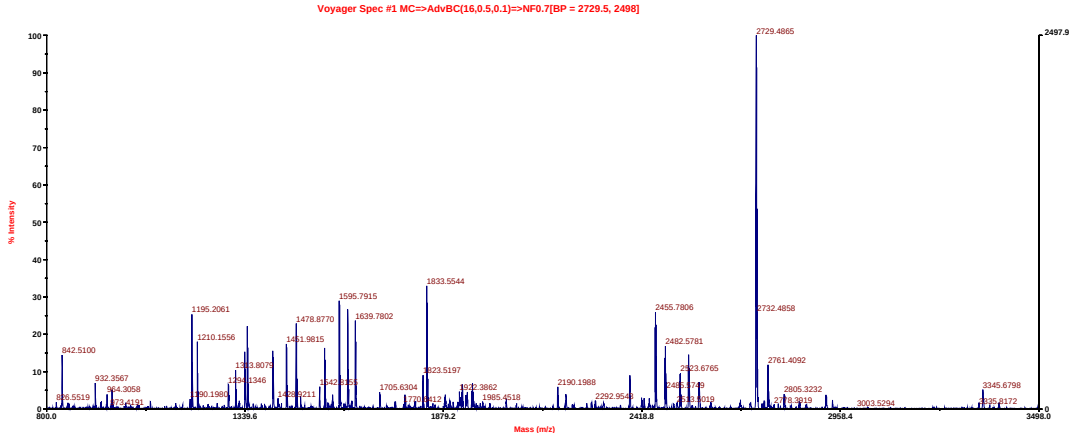

Figure 5.4 MALDI analysis of BSA derived peptides labelled with light cICAT reagent following cation-exchange column (pre-avidin) and after the avidin column (post-avidin).

and analysed by MALDI, and also diluted 1 in 10 and analysed on an LCQdeca MS/MS system. The MALDI analysis of the labelled BSA sample showed that cleavage of the biotin molecule (m/z 680.34) reduced the size of the peptide peaks, moving the peaks to the left of the spectrum (Figure 5.5). This was demonstrated by the most abundant peak in the post-avidin sample with an m/z of 2729 (Figure 5.4) that was still the most abundant peak following cleavage with an m/z of 2051 (Figure 5.5). MALDI analysis of the control sample showed that vacuum drying and re-suspension in acetic acid had changed the spectrum slightly, with previously abundant peptides becoming less abundant (Figure 5.3, Figure 5.5). This may be because the abundant peptides were less stable or dissolved less well in the acetic acid.

Several of the expected BSA peptide peaks (Table 5.1), labelled and unlabelled, could be seen among the most abundant peaks (Figure 5.5). This was confirmed when around 100 of the most abundant peaks from the labelled sample were submitted to search against the Mascot database, identifying BSA (Figure 5.6). Although the sample contained only BSA and trypsin, several other possible protein matches were listed; however, these had non-significant protein scores and were unlikely to be true matches. BSA was also identified when analysing the labelled sample on the LC-MS/MS system (Figure 5.7).

The labelling of BSA showed that the cICAT labelling worked and the technique was subsequently used to analyse proteins from virus infected cells.

5.2.2. MHV-76 vs. Int9 latently infected NS0 cells

After successfully identifying BSA labelled by the cICAT method it was decided to investigate if there was a difference in protein expression between MHV-76 and Int9 infected NS0 cells. The proteins of cells infected with MHV-76 or Int9 at a MOI of 5 for five days were extracted and fractionated into cytosolic, membrane/organelle, nuclear and cytoskeletal fractions, using a ProteoExtract® Subcellular Proteome Extraction kit, to make the protein samples less complex. A BCA Protein Assay was performed to determine the protein concentrations of the samples. Since the vtRNAs localise mainly to the cytoplasm during latency, it was decided to use the cytosolic fraction for further analysis. For each sample 100μg of cytosolic proteins were

Control: final sample

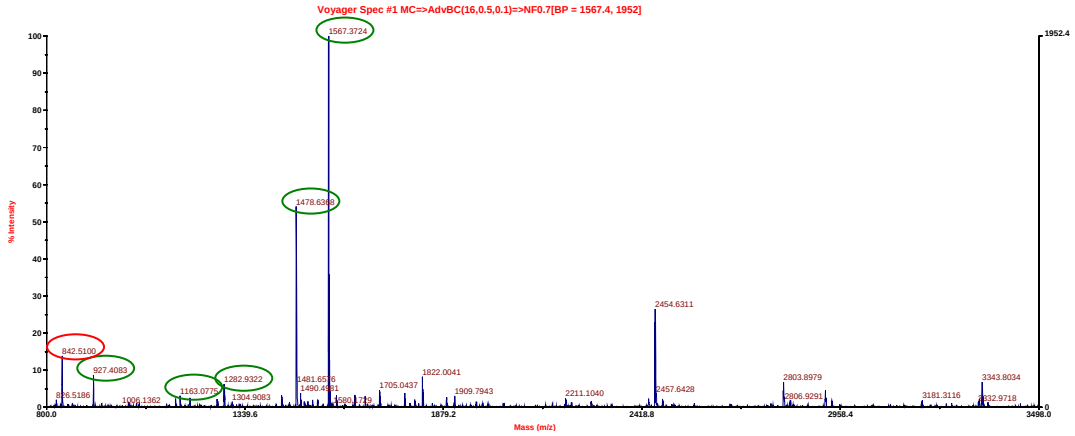

Labelled: final sample

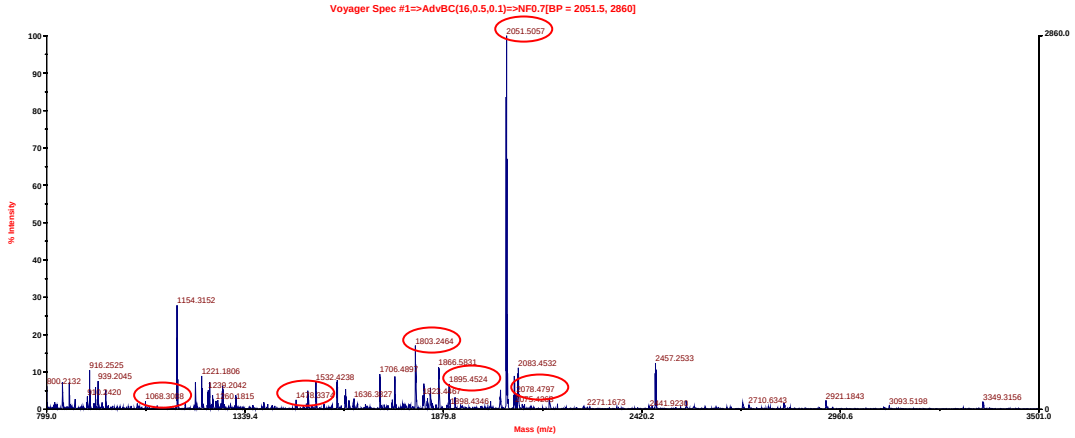

Figure 5.5 MALDI analysis of the final BSA samples, unlabelled control or labelled with light cICAT reagent. The unlabelled control had been trypsin digested, mock-labelled, dried down by vacuum dryer and resuspended in 0.5% acetic acid. Showing possible BSA peptides containing cysteines (circled in red) and not containing cysteines (circled in green).

Protein scores greater than 67 are significant (p<0.05).

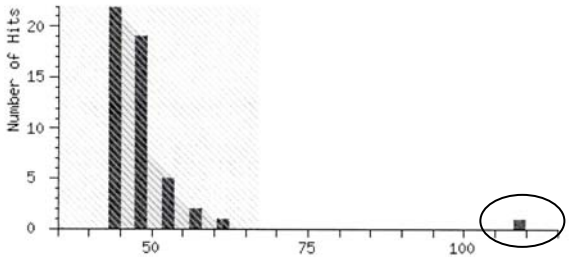

	Accession	Mass	Score	Description
1.	ALBU_BOVIN	77198	109	Serum albumin precursor - Bos taurus (Bovine)
2.	DPO1_BACST	99063	60	DNA polymerase I - Bacillus stearothermophilus (Geobacillus ste
3.	NDKA1_BOVIN	17704	59	Nucleoside diphosphate kinase A 1 - Bos taurus (Bovine)
4.	SCA4_RICAU	108679	58	Antigenic heat-stable 120 kDa protein - Rickettsia australis
5.	Y816_BACLD	8183	54	UPF0435 protein BLi00816/BL03111 - Bacillus licheniformis (stra
6.	CH601_ANADE	58226	53	60 kDa chaperonin 1 - Anaeromyxobacter dehalogenans (strain 2CI
7.	FENR2_PEA	43875	52	Ferredoxin--NADP reductase, root isozyme, chloroplast precursor
8.	RL1_DESPS	25335	52	50S ribosomal protein L1 - Desulfotalea psychrophila
9.	HCD2_MOUSE	27856	51	3-hydroxyacyl-CoA dehydrogenase type-2 - Mus musculus (Mouse)
10.	GUAA_DEIRA	56387	50	GMP synthase [glutamine-hydrolyzing] - Deinococcus radiodurans
11.	MARE1_XENTR	30869	49	Microtubule-associated protein RP/EB family member 1 - Xenopus
12.	PLEC1_RAT	540936	49	Plectin-1 - Rattus norvegicus (Rat)
13.	DYH8_MOUSE	556163	49	Ciliary dynein heavy chain 8 - Mus musculus (Mouse)
14.	HSLU_RHOPA	47686	49	ATP-dependent hsl protease ATP-binding subunit hslU - Rhodopseu
15.	MY18B_HUMAN	293639	49	Myosin-XVIIIb - Homo sapiens (Human)
16.	RPOC_LACJO	139534	48	DNA-directed RNA polymerase subunit beta' - Lactobacillus johns
17.	SRP19_HALSA	10207	48	Signal recognition particle 19 kDa protein - Halobacterium sali
18.	MYSP_ANISI	101081	48	Paramyosin - Anisakis simplex (Herring worm)
19.	CF163_BOVIN	40103	48	Uncharacterized protein C6orf163 homolog - Bos taurus (Bovine)
20.	ZN192_PANTR	70480	48	Zinc finger protein 192 - Pan troglodytes (Chimpanzee)

Figure 5.6 Results of the MALDI analysis of the BSA sample labelled with light cICAT reagent. Around 100 of the most abundant peaks were submitted to search the Swiss-Prot database, using Mascot software. BSA was identified with a significant (p<0.05) protein score of 109 that was above the threshold of 67 (as shown in the graph), indicating that this was a true match. Other possible protein matches did not have significant scores and were unlikely to be true matches.

ALBU_BOVIN
(P02769) Serum albumin precursor (Allergen Bos d 6) (BSA)

Peptide
R.LCVLHEK.T
R.LCVLHEK.T
R.NECFLSHK.D
K.QNCDQFEK.L
K.SHCIAEVEK.D
K.SHCIAEVEK.D
K.SHCIAEVEK.D
K.EACFAVEGPK.L
K.EACFAVEGPK.L
K.HLVDEPQNLIK.Q
K.HLVDEPQNLIK.Q
R.CCTKPESER.M
K.DAFLGSFLYEYSR.R
K.DAFLGSFLYEYSR.R
K.DAFLGSFLYEYSR.R
K.SLHTLFGDELCK.V
K.SLHTLFGDELCK.V
K.SLHTLFGDELCK.V
K.SLHTLFGDELCK.V
K.SLHTLFGDELCK.V
K.SLHTLFGDELCK.V
K.SLHTLFGDELCK.V
K.SLHTLFGDELCK.V
K.SLHTLFGDELCK.V
K.SLHTLFGDELCK.V
K.YICDNQDTISSK.L
K.YICDNQDTISSK.L
K.YICDNQDTISSK.L
K.DDPHACYSTVFDK.L
K.LKPDPNTLCDEFK.A
K.LKPDPNTLCDEFK.A
K.LKPDPNTLCDEFK.A
K.QEPERNECFLSHK.D
R.HPYFYAPELLYYANK.Y
R.MPCTEDYLSLILNR.L
R.MPCTEDYLSLILNR.L
R.RPCFSALTPDETYVPK.A
R.RPCFSALTPDETYVPK.A
R.RPCFSALTPDETYVPK.A
R.RPCFSALTPDETYVPK.A
R.RPCFSALTPDETYVPK.A
R.NECFLSHKDDSPDLPK.L
R.NECFLSHKDDSPDLPK.L
K.LFTFHADICTLPDTEK.Q
K.DAIPENLPPLTADFAEDKDVCK.N
K.GLVLIAFSQYLQQCPFDEHVK.L

Figure 5.7 Results of the LC-MS/MS analysis of BSA labelled with light cICAT reagent, using Mascot software to search against the Swiss-Prot database. BSA was identified with several peptides matched to BSA, as listed. Search parameters: Peptide mass tolerance ± 2 Da; Fragment mass tolerance ± 0.8 Da; missed cleavages 1.

acetone precipitated and resuspended in denaturing buffer and labelling performed according to the protocol (section 2.9.7.1). Proteins from MHV-76 infected NS0 cells were labelled with light and Int9 with heavy cICAT reagent. A vacuum dryer was used to dry down the sample prior to (nine hours) and following (20 min) cleaving of the biotin tag. The sample was resuspended in 60µl 0.5% (v/v) acetic acid and analysed on an LCQdeca MS/MS system. Only two proteins were identified, Glyceraldehyde 3-phosphate dehydrogenase (GAPDH) with one peptide labelled with light cICAT reagent and pyruvate kinase with one peptide labelled with heavy cICAT reagent (results not shown).

The MALDI analysis of samples taking during the labelling process showed that not many peptides were present following the trypsin digestion and after purification using the cation exchange and avidin columns there were few peaks with some background noise appearing, as shown by the less defined baseline (Figure 5.8). There were some peaks in the final sample following cleavage of the biotin tag, but also a lot of background noise, indicating low levels of peptides (Figure 5.9).

The fact that there were few peptides present already following the trypsin digestion indicated that there was a problem with the protein samples. It was possible that there were very few different proteins present in the cytosolic fractions or that the tryptic digestion was not working properly.

5.2.3. Troubleshooting protein extraction techniques

To determine if the low number of proteins was due to the protein fractionation, the commercial kit was compared to a different cytoplasmic protein extraction method. Proteins were extracted from uninfected NS0 cells using both the ProteoExtract® Subcellular Proteome Extraction Kit and the cytoplasmic extraction protocol and the protein concentrations determined using a BCA Protein Assay. The cytoplasmic extraction, the different fractions from the kit, as well as the cytosolic protein fractions from MHV-76 and Int9 infected NS0 cells, were analysed by SDS-PAGE in differing amounts. The cytoplasmic extract had a higher concentration of proteins; however, the gel showed that although the cytosolic fraction of uninfected NS0 cells, as well as MHV-76 and Int9 infected, had a lower concentration of proteins they did contain a lot of different proteins, although at quite low concentrations (Figure 5.10).

Post-trypsin

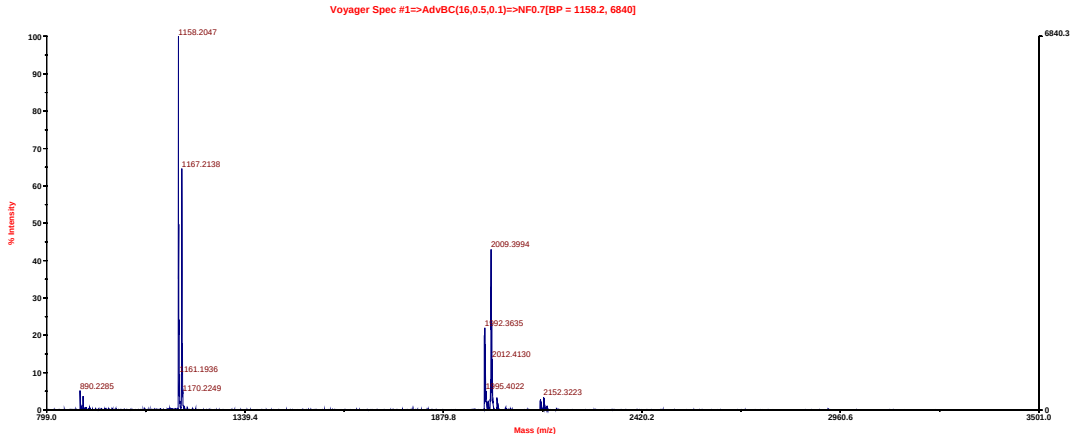

Pre-avidin

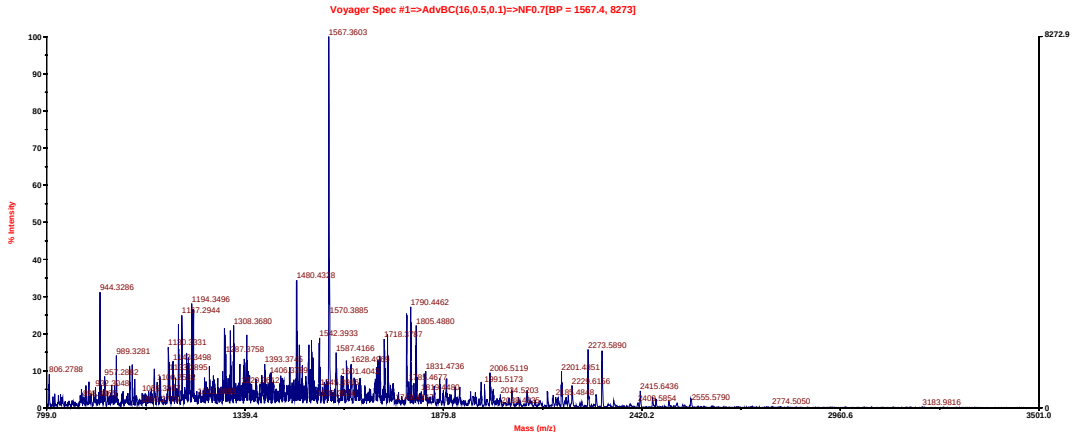

Post-avidin

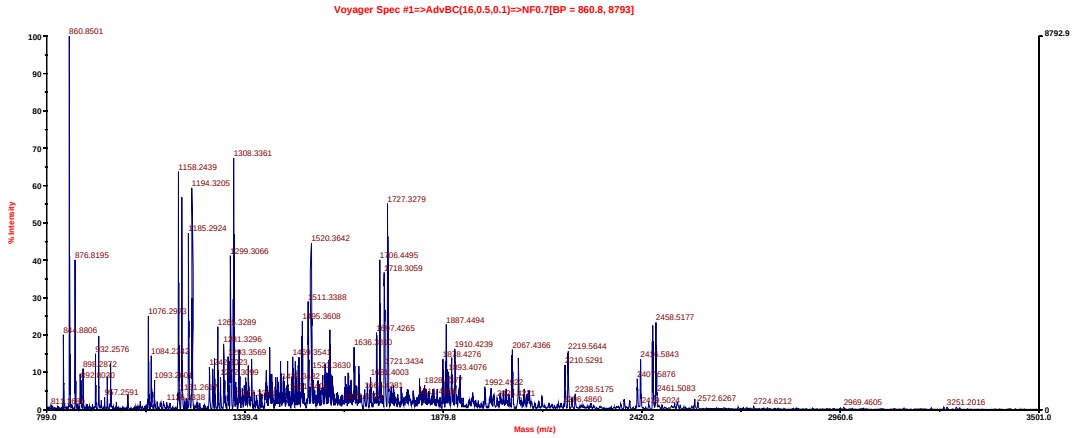

Figure 5.8 MALDI analysis of peptides from cytosolic proteins from MHV-76 or Int9 infected NS0 cells labelled with light or heavy cICAT reagent, following trypsin digestion (post-trypsin), cation-exchange column (pre-avidin) and avidin column (post-avidin).

Final sample

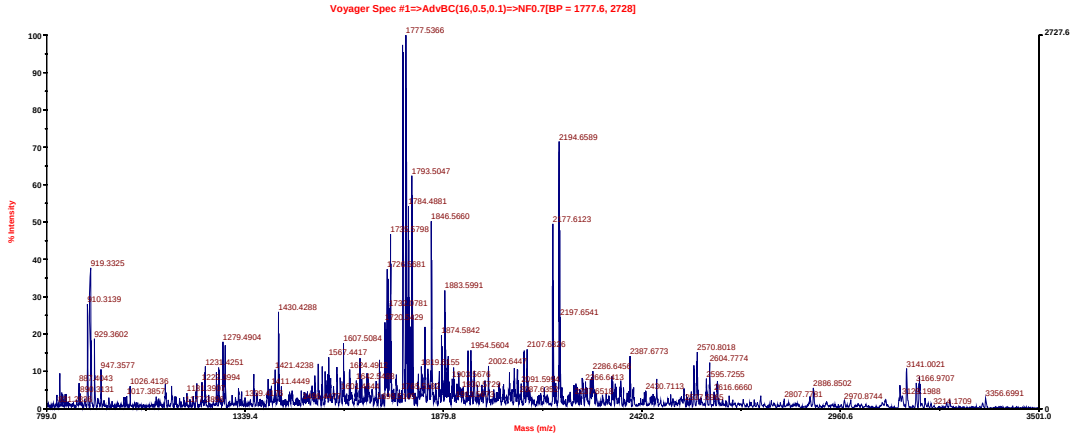

Figure 5.9 MALDI analysis of peptides from the final sample of cytosolic proteins from MHV-76 and Int9 infected NS0 cells labelled with light or heavy cICAT reagent, following cleavage of the biotin tag.

A

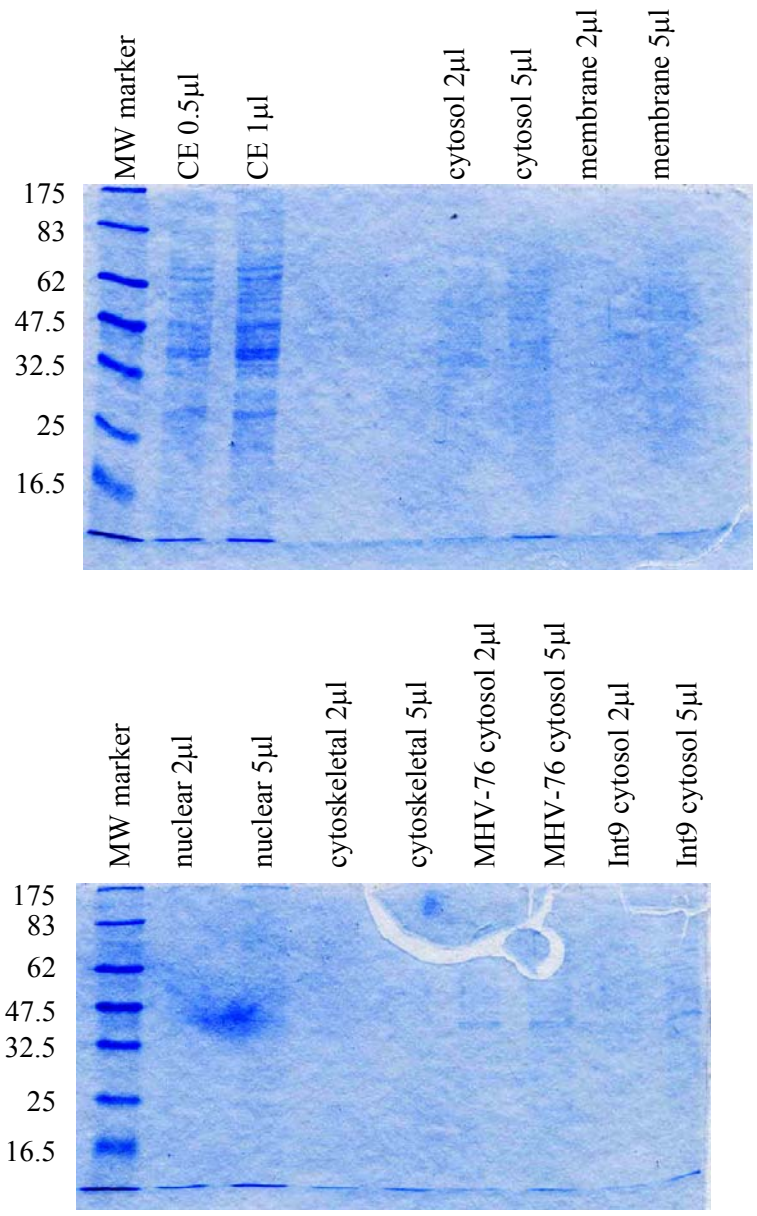

B

	proteins	µg/ml
	CE	>3495
Fractionation kit	cytosol	516
	membrane	845
	nuclear	489
	cytoskeletal	177
	MHV-76 cytosol	290
	Int9 cytosol	329

Figure 5.10 SDS-PAGE (A) showing the protein bands present in samples from NS0 cells using the cytosolic extraction (CE) and fractionation with the ProteoExtract® Subcellular Proteome Extraction Kit (cytosol, membrane, nuclear and cytoskeletal fractions), as well as the cytosolic samples of MHV-76 and Int9 infected NS0 cells used previously for the cICAT assay. The different protein concentrations for the samples are listed (B).

Since the cytoplasmic extraction generated a higher concentration of different proteins it was decided to use this extraction protocol for the cICAT labelling. It was also decided to leave out protease inhibitors in the extraction protocol to avoid the possibility of inhibiting the trypsin. To further ensure that the cytoplasmic extraction buffer would not inhibit the trypsin cleavage, even without the addition of the protease inhibitor, and to examine the effects of acetone precipitation on the proteins, tryptic digestion of BSA was performed.

BSA was dissolved in water or extraction buffer and trypsin digested in solution. In addition, BSA dissolved in extraction buffer was acetone precipitated prior to trypsin digestion. MALDI analysis of the samples showed that the trypsin digestion worked in the cytoplasmic extraction buffer; with several of the same peaks present as in the BSA digest (Figure 5.11). However, a lot of protein was lost in the acetone precipitation, with some of the BSA peptide peaks obtained, but at a very low signal with some background noise appearing. The peaks to left of the spectrum did not appear to be BSA peptide peaks, but could be from the extraction buffer or CHCA matrix. These peaks were more abundant than the BSA peaks in the acetone precipitated sample, showing that the levels of the BSA peptides in this sample were very low.

Through these experiments it was concluded that the cytoplasmic extraction protocol yielded higher levels of different proteins that should enable identification of more proteins. In addition, the acetone precipitation was identified as a source of loss of proteins and an alternative method needed to be utilised.

5.2.4. MHV-76 vs. Int9 latently infected NS0 cells- Vivaspin

Since a lot of proteins seemed to be lost in the acetone precipitation, the cICAT analysis of proteins from MHV-76 and Int9 infected cells was repeated using Vivaspins to concentrate the proteins. NS0 cells were infected with MHV-76 or Int9 at a MOI of 5 for five days, followed by cytoplasmic protein extraction and determination of protein concentration using a BCA Protein Assay. The samples were analysed by SDS-PAGE to ensure the presence of multiple proteins. Although

BSA digest

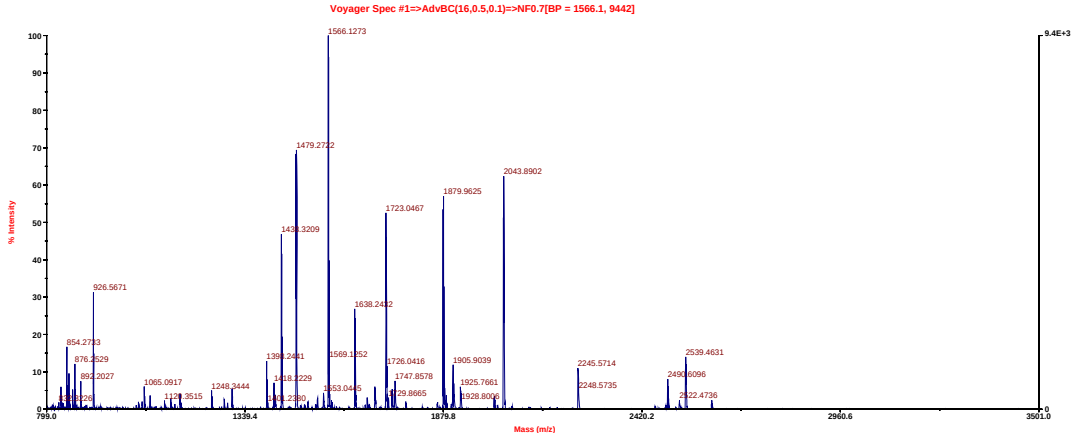

BSA CE digest

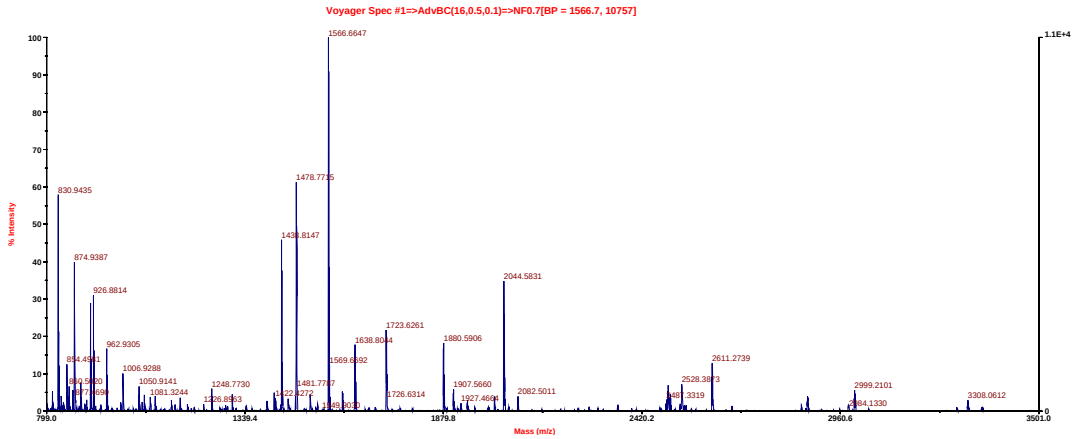

BSA CE precipitation digest

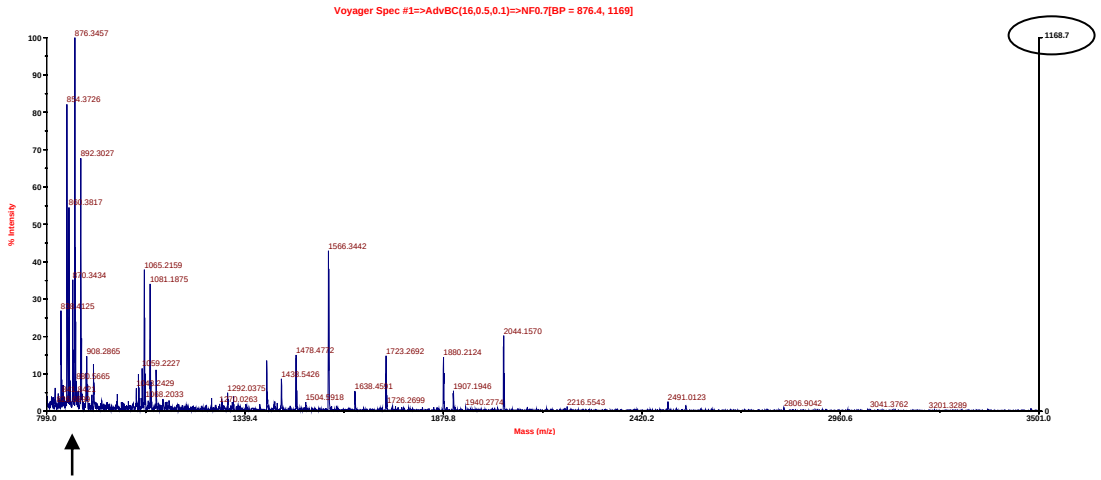

Figure 5.11 MALDI analysis of tryptic digestions of 10µg BSA in water (BSA digest), in cytoplasmic extraction buffer (BSA CE digest), mixed with cytoplasmic extraction buffer and precipitated with acetone precipitation (BSA CE precipitation digest). The low signal obtained following acetone precipitation is circled. Peaks that are from the extraction buffer or MALDI matrix are indicated by an arrow.

the protein concentrations were low there were a large number of protein bands (Figure 5.12).

Because of the low number of proteins identified in the previous assay, a larger mass of proteins were used in this experiment. For each sample 182µg of cytoplasmic proteins were concentrated using Vivaspins with a molecular weight cut off of 3000, and the assay performed according to the protocol (section 2.9.7.1) with denaturing buffer added to bring the volume up to 80µl. Proteins from MHV-76 infected NS0 cells were labelled with light and Int9 with heavy cICAT reagent. The sample was divided into two tubes for the vacuum drying step prior to cleavage of the biotin tag to try and reduce the drying time; however, it still took seven hours. The second vacuum drying step after the cleavage took almost an hour this time. The sample was resuspended in 120µl 2.5% (v/v) acetic acid and analysed by MALDI and LC-MS/MS on an LCQdeca system.

The LC-MS/MS analysis identified six proteins, with four having peptides labelled with both light and heavy cICAT reagent (Figure 5.13). This is necessary to be able to determine the differences in the abundance of proteins, and shows that the cICAT technique is working. However, many more proteins should have been identified. BSA was identified, indicating that in future experiments the cells need to be washed more rigorously prior to protein extraction, to avoid having BSA peptides overshadowing the other peptides. The MALDI analysis showed that the peptides seemed to disappear in the last step, the cleavage of the biotin tag, with a very low signal obtained and background noise appearing (Figure 5.14). Since this involved vacuum drying the sample twice, which took seven and one hour respectively, this was suspected as the cause of the loss of peptides.

Utilising Vivaspins instead of acetone precipitation to concentrate the proteins prior to labelling did lead to identification of more proteins; however, an alternative to the vacuum dryer needed to be found since the long vacuum drying times appeared to affect the peptides.

A

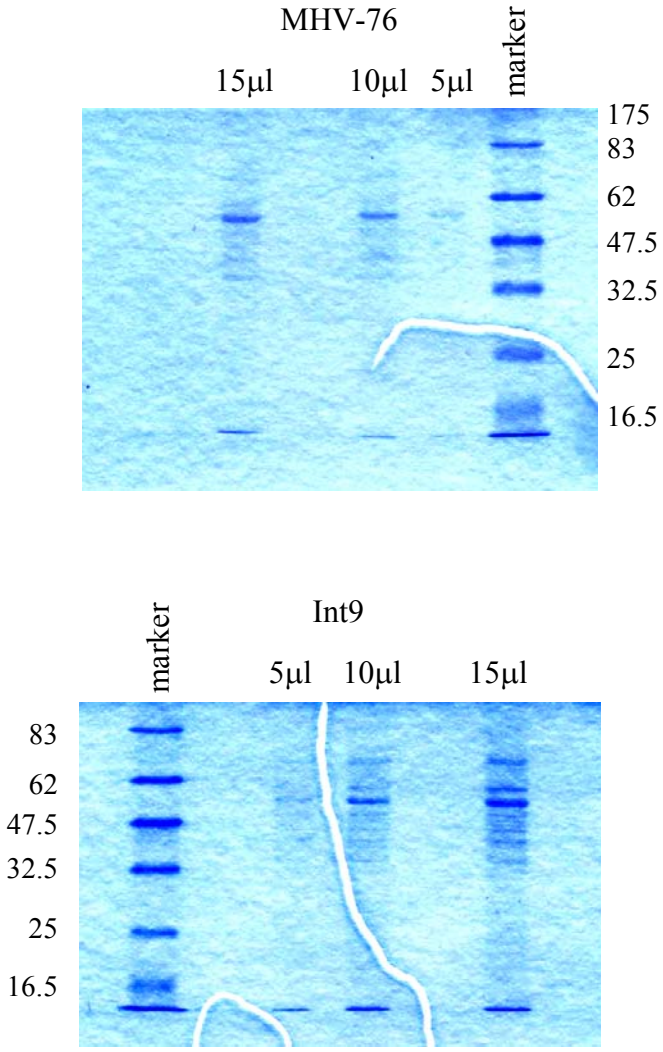

B

proteins	µg/ml
MHV-76	222
Int9	332

Figure 5.12 SDS-PAGE (A) of cytoplasmic proteins from MHV-76 and Int9 infected NS0 cells. Also listing the protein concentrations of the two samples (B).

A

```
Serum albumin precursor (Allergen Bos d 6) (BSA)
Malate dehydrogenase
60 kDa heat shock protein
Serotransferrin precursor
Aspartate aminotransferase
60 kDa heat shock protein
Protein disulfide-isomerase A6 precursor
```

B

1. ALBU_BOVIN
(P02769) Serum albumin precursor (Allergen Bos d 6) (BSA)

Observed	Peptide
534.70400	R.LCVLHEK.T + ICAT_light
639.07900	K.EACFAVEGPK.L + ICAT_light
739.78400	K.CCTESLVNR.R + 2 ICAT_light
740.11400	K.CCTESLVNR.R + 2 ICAT_light
748.38900	K.CCTESLVNR.R + 2 ICAT_heavy
762.68400	R.CCTKPESER.M + 2 ICAT_heavy
1589.96000	K.SLHTLFGDELCK.V + ICAT_light
601.74533	K.TCVADESHAGCEK.S + 2 ICAT_light
601.75533	K.TCVADESHAGCEK.S + 2 ICAT_light
607.63867	K.TCVADESHAGCEK.S + 2 ICAT_heavy
607.67867	K.TCVADESHAGCEK.S + 2 ICAT_heavy
947.89400	R.MPCTEDYLSLILNR.L + ICAT_light
952.29900	R.MPCTEDYLSLILNR.L + ICAT_heavy
1025.95900	R.RPCFSALTPDETYVPK.A + ICAT_light
1025.96400	R.RPCFSALTPDETYVPK.A + ICAT_light
1039.63400	K.LFTFHADICTLPDTEK.Q + ICAT_light
1043.83400	K.LFTFHADICTLPDTEK.Q + ICAT_heavy
1143.86400	K.ECCHGDLLECADDR.A + 3 ICAT_heavy
813.33200	K.CCAADDKEACFAVEGPK.L + 3 ICAT_light
1219.71900	K.CCAADDKEACFAVEGPK.L + 3 ICAT_light
1232.60900	K.CCAADDKEACFAVEGPK.L + 3 ICAT_heavy
830.53533	R.MPCTEDYLSLILNRLCVLHEK.T
1280.61900	K.TVMENFVAFVDKCCAADDK.E + 2 ICAT_light

2. MDHM_MOUSE
(P08249) Malate dehydrogenase

Observed	Peptide
759.26400	K.GCIVVVIPAGVPR.K + ICAT_heavy
830.15400	K.GYLGPEQLPDCLK.G + ICAT_light
1659.95000	K.GYLGPEQLPDCLK.G + ICAT_light
834.69900	K.GYLGPEQLPDCLK.G + ICAT_heavy
1669.09000	K.GYLGPEQLPDCLK.G + ICAT_heavy
964.81900	K.ETECTYFSTPLLLGK.K + ICAT_light
969.34400	K.ETECTYFSTPLLLGK.K + ICAT_heavy

Figure 5.13 Results of the LC-MS/MS analysis of peptides from cytosolic proteins from MHV-76 and Int9 infected NS0 cells labelled with light or heavy cICAT reagent, using Mascot software to search against the Swiss-Prot database. The identified proteins are listed (A) and the peptides identified for two of the proteins are shown as examples (B). Search parameters: Peptide mass tolerance ± 2 Da; Fragment mass tolerance ± 0.8 Da; missed cleavages 3. An example of a peptide identified labelled with light and heavy cICAT reagent is boxed.

Post-avidin

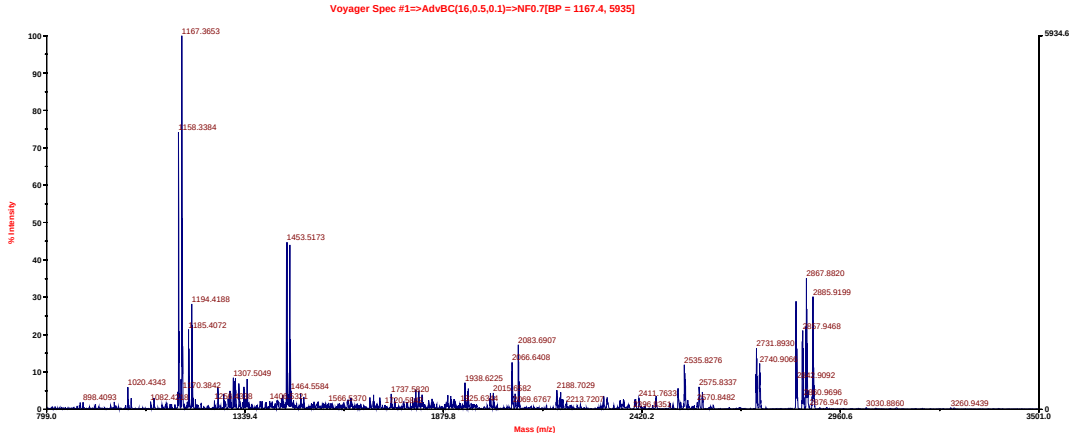

Final sample

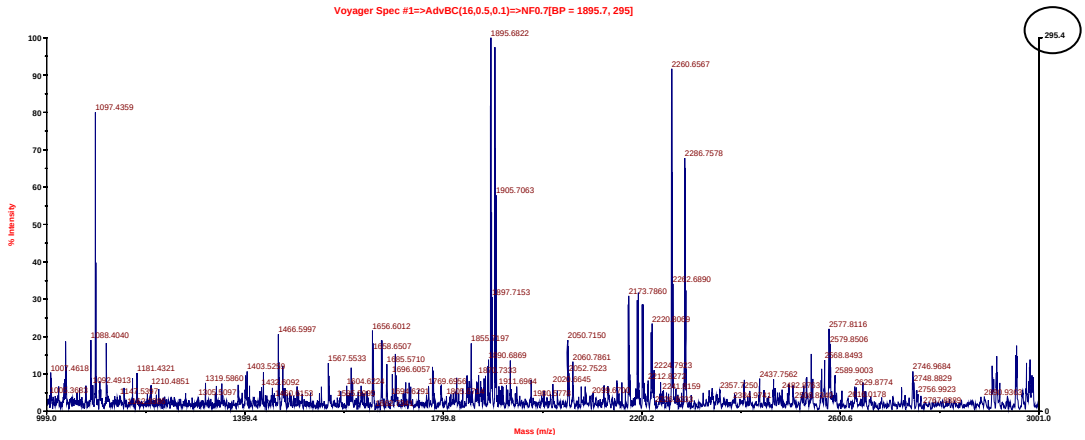

Figure 5.14 MALDI analysis of peptides from cytoplasmic proteins from MHV-76 or Int9 infected NS0 cells labelled with light or heavy cICAT reagent, after the avidin column (post-avidin) and of the final sample following vacuum drying for seven hours, cleavage of the biotin tag and vacuum drying for one hour. The very low signal obtained in the final sample is circled.

5.2.5. MHV-76 vs. Int9 latently infected NS0 cells- freeze-dryer

To minimise the loss of peptides, a freeze-dryer was used instead of the vacuum dryer for the long drying step prior to cleaving of the biotin molecule. NS0 cells were infected with MHV-76 and Int9 at a MOI of 5 for five days, the cytoplasmic proteins extracted, and the protein concentration determined with a BCA Protein Assay. A large number of proteins were present in the sample as visualised by SDS-PAGE (Figure 5.15).

For each sample 150µg of cytoplasmic proteins were concentrated using Vivaspins with a molecular weight cut off of 3000, and the assay performed according to the protocol (section 2.9.7.1) with denaturing buffer added to bring the volume up to 80µl. Proteins from MHV-76 infected NS0 cells were labelled with light and Int9 with heavy cICAT reagent. The sample was freeze-dried for four hours prior to cleaving of the biotin tag, and vacuum dried for 17 min following the cleaving. The sample was resuspended in 60µl 0.5% (v/v) acetic acid and analysed by MALDI and LC-MS/MS on an LCQdeca system. The MALDI analysis showed that the peptides were no longer lost during last step of the assay, with a high signal obtained in the final sample, nor during any other step of the assay (Figure 5.16, Figure 5.17). However, there were not as many peptide peaks as had been expected. Some pairs with a difference of 9 amu could still be identified in the final sample (Figure 5.17). The LC-MS/MS analysis identified a number of significant protein matches (Figure 5.18); however, very few cICAT light/heavy peptide pairs. The cICAT labelling was working; however, only the most abundant proteins were identified.

It was decided that the protein samples were too complex and needed to be fractionated prior to LC-MS/MS analysis. By analysing samples with smaller number of different proteins, less abundant proteins may be identified.

A

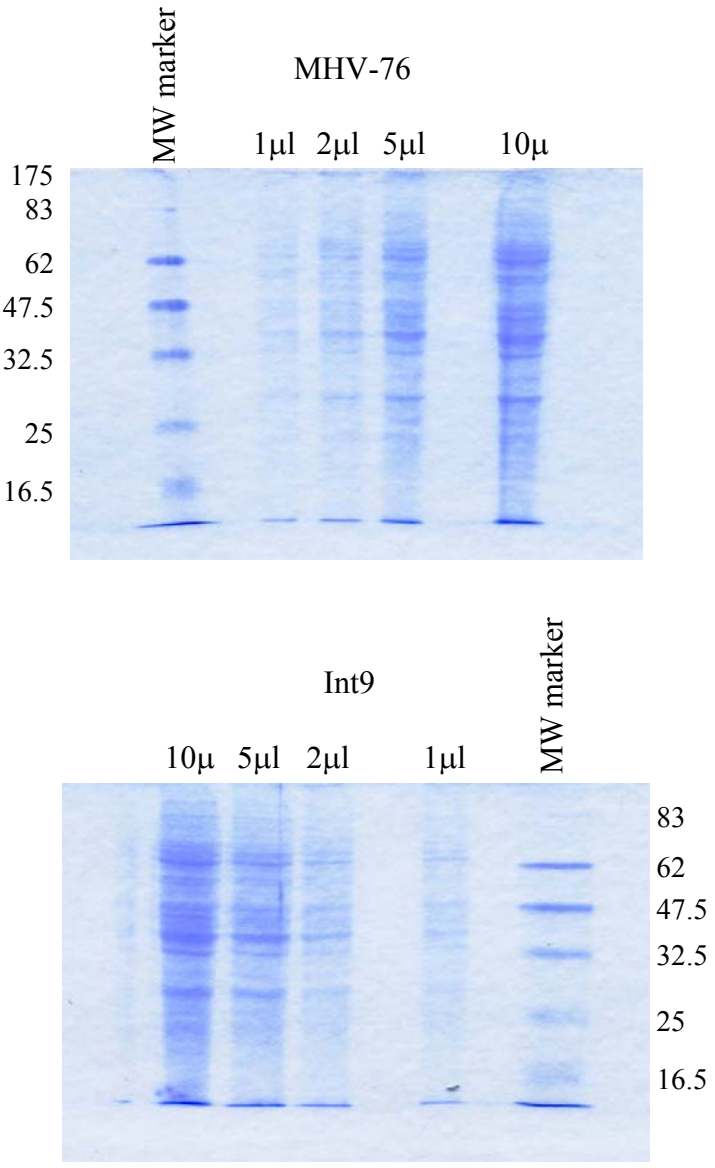

B

proteins	µg/ml
MHV-76	2712
Int9	3529

Figure 5.15 SDS-PAGE (A) of cytoplasmic proteins from MHV-76 and Int9 infected NS0 cells. Also listing the protein concentrations of the two samples (B).

Post-trypsin

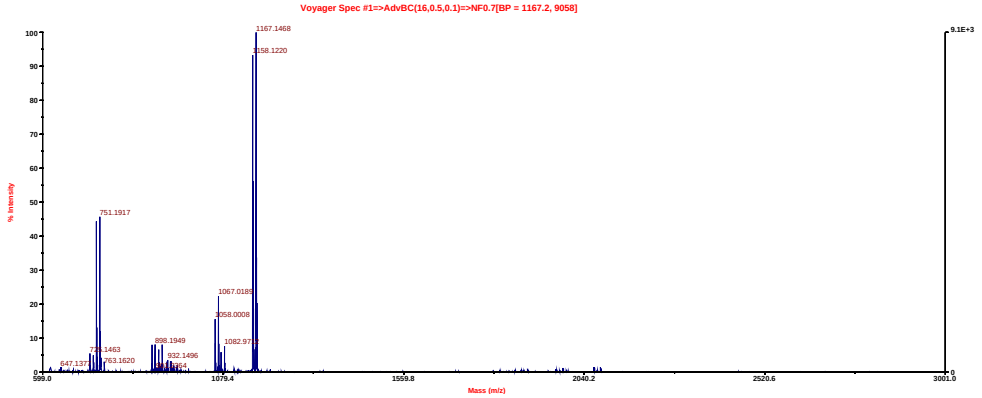

Pre-avidin

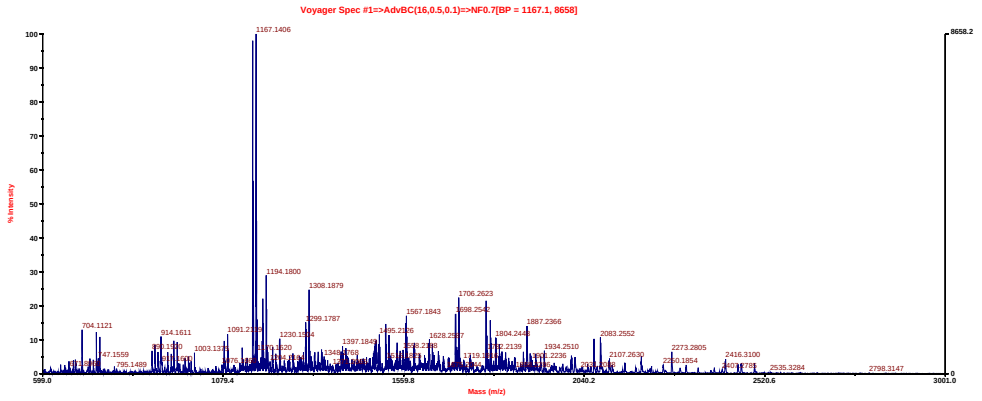

Figure 5.16 MALDI analysis of peptides from cytoplasmic proteins from MHV-76 or Int9 infected NS0 cells labelled with light or heavy cICAT reagent, following trypsin digestion (post-trypsin) and cation-exchange column (pre-avidin).

Post-avidin

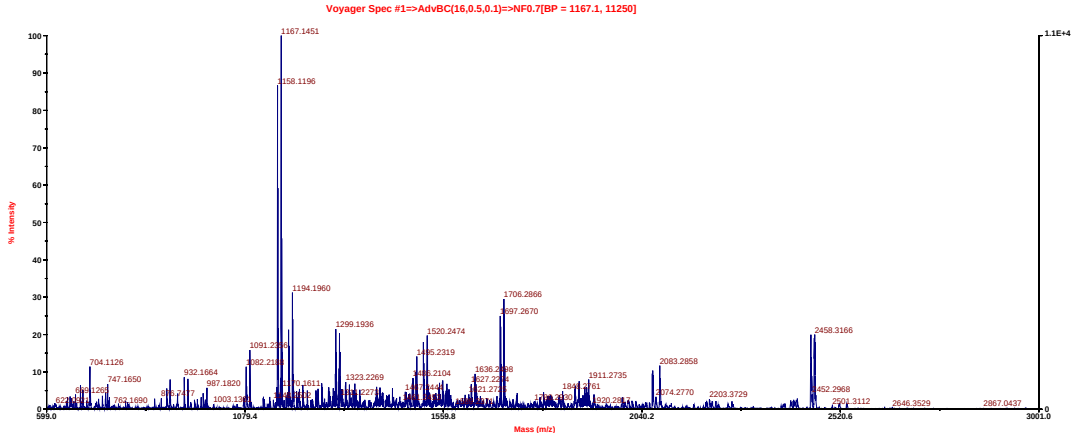

Final sample

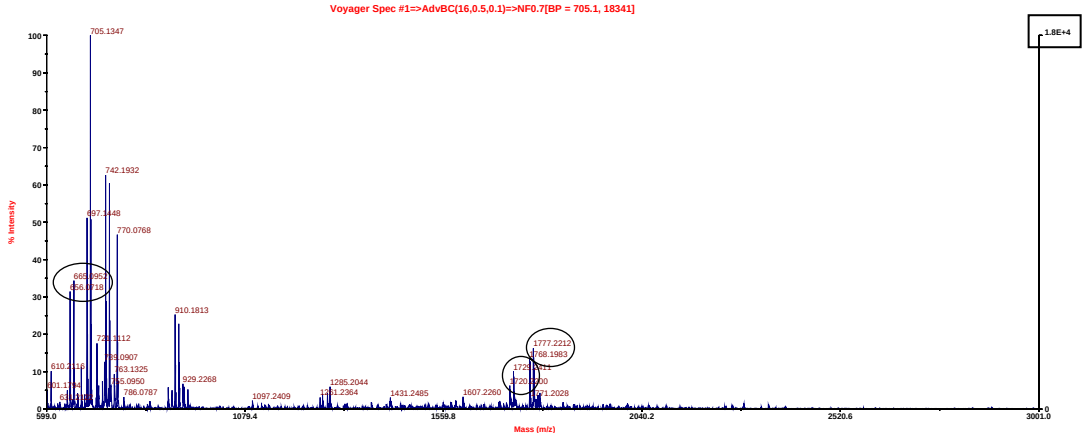

Figure 5.17 MALDI analysis of peptides from cytoplasmic proteins from MHV-76 or Int9 infected NS0 cells labelled with light or heavy cICAT reagent, after the avidin column (post-avidin) and of the final sample following freeze-drying, cleavage of the biotin tag and vacuum drying. The high signal obtained in the final sample is boxed and cICAT pairs are circled.

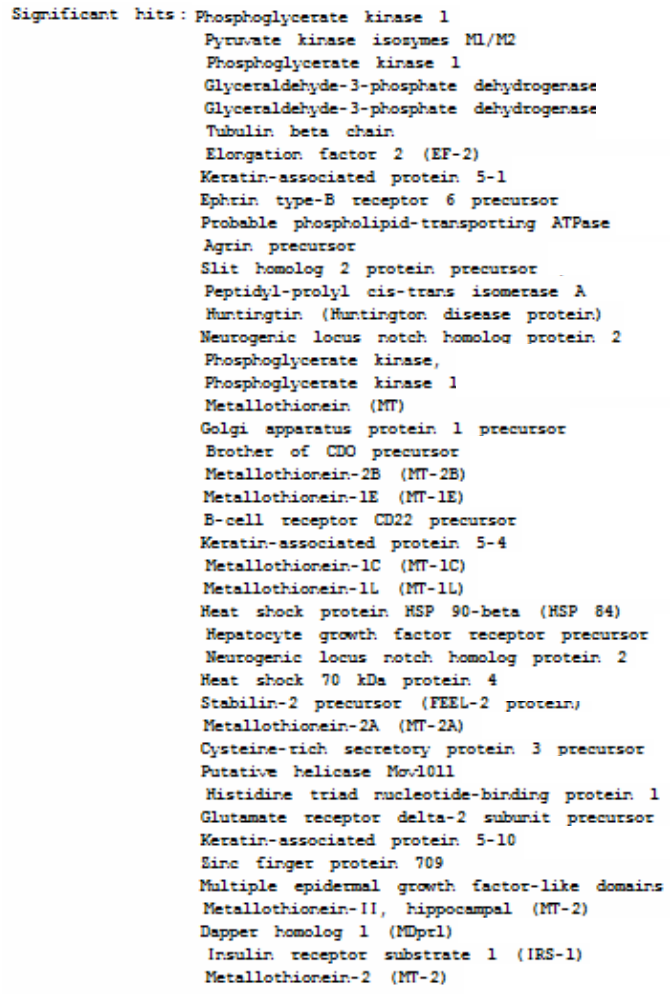

Figure 5.18 Results of the LC-MS/MS analysis of peptides from cytosolic proteins from MHV-76 or Int9 infected NS0 cells labelled with light or heavy cICAT reagent, using Mascot software to search against the Swiss-Prot database. Listing identified proteins with significant protein scores. Search parameters: Peptide mass tolerance ± 2 Da; Fragment mass tolerance ± 1.2 Da; missed cleavages 2.

5.3. 1-D PAGE cICAT

5.3.1. Assay setup

To make the protein samples less complex an alternative of the cICAT method was utilised. In the 1-D PAGE cICAT method the labelled proteins are separated by SDS-PAGE and the gel cut into pieces to fractionate the proteins (Figure 5.19). The proteins are trypsin digested in the gel and the peptides extracted prior to purification on an avidin column and cleavage of the biotin tag.

The 1-D PAGE cICAT protocol introduced more vacuum drying steps, something that had been found to be a problem previously. Therefore the effect of the vacuum drying on BSA peptides was examined.

BSA was run on SDS-PAGE in different amounts (100ng, 200ng, 300ng) and the bands excised, washed, proteins trypsin digested, and the peptides extracted according to the 1-D PAGE cICAT protocol. The extraction protocol consisted of two parts. The gel pieces were initially sonicated for 20 min in a sonic ice water bath and the supernatant collected. Further extractions were then performed three times by addition of extraction solvent (50% (v/v) ACN, 0.1% (v/v) TFA) and sonication for 20 min, removing the supernatant following each extraction. The supernatants containing the extracted peptides were pooled and vacuum dried for two hours to remove the ACN and TFA, prior to freeze drying over night.

Samples were taken for MALDI analysis after the first extraction step, following the full extraction, and after vacuum and freeze-drying and re-suspension in 100µl and 500µl avidin buffer. The MALDI analysis showed that the peptides were lost during the procedure, with most peptides obtained after the first extraction step (Figure 5.20). The following extractions with extraction solvent did not extract any further peptides, and the sample was diluted so that the peptides present initially could not be detected. These peptides were lost during the vacuum and freeze-drying. It also showed that even following the first extraction step, not many BSA peptide peaks were present (Figure 5.21). This could be because of the smaller amount of BSA used, which was chosen to replicate the amount of individual

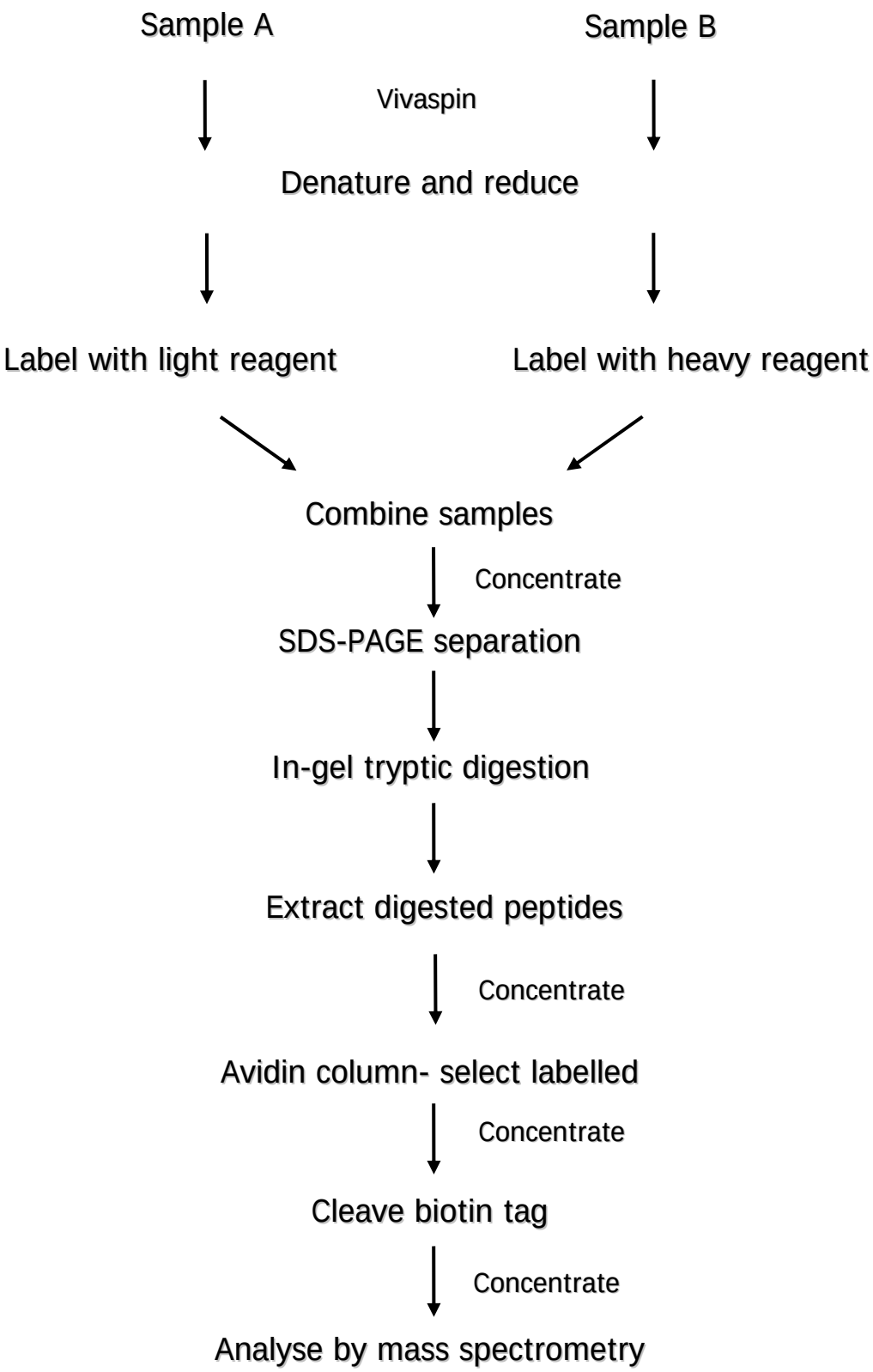

Figure 5.19 Step-by-step schematic description of the 1-D PAGE cICAT protocol.

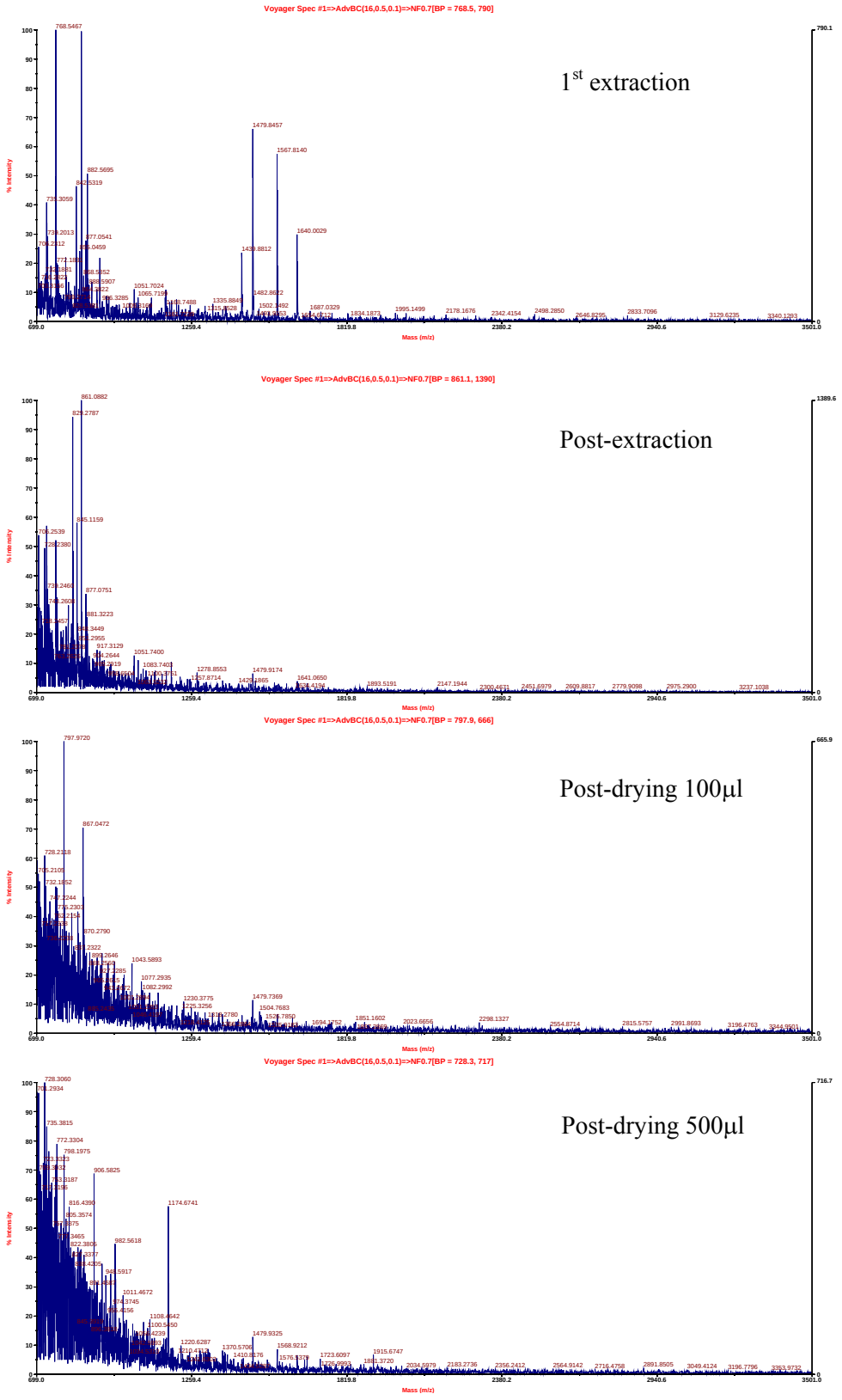

Figure 5.20 MALDI analysis of 100ng BSA in the vacuum drying test. Showing samples taken after the first and last extraction step, and following vacuum and freeze-drying and re-suspension in 100µl and 500µl avidin buffer.

1st extraction- 200ng BSA

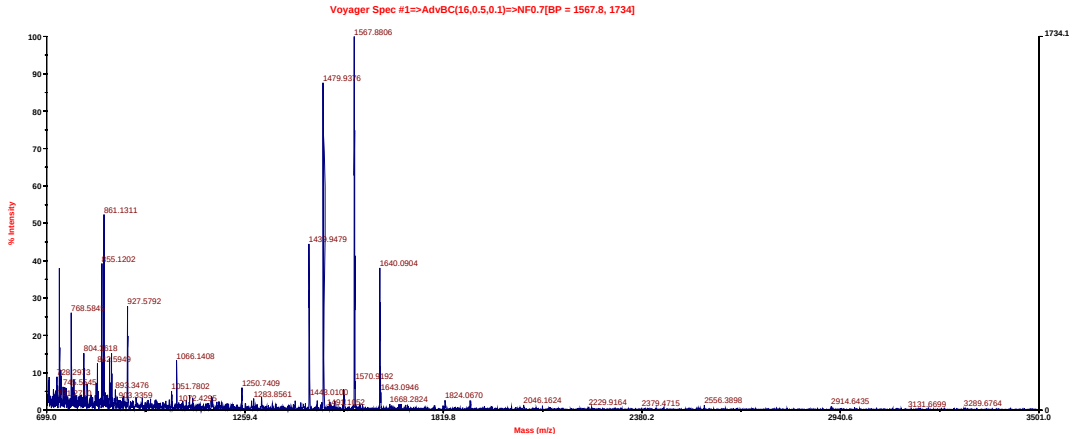

1st extraction- 300ng BSA

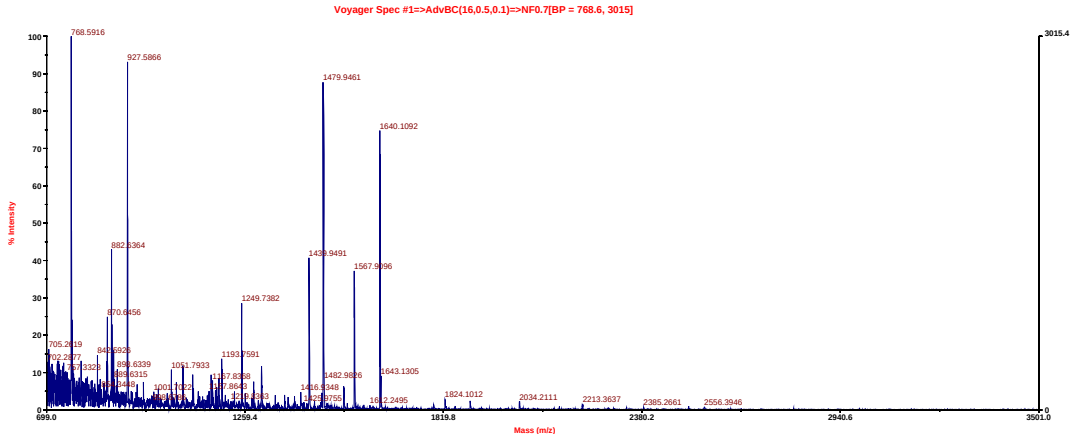

BSA digest

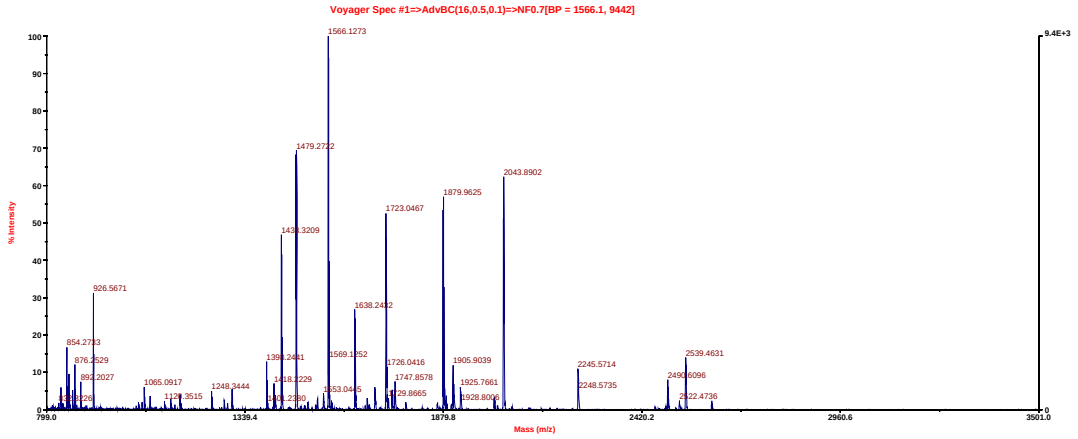

Figure 5.21 MALDI analysis of trypsin digested peptides from 200ng and 300ng BSA, following the first extraction step. Also showing the spectrum from a trypsin digest of 10μg BSA from an earlier experiment for comparison.

proteins in the cICAT labelling. It could also be because of salts present in the sample affecting the MALDI analysis.

It was concluded that the initial extraction step was sufficient to extract the peptides and that an alternative to the vacuum dryer needed to be found.

5.3.2. BSA

Following the findings in the assay setup, the 1-D PAGE cICAT protocol was tested with BSA, using ZipTips® instead of vacuum and freeze-drying to concentrate the samples during the assay, and only performing the first extraction step. The ZipTip® is a pipette tip with a bed of chromatography media in the end that allows for concentration and purification of peptides and proteins.

10µg of BSA was denatured (10µl BSA + 40µl denaturing buffer + 1µl reducing agent) and labelled with light cICAT reagent. The labelled BSA was vacuum dried 30 min to reduce the volume, run on SDS-PAGE and the band excised. There were two bands present on the gel, with the lighter band of smaller size probably consisting of unlabelled BSA. The BSA was in-gel trypsin digested and the peptides extracted, with only the first extraction step consisting of 20 min of sonication in a sonic ice water bath performed. A ZipTip® was used to concentrate the sample prior to purification using an avidin column and again prior to cleavage. Following cleavage of the biotin tag half of the sample was concentrated using a ZipTip® and half using a vacuum dryer for 25 min, prior to analysis by MALDI.

The MALDI analysis showed that there were plenty of peptide peaks in the final sample, with the final concentrating method, vacuum drying or ZipTip®, not making much difference to the sample. Problems with calibration meant that although there was plenty of peptide peaks, BSA could not be identified when searching against the database. Several BSA peptide peaks (15/24 for the ZipTip® sample, Table 5.1) could be identified manually, as indicated by the circles in Figure 5.22, and when compared to the MALDI result from the previous BSA cICAT experiment it could be concluded that the adapted 1-D PAGE cICAT assay using ZipTips® was working.

Final sample: vacuum dry

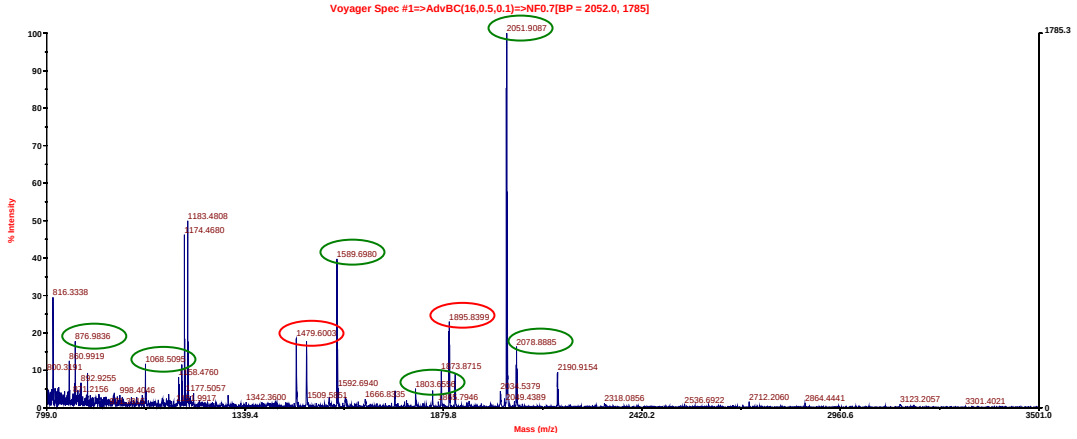

Final sample: ZipTip®

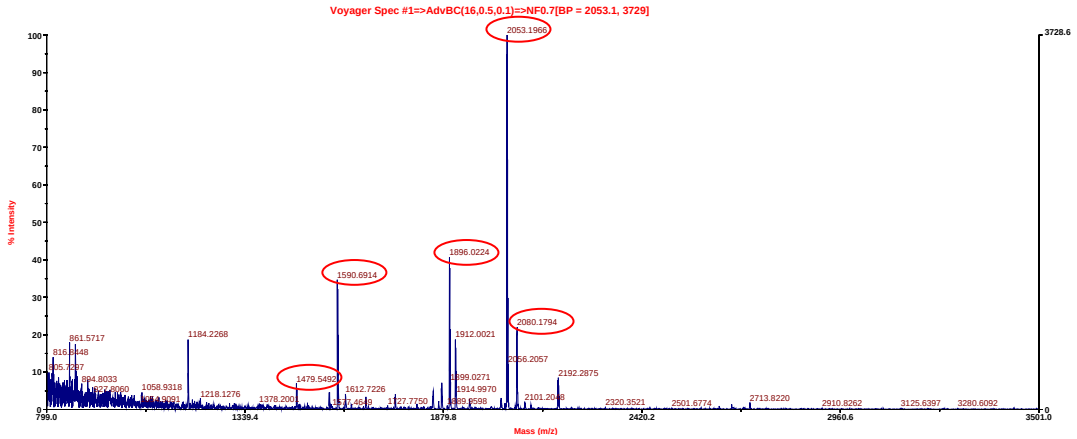

BSA digest

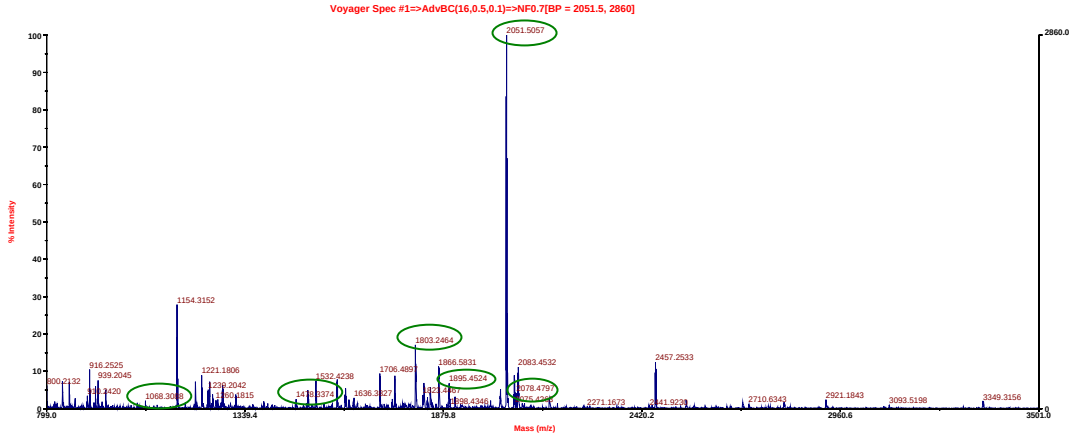

Figure 5.22 MALDI analysis of peptides from BSA labelled with light cICAT reagent. Final samples following concentration of the sample after cleavage of the biotin tag, using a vacuum dryer or a ZipTip®. Also showing the spectrum of BSA labelled with light cICAT reagent from an earlier cICAT experiment as a control. Green circles indicate BSA peptides and red circles probable BSA peptides.

5.3.3. MHV-76 vs. Int9 latently infected NS0 cells

Following all the optimisation experiments, a definitive experiment examining the differences in protein expression between MHV-76 and Int9 infected NS0 cells was performed.

NS0 cells were infected with MHV-76 and Int9 at a MOI of 5 for five days, the cytosolic proteins extracted using a ProteoExtract® Subcellular Proteome Extraction Kit, and the protein concentrations determined using a BCA Protein Assay. The extraction kit was used as this would make the protein sample less complex. 100µg of cytosolic proteins were concentrated using Vivaspins and the proteins labelled with light and heavy cICAT reagents according to the protocol (section 2.9.7.2). The samples were vacuum-dried for 30 min to reduce the sample volume prior to mixing with loading buffer and separation by SDS-PAGE. The gel strip of the lane loaded with labelled protein was cut into 11 pieces. The proteins were in-gel trypsin digested and the peptides extracted, with only the first extraction step performed. A ZipTip® was used to concentrate the sample prior to purification using an avidin column and again prior to cleavage. Following cleavage of the biotin the sample was concentrated using a vacuum drier, as this had not affected the peptides in the previous assay, and resuspended in 60µl 0.5% acetic acid. The peptides were loaded onto a ZipTip®, eluted, and briefly dried down in a vacuum dryer prior to analysing by LC-MS/MS on a LTQ.

Initially, band 3 was further processed and the other bands stored at -20°C following excising from the gel. The MALDI analysis of samples taken during the assay showed that there were plenty of peptides present following the extraction from the gel piece and that there were still many peptides in the final sample; however at low intensities (Figure 5.23). The LC-MS/MS analysis identified three proteins with significant scores and several with non-significant scores when searching against murine proteins (Figure 5.24). The protein score is calculated from the ion scores, which gives the probability that the match is a random event, with higher scores indicating a true match. In this experiment an ion score of more than 30 (significance threshold 0.05) indicated identity or extensive homology. The proteins identified are among the more abundant in the cell.

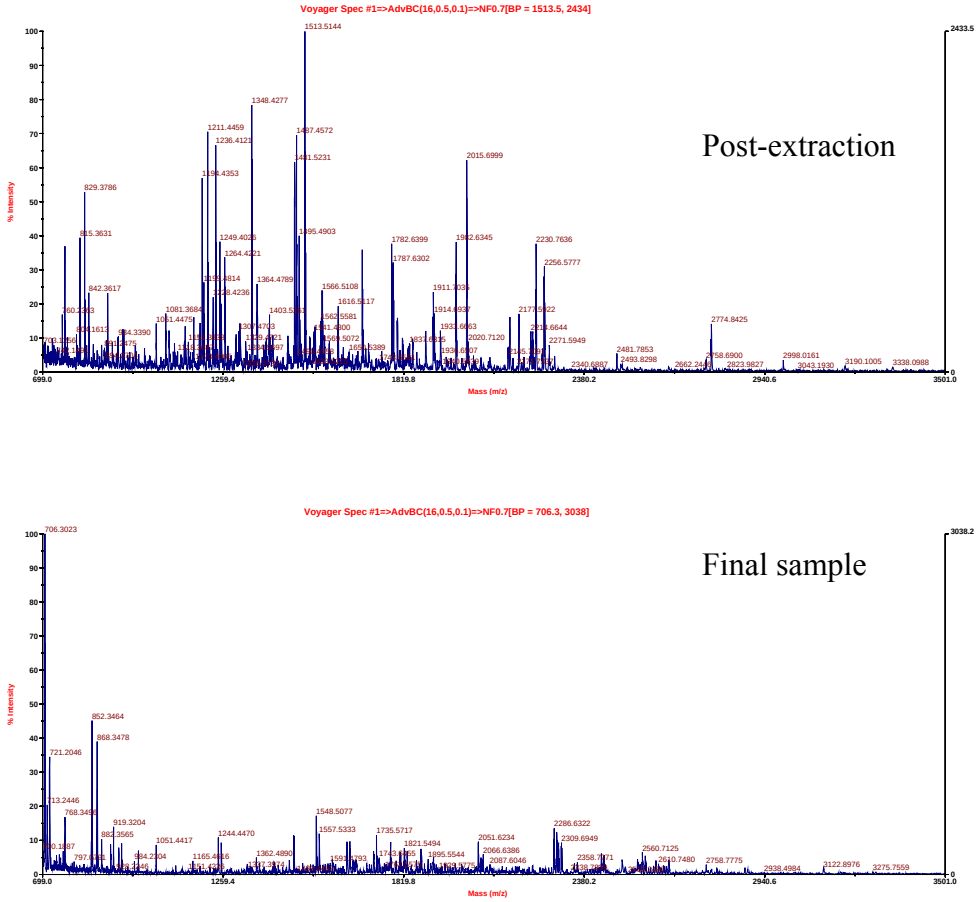

Figure 5.23 MALDI analysis of band 3 peptides in the 1-D PAGE cICAT assay. Showing samples taken following extraction of the peptides and of the final sample.

Protein hits
Heat shock protein HSP 90-beta
Heat shock cognate 71 kDa protein
Heat shock protein HSP 90-alpha
Glyceraldehyde-3-phosphate dehydrogenase
Elongation factor 2
Transitional endoplasmic reticulum ATPase
Bifunctional aminoacyl-tRNA synthetase
Aminopeptidase B
ATP-dependent RNA helicase DDX1
Arginyl-tRNA synthetase, cytoplasmic
Annexin A6
Pyruvate kinase isozymes M1/M2
Transketolase
Eukaryotic translation initiation factor 3 subunit C
Desmocollin-2 precursor
Exportin-2
ADAMTS-18 precursor
Transcription factor RFX4
Lysyl-tRNA synthetase
T-complex protein 1 subunit gamma
Asparaginyl-tRNA synthetase, cytoplasmic
26S proteasome non-ATPase regulatory subunit 2
Alpha-actinin-2
SUMO-activating enzyme subunit 2
Stress-induced-phosphoprotein 1
CTP synthase 1
Prolyl endopeptidase
Echinoderm microtubule-associated protein-like 2
Inner membrane protein COX18
Claudin-8
Programmed cell death 6-interacting protein
Alpha-actinin-4
Ubiquitin-like modifier-activating enzyme 1 X
DNA replication licensing factor MCM5
Alpha-enolase
Beta-enolase
Uncharacterized protein C20orf19 homolog
6-phosphofructokinase
Alpha-taxilin
Putative pre-mRNA-splicing factor ATP-dependent RNA helicase DHX32
Nucleolin
DNA topoisomerase 3-alpha
Asparagine synthetase [glutamine-hydrolyzing]
Scavenger receptor cysteine-rich type 1 protein M130 precursor
Phosphoglucomutase-2-like 1
Heat shock 70 kDa protein 4
UPF0474 protein C5orf41 homolog
ADAMTS-20 precursor
Alpha-N-acetylgalactosaminide alpha-2,6-sialyltransferase 5
Beta-taxilin

Figure 5.24 Results of the LC-MS/MS analysis of peptides from cytosolic proteins from MHV-76 and Int9 infected NS0 cells labelled with light or heavy cICAT reagent from band 3, using Mascot software to search against the Swiss-Prot database. Search parameters: Peptide mass tolerance ± 3 Da; Fragment mass tolerance ± 0.4 Da; missed cleavages 3. Significant protein matches are boxed.

A long list of identified peptides was produced in the LC-MS/MS analysis. Since the software to analyse the data and identify cICAT pairs was not available, the data was analysed using a program developed by Mayank B. Dutia to identify peptides with the same sequence. Several cICAT light/heavy pairs were found (Table 5.2, Table 5.3), with several proteins having more than one peptide pair labelled with light and heavy cICAT reagent. This was an improvement from the last cICAT analysis in which only a few pairs were identified and showed that fractionation of the sample improved the sensitivity of the technique. Only pairs with the same ion charge, and that had been cleaved at a lysine (K) or arginine (R) (the trypsin cleavage sites) were considered. Some peptides identified originate from the same protein, but had different numbers of missed cleavages. Since the probability of the missed cleavages would be different, these could not be considered as pairs.

The time at which the peptides came off the LC was noted and the peptide peaks manually identified in the MS spectrum to determine the peak intensities. The peptide peak intensities were used to calculate the ratio of heavy/light (Int9/MHV-76) cICAT labelled peptides (Table 5.4). The analysis showed that there were a few differences of more than 0.4 in protein levels between MHV-76 and Int9 infected NS0 cells. The differences observed all indicated that Int9 infected NS0 had higher levels of those proteins. The low ion scores and few peptides matched for individual proteins meant that it was difficult to be confident in some of the protein matches. The heat shock proteins were the protein matches that were most likely to be true because of the high ion and protein score; however, the proteins with lower protein score could still be true matches, since for many of them several peptides were identified. It is important to remember that the table here only lists pairs of labelled peptides; peptides that were labelled with only heavy or light cICAT reagent would still help give confidence in the protein match. It is difficult to have confidence in the protein matches with a protein score of 0, since these usually have very few peptide matches with low ion scores.

The average ratio of the peptide pairs identified for Heat shock protein 90-beta (Hsp90-β) was 2.2; however, for the individual peptide pairs, the ratios were inconsistent (Table 5.5). The ratios of the peptides with higher scores were 0.4 and

m/z	Ion score	Peptide	Protein / protein score
492.11	6	K.FENLCK.L + ICAT-C (C)	Heat shock protein HSP 90-beta
495.11	7	K.FENLCK.L + ICAT-C:13C(9) (C)	53
590.23	10	K.AKFENLCK.L + ICAT-C (C)	
594.79	9	K.AKFENLCK.L + ICAT-C:13C(9) (C)	
596.00	6	K.AKFENLCK.L + ICAT-C:13C(9) (C)	
720.75	6	K.CLELFSELAEDKENYK.K + ICAT-C (C)	
723.55	2	K.CLELFSELAEDKENYK.K + ICAT-C:13C(9) (C)	
763.46	35	K.CLELFSELAEDKENYKK.F + ICAT-C (C)	
767.04	28	K.CLELFSELAEDKENYKK.F + ICAT-C:13C(9) (C)	
1147.98	18	K.CLELFSELAEDKENYKK.F + ICAT-C:13C(9) (C)	
1144.64	35	K.CLELFSELAEDKENYKK.F + ICAT-C (C)	
812.26	32	K.GPAVGIDLGTTYSCVGVFQHGK.V + ICAT-C (C)	Heat shock cognate 71 kDa protein
815.59	42	K.GPAVGIDLGTTYSCVGVFQHGK.V + ICAT-C:13C(9) (C)	52
492.11	6	K.FENLCK.I + ICAT-C (C)	Heat shock protein HSP 90-alpha
495.11	7	K.FENLCK.I + ICAT-C:13C(9) (C)	46
669.78	7	K.KTKFENLCK.I + ICAT-C (C)	
675.00	13	K.KTKFENLCK.I + ICAT-C:13C(9) (C)	
1151.16	34	K.CLELFTELAEDKENYKK.F + ICAT-C (C)	
1155.39	46	K.CLELFTELAEDKENYKK.F + ICAT-C:13C(9) (C)	
577.07	3	R.VPTPNVSVVDLTCR.L + ICAT-C (C)	Glyceraldehyde-3-phosphate dehydrogenase
579.35	14	R.VPTPNVSVVDLTCR.L + ICAT-C:13C(9) (C)	34
864.23	34	R.VPTPNVSVVDLTCR.L + ICAT-C (C)	
865.23	27	R.VPTPNVSVVDLTCR.L + ICAT-C (C)	
869.20	27	R.VPTPNVSVVDLTCR.L + ICAT-C:13C(9) (C)	
775.24	26	R.CLYASVLTAQPR.L + ICAT-C (C)	Elongation factor 2
776.90	21	R.CLYASVLTAQPR.L + ICAT-C (C)	32
779.71	17	R.CLYASVLTAQPR.L + ICAT-C:13C(9) (C)	
833.34	21	R.TFCQLILDPIFK.V + ICAT-C (C)	
837.90	11	R.TFCQLILDPIFK.V + ICAT-C:13C(9) (C)	
853.24	22	R.RCLYASVLTAQPR.L + ICAT-C (C)	
858.30	11	R.RCLYASVLTAQPR.L + ICAT-C:13C(9) (C)	
868.87	7	K.DLEEDHACIPIKK.S + ICAT-C (C)	
875.67	0	K.DLEEDHACIPIKK.S + ICAT-C:13C(9) (C)	
883.14	8	R.ETVSEESNVLCLSK.S + ICAT-C (C)	
884.17	11	R.ETVSEESNVLCLSK.S + ICAT-C (C)	
887.56	8	R.ETVSEESNVLCLSK.S + ICAT-C:13C(9) (C)	
855.94	13	R.LGDVISIQPCPDVK.Y + ICAT-C (C)	Transitional endoplasmic reticulum ATPase
857.37	16	R.LGDVISIQPCPDVK.Y + ICAT-C (C)	29
861.09	12	R.LGDVISIQPCPDVK.Y + ICAT-C:13C(9) (C)	
584.18	4	K.AIANECQANFISIK.G + ICAT-C (C)	
587.71	8	K.AIANECQANFISIK.G + ICAT-C:13C(9) (C)	
1282.00	37	K.LADDVDLEQVANETHGHVGADLAALCSEAALQAIR.K + ICAT-C (C)	
1285.10	19	K.LADDVDLEQVANETHGHVGADLAALCSEAALQAIR.K + ICAT-C:13C(9) (C)	
569.28	18	K.SCQFVAVR.R + ICAT-C (C)	Bifunctional aminoacyl-tRNA synthetase
574.37	22	K.SCQFVAVR.R + ICAT-C:13C(9) (C)	22
785.55	22	R.AFFPCFDTPAVK.C + ICAT-C (C)	Aminopeptidase B
790.11	3	R.AFFPCFDTPAVK.C + ICAT-C:13C(9) (C)	22
716.20	4	K.NQALFPACVLK.N + ICAT-C (C)	ATP-dependent RNA helicase DDX1
720.40	2	K.NQALFPACVLK.N + ICAT-C:13C(9) (C)	21
682.18	9	R.LQEVFGCAIR.A + ICAT-C (C)	Arginyl-tRNA synthetase, cytoplasmic
687.18	20	R.LQEVFGCAIR.A + ICAT-C:13C(9) (C)	20
901.45	13	K.IVFVPGCSVPLTIVK.S + ICAT-C (C)	
906.31	4	K.IVFVPGCSVPLTIVK.S + ICAT-C:13C(9) (C)	
623.80	16	K.CLIEILASR.T + ICAT-C (C)	Annexin A6
627.87	17	K.CLIEILASR.T + ICAT-C:13C(9) (C)	19
765.32	29	R.NTGIICTIGPASR.S + ICAT-C (C)	Pyruvate kinase isozymes M1/M2
766.10	1	R.NTGIICTIGPASR.S + ICAT-C (C)	19
767.33	32	R.NTGIICTIGPASR.S + ICAT-C (C)	
769.04	19	R.NTGIICTIGPASR.S + ICAT-C:13C(9) (C)	
770.65	24	R.NTGIICTIGPASR.S + ICAT-C:13C(9) (C)	
1697.83	18	R.DTGNLYCTGRVDR.E + ICAT-C (C)	Desmocollin-2 precursor
1706.06	1	R.DTGNLYCTGRVDR.E + ICAT-C:13C(9) (C)	18
992.22	1	K.NLFEDQNTLTSICEK.V + ICAT-C (C)	Exportin-2
997.05	17	K.NLFEDQNTLTSICEK.V + ICAT-C:13C(9) (C)	17

Table 5.2 Peptide pairs (light/heavy) identified from band 3, showing the ion scores, protein matches and protein scores. Protein matches with high protein scores indicating true matches are in red.

m/z	Ion score	Peptide	Protein / protein score
609,18	**2**	K.ILDDICVAK.A + ICAT-C (C)	Lysyl-tRNA synthetase
613,49	**20**	K.ILDDICVAK.A + ICAT-C:13C(9) (C)	0
933,35	**21**	K.EICNAYTELNDPVR.Q + ICAT-C (C)	
937,52	**7**	K.EICNAYTELNDPVR.Q + ICAT-C:13C(9) (C)	
752,77	**14**	R.TLIQNCGASTIR.L + ICAT-C (C)	T-complex protein 1 subunit gamma
758,00	**3**	R.TLIQNCGASTIR.L + ICAT-C:13C(9) (C)	0
800,72	**20**	K.IPGGIIEDSCVLR.G + ICAT-C (C)	
804,41	**9**	K.IPGGIIEDSCVLR.G + ICAT-C:13C(9) (C)	
752,33	**21**	R.LEDLVCDVVDR.V + ICAT-C (C)	Asparaginyl-tRNA synthetase, cytoplasmic
756,54	**14**	R.LEDLVCDVVDR.V + ICAT-C:13C(9) (C)	0
828,55	**11**	R.VLVVGAGGIGCELLK.N + ICAT-C (C)	SUMO-activating enzyme subunit 2
832,86	**17**	R.VLVVGAGGIGCELLK.N + ICAT-C:13C(9) (C)	0
728,79	**3**	R.GLGLSPDLVVCR.C + ICAT-C (C)	CTP synthase 1
732,71	**10**	R.GLGLSPDLVVCR.C + ICAT-C:13C(9) (C)	0
880,56	**12**	R.VFANAPDSACVIGLR.K + ICAT-C (C)	6-phosphofructokinase, liver type
884,88	**12**	R.VFANAPDSACVIGLR.K + ICAT-C:13C(9) (C)	0
885,99	**10**	R.VFANAPDSACVIGLR.K + ICAT-C:13C(9) (C)	
585,21	**15**	QDQVCIAR + ICAT-C:13C(9) (C)	G1 to S phase transition protein 1 homolog
580,09	**10**	QDQVCIAR + ICAT-C (C)	0
634,80	**14**	ALENDPDCR + ICAT-C:13C(9) (C)	Plastin-2
631,96	**4**	ALENDPDCR + ICAT-C (C)	0
710,54	**11**	VIGSGCNLDSAR + ICAT-C (C)	L-lactate dehydrogenase A chain
715,94	**9**	VIGSGCNLDSAR + ICAT-C:13C(9) (C)	0
805,39	**11**	SCYDLSCHAR + 2 ICAT-C (C)	Glycyl-tRNA synthetase
814,10	**4**	SCYDLSCHAR + 2 ICAT-C:13C(9) (C)	0
759,23	**8**	VVVCNLYPFVK + ICAT-C:13C(9) (C)	Bifunctional purine biosynthesis protein PURH
755,93	**8**	VVVCNLYPFVK + ICAT-C (C)	0
591,67	**5**	ALCADLSPR + ICAT-C:13C(9) (C)	Xaa-Pro aminopeptidase 1
588,58	**0**	ALCADLSPR + ICAT-C (C)	0
854,34	**5**	YAAMLSCLDEAIHNVTLALKR + ICAT-C (C)	Arylsulfatase J precursor
857,26	**2**	YAAMLSCLDEAIHNVTLALKR + ICAT-C:13C(9) (C)	0
1417,70	**4**	IGTLLDAIICR + ICAT-C (C)	TP53RK-binding protein
1426,75	**2**	IGTLLDAIICR + ICAT-C:13C(9) (C)	0
627,27	**3**	CENCGKK + 2 ICAT-C:13C(9) (C)	PR domain zinc finger protein 5
619,46	**1**	CENCGKK + 2 ICAT-C (C)	0
573,44	**3**	TYGGCEGPDAMYVK + ICAT-C (C)	Transcription elongation factor B polypeptide 1
577,42	**3**	TYGGCEGPDAMYVK + ICAT-C:13C(9) (C)	0
437,64	**0**	GCLGVGDNALR + ICAT-C:13C(9) (C)	F-box/LRR-repeat protein 20
434,16	**0**	GCLGVGDNALR + ICAT-C (C)	0

Table 5.3 Peptide pairs (light/heavy) identified from band 3 with a protein score of 0, showing the ion scores, protein matches and protein scores.

Protein	Protein score	Peptide pairs ID'd	Ratio H/L
Heat shock protein HSP 90-beta	53	6	2.2
Heat shock cognate 71 kDa protein	52	1	0.6
Heat shock protein HSP 90-alpha	46	3	1.0
Glyceraldehyde-3-phosphate dehydrogenase	34	3	1.2
Elongation factor 2	32	7	0.9
Transitional endoplasmic reticulum ATPase	29	4	0.8
Bifunctional aminoacyl-tRNA synthetase	22	1	0.8
Aminopeptidase B	22	1	1.2
ATP-dependent RNA helicase DDX1	21	1	0.9
Arginyl-tRNA synthetase, cytoplasmic	20	2	0.8
Annexin A6	19	1	2.0
Pyruvate kinase isozymes M1/M2	19	6	1.2
Desmocollin-2 precursor	18	1	1.5
Exportin-2	17	1	0.9
Lysyl-tRNA synthetase	0	2	1.0
T-complex protein 1 subunit gamma	0	2	0.9
Asparaginyl-tRNA synthetase, cytoplasmic	0	1	1.3
SUMO-activating enzyme subunit 2	0	1	0.9
CTP synthase 1	0	1	0.9
6-phosphofructokinase, liver type	0	2	0.9
G1 to S phase transition protein 1 homolog	0	1	1.3
Plastin-2	0	1	0.7
L-lactate dehydrogenase A chain	0	1	2.0
Glycyl-tRNA synthetase	0	1	0.8
Bifunctional purine biosynthesis protein PURH	0	1	2.0
Xaa-Pro aminopeptidase 1	0	1	1.3
Arylsulfatase J precursor	0	1	1.1
TP53RK-binding protein	0	1	1.5
PR domain zinc finger protein 5	0	1	5.7
Transcription elongation factor B polypeptide 1	0	1	3.0
F-box/LRR-repeat protein 20	0	1	2.2

Table 5.4 Ratios of proteins from Int9 (H) and MHV-76 (L) infected NS0 cells, from band 3. Ratios with differences of at least 0.4 are indicated in red. Protein matches with high protein scores are in red, while proteins with lower protein scores are in green, and proteins with a protein score of 0 are in black.

Heat shock protein HSP 90-beta

m/z	Ion score	Intenstity	Ratio H/L	
492.11	6	5.33E+04		K.FENLCK.L + ICAT-C (C)
495.11	7	3.04E+04	**0.6**	K.FENLCK.L + ICAT-C:13C(9) (C)
590.23	10	2.13E+04		K.AKFENLCK.L + ICAT-C (C)
594.79	9	1.77E+05	**8.3**	K.AKFENLCK.L + ICAT-C:13C(9) (C)
596.00	6	2.16E+04	**1.0**	K.AKFENLCK.L + ICAT-C:13C(9) (C)
720.75	6	1.34E+05		K.CLELFSELAEDKENYK.K + ICAT-C (C)
723.55	2	2.55E+05	**1.9**	K.CLELFSELAEDKENYK.K + ICAT-C:13C(9) (C)
763.46	35	3.11E+05		K.CLELFSELAEDKENYKK.F + ICAT-C (C)
767.04	28	1.22E+05	**0.4**	K.CLELFSELAEDKENYKK.F + ICAT-C:13C(9) (C)
1147.98	18	8.47E+04	**0.9**	K.CLELFSELAEDKENYKK.F + ICAT-C:13C(9) (C)
1144.64	35	9.89E+04		K.CLELFSELAEDKENYKK.F + ICAT-C (C)

Table 5.5 Rations of individual peptide pairs of heat shock protein 90-beta. Ratios with a difference of 0.4 or more are shown in red.

0.9, indicating that there was no real difference in protein levels between the samples. Hsp90 is a molecular chaperone and is one of the most abundant proteins in the cell. It is present in two isoforms (alpha and beta) and is a multifunctional protein involved in protein folding, degradation, and transportation, as well as signalling, and histone assembly, among other functions (reviewed in Csermely *et al.* 1998). HSP90 is induced during stress, such as virus infection, and has been shown to be necessary for the replication of some viruses, such as HSV-1 (Burch and Weller 2005; Li *et al.* 2004). Hsp90-β was identified as a possible vtRNA1 binding protein in an EMSA assay, but was thought to be a contaminant (Cliffe 2005).

Two proteins with low protein scores had differences of more than 0.4. Annexin A6 is a cytosolic protein that interacts with cell-membrane components (reviewed in Moss and Morgan 2004) and Desmocollin-2 is a transmembrane glycoprotein involved in cell adhesion and possibly other processes such as tumorigenesis and signal transduction (reviewed in Dusek *et al.* 2007).

The LC-MS/MS results were also used to search against virus proteins; however, the only proteins identified had peptides with very low ion scores (results not shown) and were of no relevance to MHV-68.

Subsequently, bands 1, 2, 4, 5, 7, 9, and 11 were processed. The LC-MS/MS analysis only identified three proteins with significant scores and two with low scores (Table 5.6). The MALDI analysis showed that there were few peptides present following the extraction and that those peptides were lost during the assay (data not shown). The reason for this is unknown, perhaps the trypsin digestion or the extraction of peptides from the gel bands did not work, or maybe the avidin column was no longer binding the labelled peptides sufficiently.

One protein, Alpha-enolase, with a low protein score had a heavy to light ration of 2.0, indicating that Int9 infected NS0 cells expressed more of this protein. Alpha-enolase, a multifunctional glycolytic enzyme, is one of the most abundant cytosolic proteins (reviewed in Pancholi 2001).

Fractionation of the peptide sample by 1-D PAGE improved the sensitivity of the cICAT method and many light/heavy peptide pairs were identified. However, only

Protein	Protein score	Peptide pairs ID'd	Ratio H/L
Fructose-bisphosphate aldolase A	37	2	0.8
Triosephosphate isomerase	32	4	0.7
Pyruvate kinase isozymes M1/M2	55	2	1.0
Beta-enolase/Alpha-enolase	25	2	1.2
Alpha-enolase	25	1	2.0
Glyceraldehyde-3-phosphate dehydrogenase	0	1	0.7
Adenosine kinase	0	1	1.1
14-3-3 protein theta	0	1	1.0
GTP-binding nuclear protein Ran	0	1	2.0
14-3-3 protein zeta/delta	0	1	0.8
DNA-(apurinic or apyrimidinic site) lyase 2	0	1	0.9
FAST kinase domain-containing protein 3	0	1	2.9
Elongation factor 2	0	1	0.8
Heat shock 70 kDa protein 4	0	1	0.8
Tubulin beta-2A chain	0	1	1.0
FK506-binding protein 4	0	1	0.7
Delta-aminolevulinic acid dehydratase	0	1	5.7
Eukaryotic initiation factor 4A-II	0	1	1.0
Short transient receptor potential channel 4	0	1	0.6
Actin-binding protein anillin	0	1	0.9

Table 5.6 Ratios of proteins from Int9 (H) and MHV-76 (L) infected NS0 cells from, bands 1, 2, 4, 5, 7, 9, and 11. Ratios with differences of at least 0.4 are indicated in red. Protein matches with high protein scores are in red, while proteins with lower protein scores are in green, and proteins with a protein score of 0 are in black.

the most abundant proteins were identified, indicating that the sample was still too complex and that a different fractionation method might be needed.

5.4. Discussion

In this chapter we aimed to analyse the functions of the non-coding RNAs by investigating the differences in protein expression between MHV-76 and Int9 infected NS0 cells using the cICAT assay. This method tags the cysteine containing proteins and enables comparison of the levels of individual proteins in two samples. The cICAT and 1-D PAGE cICAT techniques have been used, for example, to identify biomarkers for chronic lymphocyteic leukaemia (CLL) and brain tumours, as well as protein changes following saline stress of yeast cells (Barnidge *et al.* 2005; Khwaja *et al.* 2007; Li *et al.* 2003). cICAT analysis of cytosolic and membrane protein fractions of B cells from patients with mutated or unmutated CLL identified nine cytosolic and four membrane proteins that had a 3-fold or greater difference in expression (Barnidge *et al.* 2005). A subset of these was confirmed by western blot analysis. Khwaja *et al.* identified 53 proteins that were differentially expressed by more than 1.1 or less than 0.9 when analysing cerebrospinal fluid from patients with two different grades of glioma and normal controls using cICAT (Khwaja *et al.* 2007). Li *et al*. used the 1-D PAGE cICAT method to analyse protein expression profiles in yeast cells following saline stress. They identified over 560 proteins, 51 of which showed more than 2-fold difference in expression (Li *et al.* 2003). These studies show that the cICAT method is a good technique to identify changes in protein expression during different conditions.

Other techniques to examine protein differences include 2D gels, SILAC and ITRAQ. SILAC and ITRAQ are similar methods to ICAT. In ITRAQ the N-termini of trypsin digested peptides are labelled with a tag. Fragmentation of this tag during MS/MS analysis creates a reporter ion with which the peptide abundance can be determined. During SILAC the cells are grown in culture with normal growth medium or growth medium containing a heavy amino acid that is incorporated into the proteins. These techniques may be better than the cICAT method; however, the facilities needed for these techniques were not available to us. The cICAT method was chosen over 2D gels since it provides a more quantitative assay. A limitation of

the cICAT assay is that only the cysteines are labelled; however, the advantage is that the biotin tag enables purification of the labelled peptides, producing a less complex sample.

The initial experiment labelling BSA with light cICAT reagent worked well, with several labelled BSA peptides identified manually and BSA correctly identified both by MALDI and LC-MS/MS. The analysis of cytosolic proteins from MHV-76 and Int9 infected NS0 cells proved more problematic. In the first experiment only two proteins were identified, even though there were a large number of proteins in the cytosolic samples, albeit at low concentration, as shown by SDS-PAGE. It was found that the proteins were lost during the acetone precipitation.

The experiment was therefore repeated using a more crude cytoplasmic protein extraction that yielded higher protein concentrations and Vivaspins to concentrate the sample instead of acetone precipitation. This time six proteins were identified in the LC-MS/MS analysis of the labelled peptides, four with peptides labelled with light and heavy cICAT reagents. The long vacuum drying steps were found to be a source of peptide loss and the experiment was therefore repeated using freeze-drying to minimise the use of the vacuum dryer. The peptides were no longer lost during the cICAT assay and several proteins were identified; however, not many light/heavy peptide pairs. The proteins identified are very abundant in the cell and after solving the problem of loss of proteins and peptides via acetone precipitation and vacuum drying, it became clear that the sample was too complex.

To fractionate the sample and make it less complex, cytosolic proteins produced with the initial fractionation kit were labelled using the 1-D PAGE cICAT protocol, which fractionates the protein sample. This technique introduced more vacuum drying steps, which had proved to be a problem earlier. In addition, testing with BSA showed that the peptides were lost during the extraction procedure. The 1-D PAGE cICAT protocol was therefore tested with BSA labelled with light cICAT reagent, using ZipTips to concentrate the sample where possible and only performing the first step of the peptide extraction. The analysis generated several peptide peaks that could manually be identified as BSA peptides labelled with light cICAT reagent showing that the adapted method was working.

The final experiment utilised all the optimisations that had been performed. The initial band to be processed, band 3, generated several peptide pairs, but only three protein matches considered significant and 11 with protein scores above zero. The protein scores are calculated from the peptide scores, which are calculated to give the probability that the peptide match is a random event, based on the quality and number of fragment ions present in the MS/MS spectra.

The average ratio of Hsp90-β was 2.2, indicating that Int9 infected NS0 cells produced more of this protein; however, the individual peptide pair ratios were inconsistent. It is possible that this protein is continuously identified because of its abundance in the cell. However, since Hsp90 has been found to be important for virus replication of e.g. HSV-1 and influenza A by interactions with the viral polymerases (Burch and Weller 2005; Chase *et al.* 2008; Li *et al.* 2004) and the fact that Hsp90-β was identified as a possible vtRNA1 interacting protein (Cliffe 2005), it is still an interesting protein. This could be further analyse by examining the Hsp90-β protein levels by western blot and possibly using Hsp90-β inhibitors such as Geldanamycin to examine the effect on Int9 infected NS0 cells.

It is not clear what functions the other proteins that appear to be up-regulated in the presence of the non-coding RNAs, Annexin A6 and Desmocollin-2, may have during virus infection. Annexin A6 is a cytosolic protein that interacts with cell-membrane components (reviewed in Moss and Morgan 2004) and Desmocollin-2 is a transmembrane glycoprotein involved in cell adhesion (reviewed in Dusek *et al.* 2007). The levels of these proteins would need to be confirmed by western blot analysis.

The other bands analysed did not generate as many protein matches as expected. The reason for this is not known, but is possible that the trypsin digestion or avidin column were not functioning properly. Due to time constraints, this could not be examined further. Three proteins with protein scores considered significant were identified and two with lower protein scores. One of these, Alpha-enolase, a glycolytic enzyme, had a ratio of 2.0 indicating that the introduction of the non-coding RNAs led to an increase of this protein; however, this would need to be

confirmed by western blot analysis. Again, this protein is one of the most abundant in the cytosol and it is not know for what purpose it would be up-regulated.

In this study we set out to identify differences in protein expression with and without the presence of the non-coding RNAs. The cICAT protocol was optimised and the 1-D PAGE cICAT protocol subsequently optimised and used. However, the assay did not generate many protein matches, making it difficult to draw any conclusions from the data. The reason for this is not know, but it is possible that the protein samples were still too complex, since only the most abundant proteins were identified. An option would be to fractionate the sample using a cation-exchange column, which would generate fewer proteins in each sample and enhanced sensitivity. The amount of protein that is fractionated in the 1-D PAGE cICAT assay is limited to the amount and volume that can be loaded in the gel lane.

As seen in this study, there are many steps in the cICAT assay at which peptides can be lost and the assay is dependent on the equipment that is available. The technique had not previously been used in the Edinburgh Protein Interaction Centre mass spectrometry facility and although considerable progress was made, because of time constraints it was not possible to achieve the aims which had been set out.

Any difference in protein levels between MHV-76 and Int9 infected cells could be because of the vtRNAs and/or the miRNAs. During the time this study was performed, the effect of miRNAs on protein levels have usually been found to be quite low, with often no more than 50% and sometimes less than 30% down-regulation observed (Bartel 2009). This small difference in protein expression may be difficult to observe using a technique to examine global protein expression; however it has been done. Baek *et al.* 2008 used SILAC to find that hundreds of proteins are down-regulated by individual miRNAs, most with low levels of down-regulation. This and the fact that uncharged tRNAs and other viral non-coding RNAs have an effect on protein expression, warrants further analysis of changes in global protein levels; perhaps by including a cation-exchange column in the cICAT protocol to fractionate the sample, or using the ITRAQ or SILAC methods, taking the samples to a laboratory where these techniques are in regular use.

An alternative to examining global protein levels would be to examine mRNA levels using microarrays; however, miRNAs often do not affect the mRNA levels of the proteins they target. It would still be worth performing microarrays to compare mRNA levels of MHV-76 and Int9 infected NS0 cells, since the vtRNAs may have an effect on mRNA levels if they are involved in gene expression.

6. Chapter Six: Conclusions

In this study we utilised insertion viruses to investigate the functions of the non-coding RNAs of MHV-68, by examining growth properties and differences in protein expression in latently infected NS0 cells. These viruses had been made through recombination of the deletant virus MHV-76 and a plasmid containing five of the vtRNAs and six of the miRNAs, resulting in two insertion viruses with the only difference to MHV-76 and the revertant virus being these non-coding RNAs. The insertion viruses had been found to act indistinguishably to MHV-76 during *in vivo* infection, with increased clearance and low levels of latency in the spleen compared to MHV-68. Therefore, we sought to investigate the functions of the non-coding RNAs during latent infection *in vitro*.

Initially, infection of the NS0 cells was investigated to ensure that this provided a suitable model for latency *in vitro*. The NS0 cell line is a murine myeloma B cell line that has been shown to support persistent infection (Sunil-Chandra *et al.* 1993). All viruses were found to infect close to 100% of the NS0 cells following infection for five days at a MOI of 5. In addition, MHV-68 infected NS0 cells expressed the vtRNAs and miRNAs during latent infection of NS0 cells, as in S11 cells. This showed that infection of NS0s provided a suitable model for latent infection. By examining the expression of the non-coding RNAs we also showed that MHV-68 expresses the miRNAs during lytic infection, which had not been confirmed at that point. We were surprised to find that the insertion viruses expressed miRNA1 at very low levels during latent infection, even though it was expressed during lytic infection. In addition, the other miRNAs were expressed at lower levels than by MHV-68. The reason for this is not known, but possible explanations include: that promoter elements needed during latent infection are missing, the non-coding RNAs affect the virus copy numbers, or the unique genes are needed for efficient expression of the non-coding RNAs.

The levels of expression of the vtRNAs during latent infection, as well as vtRNAs and miRNAs during lytic infection by the insertion viruses are not known. It would be interesting to examine this further, as it may help to explain the lower levels of miRNA expression. Since the vtRNAs are expressed on the same transcripts as the miRNAs, the levels of the vtRNAs would be expected to be low as well, if the

deficiency is at the level of transcription. However, the non-quantitative RT-PCR performed for the vtRNAs did not indicate any major differences in expression.

Despite the lack of miRNA1 expression and the lower expression of the other miRNAs, the presence of the vtRNAs and miRNAs led to a decrease in reactivation and production of lytic virus. The decrease in reactivation could be seen both by stressing the infected cells to reactivate by infective centres assay, as well as by looking at spontaneous reactivation by staining for lytic proteins. The miRNAs alone did not seem to be responsible since transfection of miRNA mimics into MHV-76 infected cells did not affect the reactivation rates, despite achieving higher miRNA levels than in insertion virus infected cells. Disruption of the miRNA biogenesis through transfection of a siRNA against Dicer did not have an effect either; however, the miRNA or Dicer knock-down was not confirmed. Transfections with the plasmid used to make the insertion viruses and vtRNAs were inconclusive and further experiments would be needed to confirm the role of the vtRNAs, or the co-operation between vtRNAs and miRNAs, in viral reactivation.

It may not be the expression of the vtRNAs, but the presence of the vtRNA genes that is causing the reduction in reactivation. tRNA genes have been shown to regulate gene expression by affecting the chromatin organisation. In budding and fission yeast, tRNA genes have been found to act as chromatin barriers that limit the spread of heterochromatin into transcriptionally active regions (Biswas *et al.* 2009; Donze *et al.* 1999; Donze and Kamakaka 2001; Scott *et al.* 2006; Scott *et al.* 2007; Simms *et al.* 2004) and have also been shown to block enhancers or silencers from affecting promoters of nearby genes (Bolton and Boeke 2003; Hull *et al.* 1994). The functions of these tRNA genes are dependent on the ability of the gene to be transcribed; however, ectopic B-box elements not linked to functional polymerase III genes have also been found to act as chromatin barriers (reviewed in McFarlane and Whitehall 2009). In mammals SINES, believed to derive from tRNAs and containing B-box elements, are thought to have a similar role; an example of this is an Alu SINE element in transgenic mice that protects neighbouring reporter genes from transcriptional interference (Willoughby *et al.* 2000). It is not clear how the tRNA genes and B-box elements exert their barrier function.

The vtRNA genes could be acting in a similar manner to keep the area active during latency by acting as chromatin barriers or blocking enhancers or silencers of nearby genes, perhaps to regulate the transcription of the miRNAs or the unique genes. M1, for example, is likely to have promoter or enhancer sequences among the vtRNA genes (pers commun Bernadette M. Dutia). However, since the insertion viruses do not contain the unique genes and the miRNAs alone were found to have no effect on viral reactivation, these could not be the cause of the reduction in reactivation seen.

It may be that there are sequences in the left end region that act as enhancers or promoters for other viral genes that may affect the reactivation, such as genes on the other side of the terminal repeats, since the genome circularises. In EBV LMP2 initiates at the right end of the genome and stretches across the terminal repeats into the left end (Laux *et al.* 1988), while in KSHV, K1 and K15 both have promoter sequences in the terminal repeats (Bowser *et al.* 2002; Wong and Damania 2006). ORF73, whose product is essential for the establishment of latency, is known to have its transcription initiation site in the terminal repeats (Coleman *et al.* 2005), that perhaps is kept active due to the presence of the vtRNA genes. It would be interesting to examine the levels of ORF73 transcription to see if it is up-regulated in Int9 infected cells, as this could explain the decrease in reactivation. It is possible that in MHV-68 one or more of the unique genes or perhaps miRNAs act to limit ORF73 transcription, allowing reactivation. To investigate the possibility of the vtRNAs as chromatin barriers, one or more cellular tRNA genes could be inserted in the left-end of MHV-76 to examine if this also leads to a reduction in reactivation.

Chromatin barriers are used in other herpesviruses to keep transcription of latency associated transcripts active during latency. HSV-1 has insulator-like elements up-stream and in the intron of the non-coding RNA LAT, that maintain chromatin boundaries, keeping heterochromatin (silencing) out and euchromatin (active) in. LAT also promotes heterochromatin on lytic promoters, which leads to lytic gene silencing during latency (Cliffe *et al.* 2009a; Wang *et al.* 2005b). Cellular non-coding RNAs have also been found to promote chromatin silencing, through recruitment of the Polycomb repressive complex 2 (PRC2) that methylates Lys 27 on histone H3 (H3K27) leading to silencing. Examples of these include: RepA that is involved in X-chromosome inactivation, the *HOX* non-coding RNA HOTAIR which represses

transcription of the *HOXD* locus of transcription factors important during early embryonic development, and *Kcnq1ot1* that confers lineage-specific silencing of the *Kcnq1* cluster of potassium channel proteins (Pandey *et al.* 2008; Rinn *et al.* 2007; Zhao *et al.* 2008).

Although the vtRNAs localise mainly in the cytoplasm, as seen by *in situ* hybridisations (see Chapter 3 and (Cliffe 2005), dot-blot analysis showed that 18% of the vtRNAs localise in the nucleoplasm during lytic infection and 19% during latent infection (Cliffe 2005). In addition, vtRNA1 was shown by EMSA to bind Jmjdla, a mouse protein of unknown function (Cliffe 2005), which has a jmjC domain. Proteins with jmjC domains have been found to be involved in modulation of heterochromatin by demethylating histones, such as H3K36, H3K9, H3K4 and H3K27 (reviewed in Klose and Zhang 2007; Swigut and Wysocka 2007). vtRNA1 could act by inhibiting the demethylation activity of Jmjdla or recruiting the protein to promote histone demethylation. The vtRNAs may also have a function in recruiting chromatin modifying complexes, such as PRC2, and this could be further investigated by RNA immunoprecipitation. It may also be of interest to investigate the differences in chromatin contents on MHV-68, MHV-76 and insertion virus genomes by chromatin immunoprecipitations (ChIPs) to determine if there is a difference in the structure of the chromatin with or without the vtRNAs.

The presence of five vtRNAs and six miRNAs led to a low level of reactivation (insertion viruses), while the presence of all non-coding RNAs as well as the four unique genes led to a higher rate of reactivation (MHV-68); however, not as high as the lack of all non-coding RNAs and the four unique genes (MHV-76). A possible explanation for this is that the non-coding RNAs and the unique genes co-operate to keep the virus latent and to keep the level of reactivation low enough to evade the immune response, but high enough to enable low level replication and spread of the viruses to permit long-term latency. The non-coding RNAs suppress reactivation, while the unique genes act to both suppress (M1) and promote (M2) reactivation (Clambey *et al.* 2000; Evans *et al.* 2008; Herskowitz *et al.* 2005; Jacoby *et al.* 2002). Without any of these genes the virus reactivates at much higher level.

The effect of the non-coding RNAs on protein expression could not be determined using the cICAT method. Despite thorough optimisation the protein samples were found to be too complex to detect anything but the most abundant proteins. Further experiments are needed to look at the differences in protein expression; however, the effects of the miRNAs on the protein levels may be difficult to examine, due to the low level of down-regulation. The fact that vtRNA1 has been found to bind to proteins (Cliffe 2005), as well as the functions of uncharged tRNAs and other viral non-coding RNAs, supports further investigation into differences in protein expression.

Uncharged tRNAs as a result of amino acid starvation are involved in regulation of protein expression in both eukaryotic and prokaryotic cells. In bacteria binding of an uncharged tRNA to the ribosome stalls translation leading to lowering of the cell's metabolism and over-expression of genes involved in amino acid synthesis (Jain *et al.* 2006). In addition, in gram-positive bacteria aminoacyl-tRNA synthetase genes and genes involved in amino acid synthesis contain T boxes to which specific tRNAs bind leading to termination of transcription. However, binding of an uncharged tRNA leads to stabilisation of an anti-terminator allowing transcription to proceed (Green *et al.* 2010). It is possible that the vtRNAs have evolved a similar mechanism in regulating viral genes.

In eukaryotic cells uncharged tRNAs activate GCN2 which phosphorylates and inactivates eIF2, resulting in reduction in global protein synthesis, activation of amino acid biosynthesis genes and genes encoding aminoacyl-tRNA synthetases, and in mammals also regulation of gene expression at different levels (Harding *et al.* 2000; Hinnebusch 2005; Jiang *et al.* 2004; Kilberg *et al.* 2005; Wek *et al.* 1995; Zhou *et al.* 2008). There is no evidence that the vtRNAs would function to down-regulate global cellular protein synthesis. Cytoplasmic protein extracts from MHV-76 and Int9 infected NS0 cells separated on a SDS-PAGE gel look very similar, with mainly the same protein bands present. Further experiments are needed to confirm this.

Several viral non-coding RNAs regulate protein synthesis. The LATs reduce the transcription of lytic genes (Chen *et al.* 1997; Garber *et al.* 1997); the EBERs and

VAI prevent virus induced inhibition of protein synthesis by inhibiting PKR activation (Clarke *et al.* 1991) (Kitajewski *et al.* 1986; O'Malley *et al.* 1986); and the HSURs up-regulate genes associated with T-cell activation (Cook *et al.* 2004; Cook *et al.* 2005).

If the vtRNAs work as chromatin barriers this would also affect the protein and mRNA levels. Taking all this in, the vtRNAs may have an effect on protein and/or mRNA levels, and it would be of interest to further examine the differences in protein and mRNA levels of cells infected with insertion virus and MHV-76. This could be done by including a cation-exchange column in the cICAT method to fractionate the sample, or by using ITRAQ or SILAC to examine changes in protein expression, and micro arrays to examine differences in mRNA levels.

The fact that the vtRNAs are selectively packaged in the virion suggests that the vtRNAs are needed either in the virion particle or immediately following infection of the cell, perhaps regulating cellular or viral protein synthesis. It is not known if the miRNAs are packaged in the virion as well.

The miRNAs did not seem to be involved in the reduction in reactivation; however, by comparison to other viral miRNAs, they are likely to target viral and/or cellular proteins such as viral proteins that are targets of the host immune response, viral gene regulators, regulators of apoptosis, or immunomodulators (Choy *et al.* 2008; Stern-Ginossar *et al.* 2007; Sullivan *et al.* 2005; Umbach *et al.* 2008). miRNA1 has a possible target site in the 3'UTR of ORF50, and this needs to be further investigated. This could be done by examining rta protein levels by western blot analysis following transfection of miRNA1 into MHV-76 infected NS0 cells; however, at present there is no antibody available to the rta. An alternative would be to transfect cells with a plasmid expressing the FLAG-tagged rta, and then miRNA1, to investigate if the rta is down-regulated by miRNA1.

The adenovirus non-coding RNAs, VAs, share several features with the vtRNAs; they are transcribed by RNA polymerase III and encode miRNAs. The VAs inhibit the processing of cellular miRNAs by out-competing binding to the Exportin-5 nuclear export factor and Dicer (Andersson *et al.* 2005; Lu and Cullen 2004). It is not known if the vtRNA/miRNA transcripts could have a similar effect in competing

with cellular miRNAs for export and processing. It is also possible that other non-coding RNAs may give rise to miRNAs.

To take the current studies further, the reactivation experiments could be repeated with a different MHV-76 stock to see if the same increased reactivation rates seen with MHV-76 compared to the revertant virus is still observed. Further, the miRNA transfection could be repeated by transfecting revertant infected NS0 cells in stead of MHV-76 infected, to ensure that there is still no effect on the reactivation rates. To ensure that the miRNAs do not have an affect on the reactivation, the siRNA against Dicer transfection should be repeated and the levels of Dicer knock-down examined by western blot analysis and the levels of miRNAs by qRT-PCR.

The current study shows that the presence of the non-coding RNAs in MHV-76 leads to a reduction in reactivation. The miRNAs alone do not have an affect on viral reactivation in this context; however, further studies are needed to determine the mechanism. To accomplish this it would be useful to examine if it is the expression or presence of the vtRNA genes that causes the reduction in latency, or if the vtRNAs and miRNAs co-operate. Virus constructs with mutations in the miRNA seed region in the MHV-68 genome and insertion of other tRNA genes or only one of the vtRNA/miRNA transcripts into the left end of MHV-76 may help to answer some of these questions.

In addition the functions of the vtRNAs will need to be investigated. Previous studies have shown that the vtRNAs interact with proteins and it would be interesting to investigate if the vtRNAs bind specific proteins such as PKR, exportin-5, Dicer, or PRC2, as well as looking at changes in protein and mRNA levels in the presence of the vtRNAs. It may also be of interest to examine if the vtRNAs bind other RNAs.

To determine the function of the miRNAs it may be useful to examine what mRNAs they interact with through RISC pull-down assays. It is not known how the vtRNA/miRNA transcripts are processed and if Drosha and Dicer are involved and this needs to be further investigated.

Further investigation into the processing and functions of the vtRNAs and miRNAs may give an insight into not just viral non-coding RNAs but also cellular non-coding RNAs and add to the understanding of the functions of RNA molecules.

7. References

Adler H, Messerle M, Wagner M and Koszinowski UH (2000). Cloning and mutagenesis of the murine gammaherpesvirus 68 genome as an infectious bacterial artificial chromosome. *J Virol.* **74** (15), 6964-6974.

Adler H, Steer B, Freimuller K and Haas J (2007). Murine gammaherpesvirus 68 contains two functional lytic origins of replication. *J Virol.* **81** (13), 7300-7305.

Ahmed M and Fraser NW (2001). Herpes simplex virus type 1 2-kilobase latency-associated transcript intron associates with ribosomal proteins and splicing factors. *J Virol.* **75** (24), 12070-12080.

Ahmed M, Lock M, Miller CG and Fraser NW (2002). Regions of the herpes simplex virus type 1 latency-associated transcript that protect cells from apoptosis in vitro and protect neuronal cells in vivo. *J Virol.* **76** (2), 717-729.

Ahn JW, Powell KL, Kellam P and Alber DG (2002). Gammaherpesvirus lytic gene expression as characterized by DNA array. *J Virol.* **76** (12), 6244-6256.

Albrecht JC and Fleckenstein B (1992). Nucleotide sequence of HSUR 6 and HSUR 7, two small RNAs of herpesvirus saimiri. *Nucleic Acids Res.* **20** (7), 1810.

Alexander JM, Nelson CA, van Berkel V, Lau EK, Studts JM, Brett TJ, Speck SH, Handel TM, Virgin HW and Fremont DH (2002). Structural basis of chemokine sequestration by a herpesvirus decoy receptor. *Cell.* **111** (3), 343-356.

Ambroziak JA, Blackbourn DJ, Herndier BG, Glogau RG, Gullett JH, McDonald AR, Lennette ET and Levy JA (1995). Herpes-like sequences in HIV-infected and uninfected Kaposi's sarcoma patients. *Science.* **268** (5210), 582-583.

Andersson J (2006). Epstein-Barr virus and Hodgkin's lymphoma. *Herpes.* **13** (1), 12-16.

Andersson MG, Haasnoot PC, Xu N, Berenjian S, Berkhout B and Akusjarvi G (2005). Suppression of RNA interference by adenovirus virus-associated RNA. *J Virol.* **79** (15), 9556-9565.

Andreoni M, Sarmati L, Nicastri E, El Sawaf G, El Zalabani M, Uccella I, Bugarini R, Parisi SG and Rezza G (2002). Primary human herpesvirus 8 infection in immunocompetent children. *JAMA.* **287** (10), 1295-1300.

Aparicio O, Razquin N, Zaratiegui M, Narvaiza I and Fortes P (2006). Adenovirus virus-associated RNA is processed to functional interfering RNAs involved in virus production. *J Virol.* **80** (3), 1376-1384.

Aparicio O, Carnero E, Abad X, Razquin N, Guruceaga E, Segura V and Fortes P (2009). Adenovirus VA RNA-derived miRNAs target cellular genes involved in cell growth, gene expression and DNA repair. *Nucleic Acids Res.*

Apcher S, Komarova A, Daskalogianni C, Yin Y, Malbert-Colas L and Fahraeus R (2009). mRNA translation regulation by the Gly-Ala repeat of Epstein-Barr virus nuclear antigen 1. *J Virol.* **83** (3), 1289-1298.

Arrand JR and Rymo L (1982). Characterization of the major Epstein-Barr virus-specific RNA in Burkitt lymphoma-derived cells. *J Virol.* **41** (2), 376-389.

Arrand JR, Young LS and Tugwood JD (1989). Two families of sequences in the small RNA-encoding region of Epstein-Barr virus (EBV) correlate with EBV types A and B. *J Virol.* **63** (2), 983-986.

Arumugaswami V, Wu TT, Martinez-Guzman D, Jia Q, Deng H, Reyes N and Sun R (2006). ORF18 is a transfactor that is essential for late gene transcription of a gammaherpesvirus. *J Virol.* **80** (19), 9730-9740.

Atanasiu D and Fraser NW (2007). The stable 2-kilobase latency-associated transcript of herpes simplex virus type 1 can alter the assembly of the 60S ribosomal subunit and is exported from nucleus to cytoplasm by a CRM1-dependent pathway. *J Virol.* **81** (14), 7695-7701.

Babcock GJ, Hochberg D and Thorley-Lawson AD (2000). The expression pattern of Epstein-Barr virus latent genes in vivo is dependent upon the differentiation stage of the infected B cell. *Immunity.* **13** (4), 497-506.

Babcock GJ, Decker LL, Volk M and Thorley-Lawson DA (1998). EBV persistence in memory B cells in vivo. *Immunity.* **9** (3), 395-404.

Baek D, Villen J, Shin C, Camargo FD, Gygi SP and Bartel DP (2008). The impact of microRNAs on protein output. *Nature.* **455** (7209), 64-71.

Bailly-Bechet M, Vergassola M and Rocha E (2007). Causes for the intriguing presence of tRNAs in phages. *Genome Res.* **17** (10), 1486-1495.

Ballestas ME, Chatis PA and Kaye KM (1999). Efficient persistence of extrachromosomal KSHV DNA mediated by latency-associated nuclear antigen. *Science.* **284** (5414), 641-644.

Bao N, Lye KW and Barton MK (2004). MicroRNA binding sites in Arabidopsis class III HD-ZIP mRNAs are required for methylation of the template chromosome. *Dev Cell.* **7** (5), 653-662.

Barends S, Rudinger-Thirion J, Florentz C, Giege R, Pleij CW and Kraal B (2004). tRNA-like structure regulates translation of Brome mosaic virus RNA. *J Virol.* **78** (8), 4003-4010.

Barnidge DR, Jelinek DF, Muddiman DC and Kay NE (2005). Quantitative protein expression analysis of CLL B cells from mutated and unmutated IgV(H) subgroups using acid-cleavable isotope-coded affinity tag reagents. *J Proteome Res.* **4** (4), 1310-1317.

Bartel DP (2009). MicroRNAs: target recognition and regulatory functions. *Cell.* **136** (2), 215-233.

Barth S, Pfuhl T, Mamiani A, Ehses C, Roemer K, Kremmer E, Jaker C, Hock J, Meister G and Grasser FA (2008). Epstein-Barr virus-encoded microRNA miR-BART2 down-regulates the viral DNA polymerase BALF5. *Nucleic Acids Res.* **36** (2), 666-675.

Barton ES, Lutzke ML, Rochford R and Virgin HWt (2005). Alpha/beta interferons regulate murine gammaherpesvirus latent gene expression and reactivation from latency. *J Virol.* **79** (22), 14149-14160.

Bechtel J, Grundhoff A and Ganem D (2005). RNAs in the virion of Kaposi's sarcoma-associated herpesvirus. *J Virol.* **79** (16), 10138-10146.

Bellare P and Ganem D (2009). Regulation of KSHV lytic switch protein expression by a virus-encoded microRNA: an evolutionary adaptation that fine-tunes lytic reactivation. *Cell Host Microbe.* **6** (6), 570-575.

Belz GT, Liu H, Andreansky S, Doherty PC and Stevenson PG (2003). Absence of a functional defect in CD8+ T cells during primary murine gammaherpesvirus-68 infection of I-A(b-/-) mice. *J Gen Virol.* **84** (Pt 2), 337-341.

Bennett NJ, May JS and Stevenson PG (2005). Gamma-herpesvirus latency requires T cell evasion during episome maintenance. *PLoS Biol.* **3** (4), e120.

Beral V, Peterman TA, Berkelman RL and Jaffe HW (1990). Kaposi's sarcoma among persons with AIDS: a sexually transmitted infection? *Lancet.* **335** (8682), 123-128.

Berger SL and Folk WR (1985). Differential activation of RNA polymerase III-transcribed genes by the polyomavirus enhancer and the adenovirus E1A gene products. *Nucleic Acids Res.* **13** (4), 1413-1428.

Bernstein E, Caudy AA, Hammond SM and Hannon GJ (2001). Role for a bidentate ribonuclease in the initiation step of RNA interference. *Nature.* **409** (6818), 363-366.

Berthomme H, Lokensgard J, Yang L, Margolis T and Feldman LT (2000). Evidence for a bidirectional element located downstream from the herpes simplex virus type 1 latency-associated promoter that increases its activity during latency. *J Virol.* **74** (8), 3613-3622.

Besecker MI, Harden ME, Li G, Wang XJ and Griffiths A (2009). Discovery of herpes B virus-encoded microRNAs. *J Virol.* **83** (7), 3413-3416.

Bhat RA and Thimmappaya B (1983). Two small RNAs encoded by Epstein-Barr virus can functionally substitute for the virus-associated RNAs in the lytic growth of adenovirus 5. *Proc Natl Acad Sci U S A.* **80** (15), 4789-4793.

Bhat RA and Thimmappaya B (1985). Construction and analysis of additional adenovirus substitution mutants confirm the complementation of VAI RNA function by two small RNAs encoded by Epstein-Barr virus. *J Virol.* **56** (3), 750-756.

Biswas M, Maqani N, Rai R, Kumaran SP, Iyer KR, Sendinc E, Smith JS and Laloraya S (2009). Limiting the extent of the RDN1 heterochromatin domain by a silencing barrier and Sir2 protein levels in Saccharomyces cerevisiae. *Mol Cell Biol.* **29** (10), 2889-2898.

Blasdell K, McCracken C, Morris A, Nash AA, Begon M, Bennett M and Stewart JP (2003). The wood mouse is a natural host for Murid herpesvirus 4. *J Gen Virol.* **84** (Pt 1), 111-113.

Blaskovic D, Stanekova D and Rajcani J (1984). Experimental pathogenesis of murine herpesvirus in newborn mice. *Acta Virol.* **28** (3), 225-231.

Blaskovic D, Stancekova M, Svobodova J and Mistrikova J (1980). Isolation of five strains of herpesviruses from two species of free living small rodents. *Acta Virol.* **24** (6), 468.

Bloom DC, Hill JM, Devi-Rao G, Wagner EK, Feldman LT and Stevens JG (1996). A 348-base-pair region in the latency-associated transcript facilitates herpes simplex virus type 1 reactivation. *J Virol.* **70** (4), 2449-2459.

Boehmer PE and Lehman IR (1997). Herpes simplex virus DNA replication. *Annu Rev Biochem.* **66**, 347-384.

Bolton EC and Boeke JD (2003). Transcriptional interactions between yeast tRNA genes, flanking genes and Ty elements: a genomic point of view. *Genome Res.* **13** (2), 254-263.

Boname JM and Stevenson PG (2001). MHC class I ubiquitination by a viral PHD/LAP finger protein. *Immunity.* **15** (4), 627-636.

Boname JM, de Lima BD, Lehner PJ and Stevenson PG (2004). Viral degradation of the MHC class I peptide loading complex. *Immunity.* **20** (3), 305-317.

Borchert GM, Lanier W and Davidson BL (2006). RNA polymerase III transcribes human microRNAs. *Nat Struct Mol Biol.* **13** (12), 1097-1101.

Bornkamm GW (2009). Epstein-Barr virus and the pathogenesis of Burkitt's lymphoma: more questions than answers. *Int J Cancer.* **124** (8), 1745-1755.

Bortz E, Whitelegge JP, Jia Q, Zhou ZH, Stewart JP, Wu TT and Sun R (2003). Identification of proteins associated with murine gammaherpesvirus 68 virions. *J Virol.* **77** (24), 13425-13432.

Bortz E, Wang L, Jia Q, Wu TT, Whitelegge JP, Deng H, Zhou ZH and Sun R (2007). Murine gammaherpesvirus 68 ORF52 encodes a tegument protein

required for virion morphogenesis in the cytoplasm. *J Virol.* **81** (18), 10137-10150.

Boshoff C and Weiss RA (2001). Epidemiology and pathogenesis of Kaposi's sarcoma-associated herpesvirus. *Philos Trans R Soc Lond B Biol Sci.* **356** (1408), 517-534.

Bowden RJ, Simas JP, Davis AJ and Efstathiou S (1997). Murine gammaherpesvirus 68 encodes tRNA-like sequences which are expressed during latency. *J Gen Virol.* **78 (Pt 7)**, 1675-1687.

Bowser BS, DeWire SM and Damania B (2002). Transcriptional regulation of the K1 gene product of Kaposi's sarcoma-associated herpesvirus. *J Virol.* **76** (24), 12574-12583.

Braaten DC, McClellan JS, Messaoudi I, Tibbetts SA, McClellan KB, Nikolich-Zugich J and Virgin HW (2006). Effective control of chronic gamma-herpesvirus infection by unconventional MHC Class Ia-independent CD8 T cells. *PLoS Pathog.* **2** (5), e37.

Branco FJ and Fraser NW (2005). Herpes simplex virus type 1 latency-associated transcript expression protects trigeminal ganglion neurons from apoptosis. *J Virol.* **79** (14), 9019-9025.

Bresnahan WA and Shenk T (2000). A subset of viral transcripts packaged within human cytomegalovirus particles. *Science.* **288** (5475), 2373-2376.

Bridgeman A, Stevenson PG, Simas JP and Efstathiou S (2001). A secreted chemokine binding protein encoded by murine gammaherpesvirus-68 is necessary for the establishment of a normal latent load. *J Exp Med.* **194** (3), 301-312.

Brooks JW, Hamilton-Easton AM, Christensen JP, Cardin RD, Hardy CL and Doherty PC (1999). Requirement for CD40 ligand, CD4(+) T cells, and B cells in an infectious mononucleosis-like syndrome. *J Virol.* **73** (11), 9650-9654.

Brooks L, Yao QY, Rickinson AB and Young LS (1992). Epstein-Barr virus latent gene transcription in nasopharyngeal carcinoma cells: coexpression of EBNA1, LMP1, and LMP2 transcripts. *J Virol.* **66** (5), 2689-2697.

Brown HJ, Song MJ, Deng H, Wu TT, Cheng G and Sun R (2003). NF-kappaB inhibits gammaherpesvirus lytic replication. *J Virol.* **77** (15), 8532-8540.

Buck AH, Santoyo-Lopez J, Robertson KA, Kumar DS, Reczko M and Ghazal P (2007). Discrete clusters of virus-encoded micrornas are associated with complementary strands of the genome and the 7.2-kilobase stable intron in murine cytomegalovirus. *J Virol.* **81** (24), 13761-13770.

Buck AH, Perot J, Chisholm MA, Kumar DS, Tuddenham L, Cognat V, Marcinowski L, Dolken L and Pfeffer S (2010). Post-transcriptional regulation of miR-27 in murine cytomegalovirus infection. *RNA.* **16** (2), 307-315.

Burch AD and Weller SK (2005). Herpes simplex virus type 1 DNA polymerase requires the mammalian chaperone hsp90 for proper localization to the nucleus. *J Virol.* **79** (16), 10740-10749.

Burkitt D (1958). A sarcoma involving the jaws in African children. *Br J Surg.* **46** (197), 218-223.

Burnside J, Bernberg E, Anderson A, Lu C, Meyers BC, Green PJ, Jain N, Isaacs G and Morgan RW (2006). Marek's disease virus encodes MicroRNAs that map to meq and the latency-associated transcript. *J Virol.* **80** (17), 8778-8786.

Cai X, Hagedorn CH and Cullen BR (2004). Human microRNAs are processed from capped, polyadenylated transcripts that can also function as mRNAs. *RNA.* **10** (12), 1957-1966.

Cai X, Lu S, Zhang Z, Gonzalez CM, Damania B and Cullen BR (2005). Kaposi's sarcoma-associated herpesvirus expresses an array of viral microRNAs in latently infected cells. *Proc Natl Acad Sci U S A.* **102** (15), 5570-5575.

Cai X, Schafer A, Lu S, Bilello JP, Desrosiers RC, Edwards R, Raab-Traub N and Cullen BR (2006). Epstein-Barr virus microRNAs are evolutionarily conserved and differentially expressed. *PLoS Pathog.* **2** (3), e23.

Caldwell RG, Wilson JB, Anderson SJ and Longnecker R (1998). Epstein-Barr virus LMP2A drives B cell development and survival in the absence of normal B cell receptor signals. *Immunity.* **9** (3), 405-411.

Cantalupo P, Doering A, Sullivan CS, Pal A, Peden KW, Lewis AM and Pipas JM (2005). Complete nucleotide sequence of polyomavirus SA12. *J Virol.* **79** (20), 13094-13104.

Cardin RD, Brooks JW, Sarawar SR and Doherty PC (1996). Progressive loss of CD8+ T cell-mediated control of a gamma-herpesvirus in the absence of CD4+ T cells. *J Exp Med.* **184** (3), 863-871.

Cen S, Khorchid A, Javanbakht H, Gabor J, Stello T, Shiba K, Musier-Forsyth K and Kleiman L (2001). Incorporation of lysyl-tRNA synthetase into human immunodeficiency virus type 1. *J Virol.* **75** (11), 5043-5048.

Chang PJ, Shedd D, Gradoville L, Cho MS, Chen LW, Chang J and Miller G (2002). Open reading frame 50 protein of Kaposi's sarcoma-associated herpesvirus directly activates the viral PAN and K12 genes by binding to related response elements. *J Virol.* **76** (7), 3168-3178.

Chang Y and Moore PS (2001). Kaposi's sarcoma-associated herpesvirus. In: *Fields virology*. Knipe DM and Howley PM (eds.); Lippincott, Williams & Wilkins.

Chang Y, Cesarman E, Pessin MS, Lee F, Culpepper J, Knowles DM and Moore PS (1994). Identification of herpesvirus-like DNA sequences in AIDS-associated Kaposi's sarcoma. *Science.* **266** (5192), 1865-1869.

Chang Y, Moore PS, Talbot SJ, Boshoff CH, Zarkowska T, Godden K, Paterson H, Weiss RA and Mittnacht S (1996). Cyclin encoded by KS herpesvirus. *Nature.* **382** (6590), 410.

Chase G, Deng T, Fodor E, Leung BW, Mayer D, Schwemmle M and Brownlee G (2008). Hsp90 inhibitors reduce influenza virus replication in cell culture. *Virology.* **377** (2), 431-439.

Chastel C, Beaucournu JP, Chastel O, Legrand MC and Le Goff F (1994). A herpesvirus from an European shrew (Crocidura russula). *Acta Virol.* **38** (5), 309.

Chekulaeva M and Filipowicz W (2009). Mechanisms of miRNA-mediated post-transcriptional regulation in animal cells. *Curr Opin Cell Biol.* **21** (3), 452-460.

Chen SH, Kramer MF, Schaffer PA and Coen DM (1997). A viral function represses accumulation of transcripts from productive-cycle genes in mouse ganglia latently infected with herpes simplex virus. *J Virol.* **71** (8), 5878-5884.

Chendrimada TP, Gregory RI, Kumaraswamy E, Norman J, Cooch N, Nishikura K and Shiekhattar R (2005). TRBP recruits the Dicer complex to Ago2 for microRNA processing and gene silencing. *Nature.* **436** (7051), 740-744.

Choi J, Means RE, Damania B and Jung JU (2001). Molecular piracy of Kaposi's sarcoma associated herpesvirus. *Cytokine Growth Factor Rev.* **12** (2-3), 245-257.

Choi YG, Dreher TW and Rao AL (2002). tRNA elements mediate the assembly of an icosahedral RNA virus. *Proc Natl Acad Sci U S A.* **99** (2), 655-660.

Choy EY, Siu KL, Kok KH, Lung RW, Tsang CM, To KF, Kwong DL, Tsao SW and Jin DY (2008). An Epstein-Barr virus-encoded microRNA targets PUMA to promote host cell survival. *J Exp Med.* **205** (11), 2551-2560.

Christensen JP and Doherty PC (1999). Quantitative analysis of the acute and long-term CD4(+) T-cell response to a persistent gammaherpesvirus. *J Virol.* **73** (5), 4279-4283.

Christensen JP, Cardin RD, Branum KC and Doherty PC (1999). CD4(+) T cell-mediated control of a gamma-herpesvirus in B cell-deficient mice is mediated by IFN-gamma. *Proc Natl Acad Sci U S A.* **96** (9), 5135-5140.

Chugh P, Matta H, Schamus S, Zachariah S, Kumar A, Richardson JA, Smith AL and Chaudhary PM (2005). Constitutive NF-kappaB activation, normal Fas-induced apoptosis, and increased incidence of lymphoma in human herpes virus 8 K13 transgenic mice. *Proc Natl Acad Sci U S A.* **102** (36), 12885-12890.

Ciampor F, Sidorenko EV, Taikova NV and Bystricka M (1981). Ultrastructural localization by immunoperoxidase techniques of influenza virus antigens in abortive infection of L cells. *Acta Virol.* **25** (6), 381-389.

Clambey ET, Virgin HWt and Speck SH (2000). Disruption of the murine gammaherpesvirus 68 M1 open reading frame leads to enhanced reactivation from latency. *J Virol.* **74** (4), 1973-1984.

Clambey ET, Virgin HWt and Speck SH (2002). Characterization of a spontaneous 9.5-kilobase-deletion mutant of murine gammaherpesvirus 68 reveals tissue-specific genetic requirements for latency. *J Virol.* **76** (13), 6532-6544.

Clarke PA, Sharp NA and Clemens MJ (1992). Expression of genes for the Epstein-Barr virus small RNAs EBER-1 and EBER-2 in Daudi Burkitt's lymphoma cells: effects of interferon treatment. *J Gen Virol.* **73 (Pt 12)**, 3169-3175.

Clarke PA, Pe'ery T, Ma Y and Mathews MB (1994). Structural features of adenovirus 2 virus-associated RNA required for binding to the protein kinase DAI. *Nucleic Acids Res.* **22** (21), 4364-4374.

Clarke PA, Schwemmle M, Schickinger J, Hilse K and Clemens MJ (1991). Binding of Epstein-Barr virus small RNA EBER-1 to the double-stranded RNA-activated protein kinase DAI. *Nucleic Acids Res.* **19** (2), 243-248.

Cliffe A (2005). The biological role of viral tRNA-like molecules in a murine gammaherpesvirus infection, PhD (The University of Edinburgh).

Cliffe AR, Garber DA and Knipe DM (2009a). Transcription of the herpes simplex virus latency-associated transcript promotes the formation of facultative heterochromatin on lytic promoters. *J Virol.* **83** (16), 8182-8190.

Cliffe AR, Nash AA and Dutia BM (2009b). Selective uptake of small RNA molecules in the virion of murine gammaherpesvirus 68. *J Virol.* **83** (5), 2321-2326.

Cohen JI (2000). Epstein-Barr virus infection. *N Engl J Med.* **343** (7), 481-492.

Cohen JI, Wang F, Mannick J and Kieff E (1989). Epstein-Barr virus nuclear protein 2 is a key determinant of lymphocyte transformation. *Proc Natl Acad Sci U S A.* **86** (23), 9558-9562.

Coleman HM, Efstathiou S and Stevenson PG (2005). Transcription of the murine gammaherpesvirus 68 ORF73 from promoters in the viral terminal repeats. *J Gen Virol.* **86** (Pt 3), 561-574.

Conrad NK and Steitz JA (2005). A Kaposi's sarcoma virus RNA element that increases the nuclear abundance of intronless transcripts. *EMBO J.* **24** (10), 1831-1841.

Conrad NK, Shu MD, Uyhazi KE and Steitz JA (2007). Mutational analysis of a viral RNA element that counteracts rapid RNA decay by interaction with the polyadenylate tail. *Proc Natl Acad Sci U S A.* **104** (25), 10412-10417.

Conrad NK, Mili S, Marshall EL, Shu MD and Steitz JA (2006). Identification of a rapid mammalian deadenylation-dependent decay pathway and its inhibition by a viral RNA element. *Mol Cell.* **24** (6), 943-953.

Cook HL, Mischo HE and Steitz JA (2004). The Herpesvirus saimiri small nuclear RNAs recruit AU-rich element-binding proteins but do not alter host AU-rich element-containing mRNA levels in virally transformed T cells. *Mol Cell Biol.* **24** (10), 4522-4533.

Cook HL, Lytle JR, Mischo HE, Li MJ, Rossi JJ, Silva DP, Desrosiers RC and Steitz JA (2005). Small nuclear RNAs encoded by Herpesvirus saimiri upregulate the expression of genes linked to T cell activation in virally transformed T cells. *Curr Biol.* **15** (10), 974-979.

Coppola MA, Flano E, Nguyen P, Hardy CL, Cardin RD, Shastri N, Woodland DL and Blackman MA (1999). Apparent MHC-independent stimulation of CD8+ T cells in vivo during latent murine gammaherpesvirus infection. *J Immunol.* **163** (3), 1481-1489.

Coscoy L and Ganem D (2000). Kaposi's sarcoma-associated herpesvirus encodes two proteins that block cell surface display of MHC class I chains by enhancing their endocytosis. *Proc Natl Acad Sci U S A.* **97** (14), 8051-8056.

Coscoy L, Sanchez DJ and Ganem D (2001). A novel class of herpesvirus-encoded membrane-bound E3 ubiquitin ligases regulates endocytosis of proteins involved in immune recognition. *J Cell Biol.* **155** (7), 1265-1273.

Cotter MA, 2nd and Robertson ES (1999). The latency-associated nuclear antigen tethers the Kaposi's sarcoma-associated herpesvirus genome to host chromosomes in body cavity-based lymphoma cells. *Virology.* **264** (2), 254-264.

Coventry VK and Conn GL (2008). Analysis of adenovirus VA RNAI structure and stability using compensatory base pair modifications. *Nucleic Acids Res.* **36** (5), 1645-1653.

Crawford DH (2001). Biology and disease associations of Epstein-Barr virus. *Philos Trans R Soc Lond B Biol Sci.* **356** (1408), 461-473.

Crawford DH, Macsween KF, Higgins CD, Thomas R, McAulay K, Williams H, Harrison N, Reid S, Conacher M, Douglas J and Swerdlow AJ (2006). A cohort study among university students: identification of risk factors for

Epstein-Barr virus seroconversion and infectious mononucleosis. *Clin Infect Dis.* **43** (3), 276-282.

Csermely P, Schnaider T, Soti C, Prohaszka Z and Nardai G (1998). The 90-kDa molecular chaperone family: structure, function, and clinical applications. A comprehensive review. *Pharmacol Ther.* **79** (2), 129-168.

Cui C, Griffiths A, Li G, Silva LM, Kramer MF, Gaasterland T, Wang XJ and Coen DM (2006). Prediction and identification of herpes simplex virus 1-encoded microRNAs. *J Virol.* **80** (11), 5499-5508.

Davis E, Caiment F, Tordoir X, Cavaille J, Ferguson-Smith A, Cockett N, Georges M and Charlier C (2005). RNAi-mediated allelic trans-interaction at the imprinted Rtl1/Peg11 locus. *Curr Biol.* **15** (8), 743-749.

Davison AJ, Eberle R, Ehlers B, Hayward GS, McGeoch DJ, Minson AC, Pellett PE, Roizman B, Studdert MJ and Thiry E (2009). The order Herpesvirales. *Arch Virol.* **154** (1), 171-177.

de Lima BD, May JS and Stevenson PG (2004). Murine gammaherpesvirus 68 lacking gp150 shows defective virion release but establishes normal latency in vivo. *J Virol.* **78** (10), 5103-5112.

de Lima BD, May JS, Marques S, Simas JP and Stevenson PG (2005). Murine gammaherpesvirus 68 bcl-2 homologue contributes to latency establishment in vivo. *J Gen Virol.* **86** (Pt 1), 31-40.

Deng H, Chu JT, Park NH and Sun R (2004). Identification of cis sequences required for lytic DNA replication and packaging of murine gammaherpesvirus 68. *J Virol.* **78** (17), 9123-9131.

Desai SM, Vaughan J and Weiss SB (1986). Identification and location of nine T5 bacteriophage tRNA genes by DNA sequence analysis. *Nucleic Acids Res.* **14** (10), 4197-4205.

Desrosiers RC, Silva DP, Waldron LM and Letvin NL (1986). Nononcogenic deletion mutants of herpesvirus saimiri are defective for in vitro immortalization. *J Virol.* **57** (2), 701-705.

Diebel KW, Smith AL and van Dyk LF (2010). Mature and functional viral miRNAs transcribed from novel RNA polymerase III promoters. *RNA.* **16** (1), 170-185.

Dieci G, Fiorino G, Castelnuovo M, Teichmann M and Pagano A (2007). The expanding RNA polymerase III transcriptome. *Trends Genet.* **23** (12), 614-622.

Dirheimer G, Keith G, Dumas P and Westhof E (1995). Primary, Secondary, and Tertiary structures of tRNAs. In: *tRNA:Structure, Biosynthesis, and Function*.

D. Söll and U. RajBhandary (eds.); American Society for Microbiology, Washington, 93-126.

Dolken L, Perot J, Cognat V, Alioua A, John M, Soutschek J, Ruzsics Z, Koszinowski U, Voinnet O and Pfeffer S (2007). Mouse cytomegalovirus microRNAs dominate the cellular small RNA profile during lytic infection and show features of posttranscriptional regulation. *J Virol.* **81** (24), 13771-13782.

Donze D and Kamakaka RT (2001). RNA polymerase III and RNA polymerase II promoter complexes are heterochromatin barriers in Saccharomyces cerevisiae. *EMBO J.* **20** (3), 520-531.

Donze D, Adams CR, Rine J and Kamakaka RT (1999). The boundaries of the silenced HMR domain in Saccharomyces cerevisiae. *Genes Dev.* **13** (6), 698-708.

Douglas J, Dutia B, Rhind S, Stewart JP and Talbot SJ (2004). Expression in a recombinant murid herpesvirus 4 reveals the in vivo transforming potential of the K1 open reading frame of Kaposi's sarcoma-associated herpesvirus. *J Virol.* **78** (16), 8878-8884.

Dreher TW (2009). Role of tRNA-like structures in controlling plant virus replication. *Virus Res.* **139** (2), 217-229.

Dreher TW, Uhlenbeck OC and Browning KS (1999). Quantitative assessment of EF-1alpha.GTP binding to aminoacyl-tRNAs, aminoacyl-viral RNA, and tRNA shows close correspondence to the RNA binding properties of EF-Tu. *J Biol Chem.* **274** (2), 666-672.

Du MQ, Liu H, Diss TC, Ye H, Hamoudi RA, Dupin N, Meignin V, Oksenhendler E, Boshoff C and Isaacson PG (2001). Kaposi sarcoma-associated herpesvirus infects monotypic (IgM lambda) but polyclonal naive B cells in Castleman disease and associated lymphoproliferative disorders. *Blood.* **97** (7), 2130-2136.

Dulebohn D, Choy J, Sundermeier T, Okan N and Karzai AW (2007). Trans-translation: the tmRNA-mediated surveillance mechanism for ribosome rescue, directed protein degradation, and nonstop mRNA decay. *Biochemistry.* **46** (16), 4681-4693.

Dupin N, Diss TL, Kellam P, Tulliez M, Du MQ, Sicard D, Weiss RA, Isaacson PG and Boshoff C (2000). HHV-8 is associated with a plasmablastic variant of Castleman disease that is linked to HHV-8-positive plasmablastic lymphoma. *Blood.* **95** (4), 1406-1412.

Dusek RL, Godsel LM and Green KJ (2007). Discriminating roles of desmosomal cadherins: beyond desmosomal adhesion. *J Dermatol Sci.* **45** (1), 7-21.

Dutia BM, Clarke CJ, Allen DJ and Nash AA (1997). Pathological changes in the spleens of gamma interferon receptor-deficient mice infected with murine gammaherpesvirus: a role for CD8 T cells. *J Virol.* **71** (6), 4278-4283.

Dutia BM, Stewart JP, Clayton RA, Dyson H and Nash AA (1999). Kinetic and phenotypic changes in murine lymphocytes infected with murine gammaherpesvirus-68 in vitro. *J Gen Virol.* **80 (Pt 10)**, 2729-2736.

Dutia BM, Roy DJ, Ebrahimi B, Gangadharan B, Efstathiou S, Stewart JP and Nash AA (2004). Identification of a region of the virus genome involved in murine gammaherpesvirus 68-induced splenic pathology. *J Gen Virol.* **85** (Pt 6), 1393-1400.

Ebrahimi B, Dutia BM, Brownstein DG and Nash AA (2001). Murine gammaherpesvirus-68 infection causes multi-organ fibrosis and alters leukocyte trafficking in interferon-gamma receptor knockout mice. *Am J Pathol.* **158** (6), 2117-2125.

Ebrahimi B, Dutia BM, Roberts KL, Garcia-Ramirez JJ, Dickinson P, Stewart JP, Ghazal P, Roy DJ and Nash AA (2003). Transcriptome profile of murine gammaherpesvirus-68 lytic infection. *J Gen Virol.* **84** (Pt 1), 99-109.

Efstathiou S, Ho YM and Minson AC (1990a). Cloning and molecular characterization of the murine herpesvirus 68 genome. *J Gen Virol.* **71 (Pt 6)**, 1355-1364.

Efstathiou S, Ho YM, Hall S, Styles CJ, Scott SD and Gompels UA (1990b). Murine herpesvirus 68 is genetically related to the gammaherpesviruses Epstein-Barr virus and herpesvirus saimiri. *J Gen Virol.* **71 (Pt 6)**, 1365-1372.

Ehlers B, Kuchler J, Yasmum N, Dural G, Voigt S, Schmidt-Chanasit J, Jakel T, Matuschka FR, Richter D, Essbauer S, Hughes DJ, Summers C, Bennett M, Stewart JP and Ulrich RG (2007). Identification of novel rodent herpesviruses, including the first gammaherpesvirus of Mus musculus. *J Virol.* **81** (15), 8091-8100.

Ehtisham S, Sunil-Chandra NP and Nash AA (1993). Pathogenesis of murine gammaherpesvirus infection in mice deficient in CD4 and CD8 T cells. *J Virol.* **67** (9), 5247-5252.

Elbashir SM, Lendeckel W and Tuschl T (2001). RNA interference is mediated by 21- and 22-nucleotide RNAs. *Genes Dev.* **15** (2), 188-200.

Elia A, Vyas J, Laing KG and Clemens MJ (2004). Ribosomal protein L22 inhibits regulation of cellular activities by the Epstein-Barr virus small RNA EBER-1. *Eur J Biochem.* **271** (10), 1895-1905.

Ensser A, Pfinder A, Muller-Fleckenstein I and Fleckenstein B (1999). The URNA genes of herpesvirus saimiri (strain C488) are dispensable for transformation of human T cells in vitro. *J Virol.* **73** (12), 10551-10555.

Epstein MA, Achong BG and Barr YM (1964). Virus Particles in Cultured Lymphoblasts from Burkitt's Lymphoma. *Lancet.* **1** (7335), 702-703.

Esteban M, Garcia MA, Domingo-Gil E, Arroyo J, Nombela C and Rivas C (2003). The latency protein LANA2 from Kaposi's sarcoma-associated herpesvirus inhibits apoptosis induced by dsRNA-activated protein kinase but not RNase L activation. *J Gen Virol.* **84** (Pt 6), 1463-1470.

Eulalio A, Huntzinger E and Izaurralde E (2008). Getting to the root of miRNA-mediated gene silencing. *Cell.* **132** (1), 9-14.

Evans AG, Moorman NJ, Willer DO and Speck SH (2006). The M4 gene of gammaHV68 encodes a secreted glycoprotein and is required for the efficient establishment of splenic latency. *Virology.* **344** (2), 520-531.

Evans AG, Moser JM, Krug LT, Pozharskaya V, Mora AL and Speck SH (2008). A gammaherpesvirus-secreted activator of Vbeta4+ CD8+ T cells regulates chronic infection and immunopathology. *J Exp Med.* **205** (3), 669-684.

Fan XC and Steitz JA (1998). Overexpression of HuR, a nuclear-cytoplasmic shuttling protein, increases the in vivo stability of ARE-containing mRNAs. *EMBO J.* **17** (12), 3448-3460.

Fan XC, Myer VE and Steitz JA (1997). AU-rich elements target small nuclear RNAs as well as mRNAs for rapid degradation. *Genes Dev.* **11** (19), 2557-2568.

Farrell MJ, Dobson AT and Feldman LT (1991). Herpes simplex virus latency-associated transcript is a stable intron. *Proc Natl Acad Sci U S A.* **88** (3), 790-794.

Felton-Edkins ZA, Kondrashov A, Karali D, Fairley JA, Dawson CW, Arrand JR, Young LS and White RJ (2006). Epstein-Barr virus induces cellular transcription factors to allow active expression of EBER genes by RNA polymerase III. *J Biol Chem.* **281** (45), 33871-33880.

Filipowicz W, Bhattacharyya SN and Sonenberg N (2008). Mechanisms of post-transcriptional regulation by microRNAs: are the answers in sight? *Nat Rev Genet.* **9** (2), 102-114.

Flano E, Woodland DL and Blackman MA (1999). Requirement for CD4+ T cells in V beta 4+CD8+ T cell activation associated with latent murine gammaherpesvirus infection. *J Immunol.* **163** (6), 3403-3408.

Flano E, Woodland DL, Blackman MA and Doherty PC (2001). Analysis of virus-specific CD4(+) t cells during long-term gammaherpesvirus infection. *J Virol.* **75** (16), 7744-7748.

Flano E, Husain SM, Sample JT, Woodland DL and Blackman MA (2000). Latent murine gamma-herpesvirus infection is established in activated B cells, dendritic cells, and macrophages. *J Immunol.* **165** (2), 1074-1081.

Flano E, Kim IJ, Moore J, Woodland DL and Blackman MA (2003). Differential gamma-herpesvirus distribution in distinct anatomical locations and cell subsets during persistent infection in mice. *J Immunol.* **170** (7), 3828-3834.

Flano E, Hardy CL, Kim IJ, Frankling C, Coppola MA, Nguyen P, Woodland DL and Blackman MA (2004). T cell reactivity during infectious mononucleosis and persistent gammaherpesvirus infection in mice. *J Immunol.* **172** (5), 3078-3085.

Florentz C and Giege R (1995). tRNA-like Structures in Plant Viral RNAs. In: *tRNA:Structure, Biosynthesis, and Function*. D. Söll and U. RajBhandary (eds.); American Society for Microbiology, Washington, 141-163.

Fok V, Mitton-Fry RM, Grech A and Steitz JA (2006). Multiple domains of EBER 1, an Epstein-Barr virus noncoding RNA, recruit human ribosomal protein L22. *RNA.* **12** (5), 872-882.

Fowler P, Marques S, Simas JP and Efstathiou S (2003). ORF73 of murine herpesvirus-68 is critical for the establishment and maintenance of latency. *J Gen Virol.* **84** (Pt 12), 3405-3416.

Ganem D (2007). Kaposi's Sarcoma-associated Herpesvirus. In: *Fields virology*, 5th edn. Knipe DM and Howley PM (eds.); Lippincott, Williams & Wilkins, Philadelphia, 2847-2888.

Gangadharan B, Hoeve MA, Allen JE, Ebrahimi B, Rhind SM, Dutia BM and Nash AA (2008). Murine gammaherpesvirus-induced fibrosis is associated with the development of alternatively activated macrophages. *J Leukoc Biol.* **84** (1), 50-58.

Garber AC, Shu MA, Hu J and Renne R (2001). DNA binding and modulation of gene expression by the latency-associated nuclear antigen of Kaposi's sarcoma-associated herpesvirus. *J Virol.* **75** (17), 7882-7892.

Garber DA, Schaffer PA and Knipe DM (1997). A LAT-associated function reduces productive-cycle gene expression during acute infection of murine sensory neurons with herpes simplex virus type 1. *J Virol.* **71** (8), 5885-5893.

Gaspar M, Gill MB, Losing JB, May JS and Stevenson PG (2008). Multiple functions for ORF75c in murid herpesvirus-4 infection. *PLoS One.* **3** (7), e2781.

Geere HM, Ligertwood Y, Templeton KM, Bennet I, Gangadharan B, Rhind SM, Nash AA and Dutia BM (2006). The M4 gene of murine gammaherpesvirus 68 modulates latent infection. *J Gen Virol.* **87** (Pt 4), 803-807.

Geraghty RJ, Krummenacher C, Cohen GH, Eisenberg RJ and Spear PG (1998). Entry of alphaherpesviruses mediated by poliovirus receptor-related protein 1 and poliovirus receptor. *Science.* **280** (5369), 1618-1620.

Ghadge GD, Swaminathan S, Katze MG and Thimmapaya B (1991). Binding of the adenovirus VAI RNA to the interferon-induced 68-kDa protein kinase correlates with function. *Proc Natl Acad Sci U S A.* **88** (16), 7140-7144.

Ghadge GD, Malhotra P, Furtado MR, Dhar R and Thimmapaya B (1994). In vitro analysis of virus-associated RNA I (VAI RNA): inhibition of the double-stranded RNA-activated protein kinase PKR by VAI RNA mutants correlates with the in vivo phenotype and the structural integrity of the central domain. *J Virol.* **68** (7), 4137-4151.

Giege R, Frugier M and Rudinger J (1998). tRNA mimics. *Curr Opin Struct Biol.* **8** (3), 286-293.

Gill MB, Edgar R, May JS and Stevenson PG (2008). A gamma-herpesvirus glycoprotein complex manipulates actin to promote viral spread. *PLoS One.* **3** (3), e1808.

Gill MB, Gillet L, Colaco S, May JS, de Lima BD and Stevenson PG (2006). Murine gammaherpesvirus-68 glycoprotein H-glycoprotein L complex is a major target for neutralizing monoclonal antibodies. *J Gen Virol.* **87** (Pt 6), 1465-1475.

Gillet L and Stevenson PG (2007). Evidence for a multiprotein gamma-2 herpesvirus entry complex. *J Virol.* **81** (23), 13082-13091.

Gillet L, Adler H and Stevenson PG (2007a). Glycosaminoglycan interactions in murine gammaherpesvirus-68 infection. *PLoS One.* **2** (4), e347.

Gillet L, Colaco S and Stevenson PG (2008). The murid herpesvirus-4 gH/gL binds to glycosaminoglycans. *PLoS One.* **3** (2), e1669.

Gillet L, May JS and Stevenson PG (2009). In vivo importance of heparan sulfate-binding glycoproteins for murid herpesvirus-4 infection. *J Gen Virol.* **90** (Pt 3), 602-613.

Gillet L, May JS, Colaco S and Stevenson PG (2007b). Glycoprotein L disruption reveals two functional forms of the murine gammaherpesvirus 68 glycoprotein H. *J Virol.* **81** (1), 280-291.

Gilligan K, Rajadurai P, Resnick L and Raab-Traub N (1990). Epstein-Barr virus small nuclear RNAs are not expressed in permissively infected cells in AIDS-associated leukoplakia. *Proc Natl Acad Sci U S A.* **87** (22), 8790-8794.

Giordani NV, Neumann DM, Kwiatkowski DL, Bhattacharjee PS, McAnany PK, Hill JM and Bloom DC (2008). During herpes simplex virus type 1 infection

of rabbits, the ability to express the latency-associated transcript increases latent-phase transcription of lytic genes. *J Virol.* **82** (12), 6056-6060.

Giuliodori S, Percudani R, Braglia P, Ferrari R, Guffanti E, Ottonello S and Dieci G (2003). A composite upstream sequence motif potentiates tRNA gene transcription in yeast. *J Mol Biol.* **333** (1), 1-20.

Glazov EA, Horwood PF, Assavalapsakul W, Kongsuwan K, Mitchell RW, Mitter N and Mahony TJ (2010). Characterization of microRNAs encoded by the bovine herpesvirus 1 genome. *J Gen Virol.* **91** (Pt 1), 32-41.

Glickman JN, Howe JG and Steitz JA (1988). Structural analyses of EBER1 and EBER2 ribonucleoprotein particles present in Epstein-Barr virus-infected cells. *J Virol.* **62** (3), 902-911.

Godden-Kent D, Talbot SJ, Boshoff C, Chang Y, Moore P, Weiss RA and Mittnacht S (1997). The cyclin encoded by Kaposi's sarcoma-associated herpesvirus stimulates cdk6 to phosphorylate the retinoblastoma protein and histone H1. *J Virol.* **71** (6), 4193-4198.

Godshalk SE, Bhaduri-McIntosh S and Slack FJ (2008). Epstein-Barr virus-mediated dysregulation of human microRNA expression. *Cell Cycle.* **7** (22), 3595-3600.

Golembe TJ, Yong J, Battle DJ, Feng W, Wan L and Dreyfuss G (2005). Lymphotropic Herpesvirus saimiri uses the SMN complex to assemble Sm cores on its small RNAs. *Mol Cell Biol.* **25** (2), 602-611.

Gong D, Qi J, Arumugaswami V, Sun R and Deng H (2009). Identification and functional characterization of the left origin of lytic replication of murine gammaherpesvirus 68. *Virology.* **387** (2), 285-295.

Gottwein E and Cullen BR (2008). Viral and cellular microRNAs as determinants of viral pathogenesis and immunity. *Cell Host Microbe.* **3** (6), 375-387.

Gottwein E, Mukherjee N, Sachse C, Frenzel C, Majoros WH, Chi JT, Braich R, Manoharan M, Soutschek J, Ohler U and Cullen BR (2007). A viral microRNA functions as an orthologue of cellular miR-155. *Nature.* **450** (7172), 1096-1099.

Gould F, Harrison SM, Hewitt EW and Whitehouse A (2009). Kaposi's sarcoma-associated herpesvirus RTA promotes degradation of the Hey1 repressor protein through the ubiquitin proteasome pathway. *J Virol.* **83** (13), 6727-6738.

Green NJ, Grundy FJ and Henkin TM (2010). The T box mechanism: tRNA as a regulatory molecule. *FEBS Lett.* **584** (2), 318-324.

Gregory RI, Chendrimada TP, Cooch N and Shiekhattar R (2005). Human RISC couples microRNA biogenesis and posttranscriptional gene silencing. *Cell.* **123** (4), 631-640.

Gregory RI, Yan KP, Amuthan G, Chendrimada T, Doratotaj B, Cooch N and Shiekhattar R (2004). The Microprocessor complex mediates the genesis of microRNAs. *Nature.* **432** (7014), 235-240.

Greijer AE, Dekkers CA and Middeldorp JM (2000). Human cytomegalovirus virions differentially incorporate viral and host cell RNA during the assembly process. *J Virol.* **74** (19), 9078-9082.

Grey F, Meyers H, White EA, Spector DH and Nelson J (2007). A human cytomegalovirus-encoded microRNA regulates expression of multiple viral genes involved in replication. *PLoS Pathog.* **3** (11), e163.

Grey F, Antoniewicz A, Allen E, Saugstad J, McShea A, Carrington JC and Nelson J (2005). Identification and characterization of human cytomegalovirus-encoded microRNAs. *J Virol.* **79** (18), 12095-12099.

Grundhoff A and Ganem D (2003). The latency-associated nuclear antigen of Kaposi's sarcoma-associated herpesvirus permits replication of terminal repeat-containing plasmids. *J Virol.* **77** (4), 2779-2783.

Grundhoff A, Sullivan CS and Ganem D (2006). A combined computational and microarray-based approach identifies novel microRNAs encoded by human gamma-herpesviruses. *RNA.* **12** (5), 733-750.

Guasparri I, Keller SA and Cesarman E (2004). KSHV vFLIP is essential for the survival of infected lymphoma cells. *J Exp Med.* **199** (7), 993-1003.

Guerrier-Takada C, van Belkum A, Pleij CW and Altman S (1988). Novel reactions of RNAase P with a tRNA-like structure in turnip yellow mosaic virus RNA. *Cell.* **53** (2), 267-272.

Guo H, Wang L, Peng L, Zhou ZH and Deng H (2009). Open reading frame 33 of a gammaherpesvirus encodes a tegument protein essential for virion morphogenesis and egress. *J Virol.* **83** (20), 10582-10595.

Hair JR, Lyons PA, Smith KG and Efstathiou S (2007). Control of Rta expression critically determines transcription of viral and cellular genes following gammaherpesvirus infection. *J Gen Virol.* **88** (Pt 6), 1689-1697.

Hammarskjold ML and Simurda MC (1992). Epstein-Barr virus latent membrane protein transactivates the human immunodeficiency virus type 1 long terminal repeat through induction of NF-kappa B activity. *J Virol.* **66** (11), 6496-6501.

Han J, Lee Y, Yeom KH, Kim YK, Jin H and Kim VN (2004). The Drosha-DGCR8 complex in primary microRNA processing. *Genes Dev.* **18** (24), 3016-3027.

Han J, Lee Y, Yeom KH, Nam JW, Heo I, Rhee JK, Sohn SY, Cho Y, Zhang BT and Kim VN (2006). Molecular basis for the recognition of primary microRNAs by the Drosha-DGCR8 complex. *Cell.* **125** (5), 887-901.

Harada F, Sawyer RC and Dahlberg JE (1975). A primer ribonucleic acid for initiation of in vitro Rous sarcarcoma virus deoxyribonucleic acid synthesis. *J Biol Chem.* **250** (9), 3487-3497.

Harada S and Kieff E (1997). Epstein-Barr virus nuclear protein LP stimulates EBNA-2 acidic domain-mediated transcriptional activation. *J Virol.* **71** (9), 6611-6618.

Harding HP, Novoa I, Zhang Y, Zeng H, Wek R, Schapira M and Ron D (2000). Regulated translation initiation controls stress-induced gene expression in mammalian cells. *Mol Cell.* **6** (5), 1099-1108.

Hardy CL, Silins SL, Woodland DL and Blackman MA (2000). Murine gamma-herpesvirus infection causes V(beta)4-specific CDR3-restricted clonal expansions within CD8(+) peripheral blood T lymphocytes. *Int Immunol.* **12** (8), 1193-1204.

Hayward GS (1999). KSHV strains: the origins and global spread of the virus. *Semin Cancer Biol.* **9** (3), 187-199.

Heldwein EE and Krummenacher C (2008). Entry of herpesviruses into mammalian cells. *Cell Mol Life Sci.* **65** (11), 1653-1668.

Henke JI, Goergen D, Zheng J, Song Y, Schuttler CG, Fehr C, Junemann C and Niepmann M (2008). microRNA-122 stimulates translation of hepatitis C virus RNA. *EMBO J.* **27** (24), 3300-3310.

Henle G, Henle W and Diehl V (1968). Relation of Burkitt's tumor-associated herpes-ytpe virus to infectious mononucleosis. *Proc Natl Acad Sci U S A.* **59** (1), 94-101.

Herold BC, WuDunn D, Soltys N and Spear PG (1991). Glycoprotein C of herpes simplex virus type 1 plays a principal role in the adsorption of virus to cells and in infectivity. *J Virol.* **65** (3), 1090-1098.

Herold BC, Visalli RJ, Susmarski N, Brandt CR and Spear PG (1994). Glycoprotein C-independent binding of herpes simplex virus to cells requires cell surface heparan sulphate and glycoprotein B. *J Gen Virol.* **75 (Pt 6)**, 1211-1222.

Herskowitz J, Jacoby MA and Speck SH (2005). The murine gammaherpesvirus 68 M2 gene is required for efficient reactivation from latently infected B cells. *J Virol.* **79** (4), 2261-2273.

Hill JM, Sedarati F, Javier RT, Wagner EK and Stevens JG (1990). Herpes simplex virus latent phase transcription facilitates in vivo reactivation. *Virology.* **174** (1), 117-125.

Hinnebusch AG (2005). Translational regulation of GCN4 and the general amino acid control of yeast. *Annu Rev Microbiol.* **59**, 407-450.

Hock J, Weinmann L, Ender C, Rudel S, Kremmer E, Raabe M, Urlaub H and Meister G (2007). Proteomic and functional analysis of Argonaute-containing mRNA-protein complexes in human cells. *EMBO Rep.* **8** (11), 1052-1060.

Holley RW, Apgar J, Everett GA, Madison JT, Marquisee M, Merrill SH, Penswick JR and Zamir A (1965). Structure of a Ribonucleic Acid. *Science.* **147**, 1462-1465.

Honess RW and Roizman B (1974). Regulation of herpesvirus macromolecular synthesis. I. Cascade regulation of the synthesis of three groups of viral proteins. *J Virol.* **14** (1), 8-19.

Howe JG and Shu MD (1988). Isolation and characterization of the genes for two small RNAs of herpesvirus papio and their comparison with Epstein-Barr virus-encoded EBER RNAs. *J Virol.* **62** (8), 2790-2798.

Howe JG and Shu MD (1989). Epstein-Barr virus small RNA (EBER) genes: unique transcription units that combine RNA polymerase II and III promoter elements. *Cell.* **57** (5), 825-834.

Hu J, Garber AC and Renne R (2002). The latency-associated nuclear antigen of Kaposi's sarcoma-associated herpesvirus supports latent DNA replication in dividing cells. *J Virol.* **76** (22), 11677-11687.

Hughes DJ, Kipar A, Milligan SG, Cunningham C, Sanders M, Quail MA, Rajandream MA, Efstathiou S, Bowden RJ, Chastel C, Bennett M, Sample JT, Barrell B, Davison AJ and Stewart JP (2009). Characterization of a novel wood mouse virus related to murid herpesvirus 4. *J Gen Virol.*

Hull MW, Erickson J, Johnston M and Engelke DR (1994). tRNA genes as transcriptional repressor elements. *Mol Cell Biol.* **14** (2), 1266-1277.

Husain SM, Usherwood EJ, Dyson H, Coleclough C, Coppola MA, Woodland DL, Blackman MA, Stewart JP and Sample JT (1999). Murine gammaherpesvirus M2 gene is latency-associated and its protein a target for CD8(+) T lymphocytes. *Proc Natl Acad Sci U S A.* **96** (13), 7508-7513.

Hussain M, Taft RJ and Asgari S (2008). An insect virus-encoded microRNA regulates viral replication. *J Virol.* **82** (18), 9164-9170.

Hutvagner G, McLachlan J, Pasquinelli AE, Balint E, Tuschl T and Zamore PD (2001). A cellular function for the RNA-interference enzyme Dicer in the maturation of the let-7 small temporal RNA. *Science.* **293** (5531), 834-838.

Hwang S, Kim KS, Flano E, Wu TT, Tong LM, Park AN, Song MJ, Sanchez DJ, O'Connell RM, Cheng G and Sun R (2009). Conserved herpesviral kinase

promotes viral persistence by inhibiting the IRF-3-mediated type I interferon response. *Cell Host Microbe.* **5** (2), 166-178.

Ibanez-Ventoso C, Vora M and Driscoll M (2008). Sequence relationships among C. elegans, D. melanogaster and human microRNAs highlight the extensive conservation of microRNAs in biology. *PLoS One.* **3** (7), e2818.

Iorio MV and Croce CM (2009). MicroRNAs in cancer: small molecules with a huge impact. *J Clin Oncol.* **27** (34), 5848-5856.

Iwakiri D, Sheen TS, Chen JY, Huang DP and Takada K (2005). Epstein-Barr virus-encoded small RNA induces insulin-like growth factor 1 and supports growth of nasopharyngeal carcinoma-derived cell lines. *Oncogene.* **24** (10), 1767-1773.

Iwakiri D, Zhou L, Samanta M, Matsumoto M, Ebihara T, Seya T, Imai S, Fujieda M, Kawa K and Takada K (2009). Epstein-Barr virus (EBV)-encoded small RNA is released from EBV-infected cells and activates signaling from Toll-like receptor 3. *J Exp Med.* **206** (10), 2091-2099.

Jaber T, Henderson G, Li S, Perng GC, Carpenter D, Wechsler SL and Jones C (2009). Identification of a novel herpes simplex virus type 1 transcript and protein (AL3) expressed during latency. *J Gen Virol.* **90** (Pt 10), 2342-2352.

Jacoby MA, Virgin HWt and Speck SH (2002). Disruption of the M2 gene of murine gammaherpesvirus 68 alters splenic latency following intranasal, but not intraperitoneal, inoculation. *J Virol.* **76** (4), 1790-1801.

Jain V, Kumar M and Chatterji D (2006). ppGpp: stringent response and survival. *J Microbiol.* **44** (1), 1-10.

Jensen KK, Chen SC, Hipkin RW, Wiekowski MT, Schwarz MA, Chou CC, Simas JP, Alcami A and Lira SA (2003). Disruption of CCL21-induced chemotaxis in vitro and in vivo by M3, a chemokine-binding protein encoded by murine gammaherpesvirus 68. *J Virol.* **77** (1), 624-630.

Jenson HB (2003). Human herpesvirus 8 infection. *Curr Opin Pediatr.* **15** (1), 85-91.

Jiang HY, Wek SA, McGrath BC, Lu D, Hai T, Harding HP, Wang X, Ron D, Cavener DR and Wek RC (2004). Activating transcription factor 3 is integral to the eukaryotic initiation factor 2 kinase stress response. *Mol Cell Biol.* **24** (3), 1365-1377.

Jiang M, Mak J, Ladha A, Cohen E, Klein M, Rovinski B and Kleiman L (1993). Identification of tRNAs incorporated into wild-type and mutant human immunodeficiency virus type 1. *J Virol.* **67** (6), 3246-3253.

Joo CH, Shin YC, Gack M, Wu L, Levy D and Jung JU (2007). Inhibition of interferon regulatory factor 7 (IRF7)-mediated interferon signal transduction

by the Kaposi's sarcoma-associated herpesvirus viral IRF homolog vIRF3. *J Virol.* **81** (15), 8282-8292.

Jopling CL, Schutz S and Sarnow P (2008). Position-dependent function for a tandem microRNA miR-122-binding site located in the hepatitis C virus RNA genome. *Cell Host Microbe.* **4** (1), 77-85.

Jopling CL, Yi M, Lancaster AM, Lemon SM and Sarnow P (2005). Modulation of hepatitis C virus RNA abundance by a liver-specific MicroRNA. *Science.* **309** (5740), 1577-1581.

Joseph AM, Babcock GJ and Thorley-Lawson DA (2000). Cells expressing the Epstein-Barr virus growth program are present in and restricted to the naive B-cell subset of healthy tonsils. *J Virol.* **74** (21), 9964-9971.

Kanda T, Otter M and Wahl GM (2001). Coupling of mitotic chromosome tethering and replication competence in epstein-barr virus-based plasmids. *Mol Cell Biol.* **21** (10), 3576-3588.

Kang W, Mukerjee R and Fraser NW (2003). Establishment and maintenance of HSV latent infection is mediated through correct splicing of the LAT primary transcript. *Virology.* **312** (1), 233-244.

Kang W, Mukerjee R, Gartner JJ, Hatzigeorgiou AG, Sandri-Goldin RM and Fraser NW (2006). Characterization of a spliced exon product of herpes simplex type-1 latency-associated transcript in productively infected cells. *Virology.* **356** (1-2), 106-114.

Kaposi M (1872). Idiopathisches multiples pigmentsarcom der haut. *Arch. Dermatol. Syphillis.* **4**, 265-273.

Katano H, Sato Y, Kurata T, Mori S and Sata T (2000). Expression and localization of human herpesvirus 8-encoded proteins in primary effusion lymphoma, Kaposi's sarcoma, and multicentric Castleman's disease. *Virology.* **269** (2), 335-344.

Kaul R, Verma SC and Robertson ES (2007). Protein complexes associated with the Kaposi's sarcoma-associated herpesvirus-encoded LANA. *Virology.* **364** (2), 317-329.

Kelly GL, Long HM, Stylianou J, Thomas WA, Leese A, Bell AI, Bornkamm GW, Mautner J, Rickinson AB and Rowe M (2009). An Epstein-Barr virus anti-apoptotic protein constitutively expressed in transformed cells and implicated in burkitt lymphomagenesis: the Wp/BHRF1 link. *PLoS Pathog.* **5** (3), e1000341.

Kerr BM, Lear AL, Rowe M, Croom-Carter D, Young LS, Rookes SM, Gallimore PH and Rickinson AB (1992). Three transcriptionally distinct forms of Epstein-Barr virus latency in somatic cell hybrids: cell phenotype dependence of virus promoter usage. *Virology.* **187** (1), 189-201.

Khvorova A, Reynolds A and Jayasena SD (2003). Functional siRNAs and miRNAs exhibit strand bias. *Cell.* **115** (2), 209-216.

Khwaja FW, Reed MS, Olson JJ, Schmotzer BJ, Gillespie GY, Guha A, Groves MD, Kesari S, Pohl J and Van Meir EG (2007). Proteomic identification of biomarkers in the cerebrospinal fluid (CSF) of astrocytoma patients. *J Proteome Res.* **6** (2), 559-570.

Kieff ED and Rickinson AB (2007). Epstein-Barr Virus and Its Replication. In: *Fields virology*, 5th edn. Knipe DM and Howley PM (eds.); Lippincott, Williams & Wilkins, Philadelphia, 2603-2654.

Kilberg MS, Pan YX, Chen H and Leung-Pineda V (2005). Nutritional control of gene expression: how mammalian cells respond to amino acid limitation. *Annu Rev Nutr.* **25**, 59-85.

Kim DH, Saetrom P, Snove O, Jr. and Rossi JJ (2008). MicroRNA-directed transcriptional gene silencing in mammalian cells. *Proc Natl Acad Sci U S A.* **105** (42), 16230-16235.

Kim IJ, Flano E, Woodland DL and Blackman MA (2002). Antibody-mediated control of persistent gamma-herpesvirus infection. *J Immunol.* **168** (8), 3958-3964.

Kim IJ, Flano E, Woodland DL, Lund FE, Randall TD and Blackman MA (2003). Maintenance of long term gamma-herpesvirus B cell latency is dependent on CD40-mediated development of memory B cells. *J Immunol.* **171** (2), 886-892.

Kim VN, Han J and Siomi MC (2009). Biogenesis of small RNAs in animals. *Nat Rev Mol Cell Biol.* **10** (2), 126-139.

Kirshner JR, Lukac DM, Chang J and Ganem D (2000). Kaposi's sarcoma-associated herpesvirus open reading frame 57 encodes a posttranscriptional regulator with multiple distinct activities. *J Virol.* **74** (8), 3586-3597.

Kitajewski J, Schneider RJ, Safer B, Munemitsu SM, Samuel CE, Thimmappaya B and Shenk T (1986). Adenovirus VAI RNA antagonizes the antiviral action of interferon by preventing activation of the interferon-induced eIF-2 alpha kinase. *Cell.* **45** (2), 195-200.

Klein G (1983). Specific chromosomal translocations and the genesis of B-cell-derived tumors in mice and men. *Cell.* **32** (2), 311-315.

Kliche S, Nagel W, Kremmer E, Atzler C, Ege A, Knorr T, Koszinowski U, Kolanus W and Haas J (2001). Signaling by human herpesvirus 8 kaposin A through direct membrane recruitment of cytohesin-1. *Mol Cell.* **7** (4), 833-843.

Klose RJ and Zhang Y (2007). Regulation of histone methylation by demethylimination and demethylation. *Nat Rev Mol Cell Biol.* **8** (4), 307-318.

Knipe DM and Cliffe A (2008). Chromatin control of herpes simplex virus lytic and latent infection. *Nat Rev Microbiol.* **6** (3), 211-221.

Komano J, Maruo S, Kurozumi K, Oda T and Takada K (1999). Oncogenic role of Epstein-Barr virus-encoded RNAs in Burkitt's lymphoma cell line Akata. *J Virol.* **73** (12), 9827-9831.

Krause PR, Croen KD, Straus SE and Ostrove JM (1988). Detection and preliminary characterization of herpes simplex virus type 1 transcripts in latently infected human trigeminal ganglia. *J Virol.* **62** (12), 4819-4823.

Krug LT, Collins CM, Gargano LM and Speck SH (2009). NF-kappaB p50 plays distinct roles in the establishment and control of murine gammaherpesvirus 68 latency. *J Virol.* **83** (10), 4732-4748.

Ku B, Woo JS, Liang C, Lee KH, Hong HS, E X, Kim KS, Jung JU and Oh BH (2008). Structural and biochemical bases for the inhibition of autophagy and apoptosis by viral BCL-2 of murine gamma-herpesvirus 68. *PLoS Pathog.* **4** (2), e25.

Laing KG, Elia A, Jeffrey I, Matys V, Tilleray VJ, Souberbielle B and Clemens MJ (2002). In vivo effects of the Epstein-Barr virus small RNA EBER-1 on protein synthesis and cell growth regulation. *Virology.* **297** (2), 253-269.

Laman H, Coverley D, Krude T, Laskey R and Jones N (2001). Viral cyclin-cyclin-dependent kinase 6 complexes initiate nuclear DNA replication. *Mol Cell Biol.* **21** (2), 624-635.

Lambeth LS, Yao Y, Smith LP, Zhao Y and Nair V (2009). MicroRNAs 221 and 222 target p27Kip1 in Marek's disease virus-transformed tumour cell line MSB-1. *J Gen Virol.* **90** (Pt 5), 1164-1171.

Lan K, Kuppers DA, Verma SC and Robertson ES (2004). Kaposi's sarcoma-associated herpesvirus-encoded latency-associated nuclear antigen inhibits lytic replication by targeting Rta: a potential mechanism for virus-mediated control of latency. *J Virol.* **78** (12), 6585-6594.

Landthaler M, Yalcin A and Tuschl T (2004). The human DiGeorge syndrome critical region gene 8 and Its D. melanogaster homolog are required for miRNA biogenesis. *Curr Biol.* **14** (23), 2162-2167.

Laux G, Perricaudet M and Farrell PJ (1988). A spliced Epstein-Barr virus gene expressed in immortalized lymphocytes is created by circularization of the linear viral genome. *EMBO J.* **7** (3), 769-774.

Lee I, Ajay SS, Yook JI, Kim HS, Hong SH, Kim NH, Dhanasekaran SM, Chinnaiyan AM and Athey BD (2009a). New class of microRNA targets containing simultaneous 5'-UTR and 3'-UTR interaction sites. *Genome Res.* **19** (7), 1175-1183.

Lee KS, Groshong SD, Cool CD, Kleinschmidt-DeMasters BK and van Dyk LF (2009b). Murine gammaherpesvirus 68 infection of IFNgamma unresponsive mice: a small animal model for gammaherpesvirus-associated B-cell lymphoproliferative disease. *Cancer Res.* **69** (13), 5481-5489.

Lee RC, Feinbaum RL and Ambros V (1993). The C. elegans heterochronic gene lin-4 encodes small RNAs with antisense complementarity to lin-14. *Cell.* **75** (5), 843-854.

Lee SI and Steitz JA (1990). Herpesvirus saimiri U RNAs are expressed and assembled into ribonucleoprotein particles in the absence of other viral genes. *J Virol.* **64** (8), 3905-3915.

Lee SI, Murthy SC, Trimble JJ, Desrosiers RC and Steitz JA (1988). Four novel U RNAs are encoded by a herpesvirus. *Cell.* **54** (5), 599-607.

Lee Y, Jeon K, Lee JT, Kim S and Kim VN (2002). MicroRNA maturation: stepwise processing and subcellular localization. *EMBO J.* **21** (17), 4663-4670.

Lee Y, Hur I, Park SY, Kim YK, Suh MR and Kim VN (2006). The role of PACT in the RNA silencing pathway. *EMBO J.* **25** (3), 522-532.

Lee Y, Kim M, Han J, Yeom KH, Lee S, Baek SH and Kim VN (2004). MicroRNA genes are transcribed by RNA polymerase II. *EMBO J.* **23** (20), 4051-4060.

Lee Y, Ahn C, Han J, Choi H, Kim J, Yim J, Lee J, Provost P, Radmark O, Kim S and Kim VN (2003). The nuclear RNase III Drosha initiates microRNA processing. *Nature.* **425** (6956), 415-419.

Lei M, Liu Y and Samuel CE (1998). Adenovirus VAI RNA antagonizes the RNA-editing activity of the ADAR adenosine deaminase. *Virology.* **245** (2), 188-196.

Lei X, Bai Z, Ye F, Xie J, Kim CG, Huang Y and Gao SJ (2010). Regulation of NF-kappaB inhibitor IkappaBalpha and viral replication by a KSHV microRNA. *Nat Cell Biol.* **12** (2), 193-199.

Leib DA, Bogard CL, Kosz-Vnenchak M, Hicks KA, Coen DM, Knipe DM and Schaffer PA (1989). A deletion mutant of the latency-associated transcript of herpes simplex virus type 1 reactivates from the latent state with reduced frequency. *J Virol.* **63** (7), 2893-2900.

Lerner MR, Andrews NC, Miller G and Steitz JA (1981). Two small RNAs encoded by Epstein-Barr virus and complexed with protein are precipitated by antibodies from patients with systemic lupus erythematosus. *Proc Natl Acad Sci U S A.* **78** (2), 805-809.

Li J, Steen H and Gygi SP (2003). Protein profiling with cleavable isotope-coded affinity tag (cICAT) reagents: the yeast salinity stress response. *Mol Cell Proteomics.* **2** (11), 1198-1204.

Li YH, Tao PZ, Liu YZ and Jiang JD (2004). Geldanamycin, a ligand of heat shock protein 90, inhibits the replication of herpes simplex virus type 1 in vitro. *Antimicrob Agents Chemother.* **48** (3), 867-872.

Liang X, Shin YC, Means RE and Jung JU (2004). Inhibition of interferon-mediated antiviral activity by murine gammaherpesvirus 68 latency-associated M2 protein. *J Virol.* **78** (22), 12416-12427.

Liang X, Collins CM, Mendel JB, Iwakoshi NN and Speck SH (2009). Gammaherpesvirus-driven plasma cell differentiation regulates virus reactivation from latently infected B lymphocytes. *PLoS Pathog.* **5** (11), e1000677.

Liang X, Pickering MT, Cho NH, Chang H, Volkert MR, Kowalik TF and Jung JU (2006). Deregulation of DNA damage signal transduction by herpesvirus latency-associated M2. *J Virol.* **80** (12), 5862-5874.

Liao HJ, Kobayashi R and Mathews MB (1998). Activities of adenovirus virus-associated RNAs: purification and characterization of RNA binding proteins. *Proc Natl Acad Sci U S A.* **95** (15), 8514-8519.

Ling PD, Tan J, Sewatanon J and Peng R (2008). Murine gammaherpesvirus 68 open reading frame 75c tegument protein induces the degradation of PML and is essential for production of infectious virus. *J Virol.* **82** (16), 8000-8012.

Liu J, Carmell MA, Rivas FV, Marsden CG, Thomson JM, Song JJ, Hammond SM, Joshua-Tor L and Hannon GJ (2004). Argonaute2 is the catalytic engine of mammalian RNAi. *Science.* **305** (5689), 1437-1441.

Liu L, Eby MT, Rathore N, Sinha SK, Kumar A and Chaudhary PM (2002). The human herpes virus 8-encoded viral FLICE inhibitory protein physically associates with and persistently activates the Ikappa B kinase complex. *J Biol Chem.* **277** (16), 13745-13751.

Lo AK, To KF, Lo KW, Lung RW, Hui JW, Liao G and Hayward SD (2007). Modulation of LMP1 protein expression by EBV-encoded microRNAs. *Proc Natl Acad Sci U S A.* **104** (41), 16164-16169.

Lu F, Weidmer A, Liu CG, Volinia S, Croce CM and Lieberman PM (2008). Epstein-Barr virus-induced miR-155 attenuates NF-kappaB signaling and stabilizes latent virus persistence. *J Virol.* **82** (21), 10436-10443.

Lu S and Cullen BR (2004). Adenovirus VA1 noncoding RNA can inhibit small interfering RNA and MicroRNA biogenesis. *J Virol.* **78** (23), 12868-12876.

Lubyova B and Pitha PM (2000). Characterization of a novel human herpesvirus 8-encoded protein, vIRF-3, that shows homology to viral and cellular interferon regulatory factors. *J Virol.* **74** (17), 8194-8201.

Lubyova B, Kellum MJ, Frisancho AJ and Pitha PM (2004). Kaposi's sarcoma-associated herpesvirus-encoded vIRF-3 stimulates the transcriptional activity of cellular IRF-3 and IRF-7. *J Biol Chem.* **279** (9), 7643-7654.

Lund E and Dahlberg JE (2006). Substrate selectivity of exportin 5 and Dicer in the biogenesis of microRNAs. *Cold Spring Harb Symp Quant Biol.* **71**, 59-66.

Lund E, Guttinger S, Calado A, Dahlberg JE and Kutay U (2004). Nuclear export of microRNA precursors. *Science.* **303** (5654), 95-98.

Lung RW, Tong JH, Sung YM, Leung PS, Ng DC, Chau SL, Chan AW, Ng EK, Lo KW and To KF (2009). Modulation of LMP2A expression by a newly identified Epstein-Barr virus-encoded microRNA miR-BART22. *Neoplasia.* **11** (11), 1174-1184.

Lybarger L, Wang X, Harris MR, Virgin HWt and Hansen TH (2003). Virus subversion of the MHC class I peptide-loading complex. *Immunity.* **18** (1), 121-130.

Ma Y and Mathews MB (1993). Comparative analysis of the structure and function of adenovirus virus-associated RNAs. *J Virol.* **67** (11), 6605-6617.

Ma Y and Mathews MB (1996). Structure, function, and evolution of adenovirus-associated RNA: a phylogenetic approach. *J Virol.* **70** (8), 5083-5099.

Mackett M, Stewart JP, de VPS, Chee M, Efstathiou S, Nash AA and Arrand JR (1997). Genetic content and preliminary transcriptional analysis of a representative region of murine gammaherpesvirus 68. *J Gen Virol.* **78 (Pt 6)**, 1425-1433.

Macrae AI, Dutia BM, Milligan S, Brownstein DG, Allen DJ, Mistrikova J, Davison AJ, Nash AA and Stewart JP (2001). Analysis of a novel strain of murine gammaherpesvirus reveals a genomic locus important for acute pathogenesis. *J Virol.* **75** (11), 5315-5327.

Macrae AI, Usherwood EJ, Husain SM, Flano E, Kim IJ, Woodland DL, Nash AA, Blackman MA, Sample JT and Stewart JP (2003). Murid herpesvirus 4 strain 68 M2 protein is a B-cell-associated antigen important for latency but not lymphocytosis. *J Virol.* **77** (17), 9700-9709.

Mador N, Goldenberg D, Cohen O, Panet A and Steiner I (1998). Herpes simplex virus type 1 latency-associated transcripts suppress viral replication and reduce immediate-early gene mRNA levels in a neuronal cell line. *J Virol.* **72** (6), 5067-5075.

Madureira PA, Matos P, Soeiro I, Dixon LK, Simas JP and Lam EW (2005). Murine gamma-herpesvirus 68 latency protein M2 binds to Vav signaling proteins and inhibits B-cell receptor-induced cell cycle arrest and apoptosis in WEHI-231 B cells. *J Biol Chem.* **280** (45), 37310-37318.

Mahajan VS, Drake A and Chen J (2009). Virus-specific host miRNAs: antiviral defenses or promoters of persistent infection? *Trends Immunol.* **30** (1), 1-7.

Maniataki E and Mourelatos Z (2005). A human, ATP-independent, RISC assembly machine fueled by pre-miRNA. *Genes Dev.* **19** (24), 2979-2990.

Marcos-Villar L, Lopitz-Otsoa F, Gallego P, Munoz-Fontela C, Gonzalez-Santamaria J, Campagna M, Shou-Jiang G, Rodriguez MS and Rivas C (2009). Kaposi's sarcoma-associated herpesvirus protein LANA2 disrupts PML oncogenic domains and inhibits PML-mediated transcriptional repression of the survivin gene. *J Virol.* **83** (17), 8849-8858.

Marques S, Alenquer M, Stevenson PG and Simas JP (2008). A single CD8+ T cell epitope sets the long-term latent load of a murid herpesvirus. *PLoS Pathog.* **4** (10), e1000177.

Marques S, Efstathiou S, Smith KG, Haury M and Simas JP (2003). Selective gene expression of latent murine gammaherpesvirus 68 in B lymphocytes. *J Virol.* **77** (13), 7308-7318.

Marquet R, Isel C, Ehresmann C and Ehresmann B (1995). tRNAs as primer of reverse transcriptases. *Biochimie.* **77** (1-2), 113-124.

Marshall L, Kenneth NS and White RJ (2008). Elevated tRNA(iMet) synthesis can drive cell proliferation and oncogenic transformation. *Cell.* **133** (1), 78-89.

Martin AP, Canasto-Chibuque C, Shang L, Rollins BJ and Lira SA (2006). The chemokine decoy receptor M3 blocks CC chemokine ligand 2 and CXC chemokine ligand 13 function in vivo. *J Immunol.* **177** (10), 7296-7302.

Martin DF, Kuppermann BD, Wolitz RA, Palestine AG, Li H and Robinson CA (1999). Oral ganciclovir for patients with cytomegalovirus retinitis treated with a ganciclovir implant. Roche Ganciclovir Study Group. *N Engl J Med.* **340** (14), 1063-1070.

Martinez-Guzman D, Rickabaugh T, Wu TT, Brown H, Cole S, Song MJ, Tong L and Sun R (2003). Transcription program of murine gammaherpesvirus 68. *J Virol.* **77** (19), 10488-10503.

Matsuda D and Dreher TW (2004). The tRNA-like structure of Turnip yellow mosaic virus RNA is a 3'-translational enhancer. *Virology.* **321** (1), 36-46.

Matsuda D, Yoshinari S and Dreher TW (2004). eEF1A binding to aminoacylated viral RNA represses minus strand synthesis by TYMV RNA-dependent RNA polymerase. *Virology.* **321** (1), 47-56.

Matta H, Surabhi RM, Zhao J, Punj V, Sun Q, Schamus S, Mazzacurati L and Chaudhary PM (2007). Induction of spindle cell morphology in human vascular endothelial cells by human herpesvirus 8-encoded viral FLICE inhibitory protein K13. *Oncogene.* **26** (11), 1656-1660.

Matta H, Punj V, Schamus S, Mazzacurati L, Chen AM, Song R, Yang T and Chaudhary PM (2008). A nuclear role for Kaposi's sarcoma-associated herpesvirus-encoded K13 protein in gene regulation. *Oncogene.* **27** (39), 5243-5253.

May JS, Walker J, Colaco S and Stevenson PG (2005a). The murine gammaherpesvirus 68 ORF27 gene product contributes to intercellular viral spread. *J Virol.* **79** (8), 5059-5068.

May JS, de Lima BD, Colaco S and Stevenson PG (2005b). Intercellular gamma-herpesvirus dissemination involves co-ordinated intracellular membrane protein transport. *Traffic.* **6** (9), 780-793.

McCormick C and Ganem D (2005). The kaposin B protein of KSHV activates the p38/MK2 pathway and stabilizes cytokine mRNAs. *Science.* **307** (5710), 739-741.

McFarlane RJ and Whitehall SK (2009). tRNA genes in eukaryotic genome organization and reorganization. *Cell Cycle.* **8** (19), 3102-3106.

McGeoch DJ, Rixon FJ and Davison AJ (2006). Topics in herpesvirus genomics and evolution. *Virus Res.* **117** (1), 90-104.

McKenna SA, Lindhout DA, Shimoike T, Aitken CE and Puglisi JD (2007). Viral dsRNA inhibitors prevent self-association and autophosphorylation of PKR. *J Mol Biol.* **372** (1), 103-113.

Meinnel T (1995). Aminoacyl-tRNA Synthetases: Occurrence, Structure, and Function In: *tRNA:Structure, Biosynthesis, and Function*. D. Söll and U. RajBhandary (eds.); American Society for Microbiology, Washington, 251-290.

Mettenleiter TC, Klupp BG and Granzow H (2006). Herpesvirus assembly: a tale of two membranes. *Curr Opin Microbiol.* **9** (4), 423-429.

Mettenleiter TC, Klupp BG and Granzow H (2009). Herpesvirus assembly: an update. *Virus Res.* **143** (2), 222-234.

Milho R, Smith CM, Marques S, Alenquer M, May JS, Gillet L, Gaspar M, Efstathiou S, Simas JP and Stevenson PG (2009). In vivo imaging of murid herpesvirus-4 infection. *J Gen Virol.* **90** (Pt 1), 21-32.

Miller CL, Lee JH, Kieff E and Longnecker R (1994). An integral membrane protein (LMP2) blocks reactivation of Epstein-Barr virus from latency following surface immunoglobulin crosslinking. *Proc Natl Acad Sci U S A.* **91** (2), 772-776.

MiRBase (2010), 'MiRBase', (updated Sept 2009) <http://www.mirbase.org/>, accessed 290110.

Mistrikova J, Rajcani J, Mrmusova M and Oravcova I (1996). Chronic infection of Balb/c mice with murine herpesvirus 72 is associated with neoplasm development. *Acta Virol.* **40** (5-6), 297-301.

Miyashita EM, Yang B, Babcock GJ and Thorley-Lawson DA (1997). Identification of the site of Epstein-Barr virus persistence in vivo as a resting B cell. *J Virol.* **71** (7), 4882-4891.

Mocarski ES, Shenk T and Pass RF (2007). Cytomegaloviruses. In: *Fields virology*, 5th edn. Knipe DM and Howley PM (eds.); Lippincott, Williams & Wilkins, Philadelphia, 2702-2772.

Montgomery RI, Warner MS, Lum BJ and Spear PG (1996). Herpes simplex virus-1 entry into cells mediated by a novel member of the TNF/NGF receptor family. *Cell.* **87** (3), 427-436.

Moore PS and Chang Y (2001). Molecular virology of Kaposi's sarcoma-associated herpesvirus. *Philos Trans R Soc Lond B Biol Sci.* **356** (1408), 499-516.

Moorman NJ, Virgin HWt and Speck SH (2003a). Disruption of the gene encoding the gammaHV68 v-GPCR leads to decreased efficiency of reactivation from latency. *Virology.* **307** (2), 179-190.

Moorman NJ, Willer DO and Speck SH (2003b). The gammaherpesvirus 68 latency-associated nuclear antigen homolog is critical for the establishment of splenic latency. *J Virol.* **77** (19), 10295-10303.

Moorman NJ, Lin CY and Speck SH (2004). Identification of candidate gammaherpesvirus 68 genes required for virus replication by signature-tagged transposon mutagenesis. *J Virol.* **78** (19), 10282-10290.

Mora AL, Woods CR, Garcia A, Xu J, Rojas M, Speck SH, Roman J, Brigham KL and Stecenko AA (2005). Lung infection with gamma-herpesvirus induces progressive pulmonary fibrosis in Th2-biased mice. *Am J Physiol Lung Cell Mol Physiol.* **289** (5), L711-721.

Morlando M, Ballarino M, Gromak N, Pagano F, Bozzoni I and Proudfoot NJ (2008). Primary microRNA transcripts are processed co-transcriptionally. *Nat Struct Mol Biol.* **15** (9), 902-909.

Mosialos G, Birkenbach M, Yalamanchili R, VanArsdale T, Ware C and Kieff E (1995). The Epstein-Barr virus transforming protein LMP1 engages signaling proteins for the tumor necrosis factor receptor family. *Cell.* **80** (3), 389-399.

Moss SE and Morgan RO (2004). The annexins. *Genome Biol.* **5** (4), 219.

Motsch N, Pfuhl T, Mrazek J, Barth S and Grasser FA (2007). Epstein-Barr virus-encoded latent membrane protein 1 (LMP1) induces the expression of the cellular microRNA miR-146a. *RNA Biol.* **4** (3), 131-137.

Muralidhar S, Veytsmann G, Chandran B, Ablashi D, Doniger J and Rosenthal LJ (2000). Characterization of the human herpesvirus 8 (Kaposi's sarcoma-associated herpesvirus) oncogene, kaposin (ORF K12). *J Clin Virol.* **16** (3), 203-213.

Muralidhar S, Pumfery AM, Hassani M, Sadaie MR, Kishishita M, Brady JN, Doniger J, Medveczky P and Rosenthal LJ (1998). Identification of kaposin (open reading frame K12) as a human herpesvirus 8 (Kaposi's sarcoma-associated herpesvirus) transforming gene. *J Virol.* **72** (6), 4980-4988.

Murphy E, Vanicek J, Robins H, Shenk T and Levine AJ (2008). Suppression of immediate-early viral gene expression by herpesvirus-coded microRNAs: implications for latency. *Proc Natl Acad Sci U S A.* **105** (14), 5453-5458.

Murthy S, Kamine J and Desrosiers RC (1986). Viral-encoded small RNAs in herpes virus saimiri induced tumors. *EMBO J.* **5** (7), 1625-1632.

Murthy SC, Trimble JJ and Desrosiers RC (1989). Deletion mutants of herpesvirus saimiri define an open reading frame necessary for transformation. *J Virol.* **63** (8), 3307-3314.

Myer VE, Lee SI and Steitz JA (1992). Viral small nuclear ribonucleoproteins bind a protein implicated in messenger RNA destabilization. *Proc Natl Acad Sci U S A.* **89** (4), 1296-1300.

Myer VE, Fan XC and Steitz JA (1997). Identification of HuR as a protein implicated in AUUUA-mediated mRNA decay. *EMBO J.* **16** (8), 2130-2139.

Nachmani D, Stern-Ginossar N, Sarid R and Mandelboim O (2009). Diverse herpesvirus microRNAs target the stress-induced immune ligand MICB to escape recognition by natural killer cells. *Cell Host Microbe.* **5** (4), 376-385.

Naito J, Mukerjee R, Mott KR, Kang W, Osorio N, Fraser NW and Perng GC (2005). Identification of a protein encoded in the herpes simplex virus type 1 latency associated transcript promoter region. *Virus Res.* **108** (1-2), 101-110.

Nanbo A, Yoshiyama H and Takada K (2005). Epstein-Barr virus-encoded poly(A)-RNA confers resistance to apoptosis mediated through Fas by blocking the PKR pathway in human epithelial intestine 407 cells. *J Virol.* **79** (19), 12280-12285.

Nanbo A, Inoue K, Adachi-Takasawa K and Takada K (2002). Epstein-Barr virus RNA confers resistance to interferon-alpha-induced apoptosis in Burkitt's lymphoma. *Embo J.* **21** (5), 954-965.

Nash AA, Dutia BM, Stewart JP and Davison AJ (2001). Natural history of murine gamma-herpesvirus infection. *Philos Trans R Soc Lond B Biol Sci.* **356** (1408), 569-579.

Nilsen TW (2007). Mechanisms of microRNA-mediated gene regulation in animal cells. *Trends Genet.* **23** (5), 243-249.

Nucifora G, Begy CR, Erickson P, Drabkin HA and Rowley JD (1993). The 3;21 translocation in myelodysplasia results in a fusion transcript between the AML1 gene and the gene for EAP, a highly conserved protein associated with the Epstein-Barr virus small RNA EBER 1. *Proc Natl Acad Sci U S A.* **90** (16), 7784-7788.

O'Malley RP, Mariano TM, Siekierka J and Mathews MB (1986). A mechanism for the control of protein synthesis by adenovirus VA RNAI. *Cell.* **44** (3), 391-400.

Obernosterer G, Leuschner PJ, Alenius M and Martinez J (2006). Post-transcriptional regulation of microRNA expression. *RNA.* **12** (7), 1161-1167.

Oda W, Mistrikova J, Stancekova M, Dutia BM, Nash AA, Takahata H, Jin Z, Oka T and Hayashi K (2005). Analysis of genomic homology of murine gammaherpesvirus (MHV)-72 to MHV-68 and impact of MHV-72 on the survival and tumorigenesis in the MHV-72-infected CB17 scid/scid and CB17+/+ mice. *Pathol Int.* **55** (9), 558-568.

Ohe K and Weissman SM (1971). The nucleotide sequence of a low molecular weight ribonucleic acid from cells infected with adenovirus 2. *J Biol Chem.* **246** (22), 6991-7009.

Osman M, Kubo T, Gill J, Neipel F, Becker M, Smith G, Weiss R, Gazzard B, Boshoff C and Gotch F (1999). Identification of human herpesvirus 8-specific cytotoxic T-cell responses. *J Virol.* **73** (7), 6136-6140.

Osterrieder N, Kamil JP, Schumacher D, Tischer BK and Trapp S (2006). Marek's disease virus: from miasma to model. *Nat Rev Microbiol.* **4** (4), 283-294.

Ouellet DL, Plante I, Landry P, Barat C, Janelle ME, Flamand L, Tremblay MJ and Provost P (2008). Identification of functional microRNAs released through asymmetrical processing of HIV-1 TAR element. *Nucleic Acids Res.* **36** (7), 2353-2365.

Palmeri D, Spadavecchia S, Carroll KD and Lukac DM (2007). Promoter- and cell-specific transcriptional transactivation by the Kaposi's sarcoma-associated herpesvirus ORF57/Mta protein. *J Virol.* **81** (24), 13299-13314.

Pancholi V (2001). Multifunctional alpha-enolase: its role in diseases. *Cell Mol Life Sci.* **58** (7), 902-920.

Pandey RR, Mondal T, Mohammad F, Enroth S, Redrup L, Komorowski J, Nagano T, Mancini-Dinardo D and Kanduri C (2008). Kcnq1ot1 antisense noncoding RNA mediates lineage-specific transcriptional silencing through chromatin-level regulation. *Mol Cell.* **32** (2), 232-246.

Parravicini C, Chandran B, Corbellino M, Berti E, Paulli M, Moore PS and Chang Y (2000). Differential viral protein expression in Kaposi's sarcoma-associated herpesvirus-infected diseases: Kaposi's sarcoma, primary effusion lymphoma, and multicentric Castleman's disease. *Am J Pathol.* **156** (3), 743-749.

Parry CM, Simas JP, Smith VP, Stewart CA, Minson AC, Efstathiou S and Alcami A (2000). A broad spectrum secreted chemokine binding protein encoded by a herpesvirus. *J Exp Med.* **191** (3), 573-578.

Pavlova IV, Virgin HWt and Speck SH (2003). Disruption of gammaherpesvirus 68 gene 50 demonstrates that Rta is essential for virus replication. *J Virol.* **77** (10), 5731-5739.

Pellet PE and Roizman B (2007). The family *Herpesviridae*: a brief introduction. In: *Fields virology*, 5th edn. Knipe DM and Howley PM (eds.); Lippincott, Williams & Wilkins, Philadelphia, 2479-2499.

Perng GC, Dunkel EC, Geary PA, Slanina SM, Ghiasi H, Kaiwar R, Nesburn AB and Wechsler SL (1994). The latency-associated transcript gene of herpes simplex virus type 1 (HSV-1) is required for efficient in vivo spontaneous reactivation of HSV-1 from latency. *J Virol.* **68** (12), 8045-8055.

Perng GC, Jones C, Ciacci-Zanella J, Stone M, Henderson G, Yukht A, Slanina SM, Hofman FM, Ghiasi H, Nesburn AB and Wechsler SL (2000). Virus-induced neuronal apoptosis blocked by the herpes simplex virus latency-associated transcript. *Science.* **287** (5457), 1500-1503.

Perng GC, Maguen B, Jin L, Mott KR, Kurylo J, BenMohamed L, Yukht A, Osorio N, Nesburn AB, Henderson G, Inman M, Jones C and Wechsler SL (2002). A novel herpes simplex virus type 1 transcript (AL-RNA) antisense to the 5' end of the latency-associated transcript produces a protein in infected rabbits. *J Virol.* **76** (16), 8003-8010.

Pertel PE, Fridberg A, Parish ML and Spear PG (2001). Cell fusion induced by herpes simplex virus glycoproteins gB, gD, and gH-gL requires a gD receptor but not necessarily heparan sulfate. *Virology.* **279** (1), 313-324.

Pfeffer S, Zavolan M, Grasser FA, Chien M, Russo JJ, Ju J, John B, Enright AJ, Marks D, Sander C and Tuschl T (2004). Identification of virus-encoded microRNAs. *Science.* **304** (5671), 734-736.

Pfeffer S, Sewer A, Lagos-Quintana M, Sheridan R, Sander C, Grasser FA, van Dyk LF, Ho CK, Shuman S, Chien M, Russo JJ, Ju J, Randall G, Lindenbach BD, Rice CM, Simon V, Ho DD, Zavolan M and Tuschl T (2005). Identification of microRNAs of the herpesvirus family. *Nat Methods.* **2** (4), 269-276.

Quinlan MP, Chen LB and Knipe DM (1984). The intranuclear location of a herpes simplex virus DNA-binding protein is determined by the status of viral DNA replication. *Cell.* **36** (4), 857-868.

Rachamadugu R, Lee JY, Wooming A and Kong BW (2009). Identification and expression analysis of infectious laryngotracheitis virus encoding microRNAs. *Virus Genes.* **39** (3), 301-308.

Rajcani J, Blaskovic D, Svobodova J, Ciampor F, Huckova D and Stanekova D (1985). Pathogenesis of acute and persistent murine herpesvirus infection in mice. *Acta Virol.* **29** (1), 51-60.

Rao AL, Dreher TW, Marsh LE and Hall TC (1989). Telomeric function of the tRNA-like structure of brome mosaic virus RNA. *Proc Natl Acad Sci U S A.* **86** (14), 5335-5339.

Rawlins DR, Milman G, Hayward SD and Hayward GS (1985). Sequence-specific DNA binding of the Epstein-Barr virus nuclear antigen (EBNA-1) to clustered sites in the plasmid maintenance region. *Cell.* **42** (3), 859-868.

Rechsteiner MP, Berger C, Zauner L, Sigrist JA, Weber M, Longnecker R, Bernasconi M and Nadal D (2008). Latent membrane protein 2B regulates susceptibility to induction of lytic Epstein-Barr virus infection. *J Virol.* **82** (4), 1739-1747.

Reich PR, Forget BG and Weissman SM (1966). RNA of low molecular weight in KB cells infected with adenovirus type 2. *J Mol Biol.* **17** (2), 428-439.

Reichman TW, Muniz LC and Mathews MB (2002). The RNA binding protein nuclear factor 90 functions as both a positive and negative regulator of gene expression in mammalian cells. *Mol Cell Biol.* **22** (1), 343-356.

Renne R, Lagunoff M, Zhong W and Ganem D (1996). The size and conformation of Kaposi's sarcoma-associated herpesvirus (human herpesvirus 8) DNA in infected cells and virions. *J Virol.* **70** (11), 8151-8154.

Renne R, Barry C, Dittmer D, Compitello N, Brown PO and Ganem D (2001). Modulation of cellular and viral gene expression by the latency-associated nuclear antigen of Kaposi's sarcoma-associated herpesvirus. *J Virol.* **75** (1), 458-468.

Rickinson AB and Kieff E (2007). Epstein-Barr Virus. In: *Fields virology*, 5th edn. Knipe DM and Howley PM (eds.); Lippincott, Williams & Wilkins, Philadelphia, 2656-2700.

Rietveld K, Pleij CW and Bosch L (1983). Three-dimensional models of the tRNA-like 3' termini of some plant viral RNAs. *EMBO J.* **2** (7), 1079-1085.

Rinn JL, Kertesz M, Wang JK, Squazzo SL, Xu X, Brugmann SA, Goodnough LH, Helms JA, Farnham PJ, Segal E and Chang HY (2007). Functional demarcation of active and silent chromatin domains in human HOX loci by noncoding RNAs. *Cell.* **129** (7), 1311-1323.

Rivas C, Thlick AE, Parravicini C, Moore PS and Chang Y (2001). Kaposi's sarcoma-associated herpesvirus LANA2 is a B-cell-specific latent viral protein that inhibits p53. *J Virol.* **75** (1), 429-438.

Robertson KA, Usherwood EJ and Nash AA (2001). Regression of a murine gammaherpesvirus 68-positive b-cell lymphoma mediated by CD4 T lymphocytes. *J Virol.* **75** (7), 3480-3482.

Robertus JD, Ladner JE, Finch JT, Rhodes D, Brown RS, Clark BF and Klug A (1974). Structure of yeast phenylalanine tRNA at 3 A resolution. *Nature.* **250** (467), 546-551.

Rock DL, Nesburn AB, Ghiasi H, Ong J, Lewis TL, Lokensgard JR and Wechsler SL (1987). Detection of latency-related viral RNAs in trigeminal ganglia of rabbits latently infected with herpes simplex virus type 1. *J Virol.* **61** (12), 3820-3826.

Rodrigues L, Pires de Miranda M, Caloca MJ, Bustelo XR and Simas JP (2006). Activation of Vav by the gammaherpesvirus M2 protein contributes to the establishment of viral latency in B lymphocytes. *J Virol.* **80** (12), 6123-6135.

Roizman B and Whitley RJ (2001). The nine ages of herpes simplex virus. *Herpes.* **8** (1), 23-27.

Roizman B, Knipe DM and Whitley RJ (2007). Herpes Simplex Viruses. In: *Fields virology*, 5th edn. Knipe DM and Howley PM (eds.); Lippincott, Williams & Wilkins, Philadelphia, 2502-2601.

Romby P, Caillet J, Ebel C, Sacerdot C, Graffe M, Eyermann F, Brunel C, Moine H, Ehresmann C, Ehresmann B and Springer M (1996). The expression of E.coli threonyl-tRNA synthetase is regulated at the translational level by symmetrical operator-repressor interactions. *EMBO J.* **15** (21), 5976-5987.

Rosa MD, Gottlieb E, Lerner MR and Steitz JA (1981). Striking similarities are exhibited by two small Epstein-Barr virus-encoded ribonucleic acids and the adenovirus-associated ribonucleic acids VAI and VAII. *Mol Cell Biol.* **1** (9), 785-796.

Roy DJ, Ebrahimi BC, Dutia BM, Nash AA and Stewart JP (2000). Murine gammaherpesvirus M11 gene product inhibits apoptosis and is expressed during virus persistence. *Arch Virol.* **145** (11), 2411-2420.

Ruf IK, Rhyne PW, Yang C, Cleveland JL and Sample JT (2000). Epstein-Barr virus small RNAs potentiate tumorigenicity of Burkitt lymphoma cells independently of an effect on apoptosis. *J Virol.* **74** (21), 10223-10228.

Russo JJ, Bohenzky RA, Chien MC, Chen J, Yan M, Maddalena D, Parry JP, Peruzzi D, Edelman IS, Chang Y and Moore PS (1996). Nucleotide sequence of the Kaposi sarcoma-associated herpesvirus (HHV8). *Proc Natl Acad Sci U S A.* **93** (25), 14862-14867.

Saini HK, Griffiths-Jones S and Enright AJ (2007). Genomic analysis of human microRNA transcripts. *Proc Natl Acad Sci U S A.* **104** (45), 17719-17724.

Samanta M, Iwakiri D and Takada K (2008). Epstein-Barr virus-encoded small RNA induces IL-10 through RIG-I-mediated IRF-3 signaling. *Oncogene.* **27** (30), 4150-4160.

Samanta M, Iwakiri D, Kanda T, Imaizumi T and Takada K (2006). EB virus-encoded RNAs are recognized by RIG-I and activate signaling to induce type I IFN. *EMBO J.* **25** (18), 4207-4214.

Samols MA, Hu J, Skalsky RL and Renne R (2005). Cloning and identification of a microRNA cluster within the latency-associated region of Kaposi's sarcoma-associated herpesvirus. *J Virol.* **79** (14), 9301-9305.

Samols MA, Skalsky RL, Maldonado AM, Riva A, Lopez MC, Baker HV and Renne R (2007). Identification of cellular genes targeted by KSHV-encoded microRNAs. *PLoS Pathog.* **3** (5), e65.

Sangster MY, Topham DJ, D'Costa S, Cardin RD, Marion TN, Myers LK and Doherty PC (2000). Analysis of the virus-specific and nonspecific B cell response to a persistent B-lymphotropic gammaherpesvirus. *J Immunol.* **164** (4), 1820-1828.

Sano M, Kato Y and Taira K (2006). Sequence-specific interference by small RNAs derived from adenovirus VAI RNA. *FEBS Lett.* **580** (6), 1553-1564.

Sarawar SR, Lee BJ, Anderson M, Teng YC, Zuberi R and Von Gesjen S (2002). Chemokine induction and leukocyte trafficking to the lungs during murine gammaherpesvirus 68 (MHV-68) infection. *Virology.* **293** (1), 54-62.

Sawtell NM and Thompson RL (1992). Herpes simplex virus type 1 latency-associated transcription unit promotes anatomical site-dependent establishment and reactivation from latency. *J Virol.* **66** (4), 2157-2169.

Sawyer RC and Dahlberg JE (1973). Small RNAs of Rous sarcoma virus: characterization by two-dimensional polyacrylamide gel electrophoresis and fingerprint analysis. *J Virol.* **12** (6), 1226-1237.

Schafer A, Cai X, Bilello JP, Desrosiers RC and Cullen BR (2007). Cloning and analysis of microRNAs encoded by the primate gamma-herpesvirus rhesus monkey rhadinovirus. *Virology.* **364** (1), 21-27.

Schwartz RA, Micali G, Nasca MR and Scuderi L (2008). Kaposi sarcoma: a continuing conundrum. *J Am Acad Dermatol.* **59** (2), 179-206; quiz 207-178.

Sciortino MT, Suzuki M, Taddeo B and Roizman B (2001). RNAs extracted from herpes simplex virus 1 virions: apparent selectivity of viral but not cellular RNAs packaged in virions. *J Virol.* **75** (17), 8105-8116.

Scott KC, Merrett SL and Willard HF (2006). A heterochromatin barrier partitions the fission yeast centromere into discrete chromatin domains. *Curr Biol.* **16** (2), 119-129.

Scott KC, White CV and Willard HF (2007). An RNA polymerase III-dependent heterochromatin barrier at fission yeast centromere 1. *PLoS One.* **2** (10), e1099.

Selbach M, Schwanhausser B, Thierfelder N, Fang Z, Khanin R and Rajewsky N (2008). Widespread changes in protein synthesis induced by microRNAs. *Nature.* **455** (7209), 58-63.

Seo GJ, Chen CJ and Sullivan CS (2009). Merkel cell polyomavirus encodes a microRNA with the ability to autoregulate viral gene expression. *Virology.* **383** (2), 183-187.

Seo GJ, Fink LH, O'Hara B, Atwood WJ and Sullivan CS (2008). Evolutionarily conserved function of a viral microRNA. *J Virol.* **82** (20), 9823-9828.

Seo T, Park J, Lim C and Choe J (2004). Inhibition of nuclear factor kappaB activity by viral interferon regulatory factor 3 of Kaposi's sarcoma-associated herpesvirus. *Oncogene.* **23** (36), 6146-6155.

Sharp TV, Schwemmle M, Jeffrey I, Laing K, Mellor H, Proud CG, Hilse K and Clemens MJ (1993). Comparative analysis of the regulation of the interferon-inducible protein kinase PKR by Epstein-Barr virus RNAs EBER-1 and EBER-2 and adenovirus VAI RNA. *Nucleic Acids Res.* **21** (19), 4483-4490.

Shen W, Sa e Silva M, Jaber T, Vitvitskaia O, Li S, Henderson G and Jones C (2009). Two small RNAs encoded within the first 1.5 kilobases of the herpes simplex virus type 1 latency-associated transcript can inhibit productive infection and cooperate to inhibit apoptosis. *J Virol.* **83** (18), 9131-9139.

Shieh MT, WuDunn D, Montgomery RI, Esko JD and Spear PG (1992). Cell surface receptors for herpes simplex virus are heparan sulfate proteoglycans. *J Cell Biol.* **116** (5), 1273-1281.

Shukla D, Liu J, Blaiklock P, Shworak NW, Bai X, Esko JD, Cohen GH, Eisenberg RJ, Rosenberg RD and Spear PG (1999). A novel role for 3-O-sulfated heparan sulfate in herpes simplex virus 1 entry. *Cell.* **99** (1), 13-22.

Siegel AM, Herskowitz JH and Speck SH (2008). The MHV68 M2 protein drives IL-10 dependent B cell proliferation and differentiation. *PLoS Pathog.* **4** (4), e1000039.

Simas JP, Bowden RJ, Paige V and Efstathiou S (1998). Four tRNA-like sequences and a serpin homologue encoded by murine gammaherpesvirus 68 are dispensable for lytic replication in vitro and latency in vivo. *J Gen Virol.* **79 (Pt 1)**, 149-153.

Simas JP, Swann D, Bowden R and Efstathiou S (1999). Analysis of murine gammaherpesvirus-68 transcription during lytic and latent infection. *J Gen Virol.* **80 (Pt 1)**, 75-82.

Simas JP, Marques S, Bridgeman A, Efstathiou S and Adler H (2004). The M2 gene product of murine gammaherpesvirus 68 is required for efficient colonization of splenic follicles but is not necessary for expansion of latently infected germinal centre B cells. *J Gen Virol.* **85** (Pt 10), 2789-2797.

Simms TA, Miller EC, Buisson NP, Jambunathan N and Donze D (2004). The Saccharomyces cerevisiae TRT2 tRNAThr gene upstream of STE6 is a barrier to repression in MATalpha cells and exerts a potential tRNA position effect in MATa cells. *Nucleic Acids Res.* **32** (17), 5206-5213.

Skalsky RL, Samols MA, Plaisance KB, Boss IW, Riva A, Lopez MC, Baker HV and Renne R (2007). Kaposi's sarcoma-associated herpesvirus encodes an ortholog of miR-155. *J Virol.* **81** (23), 12836-12845.

Soderlund H, Pettersson U, Vennstrom B, Philipson L and Mathews MB (1976). A new species of virus-coded low molecular weight RNA from cells infected with adenovirus type 2. *Cell.* **7** (4), 585-593.

Song MJ, Brown HJ, Wu TT and Sun R (2001). Transcription activation of polyadenylated nuclear rna by rta in human herpesvirus 8/Kaposi's sarcoma-associated herpesvirus. *J Virol.* **75** (7), 3129-3140.

Song MJ, Li X, Brown HJ and Sun R (2002). Characterization of interactions between RTA and the promoter of polyadenylated nuclear RNA in Kaposi's sarcoma-associated herpesvirus/human herpesvirus 8. *J Virol.* **76** (10), 5000-5013.

Song MJ, Hwang S, Wong WH, Wu TT, Lee S, Liao HI and Sun R (2005). Identification of viral genes essential for replication of murine gamma-herpesvirus 68 using signature-tagged mutagenesis. *Proc Natl Acad Sci U S A.* **102** (10), 3805-3810.

Sparks-Thissen RL, Braaten DC, Kreher S, Speck SH and Virgin HWt (2004). An optimized CD4 T-cell response can control productive and latent gammaherpesvirus infection. *J Virol.* **78** (13), 6827-6835.

Sparks-Thissen RL, Braaten DC, Hildner K, Murphy TL, Murphy KM and Virgin HWt (2005). CD4 T cell control of acute and latent murine gammaherpesvirus infection requires IFNgamma. *Virology.* **338** (2), 201-208.

Spear PG and Longnecker R (2003). Herpesvirus entry: an update. *J Virol.* **77** (19), 10179-10185.

Spivack JG and Fraser NW (1987). Detection of herpes simplex virus type 1 transcripts during latent infection in mice. *J Virol.* **61** (12), 3841-3847.

Spivack JG, Woods GM and Fraser NW (1991). Identification of a novel latency-specific splice donor signal within the herpes simplex virus type 1 2.0-kilobase latency-associated transcript (LAT): translation inhibition of LAT open reading frames by the intron within the 2.0-kilobase LAT. *J Virol.* **65** (12), 6800-6810.

Sprauge KU (1995). Transcription of Eukaryotic tRNA Genes. In: *tRNA:Structure, Biosynthesis, and Function*. D. Söll and U. RajBhandary (eds.); American Society for Microbiology, Washington, 31-50.

Stancekova M, Matis J, Raucina J, Blaskovic D and Stancek D (1987). Comparative polypeptide analysis of human, murine and strigis herpesviruses with murine cytomegalovirus by polyacrylamide gel electrophoresis. *Acta Virol.* **31** (1), 1-6.

Stapler D, Lee ED, Selvaraj SA, Evans AG, Kean LS, Speck SH, Larsen CP and Gangappa S (2008). Expansion of effector memory TCR Vbeta4+ CD8+ T cells is associated with latent infection-mediated resistance to transplantation tolerance. *J Immunol.* **180** (5), 3190-3200.

Staudt LM (2000). The molecular and cellular origins of Hodgkin's disease. *J Exp Med.* **191** (2), 207-212.

Steed A, Buch T, Waisman A and Virgin HWt (2007). Gamma interferon blocks gammaherpesvirus reactivation from latency in a cell type-specific manner. *J Virol.* **81** (11), 6134-6140.

Steiner I, Spivack JG, Lirette RP, Brown SM, MacLean AR, Subak-Sharpe JH and Fraser NW (1989). Herpes simplex virus type 1 latency-associated transcripts are evidently not essential for latent infection. *EMBO J.* **8** (2), 505-511.

Stern-Ginossar N, Saleh N, Goldberg MD, Prichard M, Wolf DG and Mandelboim O (2009). Analysis of human cytomegalovirus-encoded microRNA activity during infection. *J Virol.* **83** (20), 10684-10693.

Stern-Ginossar N, Gur C, Biton M, Horwitz E, Elboim M, Stanietsky N, Mandelboim M and Mandelboim O (2008). Human microRNAs regulate stress-induced immune responses mediated by the receptor NKG2D. *Nat Immunol.* **9** (9), 1065-1073.

Stern-Ginossar N, Elefant N, Zimmermann A, Wolf DG, Saleh N, Biton M, Horwitz E, Prokocimer Z, Prichard M, Hahn G, Goldman-Wohl D, Greenfield C, Yagel S, Hengel H, Altuvia Y, Margalit H and Mandelboim O (2007). Host immune system gene targeting by a viral miRNA. *Science.* **317** (5836), 376-381.

Stevens JG, Wagner EK, Devi-Rao GB, Cook ML and Feldman LT (1987). RNA complementary to a herpesvirus alpha gene mRNA is prominent in latently infected neurons. *Science.* **235** (4792), 1056-1059.

Stevenson PG and Doherty PC (1998). Kinetic analysis of the specific host response to a murine gammaherpesvirus. *J Virol.* **72** (2), 943-949.

Stevenson PG, Belz GT, Altman JD and Doherty PC (1998). Virus-specific CD8(+) T cell numbers are maintained during gamma-herpesvirus reactivation in CD4-deficient mice. *Proc Natl Acad Sci U S A.* **95** (26), 15565-15570.

Stevenson PG, Cardin RD, Christensen JP and Doherty PC (1999). Immunological control of a murine gammaherpesvirus independent of CD8+ T cells. *J Gen Virol.* **80 (Pt 2)**, 477-483.

Stevenson PG, May JS, Smith XG, Marques S, Adler H, Koszinowski UH, Simas JP and Efstathiou S (2002). K3-mediated evasion of CD8(+) T cells aids amplification of a latent gamma-herpesvirus. *Nat Immunol.* **3** (8), 733-740.

Stewart JP, Usherwood EJ, Ross A, Dyson H and Nash T (1998). Lung epithelial cells are a major site of murine gammaherpesvirus persistence. *J Exp Med.* **187** (12), 1941-1951.

Stuller KA and Flano E (2009). CD4 T cells mediate killing during persistent gammaherpesvirus 68 infection. *J Virol.* **83** (9), 4700-4703.

Suddath FL, Quigley GJ, McPherson A, Sneden D, Kim JJ, Kim SH and Rich A (1974). Three-dimensional structure of yeast phenylalanine transfer RNA at 3.0angstroms resolution. *Nature.* **248** (443), 20-24.

Sullivan CS, Grundhoff AT, Tevethia S, Pipas JM and Ganem D (2005). SV40-encoded microRNAs regulate viral gene expression and reduce susceptibility to cytotoxic T cells. *Nature.* **435** (7042), 682-686.

Sullivan CS, Sung CK, Pack CD, Grundhoff A, Lukacher AE, Benjamin TL and Ganem D (2009). Murine Polyomavirus encodes a microRNA that cleaves early RNA transcripts but is not essential for experimental infection. *Virology.* **387** (1), 157-167.

Sun Q, Matta H, Lu G and Chaudhary PM (2006). Induction of IL-8 expression by human herpesvirus 8 encoded vFLIP K13 via NF-kappaB activation. *Oncogene.* **25** (19), 2717-2726.

Sun R, Lin SF, Gradoville L and Miller G (1996). Polyadenylylated nuclear RNA encoded by Kaposi sarcoma-associated herpesvirus. *Proc Natl Acad Sci U S A.* **93** (21), 11883-11888.

Sunil-Chandra NP, Efstathiou S and Nash AA (1992a). Murine gammaherpesvirus 68 establishes a latent infection in mouse B lymphocytes in vivo. *J Gen Virol.* **73 (Pt 12)**, 3275-3279.

Sunil-Chandra NP, Efstathiou S and Nash AA (1993). Interactions of murine gammaherpesvirus 68 with B and T cell lines. *Virology.* **193** (2), 825-833.

Sunil-Chandra NP, Efstathiou S, Arno J and Nash AA (1992b). Virological and pathological features of mice infected with murine gamma-herpesvirus 68. *J Gen Virol.* **73 (Pt 9)**, 2347-2356.

Sunil-Chandra NP, Arno J, Fazakerley J and Nash AA (1994). Lymphoproliferative disease in mice infected with murine gammaherpesvirus 68 *Am J Pathol.* **145** (4), 818-826.

Svobodova J, Blaskovic D and Mistrikova J (1982a). Growth characteristics of herpesviruses isolated from free living small rodents. *Acta Virol.* **26** (4), 256-263.

Svobodova J, Stancekova M, Blaskovic D, Mistrikova J, Lesso J, Russ G and Masarova P (1982b). Antigenic relatedness of alphaherpesviruses isolated from free-living rodents. *Acta Virol.* **26** (6), 438-443.

Swanton C, Mann DJ, Fleckenstein B, Neipel F, Peters G and Jones N (1997). Herpes viral cyclin/Cdk6 complexes evade inhibition by CDK inhibitor proteins. *Nature.* **390** (6656), 184-187.

Swigut T and Wysocka J (2007). H3K27 demethylases, at long last. *Cell.* **131** (1), 29-32.

Tang S, Patel A and Krause PR (2009). Novel less-abundant viral microRNAs encoded by herpes simplex virus 2 latency-associated transcript and their roles in regulating ICP34.5 and ICP0 mRNAs. *J Virol.* **83** (3), 1433-1442.

Tang S, Bertke AS, Patel A, Wang K, Cohen JI and Krause PR (2008). An acutely and latently expressed herpes simplex virus 2 viral microRNA inhibits expression of ICP34.5, a viral neurovirulence factor. *Proc Natl Acad Sci U S A.* **105** (31), 10931-10936.

Tanzer A and Stadler PF (2004). Molecular evolution of a microRNA cluster. *J Mol Biol.* **339** (2), 327-335.

Tarakanova VL, Kreisel F, White DW and Virgin HWt (2008). Murine gammaherpesvirus 68 genes both induce and suppress lymphoproliferative disease. *J Virol.* **82** (2), 1034-1039.

Tarakanova VL, Suarez F, Tibbetts SA, Jacoby MA, Weck KE, Hess JL, Speck SH and Virgin HWt (2005). Murine gammaherpesvirus 68 infection is associated with lymphoproliferative disease and lymphoma in BALB beta2 microglobulin-deficient mice. *J Virol.* **79** (23), 14668-14679.

Tempera I and Lieberman PM (2009). Chromatin organization of gammaherpesvirus latent genomes. *Biochim Biophys Acta.*

Terhune SS, Schroer J and Shenk T (2004). RNAs are packaged into human cytomegalovirus virions in proportion to their intracellular concentration. *J Virol.* **78** (19), 10390-10398.

Thimmappaya B, Weinberger C, Schneider RJ and Shenk T (1982). Adenovirus VAI RNA is required for efficient translation of viral mRNAs at late times after infection. *Cell.* **31** (3 Pt 2), 543-551.

Thomas DL, Lock M, Zabolotny JM, Mohan BR and Fraser NW (2002). The 2-kilobase intron of the herpes simplex virus type 1 latency-associated transcript has a half-life of approximately 24 hours in SY5Y and COS-1 cells. *J Virol.* **76** (2), 532-540.

Thompson MP and Kurzrock R (2004). Epstein-Barr virus and cancer. *Clin Cancer Res.* **10** (3), 803-821.

Thompson RL and Sawtell NM (1997). The herpes simplex virus type 1 latency-associated transcript gene regulates the establishment of latency. *J Virol.* **71** (7), 5432-5440.

Thompson RL and Sawtell NM (2001). Herpes simplex virus type 1 latency-associated transcript gene promotes neuronal survival. *J Virol.* **75** (14), 6660-6675.

Thorley-Lawson DA and Gross A (2004). Persistence of the Epstein-Barr virus and the origins of associated lymphomas. *N Engl J Med.* **350** (13), 1328-1337.

Toczyski DP and Steitz JA (1991). EAP, a highly conserved cellular protein associated with Epstein-Barr virus small RNAs (EBERs). *EMBO J.* **10** (2), 459-466.

Townsley AC, Dutia BM and Nash AA (2004). The m4 gene of murine gammaherpesvirus modulates productive and latent infection in vivo. *J Virol.* **78** (2), 758-767.

Tripp RA, Hamilton-Easton AM, Cardin RD, Nguyen P, Behm FG, Woodland DL, Doherty PC and Blackman MA (1997). Pathogenesis of an infectious mononucleosis-like disease induced by a murine gamma-herpesvirus: role for a viral superantigen? *J Exp Med.* **185** (9), 1641-1650.

Turner A, Bruun B, Minson T and Browne H (1998). Glycoproteins gB, gD, and gHgL of herpes simplex virus type 1 are necessary and sufficient to mediate membrane fusion in a Cos cell transfection system. *J Virol.* **72** (1), 873-875.

Uchida J, Yasui T, Takaoka-Shichijo Y, Muraoka M, Kulwichit W, Raab-Traub N and Kikutani H (1999). Mimicry of CD40 signals by Epstein-Barr virus LMP1 in B lymphocyte responses. *Science.* **286** (5438), 300-303.

Umbach JL, Nagel MA, Cohrs RJ, Gilden DH and Cullen BR (2009). Analysis of human alphaherpesvirus microRNA expression in latently infected human trigeminal ganglia. *J Virol.* **83** (20), 10677-10683.

Umbach JL, Kramer MF, Jurak I, Karnowski HW, Coen DM and Cullen BR (2008). MicroRNAs expressed by herpes simplex virus 1 during latent infection regulate viral mRNAs. *Nature.* **454** (7205), 780-783.

Umbach JL, Wang K, Tang S, Krause PR, Mont EK, Cohen JI and Cullen BR (2010). Identification of viral microRNAs expressed in human sacral ganglia latently infected with herpes simplex virus 2. *J Virol.* **84** (2), 1189-1192.

Upton JW and Speck SH (2006). Evidence for CDK-dependent and CDK-independent functions of the murine gammaherpesvirus 68 v-cyclin. *J Virol.* **80** (24), 11946-11959.

Upton JW, van Dyk LF and Speck SH (2005). Characterization of murine gammaherpesvirus 68 v-cyclin interactions with cellular cdks. *Virology.* **341** (2), 271-283.

Usherwood EJ, Stewart JP and Nash AA (1996a). Characterization of tumor cell lines derived from murine gammaherpesvirus-68-infected mice. *J Virol.* **70** (9), 6516-6518.

Usherwood EJ, Ross AJ, Allen DJ and Nash AA (1996b). Murine gammaherpesvirus-induced splenomegaly: a critical role for CD4 T cells. *J Gen Virol.* **77 (Pt 4)**, 627-630.

Usherwood EJ, Stewart JP, Robertson K, Allen DJ and Nash AA (1996c). Absence of splenic latency in murine gammaherpesvirus 68-infected B cell-deficient mice. *J Gen Virol.* **77 (Pt 11)** (Library), 2819-2825.

Usherwood EJ, Roy DJ, Ward K, Surman SL, Dutia BM, Blackman MA, Stewart JP and Woodland DL (2000). Control of gammaherpesvirus latency by latent antigen-specific CD8(+) T cells. *J Exp Med.* **192** (7), 943-952.

van Berkel V, Preiter K, Virgin HWt and Speck SH (1999). Identification and initial characterization of the murine gammaherpesvirus 68 gene M3, encoding an abundantly secreted protein. *J Virol.* **73** (5), 4524-4529.

van Berkel V, Levine B, Kapadia SB, Goldman JE, Speck SH and Virgin HWt (2002). Critical role for a high-affinity chemokine-binding protein in gamma-herpesvirus-induced lethal meningitis. *J Clin Invest.* **109** (7), 905-914.

van Berkel V, Barrett J, Tiffany HL, Fremont DH, Murphy PM, McFadden G, Speck SH and Virgin HI (2000). Identification of a gammaherpesvirus selective chemokine binding protein that inhibits chemokine action. *J Virol.* **74** (15), 6741-6747.

van Dyk LF, Virgin HWt and Speck SH (2000). The murine gammaherpesvirus 68 v-cyclin is a critical regulator of reactivation from latency. *J Virol.* **74** (16), 7451-7461.

van Dyk LF, Hess JL, Katz JD, Jacoby M, Speck SH and Virgin HI (1999). The murine gammaherpesvirus 68 v-cyclin gene is an oncogene that promotes cell cycle progression in primary lymphocytes. *J Virol.* **73** (6), 5110-5122.

Ventura A, Young AG, Winslow MM, Lintault L, Meissner A, Erkeland SJ, Newman J, Bronson RT, Crowley D, Stone JR, Jaenisch R, Sharp PA and Jacks T (2008). Targeted deletion reveals essential and overlapping functions of the miR-17 through 92 family of miRNA clusters. *Cell.* **132** (5), 875-886.

Virgin HWt, Latreille P, Wamsley P, Hallsworth K, Weck KE, Dal Canto AJ and Speck SH (1997). Complete sequence and genomic analysis of murine gammaherpesvirus 68. *J Virol.* **71** (8), 5894-5904.

Wagner EK, Flanagan WM, Devi-Rao G, Zhang YF, Hill JM, Anderson KP and Stevens JG (1988a). The herpes simplex virus latency-associated transcript is spliced during the latent phase of infection. *J Virol.* **62** (12), 4577-4585.

Wagner EK, Devi-Rao G, Feldman LT, Dobson AT, Zhang YF, Flanagan WM and Stevens JG (1988b). Physical characterization of the herpes simplex virus latency-associated transcript in neurons. *J Virol.* **62** (4), 1194-1202.

Wahid AM, Coventry VK and Conn GL (2008). Systematic deletion of the adenovirus-associated RNAI terminal stem reveals a surprisingly active RNA inhibitor of double-stranded RNA-activated protein kinase. *J Biol Chem.* **283** (25), 17485-17493.

Waidner LA, Morgan RW, Anderson AS, Bernberg EL, Kamboj S, Garcia M, Riblet SM, Ouyang M, Isaacs GK, Markis M, Meyers BC, Green PJ and Burnside J (2009). MicroRNAs of Gallid and Meleagrid herpesviruses show generally conserved genomic locations and are virus-specific. *Virology.* **388** (1), 128-136.

Wakefield JK, Wolf AG and Morrow CD (1995). Human immunodeficiency virus type 1 can use different tRNAs as primers for reverse transcription but selectively maintains a primer binding site complementary to tRNA(3Lys). *J Virol.* **69** (10), 6021-6029.

Wakeling MN, Roy DJ, Nash AA and Stewart JP (2001). Characterization of the murine gammaherpesvirus 68 ORF74 product: a novel oncogenic G protein-coupled receptor. *J Gen Virol.* **82** (Pt 5), 1187-1197.

Wang GH, Garvey TL and Cohen JI (1999). The murine gammaherpesvirus-68 M11 protein inhibits Fas- and TNF-induced apoptosis. *J Gen Virol.* **80 (Pt 10)**, 2737-2740.

Wang L, Haeusler RA, Good PD, Thompson M, Nagar S and Engelke DR (2005a). Silencing near tRNA genes requires nucleolar localization. *J Biol Chem.* **280** (10), 8637-8639.

Wang QJ, Jenkins FJ, Jacobson LP, Kingsley LA, Day RD, Zhang ZW, Meng YX, Pellett PE, Kousoulas KG, Baghian A and Rinaldo CR, Jr. (2001). Primary human herpesvirus 8 infection generates a broadly specific CD8(+) T-cell response to viral lytic cycle proteins. *Blood.* **97** (8), 2366-2373.

Wang QY, Zhou C, Johnson KE, Colgrove RC, Coen DM and Knipe DM (2005b). Herpesviral latency-associated transcript gene promotes assembly of heterochromatin on viral lytic-gene promoters in latent infection. *Proc Natl Acad Sci U S A.* **102** (44), 16055-16059.

Wang Z, Yuan Z, Xiang L, Shao J and Wegrzyn G (2006). tRNA-dependent cleavage of the ColE1 plasmid-encoded RNA I. *Microbiology.* **152** (Pt 12), 3467-3476.

Warner MS, Geraghty RJ, Martinez WM, Montgomery RI, Whitbeck JC, Xu R, Eisenberg RJ, Cohen GH and Spear PG (1998). A cell surface protein with herpesvirus entry activity (HveB) confers susceptibility to infection by mutants of herpes simplex virus type 1, herpes simplex virus type 2, and pseudorabies virus. *Virology.* **246** (1), 179-189.

Wassarman DA, Lee SI and Steitz JA (1989). Nucleotide sequence of HSUR 5 RNA from herpesvirus saimiri. *Nucleic Acids Res.* **17** (3), 1258.

Watanabe A, Maruo S, Ito T, Ito M, Katsumura KR and Takada K (2009). Epstein-Barr virus-encoded Bcl-2 homologue functions as a survival factor in Wp-restricted Burkitt lymphoma cell line P3HR-1. *J Virol.*

Watanabe T, Sugaya M, Atkins AM, Aquilino EA, Yang A, Borris DL, Brady J and Blauvelt A (2003). Kaposi's sarcoma-associated herpesvirus latency-associated nuclear antigen prolongs the life span of primary human umbilical vein endothelial cells. *J Virol.* **77** (11), 6188-6196.

Webb LM, Smith VP and Alcami A (2004). The gammaherpesvirus chemokine binding protein can inhibit the interaction of chemokines with glycosaminoglycans. *FASEB J.* **18** (3), 571-573.

Weber B, Stresemann C, Brueckner B and Lyko F (2007). Methylation of human microRNA genes in normal and neoplastic cells. *Cell Cycle.* **6** (9), 1001-1005.

Weck KE, Kim SS, Virgin HI and Speck SH (1999). Macrophages are the major reservoir of latent murine gammaherpesvirus 68 in peritoneal cells. *J Virol.* **73** (4), 3273-3283.

Weck KE, Dal Canto AJ, Gould JD, O'Guin AK, Roth KA, Saffitz JE, Speck SH and Virgin HW (1997). Murine gamma-herpesvirus 68 causes severe large-vessel arteritis in mice lacking interferon-gamma responsiveness: a new model for virus-induced vascular disease. *Nat Med.* **3** (12), 1346-1353.

Wegrzyn G and Wegrzyn A (2008). Is tRNA only a translation factor or also a regulator of other processes? *J Appl Genet.* **49** (1), 115-122.

Weiss LM, Strickler JG, Warnke RA, Purtilo DT and Sklar J (1987). Epstein-Barr viral DNA in tissues of Hodgkin's disease. *Am J Pathol.* **129** (1), 86-91.

Weiss SB, Hsu WT, Foft JW and Scherberg NH (1968). Transfer RNA coded by the T4 bacteriophage genome. *Proc Natl Acad Sci U S A.* **61** (1), 114-121.

Wek SA, Zhu S and Wek RC (1995). The histidyl-tRNA synthetase-related sequence in the eIF-2 alpha protein kinase GCN2 interacts with tRNA and is required for activation in response to starvation for different amino acids. *Mol Cell Biol.* **15** (8), 4497-4506.

White RJ (2008). RNA polymerases I and III, non-coding RNAs and cancer. *Trends Genet.* **24** (12), 622-629.

Wies E, Mori Y, Hahn A, Kremmer E, Sturzl M, Fleckenstein B and Neipel F (2008). The viral interferon-regulatory factor-3 is required for the survival of KSHV-infected primary effusion lymphoma cells. *Blood.* **111** (1), 320-327.

Wightman B, Ha I and Ruvkun G (1993). Posttranscriptional regulation of the heterochronic gene lin-14 by lin-4 mediates temporal pattern formation in C. elegans. *Cell.* **75** (5), 855-862.

Willer DO and Speck SH (2003). Long-term latent murine Gammaherpesvirus 68 infection is preferentially found within the surface immunoglobulin D-negative subset of splenic B cells in vivo. *J Virol.* **77** (15), 8310-8321.

Williams H and Crawford DH (2006). Epstein-Barr virus: the impact of scientific advances on clinical practice. *Blood.* **107** (3), 862-869.

Willoughby DA, Vilalta A and Oshima RG (2000). An Alu element from the K18 gene confers position-independent expression in transgenic mice. *J Biol Chem.* **275** (2), 759-768.

Winter J, Jung S, Keller S, Gregory RI and Diederichs S (2009). Many roads to maturity: microRNA biogenesis pathways and their regulation. *Nat Cell Biol.* **11** (3), 228-234.

Wolin SL and Cedervall T (2002). The La protein. *Annu Rev Biochem.* **71**, 375-403.

Wong E, Wu TT, Reyes N, Deng H and Sun R (2007). Murine gammaherpesvirus 68 open reading frame 24 is required for late gene expression after DNA replication. *J Virol.* **81** (12), 6761-6764.

Wong EL and Damania B (2006). Transcriptional regulation of the Kaposi's sarcoma-associated herpesvirus K15 gene. *J Virol.* **80** (3), 1385-1392.

Wu TC, Mann RB, Charache P, Hayward SD, Staal S, Lambe BC and Ambinder RF (1990). Detection of EBV gene expression in Reed-Sternberg cells of Hodgkin's disease. *Int J Cancer.* **46** (5), 801-804.

Wu TT, Usherwood EJ, Stewart JP, Nash AA and Sun R (2000). Rta of murine gammaherpesvirus 68 reactivates the complete lytic cycle from latency. *J Virol.* **74** (8), 3659-3667.

Wu TT, Tong L, Rickabaugh T, Speck S and Sun R (2001). Function of Rta is essential for lytic replication of murine gammaherpesvirus 68. *J Virol.* **75** (19), 9262-9273.

Wu TT, Park T, Kim H, Tran T, Tong L, Martinez-Guzman D, Reyes N, Deng H and Sun R (2009). ORF30 and ORF34 are essential for expression of late genes in murine gammaherpesvirus 68. *J Virol.* **83** (5), 2265-2273.

Wu Y, Maruo S, Yajima M, Kanda T and Takada K (2007). Epstein-Barr virus (EBV)-encoded RNA 2 (EBER2) but not EBER1 plays a critical role in EBV-induced B-cell growth transformation. *J Virol.* **81** (20), 11236-11245.

Xia T, O'Hara A, Araujo I, Barreto J, Carvalho E, Sapucaia JB, Ramos JC, Luz E, Pedroso C, Manrique M, Toomey NL, Brites C, Dittmer DP and Harrington WJ, Jr. (2008). EBV microRNAs in primary lymphomas and targeting of CXCL-11 by ebv-mir-BHRF1-3. *Cancer Res.* **68** (5), 1436-1442.

Xu N, Segerman B, Zhou X and Akusjarvi G (2007). Adenovirus virus-associated RNAII-derived small RNAs are efficiently incorporated into the rna-induced silencing complex and associate with polyribosomes. *J Virol.* **81** (19), 10540-10549.

Yang L, Aozasa K, Oshimi K and Takada K (2004). Epstein-Barr virus (EBV)-encoded RNA promotes growth of EBV-infected T cells through interleukin-9 induction. *Cancer Res.* **64** (15), 5332-5337.

Yao Y, Zhao Y, Smith LP, Watson M and Nair V (2009). Novel microRNAs (miRNAs) encoded by herpesvirus of Turkeys: evidence of miRNA evolution by duplication. *J Virol.* **83** (13), 6969-6973.

Yao Y, Zhao Y, Xu H, Smith LP, Lawrie CH, Watson M and Nair V (2008). MicroRNA profile of Marek's disease virus-transformed T-cell line MSB-1: predominance of virus-encoded microRNAs. *J Virol.* **82** (8), 4007-4015.

Yao Y, Zhao Y, Xu H, Smith LP, Lawrie CH, Sewer A, Zavolan M and Nair V (2007). Marek's disease virus type 2 (MDV-2)-encoded microRNAs show no sequence conservation with those encoded by MDV-1. *J Virol.* **81** (13), 7164-7170.

Yates J, Warren N, Reisman D and Sugden B (1984). A cis-acting element from the Epstein-Barr viral genome that permits stable replication of recombinant

plasmids in latently infected cells. *Proc Natl Acad Sci U S A.* **81** (12), 3806-3810.

Ye FC, Zhou FC, Xie JP, Kang T, Greene W, Kuhne K, Lei XF, Li QH and Gao SJ (2008). Kaposi's sarcoma-associated herpesvirus latent gene vFLIP inhibits viral lytic replication through NF-kappaB-mediated suppression of the AP-1 pathway: a novel mechanism of virus control of latency. *J Virol.* **82** (9), 4235-4249.

Yekta S, Shih IH and Bartel DP (2004). MicroRNA-directed cleavage of HOXB8 mRNA. *Science.* **304** (5670), 594-596.

Yi R, Qin Y, Macara IG and Cullen BR (2003). Exportin-5 mediates the nuclear export of pre-microRNAs and short hairpin RNAs. *Genes Dev.* **17** (24), 3011-3016.

Yin Q, McBride J, Fewell C, Lacey M, Wang X, Lin Z, Cameron J and Flemington EK (2008). MicroRNA-155 is an Epstein-Barr virus-induced gene that modulates Epstein-Barr virus-regulated gene expression pathways. *J Virol.* **82** (11), 5295-5306.

Yin Y, Manoury B and Fahraeus R (2003). Self-inhibition of synthesis and antigen presentation by Epstein-Barr virus-encoded EBNA1. *Science.* **301** (5638), 1371-1374.

Yoshinaga S, Dean N, Han M and Berk AJ (1986). Adenovirus stimulation of transcription by RNA polymerase III: evidence for an E1A-dependent increase in transcription factor IIIC concentration. *EMBO J.* **5** (2), 343-354.

Young LS and Rickinson AB (2004). Epstein-Barr virus: 40 years on. *Nat Rev Cancer.* **4** (10), 757-768.

Zeng Y and Cullen BR (2004). Structural requirements for pre-microRNA binding and nuclear export by Exportin 5. *Nucleic Acids Res.* **32** (16), 4776-4785.

Zeng Y and Cullen BR (2005). Efficient processing of primary microRNA hairpins by Drosha requires flanking nonstructured RNA sequences. *J Biol Chem.* **280** (30), 27595-27603.

Zeng Y, Yi R and Cullen BR (2005). Recognition and cleavage of primary microRNA precursors by the nuclear processing enzyme Drosha. *EMBO J.* **24** (1), 138-148.

Zhao J, Sun BK, Erwin JA, Song JJ and Lee JT (2008). Polycomb proteins targeted by a short repeat RNA to the mouse X chromosome. *Science.* **322** (5902), 750-756.

Zhao J, Punj V, Matta H, Mazzacurati L, Schamus S, Yang Y, Yang T, Hong Y and Chaudhary PM (2007). K13 blocks KSHV lytic replication and deregulates

vIL6 and hIL6 expression: a model of lytic replication induced clonal selection in viral oncogenesis. *PLoS One.* **2** (10), e1067.

Zhao Y, Yao Y, Xu H, Lambeth L, Smith LP, Kgosana L, Wang X and Nair V (2009). A functional MicroRNA-155 ortholog encoded by the oncogenic Marek's disease virus. *J Virol.* **83** (1), 489-492.

Zhong W and Ganem D (1997). Characterization of ribonucleoprotein complexes containing an abundant polyadenylated nuclear RNA encoded by Kaposi's sarcoma-associated herpesvirus (human herpesvirus 8). *J Virol.* **71** (2), 1207-1212.

Zhong W, Wang H, Herndier B and Ganem D (1996). Restricted expression of Kaposi sarcoma-associated herpesvirus (human herpesvirus 8) genes in Kaposi sarcoma. *Proc Natl Acad Sci U S A.* **93** (13), 6641-6646.

Zhou D, Palam LR, Jiang L, Narasimhan J, Staschke KA and Wek RC (2008). Phosphorylation of eIF2 directs ATF5 translational control in response to diverse stress conditions. *J Biol Chem.* **283** (11), 7064-7073.

Zhu JY, Pfuhl T, Motsch N, Barth S, Nicholls J, Grasser F and Meister G (2009). Identification of novel Epstein-Barr virus microRNA genes from nasopharyngeal carcinomas. *J Virol.* **83** (7), 3333-3341.

Ziegelbauer JM, Sullivan CS and Ganem D (2009). Tandem array-based expression screens identify host mRNA targets of virus-encoded microRNAs. *Nat Genet.* **41** (1), 130-134.

Ziegler JL, Drew WL, Miner RC, Mintz L, Rosenbaum E, Gershow J, Lennette ET, Greenspan J, Shillitoe E, Beckstead J, Casavant C and Yamamoto K (1982). Outbreak of Burkitt's-like lymphoma in homosexual men. *Lancet.* **2** (8299), 631-633.

zur Hausen H, Schulte-Holthausen H, Klein G, Henle W, Henle G, Clifford P and Santesson L (1970). EBV DNA in biopsies of Burkitt tumours and anaplastic carcinomas of the nasopharynx. *Nature.* **228** (5276), 1056-1058.

Zwaagstra JC, Ghiasi H, Slanina SM, Nesburn AB, Wheatley SC, Lillycrop K, Wood J, Latchman DS, Patel K and Wechsler SL (1990). Activity of herpes simplex virus type 1 latency-associated transcript (LAT) promoter in neuron-derived cells: evidence for neuron specificity and for a large LAT transcript. *J Virol.* **64** (10), 5019-5028.

8. Appendix

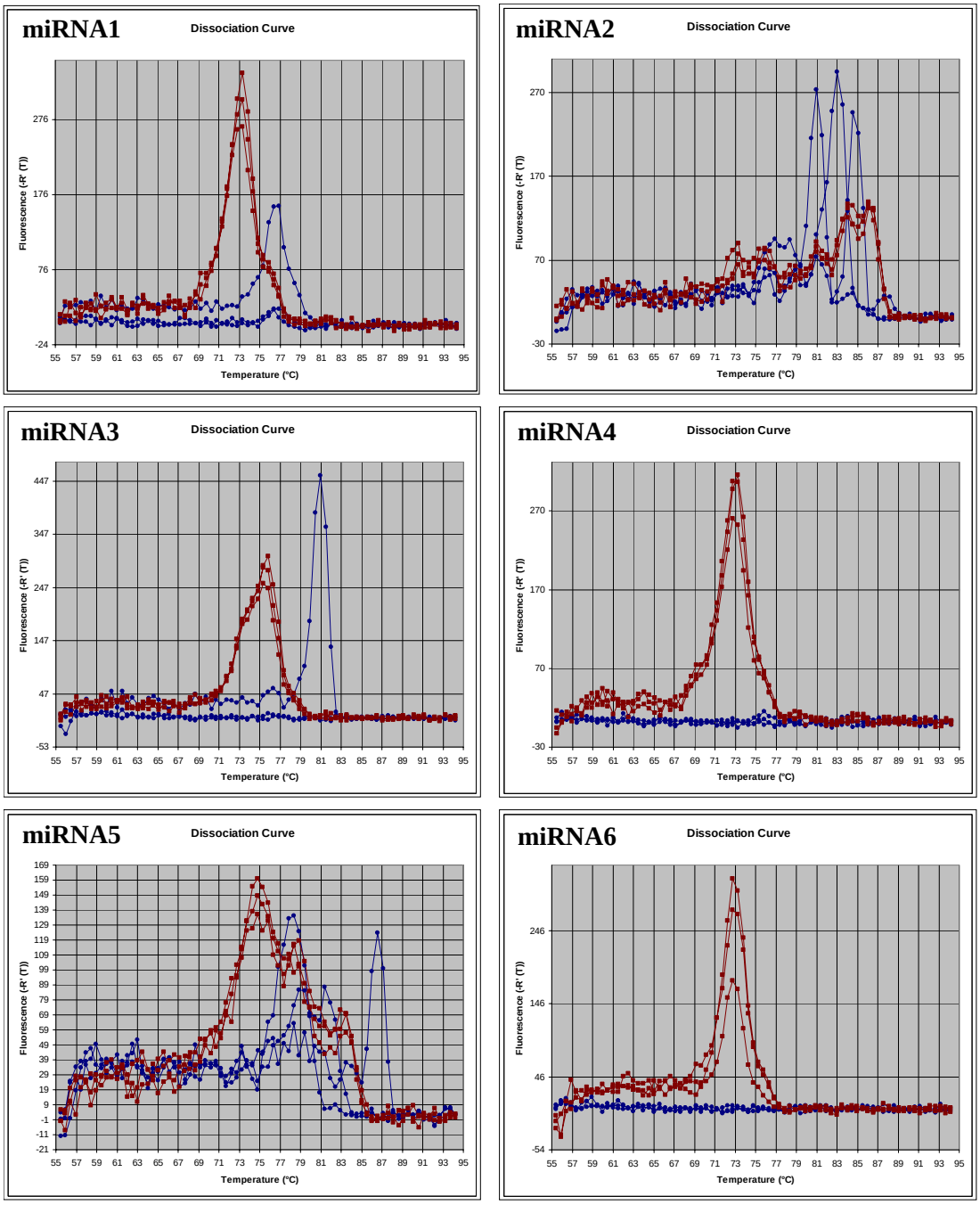

Figure 8.1 qRT-PCR dissociation curves for miRNA1-6 on RNA from mock (blue) and MHV-68 (red) infected NS0 cells.

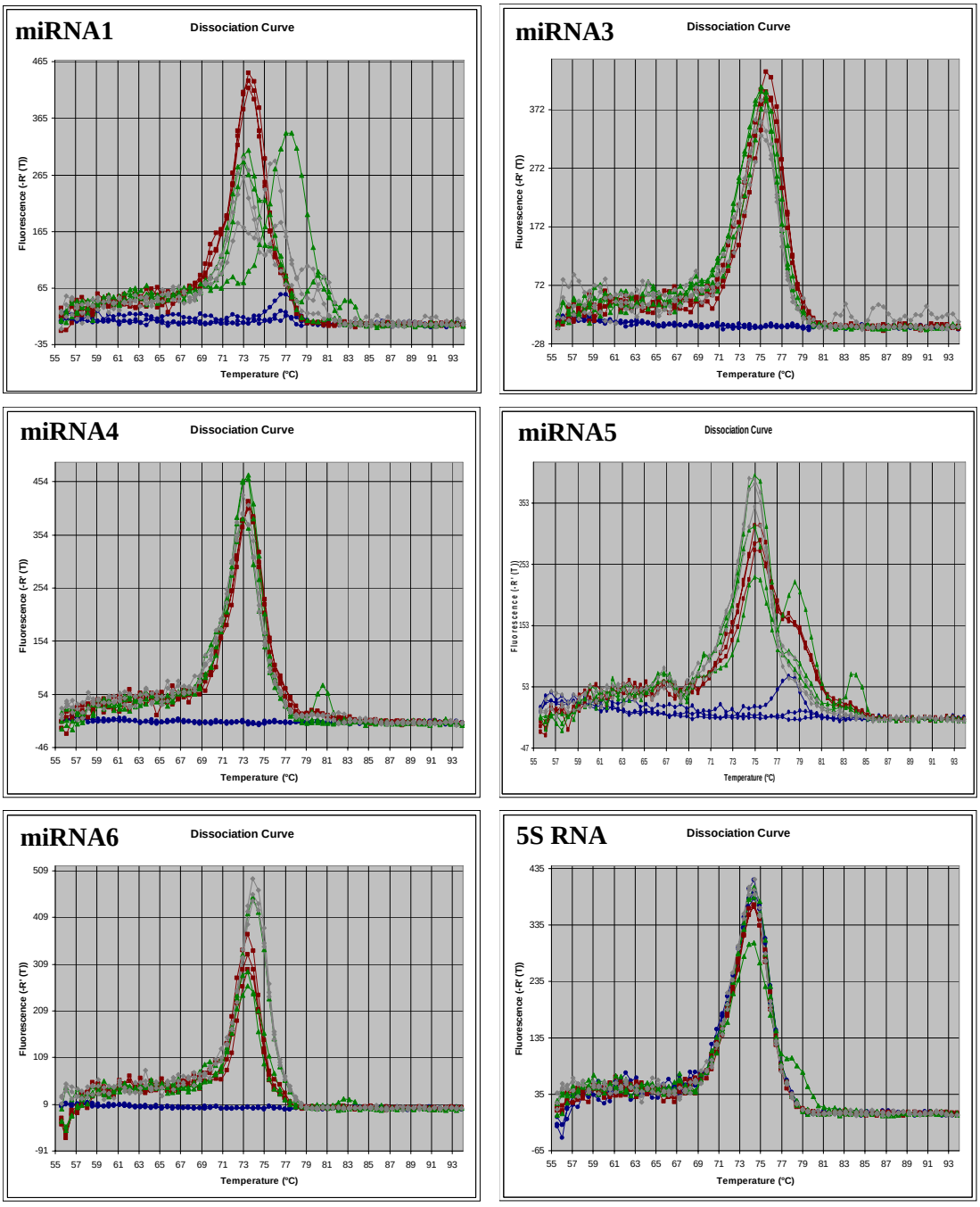

Figure 8.2 qRT-PCR dissociation curves for miRNA expression by MHV-68 (red), Int9 (green) and Int2 (grey) viruses and in mock-infected cells (blue). Showing miRNA1, 3, 4, 5, 6 and 5S ribosomal RNA dissociation curves.